Adaptive Control Based on Retrospective Cost Optimization

by

Mario A. Santillo

A dissertation submitted in partial fulfillment
of the requirements for the degree of
Doctor of Philosophy
(Aerospace Engineering)
in The University of Michigan
2009

Doctoral Committee:

Professor Dennis S. Bernstein, Chair
Professor Pierre T. Kabamba
Professor N. Harris McClamroch
Professor Jing Sun
Robert J. Fuentes, Raytheon Missile Systems

Hide not your talents, they for use were made.

What's a sun-dial in the shade?

—Benjamin Franklin

To Mom, Dad, Jason, and Michelle

Special thanks to my advisor Dennis Bernstein

Table of Contents

List of Tables

List of Figures

Chapter 1

Introduction

Feedback control is used to influence the behavior of dynamical systems. Without feedback control systems, modern technologies such as computers, aircraft, and spacecraft would not exist. One common example of control is the use of cruise control in modern automobiles. Cruise control enables the driver to set and maintain a desired vehicle speed without using the throttle. An open-loop, that is, no feedback action, method of cruise control would be to lock the throttle in a particular position; however, the vehicle speed would eventually drift given different terrains. By incorporating available sensors such as vehicle speed and engine load into a feedback loop, modern cruise controllers can accurately maintain vehicle speed over a wide variety of terrains. Additional applications of feedback control can be found in mechanical systems, electrical systems, financial systems, and even biological systems. In fact, balancing a stick on the tip of your finger is an example of feedback control; you use both your sense of sight and sense of touch to move your arm and keep the stick from falling.

Numerous design methods are commonly used in feedback control problems, ranging from classical control to modern control. Stabilizing a dynamical system when the plant parameters are uncertain or unknown, however, presents a challenging problem.

For example, consider the problem of stabilizing the equilibrium of the scalar plant

$$\dot{x}(t) = ax(t) + bu(t),$$

where $a > 0$ and $b \neq 0$. If a and b are known, then the control law $u(t) = -\text{sgn}(b)kx(t)$ stabilizes the system for all $k > a/|b|$. If a and b are uncertain, but the modeling uncertainty can be contained a priori within a given set, robust controllers [22, 25, 73, 120, 136] can be used to fix the control gain k based on the fixed level of modeling uncertainty. However, if a and b are unknown or if the modeling uncertainty cannot be ascertained a priori, knowledge of sgn b can be used to calculate either a positive high-gain feedback $u(t) = kx(t)$ or a negative high-gain feedback $u(t) = -kx(t)$ such that the closed-loop system is asymptotically stable for a sufficiently large feedback gain $k > 0$.

Unlike robust control, adaptive control algorithms tune the feedback gains in response to the true plant and exogenous signals, that is, commands and disturbances. Generally speaking, adaptive controllers require less prior modeling information than robust controllers, and thus can be viewed as highly parameter-robust control laws. The price paid for the ability of adaptive control laws to operate with limited prior modeling information is the complexity of analyzing and quantifying the stability and performance of the closed-loop system, especially in light of the fact that adaptive control laws, even for linear plants, are nonlinear.

The adaptive control literature focuses primarily on adaptive stabilization, adaptive command following, and model reference adaptive control [7, 16, 19, 24, 26, 28, 32, 46, 49, 50, 61, 65, 67, 77, 88, 90, 107, 118, 122]. These adaptive control problems have been approached using parameter-estimation-based adaptive controllers [7, 50, 90, 122], universal stabilizers [46, 47, 64, 79, 81, 86, 87, 96, 106, 130, 132], high-gain adaptive controllers [17, 18, 27, 29, 41, 46, 48, 61, 76, 77, 102], and adaptive

predictive controllers [19, 74, 88, 107].

In addition to stabilization and command following, disturbance rejection is another common objective arising in noise control, vibration suppression, and structural control [24, 32, 77, 90, 122]. Adaptive feedforward control is frequently used to reject harmonic disturbances when the disturbance spectrum is known or can be estimated [62, 80, 95]. Adaptive feedforward algorithms typically rely on least-mean-square (LMS) or recursive least-mean-square (RLMS) algorithms to update parameters. These methods include the filtered-u LMS and filtered-x LMS algorithms. However, adaptive feedforward algorithms do not account for the transfer function from the control signals to the measurements.

Model reference adaptive control (MRAC), in which a reference model is designed to generate a desired trajectory, is one of the primary approaches to adaptive control [3, 7, 32, 50, 51, 65, 68, 72, 75, 82, 85, 90–92, 94, 122, 123, 131]. In this case, the objective is to force an unknown plant to follow the output of a known reference model. In many formulations of model reference adaptive control, the control law depends on the solution of a Lyapunov equation, which, in turn depends on the reference model, and ultimately the system matrices A and B. Therefore, these control laws inherently depend on the modeling information expressed by A and B. In Chapter 5, we consider model reference adaptive control as a special case of the command-following problem; this controller does not rely on specialized assumptions about the reference model.

Stability and performance analysis of adaptive control laws often entails assumptions on the dynamics of the plant. For example, a widely invoked assumption in adaptive control is passivity [90], which is restrictive and difficult to verify in practice. A related assumption is that the plant is minimum phase or stably invertible [33, 45], which may entail the same difficulties. In fact, sampled-data control may give rise to nonminimum-phase zeros whether or not the continuous-time system is minimum

phase [8]. Since inverse-system representations are used to establish boundedness of the system inputs and outputs, nonminimum-phase zeros are known to present a challenge in proofs of stability and convergence for adaptive control algorithms [5]. Beyond these assumptions, adaptive control laws are known to be sensitive to unmodeled dynamics and sensor noise [9, 104], which motivates robust adaptive control laws [50].

In addition to these basic issues, adaptive control laws may entail unacceptable transients during adaptation, which may be exacerbated by actuator limitations [60, 98, 135]. In fact, adaptive control under extremely limited modeling information such as uncertainty in the high-frequency gain [64, 69] may yield a transient response that exceeds the practical limits of the plant. Therefore, the type and quality of the available modeling information as well as the speed of adaptation must be considered in the analysis and implementation of adaptive control laws. These issues are discussed in [5].

Certain modeling information may be required a priori to express the set in which the adaptive controller gain matrix is known to be contained. Furthermore, if the adaptive controller gain matrix is not contained within a particular set, projection algorithms may be used to force the adaptive controller gain into that set; see [7, 16, 26, 32, 50, 61, 67, 90, 118, 122]. With plant changes, however, a stabilizing adaptive controller gain may lie outside of this set, inducing an unstable closed-loop system. In addition, although many adaptive control laws assume matched uncertainty [7, 32, 90, 122], not all uncertainty is matched. This assumption frames the model assumptions on which the method is based. The adaptive controllers presented in this dissertation do not assume matched uncertainty.

Although the discrete-time adaptive control literature is more limited than the continuous-time literature, there are discrete-time versions of many continuous-time algorithms [2, 3, 7, 35, 51, 55, 66, 67, 91, 122], as well as adaptive control algorithms

unique to discrete time [28, 31–34, 66, 71, 93, 127, 134]. In [33], the authors present five algorithms for stabilization and command following of single-input single-output and multi-input multi-output minimum-phase systems. Although these algorithms require only that the command signal be bounded, they are based on the assumption that an ideal tracking controller exists. Disturbance rejection is not addressed.

In [127], a discrete-time adaptive disturbance rejection algorithm is developed based on a retrospective performance measure and ARMARKOV system representations. The retrospective performance of a system is the performance of the system at the current time assuming that the current controller was used over a past window of time. In [127], the retrospective performance is used in connection with time-series modeling of both the plant and the controller to develop an adaptive disturbance rejection algorithm that requires knowledge of only the numerator of the transfer function from the control to the performance, and does not require knowledge of the disturbance spectrum. Extensions of this method and experimental results are given in [1, 37, 42, 63, 108, 110] as well as computational fluid dynamics (CFD)-based flow control simulation results in [21, 103, 115, 116]. Robustness of the ARMARKOV adaptive disturbance rejection algorithm is studied in [109].

In this dissertation we consider discrete-time adaptive control since these control laws can be implemented directly in embedded code without requiring an intermediate discretization step with potential loss of phase margin. Furthermore, the adaptive controllers in this dissertation are developed under minimal modeling assumptions. In particular, the adaptive controllers require knowledge of the sign of the high-frequency gain and a sufficient number of Markov parameters to approximate the nonminimum-phase zeros (if any). No additional modeling information is necessary. The use of Markov parameters, or impulse response coefficients, facilitates identification and online retuning. Markov parameters are readily identifiable with least-squares (LS) or recursive least-squares (RLS) algorithms, as well as the observer/Kalman filter iden-

tification (OKID) algorithm [57]. Another application of Markov-parameter-based control is iterative learning control [83, 84], where the primary objective is repetitive-motion command following.

Applications of the adaptive control algorithms presented in this dissertation are published in [99, 117]. In [99], the adaptive control algorithm developed in Chapter 2 is used for three-degree-of-freedom angular-velocity command following in a six-degree-of-freedom Stewart platform. Closed-loop experiments were shown to reduce root mean square (RMS) angular-velocity command-following errors by at least a factor of 2 in all axes during a 10-minute test. In [117], the adaptive control algorithm developed in Chapter 5 is used to identify multi-input, multi-output, linear, time-invariant, discrete-time systems. The adaptive controller is used in feedback with an initial model to adapt the closed-loop response of the system to match the response of an unknown plant to a known input.

The remainder of this introduction summarizes the contents of Chapter 2 through Chapter 6 of this dissertation. In particular, these summaries outline the original contributions of each chapter. Two primary areas of research are presented in this dissertation. Specifically, Chapter 2 focuses on gradient-based adaptive control, while Chapters 3-6 relate to retrospective-cost-based adaptive control. Detailed literature reviews are provided at the beginning of each individual chapter.

Chapter 2 Summary

The results of Chapter 2 are an extension of the work presented in [36, Chapter VII], where an adaptive controller is developed that requires limited model information for stabilization, command following, and disturbance rejection for multi-input, multi-output, linear, time-invariant, minimum-phase, discrete-time systems. Specifically, the controller requires knowledge of the open-loop system's relative degree and a bound on the first nonzero Markov parameter. Notably, the controller does not

require knowledge of the command or disturbance spectrum as long as the command and disturbance signals are generated by Lyapunov-stable linear systems.

The original contribution of Chapter 2, beyond the material presented in [36, Chapter VII], is the use of a logarithmic Lyapunov function to prove Lyapunov stability for systems whose exogenous dynamics are unknown and unmeasured. In addition, we construct the adaptive update law as a gradient-based adaptive control algorithm. Since an ideal deadbeat internal model controller is proven to exist, the gradient-based construction allows us to compute and implement an optimal gradient step size. Furthermore, the gradient-based construction provides a framework for directly analyzing tradeoffs between transient performance and modeling accuracy. Finally, we derive an inverse system representation for multi-input, multi-output, minimum-phase systems which is necessary for the proof of Theorem 2.6.1.

Chapter 2 uses three key tools to prove global convergence of the performance variable. First, we use a nonminimal state-space realization of the plant. Similar nonminimal state-space realizations are considered in [23, 30, 32, 38, 101, 124, 127, 134]. Second, we prove the existence of an ideal fixed-gain controller that incorporates a deadbeat internal model controller, also developed in Chapter 2. Lastly, using a logarithmic Lyapunov function, we prove global asymptotic convergence for command following and disturbance rejection as well as Lyapunov stability of the closed-loop adaptive system when the open-loop system is asymptotically stable. Since we use a logarithmic Lyapunov function, we do not need to make use of the key technical lemma [32], which is limited to output convergence. The key technical lemma along with logarithmic Lyapunov functions [2, 3, 34, 35, 53–56, 59] are the two principal techniques used to prove stability for discrete-time adaptive systems.

Chapter 3 Summary

Chapter 3 begins the main topic of this dissertation. Since the method of proof for the gradient-based adaptive control algorithm presented in Chapter 2 cannot be extended to nonminimum-phase systems, we now focus on retrospective-cost-based adaptive control. In particular, this chapter investigates full-state-feedback stabilization in multi-input, linear, time-invariant, discrete-time systems. Retrospective cost optimization [127] is a measure of performance at the current time based on a past window of data and without assumptions about the command or disturbance signals. In particular, retrospective cost optimization acts as an inner loop to the adaptive control algorithm by modifying the performance variables based on the difference between the actual past control inputs and the recomputed past control inputs based on the current control law. This technique is inherent in [127] in the use of the estimated performance variable, but is more fully developed in this dissertation.

The original contribution of Chapter 3 is the development of a retrospective-cost-based adaptive controller for full-state-feedback stabilization. Furthermore, we prove Lyapunov stability of the closed-loop system for a special case. We also present numerical examples to illustrate the robustness of the algorithm under conditions of Markov-parameter uncertainty. Theoretical and numerical results suggest that the converged adaptive controller has a downward adaptive gain margin of 6 dB and an infinite upward adaptive gain margin, which is reminiscent of continuous-time fixed-gain LQR control. Guaranteed stability margins for discrete-time fixed-gain LQR are discussed in [119], but the margins are found to be inferior to their continuous-time counterparts.

Chapter 4 Summary

To further develop retrospective-cost-based adaptive control, the results of Chapter 4 generalize the results of Chapter 3 to static-output-feedback stabilization.

Specifically, we construct a retrospective-cost-based adaptive controller for multi-input, multi-output, linear, time-invariant, discrete-time systems with knowledge of the sign of the high-frequency gain and a sufficient number of Markov parameters to approximate the nonminimum-phase zeros (if any). No additional information about the poles or zeros need be known. In addition, we develop a theoretical link between nonminimum-phase zero information and Markov parameters. This link is detailed in Appendix A. We also present numerical examples to illustrate the robustness of the algorithm under conditions of Markov parameter uncertainty.

Chapter 5 Summary

The results of Chapter 5 are based on the adaptive control algorithms developed in [127] as well as Chapter 3 and Chapter 4 of this dissertation. Specifically, Chapter 5 generalizes the results of Chapter 3 and Chapter 4 to dynamic compensation for stabilization, command following, disturbance rejection, and model reference adaptive control. We construct a retrospective-cost-based adaptive controller for multi-input, multi-output, linear, time-invariant, discrete-time systems with knowledge of the sign of the high-frequency gain and a sufficient number of Markov parameters to approximate the nonminimum-phase zeros (if any). No additional information about the poles or the zeros need be known.

A novel feature of the adaptive control algorithms developed in Chapters 3-5 of this dissertation is the use of an adjustable learning-rate parameter α which allows us to develop Newton-step-based adaptive update laws. In addition, Chapter 5 further develops the theoretical link between Markov parameters and nonminimum-phase zeros. We also develop preliminary metrics for analyzing the gain and phase margins for discrete-time adaptive systems. Finally, numerical robustness analysis with uncertainty in the required modeling information is presented for plants that are multi-input, multi-output, nonminimum phase, and possibly unstable. These

numerical studies show that the adaptive control algorithm is effective for handling nonminimum-phase zeros under minimal modeling assumptions. These studies also provide guidance into the choice of the learning-rate parameter α for stable response and acceptable transient behavior.

Chapter 6 Summary

Adaptive control algorithms can be classified as either direct or indirect, depending on whether they employ an explicit parameter estimation algorithm within the overall adaptive scheme; see [32, 50, 77, 90]. Most direct adaptive control algorithms, with the exception of universal adaptive control algorithms [46, 47, 64, 79, 81, 86, 87, 96, 106, 130, 132], require some prior modeling information, such as the sign of the high-frequency gain. By updating the required modeling information, perhaps through closed-loop identification, a direct adaptive control algorithm can be converted to an indirect adaptive control algorithm, which may yield greater versatility in practice.

The results of Chapter 6 extend the results of Chapter 5. Specifically, the direct adaptive controller developed in Chapter 5 is augmented with recursive least-squares estimation to form a discrete-time indirect adaptive control law that is effective for systems that are multi-input, multi-output, and/or nonminimum phase. Recursive least-squares estimation is used for concurrent Markov parameter updating. We present numerical examples to illustrate the algorithm's effectiveness in handling nonminimum-phase zeros as plant changes occur. These results are noteworthy since nonminimum-phase zeros are known to be challenging for adaptive control algorithms [5]. Numerical results show that the algorithm is able to update the Markov parameters and maintain stabilization of the system.

Chapter 2

Adaptive Gradient-Based Dynamic Compensation

In this chapter, we present an adaptive controller that requires limited model information for stabilization, command following, and disturbance rejection for multi-input, multi-output, linear, time-invariant, minimum-phase, discrete-time systems. Specifically, the controller requires knowledge of the open-loop system's relative degree and a bound on the first nonzero Markov parameter. Notably, the controller does not require knowledge of the command or disturbance spectrum as long as the command and disturbance signals are generated by Lyapunov-stable linear systems. Thus, the command and disturbance are combinations of discrete-time sinusoids and steps. In addition, the controller uses feedback action only and thus does not require a direct measurement of the command or disturbance signals. We prove global asymptotic convergence for command following and disturbance rejection.

The results of this chapter are an extension of the work presented in [36, Chapter VII]. Beyond the material presented in [36, Chapter VII], this dissertation incorporates a logarithmic Lyapunov function to prove Lyapunov stability for systems whose exogenous dynamics are unknown and unmeasured. In addition, the adaptive update law is now constructed as a gradient-based adaptive control algorithm. In contrast to [127], which was only able to compute an implementable gradient step size, we

prove the existence of an ideal deadbeat internal model controller, and thus, we are now able to compute the optimal gradient step size. Furthermore, the gradient-based construction provides a framework for directly analyzing tradeoffs between transient performance and modeling accuracy. Finally, an appendix includes the derivation of an inverse system representation for multi-input, multi-output, minimum-phase systems. This derivation is necessary for the proof of Theorem 2.6.1. A precursor to the results of this chapter is given in [39], while the full results and methods of this chapter are published in [45]. An application of this algorithm to 3-axis angular velocity command following in a six-degree-of-freedom Stewart platform is published in [99], and a variation of the adaptive control algorithm developed in this chapter is implemented on an experimental testbed in [43] to demonstrate broadband adaptive disturbance rejection.

2.1 Introduction

The adaptive control literature focuses primarily on adaptive stabilization, adaptive tracking, and model reference adaptive control [7, 28, 32, 50, 67, 90, 122]. These adaptive control problems have been approached using parameter-estimation-based adaptive controllers [7, 50, 90, 122], universal stabilizers [47, 79, 81, 86, 96, 106, 130], and high-gain adaptive controllers [18, 27, 29, 41, 46, 48, 61, 76, 77, 102]. In addition to stabilization and command following, disturbance rejection is a third common objective, arising in noise control, vibration suppression, and structural control. In the present chapter, we consider the combined stabilization, command following, and disturbance rejection problem for uncertain minimum-phase discrete-time systems with command and disturbance signals generated by exogenous dynamics with unknown spectra. Furthermore, unlike adaptive feedforward control, we do not require a direct measurement of the command or disturbance signals.

Adaptive feedforward control is frequently used to reject harmonic disturbances when the disturbance spectrum is known or can be estimated [62, 80, 95]. Adaptive feedforward algorithms typically rely on least-mean-square (LMS) or recursive least-mean-square (RLMS) algorithms to update parameters. These methods include the filtered-u LMS and filtered-x LMS algorithms. However, adaptive feedforward algorithms do not account for the transfer function from the control signals to the measurements.

In [127], a discrete-time adaptive disturbance rejection algorithm is developed based on a retrospective performance measure. The retrospective performance of a system is the performance of the system at the current time assuming that the current controller was used over a past window of time. In [127], the retrospective performance is used in connection with time-series modeling of both the plant and the controller to develop an adaptive disturbance rejection algorithm that requires knowledge of only the numerator of the transfer function from the control to the performance, and does not require knowledge of the disturbance spectrum. Extensions of this method and experimental results are given in [42, 63, 108, 110].

Although the discrete-time adaptive control literature is more limited than the continuous-time literature, there are discrete-time versions of many continuous-time algorithms [2, 3, 7, 35, 51, 55, 66, 67, 91, 122], as well as adaptive control algorithms unique to discrete time [32, 33, 71, 134]. In [33], the authors present five algorithms for stabilization and command following of single-input single-output (SISO) and multi-input multi-output (MIMO) minimum-phase systems. Although these algorithms require only that the command signal be bounded, they are based on the assumption that an ideal tracking controller exists. Disturbance rejection is not addressed. In [78], the authors consider output regulation with a known plant and an unknown exosystem that generates reference and disturbance signals.

In the present chapter, we develop a discrete-time adaptive MIMO output feed-

back controller for stabilization, command following, and disturbance rejection in minimum-phase systems. This Markov-parameter-based adaptive control algorithm requires knowledge of only the open-loop system's relative degree and a bound on the first nonzero Markov parameter. We assume that the command and disturbance signals are generated by a Lyapunov-stable linear system so that the command and disturbance signals consist of discrete-time sinusoids and steps. However, we do not require any information regarding the spectrum of the command or the disturbance, and we do not require a direct measurement of the command or the disturbance. We prove globally asymptotic command following and disturbance rejection, as well as Lyapunov stability of the closed-loop error system when the open-loop dynamics are asymptotically stable. If there are no command or disturbance signals, then we prove output stabilization, that is, global asymptotic convergence of the output to zero.

The present chapter uses three key tools to prove global convergence of the performance variable. First, we use a nonminimal state-space realization of the plant. Similar nonminimal state-space realizations are considered in [23, 30, 32, 38, 124, 134]. The nonminimal state-space realization has a state that consists entirely of delayed inputs and outputs, which allows us to represent dynamic output feedback as static full-state feedback. More precisely, dynamic output feedback can be written as the product of a known feedback vector and a matrix of estimated controller parameters. Second, we prove the existence of an ideal fixed-gain controller that incorporates a deadbeat internal model controller. For more information on deadbeat internal model control, see [40]. Lastly, we use a logarithmic Lyapunov-like function to prove asymptotic command following and disturbance rejection. Logarithmic Lyapunov functions, that is, quadratic functions that incorporate a logarithm, are used in [2, 3, 35, 53–56, 59] to prove Lyapunov stability of discrete-time systems. In [128], a quadratic Lyapunov-like function is used to establish convergence of discrete-time systems. Using the logarithmic Lyapunov function, we prove global asymptotic convergence for

command following and disturbance rejection as well as Lyapunov stability of the adaptive system when the open-loop system is asymptotically stable.

2.2 Problem Formulation

Consider the MIMO discrete-time system

$$x(k+1) = Ax(k) + Bu(k) + D_1 w(k), \tag{2.1}$$

$$y(k) = Cx(k) + D_2 w(k), \tag{2.2}$$

where $x(k) \in \mathbb{R}^n$, $y(k) \in \mathbb{R}^{l_y}$, $u(k) \in \mathbb{R}^{l_u}$, $w(k) \in \mathbb{R}^{l_w}$, and $k \geq 0$. Our goal is to design an adaptive output feedback controller under which the performance variable y converges to zero in the presence of the exogenous signal w. Note that w can represent either a command signal to be followed, an external disturbance to be rejected, or both. For example, if $D_1 = 0$ and $D_2 \neq 0$, then the objective is to have the output Cx follow the command signal $-D_2 w$. On the other hand, if $D_1 \neq 0$ and $D_2 = 0$, then the objective is to reject the disturbance w from the performance measurement Cx. The combined command following and disturbance rejection problem is considered when D_1 and D_2 are block matrices. More precisely, if $D_1 = \left[\begin{array}{cc} \hat{D}_1 & 0 \end{array}\right]$, $D_2 = \left[\begin{array}{cc} 0 & \hat{D}_2 \end{array}\right]$, and $w(k) = \left[\begin{array}{c} w_1(k) \\ w_2(k) \end{array}\right]$, then the objective is to have Cx follow the command $-\hat{D}_2 w_2$ while rejecting the disturbance w_1. Lastly, if D_1 and D_2 are empty matrices, then the objective is output stabilization, that is, global asymptotic convergence of $y = Cx$ (and thus x) to zero.

In the nonadaptive case, a sufficient condition for command following and disturbance rejection is $l_u \geq l_y$ [40, 44]. Furthermore, we require that $l_y \geq l_u$ because the construction of an ideal fixed-gain controller in Section 2.4 requires that the first nonzero Markov parameter from u to y be left invertible. Thus, we require that

$l_y = l_u$. Henceforth, $l \triangleq l_y = l_u$.

Next, define the transfer function matrix

$$G_{yu}(z) \triangleq C(zI - A)^{-1}B = \sum_{i=d}^{\infty} z^{-i} H_i, \tag{2.3}$$

and define d to be the smallest positive integer i such that the ith Markov parameter $H_i \triangleq CA^{i-1}B$ is nonzero. We make the following assumptions:

(A1) The triple (A, B, C) is controllable and observable.

(A2) If $\lambda \in \mathbb{C}$ and $\operatorname{rank} \begin{bmatrix} A - \lambda I & B \\ C & 0 \end{bmatrix} < \text{normal rank} \begin{bmatrix} A - zI & B \\ C & 0 \end{bmatrix}$, then $|\lambda| < 1$.

(A3) d is known.

(A4) H_d is nonsingular.

(A5) There exists $\bar{H}_d \in \mathbb{R}^{l \times l}$ such that $2H_d^{\mathrm{T}} H_d \leq H_d^{\mathrm{T}} \bar{H}_d + \bar{H}_d^{\mathrm{T}} H_d$ and $\bar{H}_d$ is known.

(A6) There exists an integer $\bar{n}$ such that $n \leq \bar{n}$ and $\bar{n}$ is known.

(A7) The performance variable $y(k)$ is measured and available for feedback.

(A8) The exogenous signal $w(k)$ is generated by

$$x_w(k+1) = A_w x_w(k), \tag{2.4}$$
$$w(k) = C_w x_w(k), \tag{2.5}$$

where $x_w \in \mathbb{R}^{n_w}$ and A_w has distinct eigenvalues, all of which are on the unit circle.

(A9) There exists an integer $\bar{n}_w$ such that $n_w \leq \bar{n}_w$ and $\bar{n}_w$ is known.

(A10) The exogenous signal $w(k)$ is not measured.

(A11) $A, B, C, D_1, D_2, A_w, C_w, n, n_w$, and H_d are not known.

Assumption (A1) implies that the McMillan degree of $G_{yu}(z)$ is n. In the SISO case, assumption (A1) prevents pole-zero cancellation when forming the transfer function $G_{yu}(z)$, which implies that the order of $G_{yu}(z)$ is n.

Let $G_{yu}(z)$ have a left coprime matrix-fraction description $G_{yu}(z) = \mu(z)^{-1}\nu(z)$, where $\mu(z)$ and $\nu(z)$ are $l \times l$ polynomial matrices. Without loss of generality, we assume that $\mu(z)$ is in column-Hermite form, that is, $\mu(z)$ is upper triangular where each diagonal entry is a monic polynomial whose degree is higher than the degree of all of the remaining entries in its column [58, Theorem 6.3-2]. Thus, we can write

$$\mu(z) = z^m\mu_0 + z^{m-1}\mu_1 + \cdots + z\mu_{m-1} + \mu_m, \tag{2.6}$$

where $m \leq n$ and $\mu_0, \ldots, \mu_m \in \mathbb{R}^{l\times l}$ are upper triangular. Note that the leading coefficient matrix μ_0 is not necessarily I_l. However, it can be seen that there exists an $l \times l$ upper-triangular polynomial matrix

$$Q(z) \triangleq \begin{bmatrix} z^{h_{11}} & q_{12}z^{h_{12}} & \cdots & q_{1l}z^{h_{1l}} \\ & z^{h_{22}} & \cdots & q_{2l}z^{h_{2l}} \\ & & \ddots & \vdots \\ & & & z^{h_{ll}} \end{bmatrix}, \tag{2.7}$$

such that the leading term of $\alpha(z) \triangleq Q(z)\mu(z)$ is $z^m I_l$. Thus, we can write

$$\alpha(z) = z^m I_l + z^{m-1}\alpha_1 + z^{m-2}\alpha_2 + \cdots + z\alpha_{m-1} + \alpha_m, \tag{2.8}$$

where $\alpha_1, \ldots, \alpha_m \in \mathbb{R}^{l\times l}$. Furthermore, $G_{yu}(z)$ has the matrix-fraction description $G_{yu}(z) = \alpha(z)^{-1}\beta(z)$, where $\beta(z) \triangleq Q(z)\nu(z)$, and we can write

$$\beta(z) = z^{m-d}\beta_d + z^{m-d-1}\beta_{d+1} + \cdots + z\beta_{m-1} + \beta_m, \tag{2.9}$$

where $\beta_d, \ldots, \beta_m \in \mathbb{R}^{l \times l}$. Note that if the input to G_{yu} is $u = \delta(0)e_i$, where $\delta(0)$ is the unit impulse at $k = 0$ and e_i is the ith column of I_l, then the output is

$$y(k) = \begin{cases} 0, & 0 \leq k < d, \\ \beta_d e_i, & k = d. \end{cases} \tag{2.10}$$

Thus, it follows that $\beta_d = H_d$. Note that $\alpha(z)$ and $\beta(z)$ are not necessarily left coprime. However, since $\mu(z)$ and $\nu(z)$ are left coprime, it follows that $Q(z)$ is the greatest common left divisor of $\alpha(z)$ and $\beta(z)$. Furthermore, since $\det Q(z) = z^{h_{11}+\cdots+h_{ll}}$, the pole-zero cancellation that occurs when forming the transfer function $G_{yu}(z) = \alpha(z)^{-1}\beta(z)$ occurs only at $z = 0$.

Define the transfer function matrix

$$G_{yw}(z) \stackrel{\triangle}{=} C(zI - A)^{-1}D_1 + D_2, \tag{2.11}$$

and, assuming that G_{yw} has a matrix-fraction description of the form $G_{yw} = \alpha(z)^{-1}\gamma(z)$, which is not necessarily left coprime, we can write

$$\gamma(z) = z^m\gamma_0 + z^{m-1}\gamma_1 + \cdots + z\gamma_{m-1} + \gamma_m, \tag{2.12}$$

where $\gamma_0, \ldots, \gamma_m \in \mathbb{R}^{l \times l_w}$. Therefore, for $k \geq m$, the state-space system (2.1), (2.2) has the time-series representation

$$y(k) = \sum_{i=1}^{m} -\alpha_i y(k-i) + \sum_{i=d}^{m} \beta_i u(k-i) + \sum_{i=0}^{m} \gamma_i w(k-i). \tag{2.13}$$

Definition 2.2.1. *Let G be a strictly proper transfer function matrix. Then the* normal rank *of G is rank G = rank $G(\lambda)$ for almost all $\lambda \in \mathbb{C}$.*

Next, note that it follows from (2.3) and assumption (A4) that, for all sufficiently large $\lambda \in \mathbb{C}$, rank $G_{yu}(\lambda) = l$. Thus, $G_{yu}(z)$ has full normal rank, that is,

normal rank $G_{yu} = l$. Consequently, normal rank $\nu = l$.

Definition 2.2.2. *Let G be a strictly proper $s \times t$ transfer function matrix with the Smith-McMillan form*

$$G(z) = U_1(z) \begin{bmatrix} \frac{q_1(z)}{p_1(z)} & & & 0 \\ & \ddots & & \\ & & \frac{q_r(z)}{p_r(z)} & \\ 0 & & & 0_{(s-r)\times(t-r)} \end{bmatrix} U_2(z), \tag{2.14}$$

where $r =$ normal rank G, U_1 and U_2 are unimodular matrices, and $q_1, \ldots, q_r, p_1, \ldots, p_r$ are monic polynomials such that, for all $i = 1, \ldots, r$, q_i and p_i are coprime and, for all $i = 1, \ldots, r-1$, p_{i+1} divides p_i and q_i divides q_{i+1}. Then the poles *of G, counting multiplicity, are the roots of $p_1 \cdots p_r$, and the* transmission zeros *of G, counting multiplicity, are the roots of $q_1 \cdots q_r$.*

Lemma 2.2.3. *Let G be a strictly proper $s \times t$ transfer function matrix with a left coprime matrix-fraction description $G(z) = P(z)^{-1}Z(z)$. Then $\lambda \in \mathbb{C}$ is a transmission zero of G if and only if rank $Z(\lambda) <$ normal rank Z. Furthermore, $p \in \mathbb{C}$ is a pole of G if and only if $\det P(p) = 0$.*

Assumption (A2) states that the invariant zeros of (A, B, C) are contained in the open unit circle. Since, by assumption (A1), (A, B, C) is minimal, it follows that the invariant zeros of (A, B, C) are exactly the transmission zeros of $G_{yu}(z)$. Therefore, assumption (A2) is equivalent to the assumption that the transmission zeros of $G_{yu}(z)$ are contained in the open unit circle. Since $\mu(z)$ and $\nu(z)$ are left coprime, it follows from Lemma 2.2.3 that assumption (A2) is equivalent to the assumption that, if $\lambda \in \mathbb{C}$ and rank $\nu(\lambda) <$ normal rank ν, then $|\lambda| < 1$. Furthermore, since normal rank $\nu = l$ by assumption (A4), it follows that assumption (A2) implies that, if $\lambda \in \mathbb{C}$ and $\det \nu(\lambda) = 0$, then $|\lambda| < 1$. Consequently, since

$\det \beta(\lambda) = \det Q(\lambda) \det \nu(\lambda) = z^{h_{11}+\cdots+h_{ll}} \det \nu(\lambda)$, it follows that, if $\lambda \in \mathbb{C}$ and $\det \beta(\lambda) = 0$, then $|\lambda| < 1$.

For SISO systems, assumption (A5) specializes to the assumption that sgn H_d is known and an upper bound on the magnitude $|H_d|$ is known. For MIMO systems, assumption (A5) is a generalization of this SISO assumption. In particular, if H_d is positive definite, then assumption (A5) specializes to the assumption that an upper bound on the magnitude of $\lambda_{\max}(H_d)$ is known. Similarly, if H_d is negative definite, then assumption (A5) specializes to the assumption that an upper bound on the magnitude of $|\lambda_{\min}(H_d)|$ is known. More precisely, if H_d is positive definite, then assumption (A5) is satisfied with $\bar{H}_d > \lambda_{\max}(H_d) I_l$, while, if H_d is negative definite, then assumption (A5) is satisfied with $\bar{H}_d > |\lambda_{\min}(H_d)| I_l$. Note that assumptions (A4) and (A5) imply that $\bar{H}_d$ is nonsingular.

Assumption (A8) restricts our consideration to command and disturbance signals that consist of discrete-time sinusoids and steps. The assumption that the eigenvalues of A_w are distinct entails no loss in generality compared to the assumption that the eigenvalues of A_w are semisimple, that is, appear only in Jordan blocks of order 1. For example, consider the system

$$x_w(k+1) = \begin{bmatrix} \lambda & 0 \\ 0 & \lambda \end{bmatrix} x_w(k), \quad w(k) = x_w(k), \tag{2.15}$$

where $x_w(k) \stackrel{\triangle}{=} [x_{w1}(k) \quad x_{w2}(k)]^{\mathrm{T}}$. We consider two cases. First, suppose that $x_{w1}(0) \neq 0$ and construct the system

$$x_{w\mathrm{r}}(k+1) = \lambda x_{w\mathrm{r}}(k), \quad w_{\mathrm{r}}(k) = \begin{bmatrix} 1 \\ \frac{x_{w2}(0)}{x_{w1}(0)} \end{bmatrix} x_{w\mathrm{r}}(k). \tag{2.16}$$

Then, with $x_{wr}(0) = x_{w1}(0)$, it follows that

$$w_{\mathrm{r}}(k) = \begin{bmatrix} 1 \\ \frac{x_{w2}(0)}{x_{w1}(0)} \end{bmatrix} \lambda^k x_{wr}(0) = \begin{bmatrix} \lambda^k x_{w1}(0) \\ \lambda^k x_{w2}(0) \end{bmatrix} = w(k). \tag{2.17}$$

A similar argument applies to the case $x_{w2}(0) \neq 0$. Therefore, it follows that there exists a system with distinct eigenvalues whose output is identical to the output of (2.4), (2.5). Or course, Jordan blocks of order greater than 1 give rise to unbounded disturbances, which are not considered.

Assumption (A10) implies that a direct measurement of the command and disturbance is not required, while assumption (A11) implies that the spectrum of the command and disturbance signals is unknown. We stress that $y(k)$ is the only signal available for feedback.

2.3 Nonminimal State Space Realization

We use a nonminimal state-space realization of the time-series system (2.13) whose state consists entirely of measured information. More specifically, the state consists of past values of the performance variable $y(k)$ and the control $u(k)$. To construct the nonminimal state-space realization of the time-series system (2.13), we introduce the following notation. For a positive integer p, define the nilpotent matrix

$$\mathcal{N}_p \triangleq \begin{bmatrix} 0_{l\times l} & \cdots & 0_{l\times l} & 0_{l\times l} \\ I_l & \cdots & 0_{l\times l} & 0_{l\times l} \\ \vdots & \ddots & \vdots & \vdots \\ 0_{l\times l} & \cdots & I_l & 0_{l\times l} \end{bmatrix} \in \mathbb{R}^{lp\times lp}, \tag{2.18}$$

and define

$$E_1 \triangleq \begin{bmatrix} I_l \\ 0_{l(p-1)\times l} \end{bmatrix} \in \mathbb{R}^{lp\times l}, \tag{2.19}$$

where the dimension p is given by context.

Now, let $n_\mathrm{c} \geq m$ and consider the $2ln_\mathrm{c}$-order nonminimal state-space realization of (2.13)

$$\phi(k+1) = \mathcal{A}\phi(k) + \mathcal{B}u(k) + \mathcal{D}_1 W(k), \tag{2.20}$$

$$y(k) = \mathcal{C}\phi(k) + \mathcal{D}_2 W(k), \tag{2.21}$$

where

$$\mathcal{A} \triangleq \mathcal{A}_\mathrm{nil} + \begin{bmatrix} E_1\mathcal{C} \\ 0_{ln_\mathrm{c}\times 2ln_\mathrm{c}} \end{bmatrix}, \quad \mathcal{B} \triangleq \begin{bmatrix} 0_{ln_\mathrm{c}\times l} \\ E_1 \end{bmatrix}, \tag{2.22}$$

$$\mathcal{C} \triangleq \begin{bmatrix} -\alpha_1 & \cdots & -\alpha_m & 0_{l\times l(n_\mathrm{c}-m)} & 0_{l\times l(d-1)} & \beta_d & \cdots & \beta_m & 0_{l\times l(n_\mathrm{c}-m)} \end{bmatrix}, \tag{2.23}$$

$$\mathcal{D}_1 \triangleq \begin{bmatrix} E_1\mathcal{D}_2 \\ 0_{ln_\mathrm{c}\times(m+1)l_w} \end{bmatrix}, \quad \mathcal{D}_2 \triangleq \begin{bmatrix} \gamma_0 & \cdots & \gamma_m \end{bmatrix}; \tag{2.24}$$

$$\mathcal{A}_\mathrm{nil} \triangleq \begin{bmatrix} \mathcal{N}_{n_\mathrm{c}} & 0_{ln_\mathrm{c}\times ln_\mathrm{c}} \\ 0_{ln_\mathrm{c}\times ln_\mathrm{c}} & \mathcal{N}_{n_\mathrm{c}} \end{bmatrix} \tag{2.25}$$

is nilpotent; and

$$\phi(k) \triangleq \begin{bmatrix} y(k-1) \\ \vdots \\ y(k-n_{\mathrm{c}}) \\ u(k-1) \\ \vdots \\ u(k-n_{\mathrm{c}}) \end{bmatrix}, \qquad W(k) \triangleq \begin{bmatrix} w(k) \\ \vdots \\ w(k-m) \end{bmatrix}. \tag{2.26}$$

Note that the definition of $\mathcal{C}$ in (2.23) requires $n_{\mathrm{c}} \geq m$. The triple $(\mathcal{A}, \mathcal{B}, \mathcal{C})$ is stabilizable and detectable. However, $(\mathcal{A}, \mathcal{B}, \mathcal{C})$ is neither controllable nor observable. In particular, $(\mathcal{A}, \mathcal{B}, \mathcal{C})$ has n controllable and observable eigenvalues, while the remaining $2ln_{\mathrm{c}} - n$ eigenvalues are located at 0. Moreover, $(\mathcal{A}, \mathcal{B})$ has $ln_{\mathrm{c}} - n$ uncontrollable eigenvalues at 0, while $(\mathcal{A}, \mathcal{C})$ has ln_{c} unobservable eigenvalues at 0. Note that in this basis, the state $\phi(k)$ contains only past values of the performance variable y and the control u.

Now, we consider the time-series controller

$$u(k) = \sum_{i=1}^{n_{\mathrm{c}}} M_i u(k-i) + \sum_{i=1}^{n_{\mathrm{c}}} N_i y(k-i), \tag{2.27}$$

where, for all $i = 1, \ldots, n_{\mathrm{c}}$, $M_i \in \mathbb{R}^{l \times l}$ and $N_i \in \mathbb{R}^{l \times l}$. The control can be written as

$$u(k) = \theta \phi(k), \tag{2.28}$$

where

$$\theta \triangleq \begin{bmatrix} N_1 & \cdots & N_{n_{\mathrm{c}}} & M_1 & \cdots & M_{n_{\mathrm{c}}} \end{bmatrix} \in \mathbb{R}^{l \times 2ln_{\mathrm{c}}}. \tag{2.29}$$

The control (2.28), which is dynamic output feedback in terms of y, can be com-

puted by recording and using n_c past values of the performance variable y and the control u. However, (2.28) is a full-state-feedback control law for the nonminimal state-space system (2.20)-(2.25). The closed-loop system consisting of (2.20)-(2.25) with the linear time-invariant feedback (2.28) is

$$\phi(k+1) = \tilde{\mathcal{A}}\phi(k) + \mathcal{D}_1 W(k), \tag{2.30}$$

$$y(k) = \mathcal{C}\phi(k) + \mathcal{D}_2 W(k), \tag{2.31}$$

where

$$\tilde{\mathcal{A}} \triangleq \mathcal{A} + \mathcal{B}\theta = \mathcal{A}_{\text{nil}} + \begin{bmatrix} E_1\mathcal{C} \\ E_1\theta \end{bmatrix}. \tag{2.32}$$

2.4 Ideal Fixed-Gain Controller

In this section, we prove existence and derive properties of an ideal fixed-gain controller of the form (2.27) for the open-loop system (2.1) and (2.2). This controller, whose structure is illustrated in Figure 2.1, is used in subsequent sections to construct an error system for analyzing the adaptive closed-loop system. We stress that the ideal controller is not intended for implementation. An ideal fixed-gain controller consists of two distinct parts, specifically, a precompensator, which cancels the transmission zeros of the open-loop system, and a deadbeat internal model controller, which operates in feedback on the observable states of the precompensator cascaded with the open-loop system.

First, we demonstrate how to construct the ideal fixed-gain controller. Using

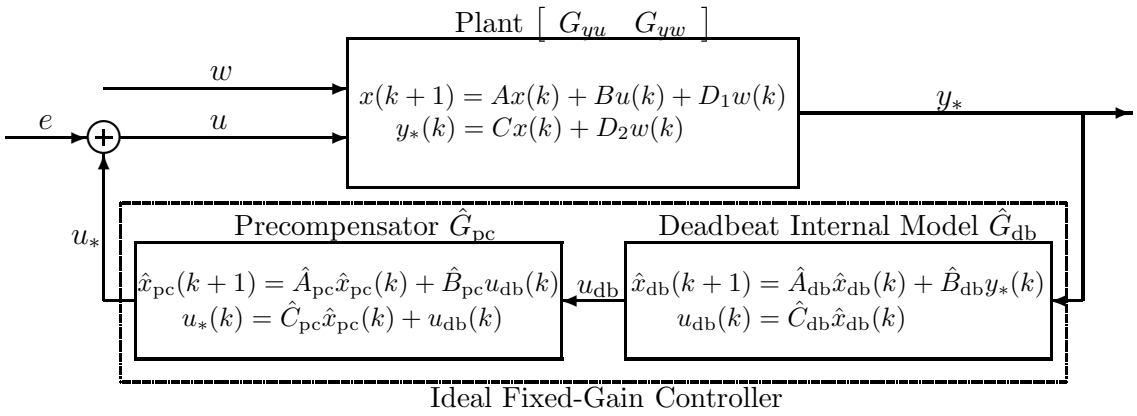

Figure 2.1 Closed-loop system with the ideal fixed-gain controller. The pseudo-input e facilitates the proof of Theorem 2.4.1 but is otherwise set to zero.

assumption (A4), consider the $l \times l$ exactly proper precompensator

$$u_*(k) = -H_d^{-1} \sum_{i=1}^{m-d} \beta_{d+i} u_*(k-i) + u_{\rm db}(k), \tag{2.33}$$

which has a minimal state-space realization of the form

$$\hat{x}_{\rm pc}(k+1) = \hat{A}_{\rm pc}\hat{x}_{\rm pc}(k) + \hat{B}_{\rm pc}u_{\rm db}(k), \tag{2.34}$$

$$u_*(k) = \hat{C}_{\rm pc}\hat{x}_{\rm pc}(k) + u_{\rm db}(k), \tag{2.35}$$

where $\hat{x}_{\rm pc} \in \mathbb{R}^{\hat{n}_{\rm pc}}$ and $\hat{n}_{\rm pc}$ is the McMillan degree of $\hat{G}_{\rm pc}(z) \triangleq \beta(z)^{-1} z^{m-d} H_d$, which is the transfer function from $u_{\rm db}$ to u_*. Note that $\hat{n}_{\rm pc} \leq l(m-d)$. The poles of the precompensator $\hat{G}_{\rm pc}(z)$ are exactly the transmission zeros of the open-loop transfer function $G_{yu}(z)$. Furthermore, assumption (A2) implies that the transmission zeros of $G_{yu}(z)$, and thus the poles of $\hat{G}_{\rm pc}(z)$, are asymptotically stable. Therefore, the cascade

$$\begin{aligned} G_{yu}(z)\hat{G}_{\rm pc}(z) &= \alpha(z)^{-1}\beta(z)\beta(z)^{-1}z^{m-d}H_d \\ &= \alpha(z)^{-1}z^{m-d}H_d \end{aligned} \tag{2.36}$$

has asymptotically stable pole-zero cancellation. Let n_{o} be the McMillan degree of $G_{yu}(z)\hat{G}_{\mathrm{pc}}(z)$, and note that $n_{\mathrm{o}} \leq lm$.

Define the pseudo-input

$$e(k) \triangleq u(k) - u_*(k), \tag{2.37}$$

and cascade the precompensator (2.34), (2.35) with the open-loop system (2.1), (2.2) to obtain

$$\begin{aligned}\begin{bmatrix} x(k+1) \\ \hat{x}_{\mathrm{pc}}(k+1) \end{bmatrix} &= \begin{bmatrix} A & B\hat{C}_{\mathrm{pc}} \\ 0 & \hat{A}_{\mathrm{pc}} \end{bmatrix} \begin{bmatrix} x(k) \\ \hat{x}_{\mathrm{pc}}(k) \end{bmatrix} + \begin{bmatrix} B \\ \hat{B}_{\mathrm{pc}} \end{bmatrix} u_{\mathrm{db}}(k) \\ &\quad + \begin{bmatrix} B \\ 0 \end{bmatrix} e(k) + \begin{bmatrix} D_1 \\ 0 \end{bmatrix} w(k), \end{aligned} \tag{2.38}$$

$$y_*(k) = \begin{bmatrix} C & 0 \end{bmatrix} \begin{bmatrix} x(k) \\ \hat{x}_{\mathrm{pc}}(k) \end{bmatrix} + D_2 w(k), \tag{2.39}$$

where y_* is the ideal system output. Since the poles of $\hat{G}_{\mathrm{pc}}(z)$ cancel the transmission zeros of $G_{yu}(z)$, it follows that

$$\left(\begin{bmatrix} A & B\hat{C}_{\mathrm{pc}} \\ 0 & \hat{A}_{\mathrm{pc}} \end{bmatrix}, \begin{bmatrix} B \\ \hat{B}_{\mathrm{pc}} \end{bmatrix}, \begin{bmatrix} C & 0 \end{bmatrix} \right) \tag{2.40}$$

is not minimal. However, since (A, B) and $(\hat{A}_{\mathrm{pc}}, \hat{B}_{\mathrm{pc}})$ are controllable, it follows that (2.40) is controllable. Thus,

$$\left(\begin{bmatrix} A & B\hat{C}_{\mathrm{pc}} \\ 0 & \hat{A}_{\mathrm{pc}} \end{bmatrix}, \begin{bmatrix} C & 0 \end{bmatrix} \right) \tag{2.41}$$

is not observable. In fact, it follows from the pole-zero cancellations between $\hat{G}_{\mathrm{pc}}(z)$

and $G_{yu}(z)$ that the unobservable modes of (2.41) are exactly the poles of $\hat{G}_{\rm pc}(z)$, all of which are asymptotically stable.

Next, let $\hat{x}_{\rm db} \in \mathbb{R}^{\hat{n}_{\rm db}}$, and let

$$\hat{x}_{\rm db}(k+1) = \hat{A}_{\rm db}\hat{x}_{\rm db}(k) + \hat{B}_{\rm db}y_*(k), \tag{2.42}$$

$$u_{\rm db}(k) = \hat{C}_{\rm db}\hat{x}_{\rm db}(k), \tag{2.43}$$

be an internal model controller (whose existence is shown in Section 2.9) for the observable states of (2.38) and (2.39) that guarantees exact command following and disturbance rejection in finite time, that is, (2.42), (2.43) is a deadbeat internal model controller. Thus, the ideal fixed-gain controller consists of the precompensator (2.34), (2.35) and the deadbeat internal model controller (2.42), (2.43). Define the transfer function matrix of the deadbeat internal model controller (2.42), (2.43) by

$$\hat{G}_{\rm db}(z) \triangleq \hat{C}_{\rm db}(zI - \hat{A}_{\rm db})^{-1}\hat{B}_{\rm db}.$$

The following theorem constructs the ideal fixed-gain controller

$$u_*(k) = \sum_{i=1}^{n_{\rm c}} M_{*i}u_*(k-i) + \sum_{i=1}^{n_{\rm c}} N_{*i}y_*(k-i), \tag{2.44}$$

which can be expressed as

$$u_*(k) = \theta_*\phi_{**}(k), \tag{2.45}$$

where

$$\theta_* \triangleq \left[\begin{array}{cccccc} N_{*1} & \cdots & N_{*n_{\rm c}} & M_{*1} & \cdots & M_{*n_{\rm c}} \end{array} \right] \tag{2.46}$$

and

$$\phi_{**}(k) \triangleq \begin{bmatrix} y_*(k-1) \\ \vdots \\ y_*(k-n_{\mathrm{c}}) \\ u_*(k-1) \\ \vdots \\ u_*(k-n_{\mathrm{c}}) \end{bmatrix}. \tag{2.47}$$

The closed-loop system with the ideal fixed-gain controller is shown in Figure 2.1 and is given by

$$\phi(k+1) = \tilde{\mathcal{A}}_*\phi(k) + \mathcal{D}_1 W(k), \tag{2.48}$$

$$y(k) = \mathcal{C}\phi(k) + \mathcal{D}_2 W(k), \tag{2.49}$$

where

$$\tilde{\mathcal{A}}_* \triangleq \mathcal{A} + \mathcal{B}\theta_* = \mathcal{A}_{\mathrm{nil}} + \begin{bmatrix} E_1\mathcal{C} \\ E_1\theta_* \end{bmatrix}. \tag{2.50}$$

Theorem 2.4.1. *Consider the ideal closed-loop system consisting of (2.48), (2.49), where $\tilde{\mathcal{A}}_*$, $\mathcal{B}$, and $\mathcal{C}$ are given by (2.50), (2.22), and (2.23), respectively. Furthermore, let*

$$n_{\mathrm{c}} \geq n_{\mathrm{o}} + 2ln_w + m - d. \tag{2.51}$$

Then there exists an ideal linear output-feedback controller (2.44) of order n_{c} such that the following statements hold:

(i) *For all initial conditions* $\phi_{**}(0)$ *and* $x_w(0)$ *and all integers* $k \geq k_0$*, where*

$$k_0 \triangleq n_{\mathrm{o}} + n_{\mathrm{c}} + d - m, \tag{2.52}$$

it follows that $y_*(k) = 0$*.*

(ii) $\tilde{\mathcal{A}}_*$ *is asymptotically stable.*

(iii) *For* $i = 1, 2, 3, \ldots,$

$$\mathcal{C}\tilde{\mathcal{A}}_*^{i-1}\mathcal{B} = \begin{cases} H_d, & i = d, \\ 0, & i \neq d. \end{cases} \tag{2.53}$$

Proof. We show that a time-series representation of the fixed-gain controller (2.34), (2.35), (2.42), and (2.43) depicted in Figure 2.1 exists and satisfies *(i)-(iii)*.

First, consider the cascade (2.38), (2.39), and recall that (2.40) is controllable but not observable. Furthermore, the unobservable modes of (2.41) are precisely the poles of $\hat{G}_{\mathrm{pc}}(z)$, all of which are asymptotically stable because of assumption (A2). Therefore, it follows from the Kalman decomposition that there exists a nonsingular matrix $T \in \mathbb{R}^{(n+\hat{n}_{\mathrm{pc}})\times(n+\hat{n}_{\mathrm{pc}})}$ such that

$$\begin{bmatrix} A_{\mathrm{o}} & 0 \\ A_{21} & A_{\bar{\mathrm{o}}} \end{bmatrix} = T \begin{bmatrix} A & B\hat{C}_{\mathrm{pc}} \\ 0 & \hat{A}_{\mathrm{pc}} \end{bmatrix} T^{-1}, \tag{2.54}$$

$$\begin{bmatrix} C_{\mathrm{o}} & 0 \end{bmatrix} = \begin{bmatrix} C & 0 \end{bmatrix} T^{-1}, \tag{2.55}$$

where $A_{\mathrm{o}} \in \mathbb{R}^{n_{\mathrm{o}}\times n_{\mathrm{o}}}$, $(A_{\mathrm{o}}, C_{\mathrm{o}})$ is observable, and $A_{\bar{\mathrm{o}}}$ is asymptotically stable.

Now, defining $\begin{bmatrix} x_{\mathrm{o}}(k) \\ x_{\bar{\mathrm{o}}}(k) \end{bmatrix} \triangleq T \begin{bmatrix} x(k) \\ \hat{x}_{\mathrm{pc}}(k) \end{bmatrix}$, where $x_{\mathrm{o}}(k) \in \mathbb{R}^{n_{\mathrm{o}}}$, and applying this

change of basis to the cascade (2.38) and (2.39) yields

$$\begin{bmatrix} x_{\mathrm{o}}(k+1) \\ x_{\bar{\mathrm{o}}}(k+1) \end{bmatrix} = \begin{bmatrix} A_{\mathrm{o}} & 0 \\ A_{21} & A_{\bar{\mathrm{o}}} \end{bmatrix} \begin{bmatrix} x_{\mathrm{o}}(k) \\ x_{\bar{\mathrm{o}}}(k) \end{bmatrix} + \begin{bmatrix} B_{\mathrm{o}} \\ B_{\bar{\mathrm{o}}} \end{bmatrix} u_{\mathrm{db}}(k) + \begin{bmatrix} B_{e,\mathrm{o}} \\ B_{e,\bar{\mathrm{o}}} \end{bmatrix} e(k) + \begin{bmatrix} D_{1,\mathrm{o}} \\ D_{1,\bar{\mathrm{o}}} \end{bmatrix} w(k), \tag{2.56}$$

$$y_*(k) = \begin{bmatrix} C_{\mathrm{o}} & 0 \end{bmatrix} \begin{bmatrix} x_{\mathrm{o}}(k) \\ x_{\bar{\mathrm{o}}}(k) \end{bmatrix} + D_2 w(k), \tag{2.57}$$

where $x_{\mathrm{o}} \in \mathbb{R}^{n_{\mathrm{o}}}$ and

$$\begin{bmatrix} B_{\mathrm{o}} \\ B_{\bar{\mathrm{o}}} \end{bmatrix} = T \begin{bmatrix} B \\ \hat{B}_{\mathrm{pc}} \end{bmatrix}, \quad \begin{bmatrix} B_{e,\mathrm{o}} \\ B_{e,\bar{\mathrm{o}}} \end{bmatrix} = T \begin{bmatrix} B \\ 0 \end{bmatrix}, \quad \begin{bmatrix} D_{1,\mathrm{o}} \\ D_{1,\bar{\mathrm{o}}} \end{bmatrix} = T \begin{bmatrix} D_1 \\ 0 \end{bmatrix}. \tag{2.58}$$

Note that $(A_{\mathrm{o}}, B_{\mathrm{o}}, C_{\mathrm{o}})$ is a minimal realization of the transfer function matrix

$$\begin{aligned} G_{\mathrm{o}}(z) &\stackrel{\triangle}{=} C_{\mathrm{o}}[zI - A_{\mathrm{o}}]^{-1} B_{\mathrm{o}} = G_{yu}(z)\hat{G}_{\mathrm{pc}}(z) \\ &= \alpha(z)^{-1} z^{m-d} H_d. \end{aligned} \tag{2.59}$$

Next, we consider a deadbeat internal model controller of the form (2.42), (2.43) designed for the observable subsystem of (2.56), (2.57) given by

$$x_{\mathrm{o}}(k+1) = A_{\mathrm{o}} x_{\mathrm{o}}(k) + B_{\mathrm{o}} u_{\mathrm{db}}(k) + B_{e,\mathrm{o}} e(k) + D_{1,\mathrm{o}} w(k), \tag{2.60}$$

$$y_*(k) = C_{\mathrm{o}} x_{\mathrm{o}}(k) + D_2 w(k). \tag{2.61}$$

The invariant zeros of $(A_{\mathrm{o}}, B_{\mathrm{o}}, C_{\mathrm{o}})$ are located at the origin and thus do not coincide with the eigenvalues of A_w by assumption (A8). Since, in addition, $(A_{\mathrm{o}}, B_{\mathrm{o}}, C_{\mathrm{o}})$ is minimal, the dimension of y equals the dimension of u, and normal rank $G_{\mathrm{o}} = l$,

it follows from Theorem 2.9.1 with $\hat{n} = n_{\mathrm{o}}$, $\hat{n}_w = n_w$, and $\hat{l}_y = l$ that, for all $\hat{n}_{\mathrm{db}}$ satisfying

$$\hat{n}_{\mathrm{db}} \geq n_{\mathrm{o}} + 2ln_w, \tag{2.62}$$

there exists a discrete-time controller (2.42), (2.43) such that the dynamics matrix

$$\tilde{\mathcal{A}}_{\mathrm{dbo}} \triangleq \begin{bmatrix} A_{\mathrm{o}} & B_{\mathrm{o}}\hat{C}_{\mathrm{db}} \\ \hat{B}_{\mathrm{db}}C_{\mathrm{o}} & \hat{A}_{\mathrm{db}} \end{bmatrix}, \tag{2.63}$$

of the closed-loop system (2.42), (2.43), (2.60), and (2.61), which represents the feedback interconnection of G_{o} and $\hat{G}_{\mathrm{db}}$, is nilpotent. Furthermore, with $e(k) \equiv 0$, for all initial conditions $(x_{\mathrm{o}}(0), x_{\bar{\mathrm{o}}}(0), \hat{x}_{\mathrm{db}}(0), x_w(0))$ and all integers $k \geq n_{\mathrm{o}} + \hat{n}_{\mathrm{db}}$, it follows that $y_*(k) = 0$.

The closed-loop system (2.42), (2.43), (2.56), and (2.57) is

$$\begin{aligned} \begin{bmatrix} x_{\mathrm{o}}(k+1) \\ \hat{x}_{\mathrm{db}}(k+1) \\ x_{\bar{\mathrm{o}}}(k+1) \end{bmatrix} &= \begin{bmatrix} A_{\mathrm{o}} & B_{\mathrm{o}}\hat{C}_{\mathrm{db}} & 0 \\ \hat{B}_{\mathrm{db}}C_{\mathrm{o}} & \hat{A}_{\mathrm{db}} & 0 \\ A_{21} & B_{\bar{\mathrm{o}}}\hat{C}_{\mathrm{db}} & A_{\bar{\mathrm{o}}} \end{bmatrix} \begin{bmatrix} x_{\mathrm{o}}(k) \\ \hat{x}_{\mathrm{db}}(k) \\ x_{\bar{\mathrm{o}}}(k) \end{bmatrix} \\ &\quad + \begin{bmatrix} B_{e,\mathrm{o}} \\ 0 \\ B_{e,\bar{\mathrm{o}}} \end{bmatrix} e(k) + \begin{bmatrix} D_{1,\mathrm{o}} \\ \hat{B}_{\mathrm{db}}D_2 \\ D_{1,\bar{\mathrm{o}}} \end{bmatrix} w(k), \end{aligned} \tag{2.64}$$

$$y_*(k) = \begin{bmatrix} C_{\mathrm{o}} & 0 & 0 \end{bmatrix} \begin{bmatrix} x_{\mathrm{o}}(k) \\ \hat{x}_{\mathrm{db}}(k) \\ x_{\bar{\mathrm{o}}}(k) \end{bmatrix} + D_2 w(k). \tag{2.65}$$

Since $\tilde{\mathcal{A}}_{\mathrm{dbo}}$ is nilpotent and $A_{\bar{\mathrm{o}}}$ is asymptotically stable, it follows that

$$\begin{bmatrix} A_{\mathrm{o}} & B_{\mathrm{o}}\hat{C}_{\mathrm{db}} & 0 \\ \hat{B}_{\mathrm{db}}C_{\mathrm{o}} & \hat{A}_{\mathrm{db}} & 0 \\ A_{21} & B_{\bar{\mathrm{o}}}\hat{C}_{\mathrm{db}} & A_{\bar{\mathrm{o}}} \end{bmatrix} \tag{2.66}$$

is asymptotically stable.

To construct the ideal fixed gain controller, we first write the transfer function matrix of (2.42), (2.43) as

$$\hat{G}_{\mathrm{db}}(z) = \hat{M}(z)^{-1}\hat{N}(z), \tag{2.67}$$

where

$$\hat{M}(z) = z^{\hat{n}_{\mathrm{db}}}I_l + z^{\hat{n}_{\mathrm{db}}-1}\hat{M}_1 + \cdots + z\hat{M}_{\hat{n}_{\mathrm{db}}-1} + \hat{M}_{\hat{n}_{\mathrm{db}}}, \tag{2.68}$$

$$\hat{N}(z) = z^{\hat{n}_{\mathrm{db}}-1}\hat{N}_1 + z^{\hat{n}_{\mathrm{db}}-2}\hat{N}_2 + \cdots + z\hat{N}_{\hat{n}_{\mathrm{db}}-1} + \hat{N}_{\hat{n}_{\mathrm{db}}}, \tag{2.69}$$

where, for $i = 1, \ldots, \hat{n}_{\mathrm{db}}$, $\hat{M}_i \in \mathbb{R}^{l\times l}$ and $\hat{N}_i \in \mathbb{R}^{l\times l}$. Therefore, (2.42), (2.43) has the time-series representation

$$u_{\mathrm{db}}(k) = -\sum_{i=1}^{\hat{n}_{\mathrm{db}}} \hat{M}_i u_{\mathrm{db}}(k-i) + \sum_{i=1}^{\hat{n}_{\mathrm{db}}} \hat{N}_i y_*(k-i). \tag{2.70}$$

Now, let $\hat{n}_{\mathrm{db}} = n_{\mathrm{c}} + d - m$, and note that, since (2.51) holds, $\hat{n}_{\mathrm{db}} = n_{\mathrm{c}} + d - m \geq n_{\mathrm{o}} + 2ln_w$, as required by (2.62). With $e(k) \equiv 0$, and thus $u(k) = u_*(k)$ for all $k \geq k_0$, the ideal fixed-gain controller, which consists of the precompensator (2.33) and the deadbeat internal model controller (2.70), is given by (2.44), where, for

$i = 1, 2, \ldots, n_{\mathrm{c}}$,

$$M_{*i} \triangleq -H_d^{-1}\beta_{d+i} - \sum_{j=1}^{i} \hat{M}_j H_d^{-1}\beta_{d+i-j}, \tag{2.71}$$

$$N_{*i} \triangleq \hat{N}_i, \tag{2.72}$$

where, for all $i > m$, $\beta_i = 0$, and, for all $i > \hat{n}_{\mathrm{db}}$, $\hat{M}_i = \hat{N}_i = 0$.

To show *(i)*, consider the $2ln_{\mathrm{c}}$-order nonminimal state-space realization of the controller (2.45), (2.71), and (2.72) given by

$$\phi_{**}(k+1) = \mathcal{A}_{\mathrm{c}}\phi_{**}(k) + \mathcal{B}_{\mathrm{c}}y_*(k), \tag{2.73}$$

$$u_*(k) = \mathcal{C}_{\mathrm{c}}\phi_{**}(k), \tag{2.74}$$

where

$$\mathcal{A}_{\mathrm{c}} \triangleq \mathcal{A}_{\mathrm{nil}} + \left[\begin{array}{c} 0_{ln_{\mathrm{c}}\times 2ln_{\mathrm{c}}} \\ E_1\theta_* \end{array}\right], \quad \mathcal{B}_{\mathrm{c}} \triangleq \left[\begin{array}{c} E_1 \\ 0_{ln_{\mathrm{c}}\times l} \end{array}\right], \quad \mathcal{C}_{\mathrm{c}} \triangleq \theta_*. \tag{2.75}$$

Note that $\mathcal{A}_{\mathrm{c}} = \mathcal{A} + \mathcal{B}\mathcal{C}_{\mathrm{c}} - \mathcal{B}_{\mathrm{c}}\mathcal{C}$. Therefore, the ideal closed-loop system (2.20)-(2.25) and (2.73)-(2.75) is

$$\left[\begin{array}{c} \phi_*(k+1) \\ \phi_{**}(k+1) \end{array}\right] = \left[\begin{array}{cc} \mathcal{A} & \mathcal{B}\mathcal{C}_{\mathrm{c}} \\ \mathcal{B}_{\mathrm{c}}\mathcal{C} & \mathcal{A}_{\mathrm{c}} \end{array}\right] \left[\begin{array}{c} \phi_*(k) \\ \phi_{**}(k) \end{array}\right] + \left[\begin{array}{c} \mathcal{B} \\ 0 \end{array}\right] e(k) + \left[\begin{array}{c} \mathcal{D}_1 \\ \mathcal{B}_{\mathrm{c}}\mathcal{D}_2 \end{array}\right] W(k), \tag{2.76}$$

$$y_*(k) = \left[\begin{array}{cc} \mathcal{C} & 0 \end{array}\right] \left[\begin{array}{c} \phi_*(k) \\ \phi_{**}(k) \end{array}\right] + \mathcal{D}_2 W(k), \tag{2.77}$$

where

$$\phi_*(k) \triangleq \begin{bmatrix} y_*(k-1) \\ \vdots \\ y_*(k-n_{\rm c}) \\ u(k-1) \\ \vdots \\ u(k-n_{\rm c}) \end{bmatrix}. \tag{2.78}$$

The closed-loop system (2.76) and (2.77) is a nonminimal representation of the closed-loop system (2.64) and (2.65). Furthermore, every unobservable or uncontrollable mode of (2.76) and (2.77) is located at zero. Thus, the spectrum of

$$\tilde{\mathcal{A}}_{\rm cl} \triangleq \begin{bmatrix} \mathcal{A} & \mathcal{B}\mathcal{C}_{\rm c} \\ \mathcal{B}_{\rm c}\mathcal{C} & \mathcal{A}_{\rm c} \end{bmatrix} \tag{2.79}$$

consists of the eigenvalues of (2.66) as well as $4ln_{\rm c} - n - \hat{n}_{\rm pc} - \hat{n}_{\rm db}$ eigenvalues located at 0. Therefore, since (2.66) is asymptotically stable, it follows that (2.79) is asymptotically stable. Furthermore, since (2.76), (2.77) is a nonminimal representation of (2.64), (2.65), it follows that, with $e(k) \equiv 0$, for all initial conditions $\phi_{**}(0)$ and $x_w(0)$ and all $k \geq n_{\rm o} + \hat{n}_{\rm db} = k_0$, it follows that $y_*(k) = 0$. Thus, we have verified *(i)*.

To show *(ii)*, consider the change of basis

$$\begin{bmatrix} \tilde{\mathcal{A}}_* & \mathcal{B}\mathcal{C}_{\rm c} \\ 0 & \mathcal{A}_{\rm nil} \end{bmatrix} = \begin{bmatrix} I & 0 \\ -I & I \end{bmatrix} \begin{bmatrix} \mathcal{A} & \mathcal{B}\mathcal{C}_{\rm c} \\ \mathcal{B}_{\rm c}\mathcal{C} & \mathcal{A}_{\rm c} \end{bmatrix} \begin{bmatrix} I & 0 \\ I & I \end{bmatrix}, \tag{2.80}$$

$$\begin{bmatrix} \mathcal{B} \\ -\mathcal{B} \end{bmatrix} = \begin{bmatrix} I & 0 \\ -I & I \end{bmatrix} \begin{bmatrix} \mathcal{B} \\ 0 \end{bmatrix}, \tag{2.81}$$

$$\begin{bmatrix} \mathcal{C} & 0 \end{bmatrix} = \begin{bmatrix} \mathcal{C} & 0 \end{bmatrix} \begin{bmatrix} I & 0 \\ I & I \end{bmatrix}. \tag{2.82}$$

Since (2.79) is asymptotically stable and $\mathcal{A}_{\rm nil}$ is nilpotent, it follows from (2.80) that $\tilde{\mathcal{A}}_*$ is asymptotically stable, verifying *(ii)*.

To show *(iii)*, we compute the closed-loop Markov parameters $\tilde{H}_{y_*e,i}$ from the pseudo-input e to the performance variable y_* using a state-space realization of the closed-loop system and a transfer function matrix representation of the closed-loop system. First, consider the nonminimal state-space realization (2.76) and (2.77). For $i = 1, 2, \ldots$, define the Markov parameters

$$\begin{aligned} \tilde{H}_{y_*e,i} &\triangleq \begin{bmatrix} \mathcal{C} & 0 \end{bmatrix} \begin{bmatrix} \mathcal{A} & \mathcal{B}\mathcal{C}_{\rm c} \\ \mathcal{B}_{\rm c}\mathcal{C} & \mathcal{A}_{\rm c} \end{bmatrix}^{i-1} \begin{bmatrix} \mathcal{B} \\ 0 \end{bmatrix} \\ &= \begin{bmatrix} \mathcal{C} & 0 \end{bmatrix} \begin{bmatrix} \tilde{\mathcal{A}}_* & \mathcal{B}\mathcal{C}_{\rm c} \\ 0 & \mathcal{A}_{\rm nil} \end{bmatrix}^{i-1} \begin{bmatrix} \mathcal{B} \\ -\mathcal{B} \end{bmatrix} \\ &= \mathcal{C}\tilde{\mathcal{A}}_*^{i-1}\mathcal{B} + \sum_{j=1}^{i-1} -\mathcal{C}\tilde{\mathcal{A}}_*^{j-1}\mathcal{B}M_{*i-j}, \end{aligned} \tag{2.83}$$

where $M_{*i} = \mathcal{C}_{\rm c}\mathcal{A}_{\rm nil}^{i-1}\mathcal{B}$ for $i = 1, 2, \ldots, n_{\rm c}$ and $M_{*i} = 0$ for all $i > n_{\rm c}$.

Next, consider the transfer function matrix representation of the open-loop system

$$\begin{aligned} y_* &= G_{yu}(z)u + G_{yw}(z)w \\ &= G_{yu}(z)u_* + G_{yu}(z)e + G_{yw}(z)w \\ &= G_{yu}(z)\hat{G}_{\rm pc}(z)\hat{G}_{\rm db}(z)y_* + G_{yu}(z)e + G_{yw}(z)w, \end{aligned} \tag{2.84}$$

which implies that the closed-loop system is

$$y_* = \tilde{G}_{ye}e + \tilde{G}_{yw}w, \tag{2.85}$$

where

$$\begin{aligned} \tilde{G}_{ye} &\triangleq [I_l - G_{yu}(z)\hat{G}_{\rm pc}(z)\hat{G}_{\rm db}(z)]^{-1}G_{yu}(z) \\ &= [I_l - \alpha(z)^{-1}z^{m-d}H_d\hat{M}(z)^{-1}\hat{N}(z)]^{-1}\alpha(z)^{-1}\beta(z) \\ &= [\alpha(z) - z^{m-d}H_d\hat{M}(z)^{-1}\hat{N}(z)]^{-1}\beta(z) \\ &= \tilde{D}(z)^{-1}\hat{M}(z)H_d^{-1}\beta(z), \end{aligned} \tag{2.86}$$

$$\begin{aligned} \tilde{G}_{yw} &\triangleq [I_l - G_{yu}(z)\hat{G}_{\rm pc}(z)\hat{G}_{\rm db}(z)]^{-1}G_{yw}(z) \\ &= \tilde{D}(z)^{-1}\hat{M}(z)H_d^{-1}\gamma(z), \end{aligned} \tag{2.87}$$

and $\tilde{D}(z) \triangleq \hat{M}(z)H_d^{-1}\alpha(z) - z^{m-d}\hat{N}(z)$. Notice that $\tilde{D}(z)$ can be written as

$$\tilde{D}(z) = z^{m+\hat{n}_{\rm db}}H_d^{-1} + z^{m+\hat{n}_{\rm db}-1}\tilde{D}_1 + \cdots + \tilde{D}_{m+\hat{n}_{\rm db}}, \tag{2.88}$$

where, for $i = 1, 2, \ldots, m + \hat{n}_{\rm db}$, $\tilde{D}_i \in \mathbb{R}^{l\times l}$. Since (2.63) is nilpotent, it follows that the poles of $\tilde{G}_{ye}$ and $\tilde{G}_{yw}$ are located at zero; in particular, $\det \tilde{D}(z) = z^{l(m+\hat{n}_{\rm db})}\det H_d^{-1}$. In fact, it follows from (2.88) that the coefficients of the deadbeat

controller $\hat{M}(z)^{-1}\hat{N}(z)$ can be chosen so that $\tilde{D}_1 = \cdots = \tilde{D}_{m+\hat{n}_{\rm db}} = 0$, and thus

$$\tilde{G}_{ye}(z) = \left[z^{m+\hat{n}_{\rm db}} H_d^{-1}\right]^{-1} \tilde{N}(z) = z^{-m-\hat{n}_{\rm db}} H_d \tilde{N}(z), \tag{2.89}$$

where

$$\tilde{N}(z) \stackrel{\triangle}{=} \hat{M}(z) H_d^{-1} \beta(z) = z^{m+\hat{n}_{\rm db}} \tilde{N}_0 + \cdots + N_{m+\hat{n}_{\rm db}} \tag{2.90}$$

and

$$\tilde{N}_i = \begin{cases} 0, & 0 \le i < d, \\ I_l, & i = d, \\ H_d^{-1}\beta_i + \sum_{j=1}^{i-d} \hat{M}_j H_d^{-1} \beta_{i-j}, & d < i \le m + \hat{n}_{\rm db}. \end{cases} \tag{2.91}$$

Therefore, it follows from (2.71) that

$$\tilde{N}_i = \begin{cases} 0, & 0 \le i < d, \\ I_l, & i = d, \\ -M_{*i-d}, & d < i \le m + \hat{n}_{\rm db}. \end{cases} \tag{2.92}$$

It follows from (2.89) that the closed-loop Markov parameters $\tilde{H}_{y_* e,i}$ from the pseudo-input e to the performance variable y_* are $\tilde{H}_{y_* e,i} = H_d \tilde{N}_i$ for $i = 1, 2, \ldots, m + \hat{n}_{\rm db}$ and $\tilde{H}_{y_* e,i} = 0$ for $i > m + \hat{n}_{\rm db}$, which implies

$$\tilde{H}_{y_* e,i} = \begin{cases} 0, & 0 \le i < d, \\ H_d, & i = d, \\ -H_d M_{*i-d}, & d < i \le m + \hat{n}_{\rm db}, \\ 0, & i > m + \hat{n}_{\rm db}. \end{cases} \tag{2.93}$$

Then property *(iii)* follows from comparing the expressions for $\tilde{H}_{y_* e,i}$ given by (2.83)

and (2.93). More specifically, since (2.93) implies that $\tilde{H}_{y_*e,1} = \cdots = \tilde{H}_{y_*e,d-1} = 0$, it follows from (2.83) that $\mathcal{C}\mathcal{B} = \mathcal{C}\tilde{\mathcal{A}}_*\mathcal{B} = \cdots = \mathcal{C}\tilde{\mathcal{A}}_*^{d-2}\mathcal{B} = 0$. Next, since $\mathcal{C}\mathcal{B} = \mathcal{C}\tilde{\mathcal{A}}_*\mathcal{B} = \cdots = \mathcal{C}\tilde{\mathcal{A}}_*^{d-2}\mathcal{B} = 0$ and $\tilde{H}_{y_*e,d} = H_d$ (using (2.93)), it follows from (2.83) that $\mathcal{C}\tilde{\mathcal{A}}_*^{d-1}\mathcal{B} = H_d$. Now, since $\mathcal{C}\mathcal{B} = \mathcal{C}\tilde{\mathcal{A}}_*\mathcal{B} = \cdots = \mathcal{C}\tilde{\mathcal{A}}_*^{d-2}\mathcal{B} = 0$, $\mathcal{C}\tilde{\mathcal{A}}_*^{d-1}\mathcal{B} = H_d$, and $\tilde{H}_{y_*e,d+1} = -H_dM_{*1}$ (using (2.93)), it follows from (2.83) that $\mathcal{C}\tilde{\mathcal{A}}_*^{d}\mathcal{B} = 0$. Lastly, since $\mathcal{C}\mathcal{B} = \mathcal{C}\tilde{\mathcal{A}}_*\mathcal{B} = \cdots = \mathcal{C}\tilde{\mathcal{A}}_*^{d-2}\mathcal{B} = 0$, $\mathcal{C}\tilde{\mathcal{A}}_*^{d-1}\mathcal{B} = H_d$, $\mathcal{C}\tilde{\mathcal{A}}_*^{d}\mathcal{B} = 0$, and $\tilde{H}_{y_*e,d+2} = -H_dM_{*2}$ (using (2.93)), it follows from (2.83) that $\mathcal{C}\tilde{\mathcal{A}}_*^{d+1}\mathcal{B} = 0$. Continuing this analysis yields $\mathcal{C}\mathcal{B} = \mathcal{C}\tilde{\mathcal{A}}_*\mathcal{B} = \cdots = \mathcal{C}\tilde{\mathcal{A}}_*^{d-2}\mathcal{B} = 0$, $\mathcal{C}\tilde{\mathcal{A}}_*^{d-1}\mathcal{B} = H_d$, and $\mathcal{C}\tilde{\mathcal{A}}_*^{d}\mathcal{B} = \mathcal{C}\tilde{\mathcal{A}}_*^{d+1}\mathcal{B} = \cdots = 0$. □

2.5 Error System

We now construct an error system using the ideal fixed-gain controller and a controller whose gains are updated by an adaptive law. By assumption (A11), the controller order n_c given by (2.51) is unknown. However, since $m \leq n$ and $n_o \leq lm$, it follows that $n_o + m + 2ln_w - d \leq (l+1)\bar{n} + 2l\bar{n}_w - d$. Therefore, if

$$n_c \geq (l+1)\bar{n} + 2l\bar{n}_w - d, \tag{2.94}$$

then n_c satisfies (2.51). Assumptions (A3), (A6), and (A9) imply that the lower bound on n_c given by (2.94) is known.

The closed-loop system consisting of (2.20)-(2.25) with the ideal feedback (2.45) is

$$\phi_{**}(k+1) = \tilde{\mathcal{A}}_*\phi_{**}(k) + \mathcal{D}_1W(k), \tag{2.95}$$

$$y_*(k) = \mathcal{C}\phi_{**}(k) + \mathcal{D}_2W(k), \tag{2.96}$$

where, by *(ii)* of Theorem 2.4.1, $\tilde{\mathcal{A}}_*$ is asymptotically stable.

Next, consider the controller

$$u(k) = \sum_{i=1}^{n_c} M_i(k)u(k-i) + \sum_{i=1}^{n_c} N_i(k)y(k-i), \tag{2.97}$$

where, for all $i = 1, \ldots, n_c$, $M_i : \mathbb{N} \to \mathbb{R}^{l\times l}$ and $N_i : \mathbb{N} \to \mathbb{R}^{l\times l}$ are given by the adaptive law presented in the following section. The control can be expressed as

$$u(k) = \theta(k)\phi(k), \tag{2.98}$$

where

$$\theta(k) \triangleq \left[\begin{array}{cccccc} N_1(k) & \cdots & N_{n_c}(k) & M_1(k) & \cdots & M_{n_c}(k) \end{array} \right]. \tag{2.99}$$

Inserting (2.98) into (2.20) yields

$$\phi(k+1) = \mathcal{A}\phi(k) + \mathcal{B}\theta(k)\phi(k) + \mathcal{D}_1 W(k). \tag{2.100}$$

Next, defining

$$\tilde{\theta}(k) \triangleq \theta(k) - \theta_*, \tag{2.101}$$

and substituting $\theta(k) = \tilde{\theta}(k) + \theta_*$ into (2.100), the closed-loop system consisting of (2.20), (2.21) with the time-varying feedback (2.98) becomes

$$\phi(k+1) = \tilde{\mathcal{A}}_*\phi(k) + \mathcal{B}\tilde{\theta}(k)\phi(k) + \mathcal{D}_1 W(k), \tag{2.102}$$

$$y(k) = \mathcal{C}\phi(k) + \mathcal{D}_2 W(k). \tag{2.103}$$

Now, we construct an error system by combining the ideal closed-loop system

(2.95), (2.96) with the closed-loop system (2.102), (2.103). Define the error state

$$\tilde{\phi}(k) \triangleq \phi(k) - \phi_{**}(k), \tag{2.104}$$

and subtract (2.95), (2.96) from (2.102), (2.103) to obtain

$$\tilde{\phi}(k+1) = \tilde{\mathcal{A}}_*\tilde{\phi}(k) + \mathcal{B}\tilde{\theta}(k)\phi(k), \tag{2.105}$$

$$\tilde{y}(k) = \mathcal{C}\tilde{\phi}(k), \tag{2.106}$$

where

$$\tilde{y}(k) \triangleq y(k) - y_*(k). \tag{2.107}$$

Note that the Markov parameters of the error system (2.105), (2.106) are given by *(iii)* of Theorem 2.4.1.

The following proposition shows that $y(k)$ is linear in the estimation error $\tilde{\theta}(k)$. This proposition is essential for developing the adaptive law and analyzing the stability of the error system.

Proposition 2.5.1. *Consider the error system (2.105) and (2.106). For all $k \geq k_0$,*

$$\tilde{y}(k) = y(k) = H_d\tilde{\theta}(k-d)\phi(k-d). \tag{2.108}$$

Proof. Substituting (2.105) into (2.106) yields

$$\tilde{y}(k) = \sum_{i=1}^{k} \mathcal{C}\tilde{\mathcal{A}}_*^{i-1}\mathcal{B}\tilde{\theta}(k-i)\phi(k-i). \tag{2.109}$$

It now follows from *(iii)* of Theorem 2.4.1 and (2.109) that $\tilde{y}(k) = H_d\tilde{\theta}(k-d)\phi(k-d)$. Furthermore, it follows from *(i)* of Theorem 2.4.1 that, for all $k \geq k_0$, $y_*(k) = 0$, that

is, $\tilde{y}(k) = y(k)$. Hence, for all $k \geq k_0$, (2.108) holds. $\square$

2.6 Adaptive Controller and Stability Analysis

We now present the adaptive law for the controller (2.98), (2.99) and analyze the properties of the closed-loop error system. Consider the cost function

$$\mathcal{J}(k) \triangleq \frac{1}{2}\tilde{y}^{\mathrm{T}}(k)\tilde{y}(k). \tag{2.110}$$

Substituting (2.108) into (2.110), the gradient of $\mathcal{J}(k)$ with respect to $\tilde{\theta}(k-d)$ is given by

$$\frac{\partial \mathcal{J}(k)}{\partial \tilde{\theta}(k-d)} = H_d^{\mathrm{T}} y(k) \phi^{\mathrm{T}}(k-d). \tag{2.111}$$

Since, by assumption (A11), H_d is unknown, we replace H_d in (2.111) with $\bar{H}_d$, and, in place of (2.111), we use the implementable gradient

$$G(k) \triangleq \bar{H}_d^{\mathrm{T}} y(k) \phi^{\mathrm{T}}(k-d). \tag{2.112}$$

Note that the implementable gradient (2.112) can be used in practice due to assumptions (A3), (A5), and (A7).

Now, consider the adaptive law

$$\theta(k+1) = \theta(k-d) - \eta(k) G(k), \tag{2.113}$$

where $\eta : \mathbb{N} \to [0, \infty)$ is a step-size function. Note that if $G(k) = 0$ then $\eta(k)$ is irrelevant. In accordance with assumptions (A10) and (A11), the adaptive control law (2.113) does not require a measurement of the exogenous signal $w(k)$ and does not use knowledge of the exogenous dynamics (2.4), (2.5).

Subtracting θ_* from both sides of (2.113) yields the estimator-error update equation

$$\tilde{\theta}(k+1) = \tilde{\theta}(k-d) - \eta(k)G(k). \tag{2.114}$$

The closed-loop error system is thus given by

$$Y(k+1) = \mathcal{A}_Y Y(k) + \mathcal{B}_Y y(k), \tag{2.115}$$

$$\tilde{\theta}(k+1) = \tilde{\theta}(k-d) - \eta(k)G(k), \tag{2.116}$$

$$\vdots$$

$$\tilde{\theta}(k-d+1) = \tilde{\theta}(k-2d) - \eta(k-d)G(k-d), \tag{2.117}$$

where

$$\mathcal{A}_Y \triangleq \mathcal{N}_{l(n_c+d)}, \qquad \mathcal{B}_Y \triangleq \begin{bmatrix} I_l \\ 0_{l(n_c+d-1)\times l} \end{bmatrix}, \qquad Y(k) \triangleq \begin{bmatrix} y(k-1) \\ \vdots \\ y(k-n_c-d) \end{bmatrix}. \tag{2.118}$$

Theorem 2.6.1. *Consider the open-loop system (2.1), (2.2) satisfying assumptions (A1)-(A11) and the adaptive feedback controller (2.94), (2.98), (2.99), (2.108), and (2.113). Furthermore, for all $k \geq k_0$, let $\zeta(k) \in \mathbb{R}$ be such that*

$$0 < \zeta_{\mathrm{l}} \triangleq \inf_{j \geq k_0} \zeta(j) \leq \zeta(k) \leq \zeta_{\mathrm{u}} \triangleq \sup_{j \geq k_0} \zeta(j) < 2. \tag{2.119}$$

Finally, for all $k \in \mathbb{N}$ such that $G(k) \neq 0$, let $\eta(k) \in [0, \infty)$ satisfy

$$\eta(k) = 0, \quad \textit{if} \quad k < k_0, \tag{2.120}$$

$$\eta(k) = \zeta(k)\eta_{\mathrm{opt}}(k), \quad \textit{if} \quad k \geq k_0, \tag{2.121}$$

where

$$\eta_{\mathrm{opt}}(k) \triangleq \frac{\|y(k)\|_2^2}{\|G(k)\|_{\mathrm{F}}^2}. \tag{2.122}$$

Then, for all initial conditions $x(0)$ and $\theta(0)$, $\theta(k)$ is bounded, $u(k)$ is bounded, $\lim_{k\to\infty} y(k) = 0$, and $x(k)$ satisfying (2.1) is bounded. If, in addition, the open-loop dynamics matrix A is asymptotically stable and $u(k) = 0$ for all $k = 0, \ldots, k_0 - 1$, then, for all $x_w(0)$, the zero solution of the closed-loop error system (2.115)-(2.117) is Lyapunov stable.

Proof. Let $k \geq k_0$ so that, by Proposition 2.5.1, $\tilde{y}(k) = y(k)$. Consider the quadratic function

$$J(Y) \triangleq Y^{\mathrm{T}} \mathcal{P} Y, \tag{2.123}$$

where $\mathcal{P} > 0$ satisfies the discrete-time Lyapunov equation

$$\mathcal{P} = \mathcal{A}_Y^{\mathrm{T}} \mathcal{P} \mathcal{A}_Y + \mathcal{Q} + \alpha I, \tag{2.124}$$

where $\mathcal{Q} > 0$ and $\alpha > 0$. Note that $\mathcal{P}$ exists since $\mathcal{A}_Y$ is asymptotically stable. Defining

$$\Delta J(k) \triangleq J(Y(k+1)) - J(Y(k)), \tag{2.125}$$

it follows from (2.115) that

$$\begin{aligned}
\Delta J(k) &= Y^{\mathrm{T}}(k+1)\mathcal{P}Y(k+1) - Y^{\mathrm{T}}(k)\mathcal{P}Y(k) \\
&= -Y^{\mathrm{T}}(k)\left(\mathcal{Q}+\alpha I\right)Y(k) + Y^{\mathrm{T}}(k)\mathcal{A}_Y^{\mathrm{T}}\mathcal{P}\mathcal{B}_Y y(k) \\
&\quad + y^{\mathrm{T}}(k)\mathcal{B}_Y^{\mathrm{T}}\mathcal{P}\mathcal{A}_Y Y(k) + y^{\mathrm{T}}(k)\mathcal{B}_Y^{\mathrm{T}}\mathcal{P}\mathcal{B}_Y y(k) \\
&\leq -Y^{\mathrm{T}}(k)\left(\mathcal{Q}+\alpha I\right)Y(k) + y^{\mathrm{T}}(k)\mathcal{B}_Y^{\mathrm{T}}\mathcal{P}\mathcal{B}_Y y(k) + \alpha Y^{\mathrm{T}}(k)Y(k) \\
&\quad + \frac{1}{\alpha}y^{\mathrm{T}}(k)\left[\mathcal{B}_Y^{\mathrm{T}}\mathcal{P}\mathcal{A}_Y\mathcal{A}_Y^{\mathrm{T}}\mathcal{P}\mathcal{B}_Y\right]y(k) \\
&\leq -Y^{\mathrm{T}}(k)\mathcal{Q}Y(k) + \sigma_1 y^{\mathrm{T}}(k)y(k), \qquad (2.126)
\end{aligned}$$

where $\sigma_1 \triangleq \lambda_{\max}\left(\mathcal{B}_Y^{\mathrm{T}}\mathcal{P}\mathcal{B}_Y + \frac{1}{\alpha}\mathcal{B}_Y^{\mathrm{T}}\mathcal{P}\mathcal{A}_Y\mathcal{A}_Y^{\mathrm{T}}\mathcal{P}\mathcal{B}_Y\right)$.

Now, consider the positive-definite, radially unbounded Lyapunov-like function

$$\begin{aligned}
V(Y(k),\tilde{\theta}(k),\ldots,\tilde{\theta}(k-d)) &\triangleq \ln\left(1 + a_1 Y^{\mathrm{T}}(k)\mathcal{P}Y(k)\right) + a_2\sum_{i=0}^{d}\|\tilde{\theta}(k-i)\|_{\mathrm{F}}^2 \\
&= \ln\left(1 + a_1 J(Y(k))\right) + a_2\sum_{i=0}^{d}\|\tilde{\theta}(k-i)\|_{\mathrm{F}}^2, \qquad (2.127)
\end{aligned}$$

where $a_1 > 0$ and $a_2 > 0$ are specified below. The Lyapunov-like difference is thus given by

$$\begin{aligned}
\Delta V(k) &\triangleq V(Y(k+1),\tilde{\theta}(k+1),\ldots,\tilde{\theta}(k-d+1)) \\
&\quad - V(Y(k),\tilde{\theta}(k),\ldots,\tilde{\theta}(k-d)). \qquad (2.128)
\end{aligned}$$

Evaluating $\Delta V(k)$ along the trajectories of the closed-loop error system (2.115)-

(2.117) yields

$$\begin{aligned}
\Delta V(k) =& \ln\left[1 + a_1 Y^{\mathrm{T}}(k+1)\mathcal{P}Y(k+1)\right] - \ln\left[1 + a_1 Y^{\mathrm{T}}(k)\mathcal{P}Y(k)\right] \\
&+ a_2\eta^2(k)\|G(k)\|_{\mathrm{F}}^2 - 2a_2\eta(k)\left[\mathrm{tr}\,\left(\tilde{\theta}(k-d)G^{\mathrm{T}}(k)\right)\right] \\
=& \ln\left[1 + a_1 J(Y(k)) + a_1\Delta J(k)\right] - \ln\left[1 + a_1 J(Y(k))\right] + a_2\eta^2(k)\|G(k)\|_{\mathrm{F}}^2 \\
&- 2a_2\eta(k)\left[\mathrm{tr}\,\left(\tilde{\theta}(k-d)\phi(k-d)y^{\mathrm{T}}(k)\bar{H}_d\right)\right] \\
=& \ln\left[1 + a_1 J(Y(k)) + a_1\Delta J(k)\right] - \ln\left[1 + a_1 J(Y(k))\right] + a_2\eta^2(k)\|G(k)\|_{\mathrm{F}}^2 \\
&- a_2\left(2\eta(k)\phi^{\mathrm{T}}(k-d)\tilde{\theta}^{\mathrm{T}}(k-d)H_d^{\mathrm{T}}\bar{H}_d\tilde{\theta}(k-d)\phi(k-d)\right) \\
=& \ln\left[1 + a_1 J(Y(k)) + a_1\Delta J(k)\right] - \ln\left[1 + a_1 J(Y(k))\right] + a_2\eta^2(k)\|G(k)\|_{\mathrm{F}}^2 \\
&- a_2\eta(k)\phi^{\mathrm{T}}(k-d)\tilde{\theta}^{\mathrm{T}}(k-d)\left[H_d^{\mathrm{T}}\bar{H}_d + \bar{H}_d^{\mathrm{T}}H_d\right]\tilde{\theta}(k-d)\phi(k-d).
\end{aligned} \tag{2.129}$$

By assumption (A5) and using (2.108), we have

$$\begin{aligned}
\Delta V(k) \le& \ln\left(1 + \frac{a_1\Delta J(k)}{1 + a_1 J(Y(k))}\right) + a_2\left[-2\eta(k)\phi^{\mathrm{T}}(k-d)\tilde{\theta}^{\mathrm{T}}(k-d)\times\right. \\
&\left. H_d^{\mathrm{T}}H_d\tilde{\theta}(k-d)\phi(k-d) + \eta^2(k)\|G(k)\|_{\mathrm{F}}^2\right] \\
=& \ln\left(1 + \frac{a_1\Delta J(k)}{1 + a_1 J(Y(k))}\right) + a_2\left[-2\eta(k)\|y(k)\|_2^2 + \eta^2(k)\|G(k)\|_{\mathrm{F}}^2\right] \\
=& \ln\left(1 + \frac{a_1\Delta J(k)}{1 + a_1 J(Y(k))}\right) - 2a_2\eta(k)\|y(k)\|_2^2 + a_2\eta^2(k)\frac{\|y(k)\|_2^2}{\eta_{\mathrm{opt}}(k)} \\
=& \ln\left(1 + \frac{a_1\Delta J(k)}{1 + a_1 J(Y(k))}\right) - 2a_2\eta_{\mathrm{opt}}^2(k)\frac{\eta(k)}{\eta_{\mathrm{opt}}(k)}\frac{\|y(k)\|_2^2}{\eta_{\mathrm{opt}}(k)} \\
&+ a_2\eta_{\mathrm{opt}}^2(k)\left(\frac{\eta(k)}{\eta_{\mathrm{opt}}(k)}\right)^2\frac{\|y(k)\|_2^2}{\eta_{\mathrm{opt}}(k)} \\
=& \ln\left(1 + \frac{a_1\Delta J(k)}{1 + a_1 J(Y(k))}\right) - a_2\eta_{\mathrm{opt}}^2(k)\left[2\zeta(k) - \zeta^2(k)\right]\|G(k)\|_{\mathrm{F}}^2 \\
\le& \ln\left(1 + \frac{a_1\Delta J(k)}{1 + a_1 J(Y(k))}\right) - a_2\kappa\eta_{\mathrm{opt}}^2(k)\|G(k)\|_{\mathrm{F}}^2 \\
=& \ln\left(1 + \frac{a_1\Delta J(k)}{1 + a_1 J(Y(k))}\right) - a_2\kappa\frac{\|y(k)\|_2^4}{\|G(k)\|_{\mathrm{F}}^2},
\end{aligned} \tag{2.130}$$

where κ is defined by

$$\begin{aligned}\kappa &\triangleq \inf_{j\geq k_0}\left[2\zeta(j)-\zeta^2(j)\right]\\ &= \min\{2\zeta_{\rm l}-\zeta_{\rm l}^2, 2\zeta_{\rm u}-\zeta_{\rm u}^2\}.\end{aligned} \tag{2.131}$$

Since $0<\zeta_{\rm l}\leq\zeta_{\rm u}<2$, it follows that κ is positive.

Since, for all $x>0$, $\ln x\leq x-1$, using

$$\|G(k)\|_{\rm F}^2\leq\sigma_{\max}^2(\bar{H}_d)\|y(k)\|_2^2\|\phi(k-d)\|_2^2 \tag{2.132}$$

and (2.126) we have

$$\begin{aligned}\Delta V(k) &\leq a_1\frac{\Delta J(k)}{1+a_1J(Y(k))}-a_2\kappa\frac{y^{\rm T}(k)y(k)}{\sigma_{\max}^2(\bar{H}_d)\|\phi(k-d)\|_2^2}\\ &\leq -a_1\frac{Y^{\rm T}(k)\mathcal{Q}Y(k)}{1+a_1Y^{\rm T}(k)\mathcal{P}Y(k)}+a_1\sigma_1\frac{y^{\rm T}(k)y(k)}{1+a_1Y^{\rm T}(k)\mathcal{P}Y(k)}\\ &\quad -a_2\kappa\frac{y^{\rm T}(k)y(k)}{\sigma_{\max}^2(\bar{H}_d)\|\phi(k-d)\|_2^2}.\end{aligned} \tag{2.133}$$

Furthermore, defining

$$U_0(k)\triangleq\begin{bmatrix}u(k-1)\\ \vdots\\ u(k-n_c)\end{bmatrix},\quad Y_0(k)\triangleq\begin{bmatrix}y(k-1)\\ \vdots\\ y(k-n_c)\end{bmatrix}, \tag{2.134}$$

it follows from $\|\phi(k-d)\|_2^2=\|Y_0(k-d)\|_2^2+\|U_0(k-d)\|_2^2$ that

$$\begin{aligned}\Delta V(k) \leq & -a_1\frac{Y^{\rm T}(k)\mathcal{Q}Y(k)}{1+a_1Y^{\rm T}(k)\mathcal{P}Y(k)}+a_1\sigma_1\frac{y^{\rm T}(k)y(k)}{1+a_1\lambda_{\min}(\mathcal{P})\,||Y(k)||_2^2}\\ &-a_2\kappa\frac{y^{\rm T}(k)y(k)}{\sigma_{\max}^2(\bar{H}_d)\left[||Y_0(k-d)||_2^2+||U_0(k-d)||_2^2\right]}.\end{aligned} \tag{2.135}$$

Assumption (A2) implies that the invariant zeros of the system (2.1)-(2.5) from

u to y are asymptotically stable. Thus, it follows from Theorem 2.10.1 with $p = n_{\rm c}$ that there exist $b_1 > 0$ and $b_2 > 0$ such that

$$\begin{aligned}
||U_0(k-d)||_2^2 &\leq b_1 + b_2 \left|\left|\left|\begin{bmatrix} y(k-1) \\ \vdots \\ y(k-n_{\rm c}-1) \end{bmatrix}\right|\right|\right|_2^2 \\
&= b_1 + b_2 \left|\left|\left|\begin{bmatrix} Y_0(k) \\ y(k-n_{\rm c}-1) \end{bmatrix}\right|\right|\right|_2^2 \\
&\leq b_1 + b_2 \left|\left|\left|\begin{bmatrix} Y_0(k) \\ y(k-n_{\rm c}-1) \\ y(k-n_{\rm c}-2) \\ \vdots \\ y(k-n_{\rm c}-d) \end{bmatrix}\right|\right|\right|_2^2 \\
&= b_1 + b_2 \, ||Y(k)||_2^2 . \qquad (2.136)
\end{aligned}$$

Therefore, since $\|Y_0(k-d)\|_2^2 \leq \|Y(k)\|_2^2$, it follows that

$$\begin{aligned}
\Delta V(k) \leq & -a_1 \frac{Y^{\rm T}(k)\mathcal{Q}Y(k)}{1 + a_1 Y^{\rm T}(k)\mathcal{P}Y(k)} + a_1\sigma_1 \frac{y^{\rm T}(k)y(k)}{1 + a_1\lambda_{\min}(\mathcal{P})\,||Y(k)||_2^2} \\
& - a_2\kappa \frac{y^{\rm T}(k)y(k)}{\sigma_{\max}^2(\bar{H}_d)\left[b_1 + ||Y_0(k-d)||_2^2 + b_2\,||Y(k)||_2^2\right]} \\
\leq & -a_1 \frac{Y^{\rm T}(k)\mathcal{Q}Y(k)}{1 + a_1 Y^{\rm T}(k)\mathcal{P}Y(k)} + a_1\sigma_1 \frac{y^{\rm T}(k)y(k)}{1 + a_1\lambda_{\min}(\mathcal{P})\,||Y(k)||_2^2} \\
& - a_2\kappa \frac{y^{\rm T}(k)y(k)}{\sigma_{\max}^2(\bar{H}_d)\left[b_1 + (b_2+1)\,||Y(k)||_2^2\right]} \\
= & -a_1 \frac{Y^{\rm T}(k)\mathcal{Q}Y(k)}{1 + a_1 Y^{\rm T}(k)\mathcal{P}Y(k)} + a_1\sigma_1 \frac{y^{\rm T}(k)y(k)}{1 + a_1\lambda_{\min}(\mathcal{P})\,||Y(k)||_2^2} \\
& - a_2\kappa \frac{b_3 y^{\rm T}(k)y(k)}{1 + b_4\,||Y(k)||_2^2}, \qquad (2.137)
\end{aligned}$$

where $b_3 \triangleq \frac{1}{\sigma_{\max}^2(\bar{H}_d)b_1}$ and $b_4 \triangleq \frac{b_2+1}{b_1}$.

Next, letting $a_1 \triangleq \frac{b_4}{\lambda_{\min}(\mathcal{P})}$ and $a_2 \triangleq \frac{a_1\sigma_1}{b_3\kappa}$, it follows that

$$\Delta V(k) \leq -W(Y(k)), \tag{2.138}$$

where

$$W(Y(k)) \triangleq a_1 \frac{Y^{\mathrm{T}}(k)\mathcal{Q}Y(k)}{1 + a_1 Y^{\mathrm{T}}(k)\mathcal{P}Y(k)}. \tag{2.139}$$

To show that $\tilde{\theta}(k)$ and $Y(k)$ are bounded, summing (2.138) from k_0 to $k-1$, where $k_0 \leq k-1$, yields

$$\begin{aligned} V(Y(k), \tilde{\theta}(k), \ldots, \tilde{\theta}(k-d)) &= V(Y(k_0), \tilde{\theta}(k_0), \ldots, \tilde{\theta}(k_0-d)) + \sum_{j=k_0}^{k-1} \Delta V(j) \\ &\leq V(Y(k_0), \tilde{\theta}(k_0), \ldots, \tilde{\theta}(k_0-d)) - \sum_{j=k_0}^{k-1} W(Y(j)) \\ &\leq V(Y(k_0), \tilde{\theta}(k_0), \ldots, \tilde{\theta}(k_0-d)). \end{aligned} \tag{2.140}$$

Thus, $V(Y(k), \tilde{\theta}(k), \ldots, \tilde{\theta}(k-d))$ is bounded. Since $V(Y(k), \tilde{\theta}(k), \ldots, \tilde{\theta}(k-d))$ is positive definite and radially unbounded, it follows that $\tilde{\theta}(k)$ and $Y(k)$ are bounded. Thus, $\theta(k) = \tilde{\theta}(k) + \theta_*$ is bounded.

Now, we show that $\lim_{k\to\infty} Y(k) = 0$. Since V is positive definite, it follows from (2.138) that

$$\begin{aligned} 0 &\leq \lim_{k\to\infty} \sum_{j=k_0}^{k} W(Y(j)) \\ &\leq -\lim_{k\to\infty} \sum_{j=k_0}^{k} \Delta V(j) \\ &= V(Y(k_0), \tilde{\theta}(k_0), \ldots, \tilde{\theta}(k_0-d)) - \lim_{k\to\infty} V(Y(k), \tilde{\theta}(k), \ldots, \tilde{\theta}(k-d)) \\ &\leq V(Y(k_0), \tilde{\theta}(k_0), \ldots, \tilde{\theta}(k_0-d)), \end{aligned} \tag{2.141}$$

where all three limits exist. Thus, $\lim_{k\to\infty} W(Y(k)) = 0$. Next, note that

$$0 \leq \upsilon(\|Y(k)\|) \leq W(Y(k)), \tag{2.142}$$

where

$$\upsilon(\|Y(k)\|) \stackrel{\triangle}{=} \frac{a_1 \lambda_{\min}(\mathcal{Q}) \|Y(k)\|_2^2}{1 + a_1 \lambda_{\max}(\mathcal{P}) \|Y(k)\|_2^2}. \tag{2.143}$$

Thus $\lim_{k\to\infty} \upsilon(\|Y(k)\|) = 0$. Rewriting (2.143) as

$$\|Y(k)\| = \sqrt{\frac{\upsilon(\|Y(k)\|)}{a_1 \left(\lambda_{\min}(\mathcal{Q}) - \upsilon(\|Y(k)\|)\lambda_{\max}(\mathcal{P})\right)}}, \tag{2.144}$$

it follows that $\lim_{k\to\infty} Y(k) = 0$, and thus $\lim_{k\to\infty} y(k) = 0$. Finally, it follows from (2.136) that $u(k)$ is bounded. Thus, $\phi(k)$ is bounded. Since $\phi(k)$ is the state of the nonminimal state-space realization (2.20)-(2.25) of the time-series representation (2.13) for the original state-space system (2.1), (2.2), it follows that $x(k)$ is bounded.

To prove the last statement of Theorem 2.6.1, let $x_w(0)$ be given and let

$$\mathcal{X}(k) \stackrel{\triangle}{=} \begin{bmatrix} Y(k) \\ \tilde{\theta}(k-d) \\ \vdots \\ \tilde{\theta}(k-2d) \end{bmatrix} \tag{2.145}$$

be the state of the closed-loop error system (2.115)-(2.117). Since V is positive definite and, by (2.138), ΔV is negative semidefinite, it follows from [77, Lemma A.3.12] that the zero solution of the closed-loop error system is Lyapunov stable starting at k_0. Therefore, given $\varepsilon_0 > 0$, there exists $\delta_0 > 0$ such that, if $\|\mathcal{X}(k_0)\| < \delta_0$, then $\|\mathcal{X}(k)\| < \varepsilon_0$ for all $k \geq k_0$.

Now, assume that the open-loop dynamics matrix A is asymptotically stable and

that $u(k) = 0$ for all $k < k_0$. Then, it follows that there exists $\delta_1 > 0$ such that, if $\|\mathcal{X}(0)\| < \delta_1$, then $\|\mathcal{X}(k)\| < \delta_0$ for all $k = 0, \ldots, k_0 - 1$. Consequently, for all $\varepsilon_0 > 0$, there exists $\delta_1 > 0$ such that, if $\|\mathcal{X}(0)\| < \delta_1$, then $\|\mathcal{X}(k)\| < \varepsilon_0$ for all $k \geq 0$. Therefore, the zero solution of the closed-loop error system (2.115)-(2.117) is Lyapunov stable starting at $k = 0$. □

The step size $\eta_{\mathrm{opt}}(k)$ given by (2.122) has the following interpretation. Note that (2.130) can be written as

$$\Delta V(k) \leq \ln\left(1 + \frac{a_1 \Delta J(k)}{1 + a_1 J(Y(k))}\right) + a_2 \left[(\eta(k) - \eta_{\mathrm{opt}}(k))^2 - \eta_{\mathrm{opt}}^2(k)\right] \|G(k)\|_{\mathrm{F}}^2. \tag{2.146}$$

Since the quadratic function $(\eta(k) - \eta_{\mathrm{opt}}(k))^2 - \eta_{\mathrm{opt}}^2(k)$ achieves its minimum at $\eta(k) = \eta_{\mathrm{opt}}(k)$, it follows that the upper bound for $\Delta V(k)$ given by (2.146) is minimized by $\eta(k) = \eta_{\mathrm{opt}}(k)$.

An analogous optimal step size is constructed in [127], where an ideal (not necessarily deadbeat) controller is assumed to exist. However, in the present chapter, an ideal deadbeat internal model controller is proven to exist and have the properties given by Theorem 2.4.1 and Proposition 2.5.1. Hence, for all $k \geq k_0$, $\tilde{y}(k) = y(k)$ is known, and thus $\eta_{\mathrm{opt}}(k)$ is computable.

In [127], $\tilde{y}(k) = y(k) - y_*(k)$ is unknown since $y_*(k)$ is unknown, and thus the optimal step size is not computable in [127]. To obtain a computable step size in [127], several implementable step sizes are defined. We can construct an analogous step size $\eta_{\mathrm{imp}}(k)$. Specifically, $\eta_{\mathrm{imp}}(k)$ defined by

$$\eta_{\mathrm{imp}}(k) \triangleq \frac{1}{\varepsilon + \sigma_{\max}^2(\bar{H}_d)\|\phi(k-d)\|_2^2}, \tag{2.147}$$

where $\varepsilon \geq 0$, satisfies

$$\eta_{\text{imp}}(k) \leq \eta_{\text{opt}}(k). \tag{2.148}$$

Theorem 2.6.1 holds with (2.121) replaced by

$$\eta(k) = \zeta(k)\eta_{\text{imp}}(k). \tag{2.149}$$

However, (2.147) is not needed in the present chapter since $\tilde{y}(k) = y(k)$ is known for all $k \geq k_0$ and thus $\eta_{\text{opt}}(k)$ is computable and thus implementable.

Let $\{\psi(k)\}_{k=k_0}^{\infty}$ satisfy

$$\frac{\zeta_{\text{u}}}{2} < \sup_{j \geq k_0} \psi(j) < \infty, \tag{2.150}$$

and define $\hat{\zeta}(k) \stackrel{\triangle}{=} \frac{\zeta(k)}{\psi(k)}$. Then, if (2.119) holds for $\{\zeta(k)\}_{k=k_0}^{\infty}$, then it also holds with $\{\zeta(k)\}_{k=k_0}^{\infty}$ replaced by $\{\hat{\zeta}(k)\}_{k=k_0}^{\infty}$. The term $\psi(k)$ can be viewed as a tuning variable relating to the magnitude of the bound $\bar{H}_d$ representing the accuracy with which H_d is modeled. In particular, by defining the time-varying bound

$$\bar{H}_{d,k} \stackrel{\triangle}{=} \sqrt{\psi(k)}\bar{H}_d, \tag{2.151}$$

$\bar{H}_d$ can be replaced with $\bar{H}_{d,k}$ in assumption (A5) and (2.112). The example in the next section shows that the transient response is directly related to $\psi(k)$ and thus $\zeta(k)$. Therefore $\psi(k)$ and $\zeta(k)$ are indirectly related to the conservatism of the bound $\bar{H}_d$ on the first nonzero Markov parameter.

2.7 Mass-Spring-Dashpot Example

Consider the 3-mass structure with all possible spring and dashpot connections given by

$$M\ddot{q} + C\dot{q} + Kq = \mu \begin{bmatrix} 0 \\ u \\ 0 \end{bmatrix} + \mu \begin{bmatrix} w_1 \\ w_2 \\ w_3 \end{bmatrix}, \tag{2.152}$$

where

$$M \triangleq \operatorname{diag}(m_1, m_2, m_3), \tag{2.153}$$

$$C \triangleq \begin{bmatrix} c_1 + c_{1,2} + c_{1,3} & -c_{1,2} & -c_{1,3} \\ -c_{1,2} & c_{1,2} + c_2 + c_{2,3} & -c_{2,3} \\ -c_{1,3} & -c_{2,3} & c_{1,3} + c_{2,3} + c_3 \end{bmatrix}, \tag{2.154}$$

$$K \triangleq \begin{bmatrix} k_1 + k_{1,2} + k_{1,3} & -k_{1,2} & -k_{1,3} \\ -k_{1,2} & k_{1,2} + k_2 + k_{2,3} & -k_{2,3} \\ -k_{1,3} & -k_{2,3} & k_{1,3} + k_{2,3} + k_3 \end{bmatrix}, \tag{2.155}$$

$$q \triangleq \begin{bmatrix} q_1 & q_2 & q_3 \end{bmatrix}^{\mathrm{T}}, \tag{2.156}$$

u is the control, and w_1, w_2, and w_3 are disturbances. For this example, the masses are $m_1 = 0.01$ kg, $m_2 = 0.02$ kg, $m_3 = 0.01$ kg; the damping coefficients are $c_1 = 5$ kg/sec, $c_2 = 3$ kg/sec, $c_3 = 4$ kg/sec, $c_{1,2} = 0.1$ kg/sec, $c_{1,3} = 0.2$ kg/sec, $c_{2,3} = 0.3$ kg/sec; and the spring constants are $k_1 = 11$ kg/sec^2, $k_2 = 12$ kg/sec^2, $k_3 = 13$ kg/sec^2, $k_{1,2} = 70$ kg/sec^2, $k_{1,3} = 60$ kg/sec^2, $k_{2,3} = 30$ kg/sec^2. The input gain $\mu = 10^4$ is used for numerical conditioning.

The control objective is to reject the disturbances w_1, w_2, and w_3 while forcing the position of m_2 to follow the command w_4. Thus the performance variable is given

by $y = q_2 - w_4$. We assume that the command and disturbance signals are generated by a Lyapunov-stable discrete-time linear system whose spectrum is unknown.

The continuous-time system (2.152)-(2.156) is sampled at 100 Hz with input provided by a zero-order hold. It follows from [20] that the resulting sampled-data system is minimum phase from u to y. Thus assumption (A2) is satisfied. Furthermore, the sampled-data system has a delay $d = 1$, and the first nonzero Markov parameter is $H_1 = 0.3$. Let the bound on the first nonzero Markov parameter be $\bar{H}_1 = 1.5H_1 = 0.45$, which satisfies assumption (A5). Thus the mass-spring-dashpot sampled-data system satisfies assumptions (A1)-(A11).

The unknown disturbance signals are discrete sinusoids with frequency $\omega_1 = 5$ Hz, and the unknown command signal is a discrete sinusoid with frequency $\omega_2 = 13$ Hz plus a constant bias. More specifically, the unknown disturbance and command signals are

$$w_1(k) = \sin 2\pi\omega_1 T_s k, \tag{2.157}$$

$$w_2(k) = -1.5 \sin 2\pi\omega_1 T_s k, \tag{2.158}$$

$$w_3(k) = 2 \sin 2\pi\omega_1 T_s k, \tag{2.159}$$

$$w_4(k) = \sin 2\pi\omega_2 T_s k + 7, \tag{2.160}$$

where the sample time is $T_s = 0.01$ sec. The open-loop system is given the initial conditions $q(0) = \begin{bmatrix} 1 & 2 & 0 \end{bmatrix}^{\mathrm{T}}$ m and $\dot{q}(0) = \begin{bmatrix} -1 & -2 & 0 \end{bmatrix}^{\mathrm{T}}$ m/s. Figure 2.2 is a time history of the performance variable y. The system is allowed to run open loop for 5 seconds. Then the adaptive controller (2.98) and (2.113) with $n_c = 20$, $d = 1$, $\bar{H}_1 = 0.45$, and $\eta(k) = \eta_{\mathrm{opt}}(k)$ is implemented in feedback with the initial condition $\theta(0) = 0$. The performance variable y converges to zero, which implies that the position q_2 asymptotically follows the command w_4 and rejects the disturbances w_1, w_2, and w_3. In particular, Figure 2.3 shows that the controller places poles at

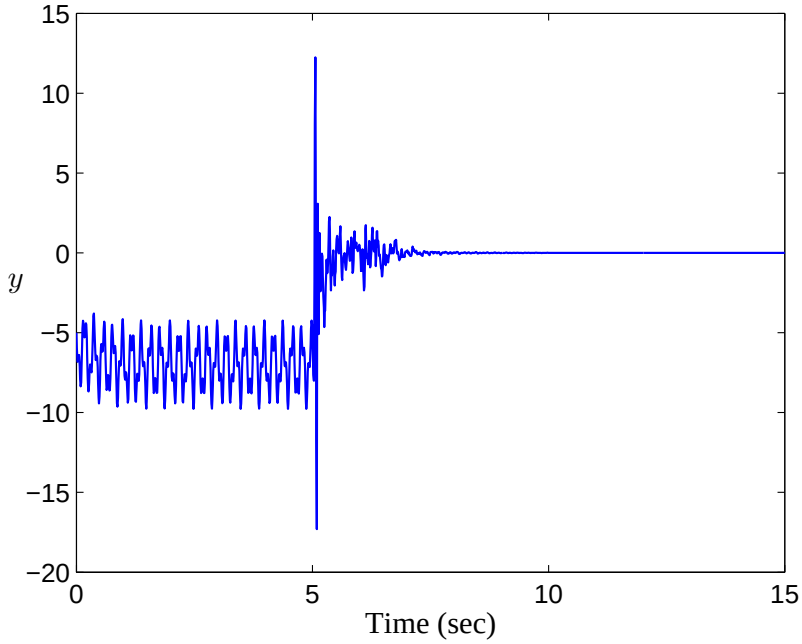

Figure 2.2 The adaptive controller with $\eta(k) = \eta_{\text{opt}}(k)$ (that is, $\zeta(k) \equiv 1$) is implemented in the feedback loop after 5 seconds. The performance variable y converges to zero.

the disturbance frequencies $\omega_1 = 5$ Hz and $\omega_2 = 13$ Hz. Note that $k_0 = 21$, which corresponds to 0.21 sec.

The controller's transient performance has significant peaks, as shown in Figure 2.2. This transient behavior is due in part to the bound $\bar{H}_1$ on the first nonzero Markov parameter H_1. However, the speed of adaptation and thus the transient performance are directly influenced by $\zeta(k)$. Specifically, the controller adapts more slowly when $\zeta(k)$ is small and more quickly when $\zeta(k)$ is large. To demonstrate this effect, consider the adaptive controller (2.98) and (2.113) with $\eta(k) = \frac{1}{5}\eta_{\text{opt}}(k)$. After the system is allowed to run open loop for 5 seconds, the adaptive controller (2.98) and (2.113) with $n_{\text{c}} = 20$, $d = 1$, $\bar{H}_1 = 0.45$, and $\eta(k) = \frac{1}{5}\eta_{\text{opt}}(k)$ is implemented in feedback with the initial condition $\theta(0) = 0$. Figure 2.4 shows that the performance variable y converges to zero with improved transient performance, but at the expense of convergence time. Equivalently, setting $\zeta(k) \equiv 1$, $\psi(k) \equiv 5$, and replacing $\bar{H}_1$ with $\bar{H}_{1,k} \equiv 0.45\sqrt{5} = 1.0$ yields the same result. In this case, the transient performance is

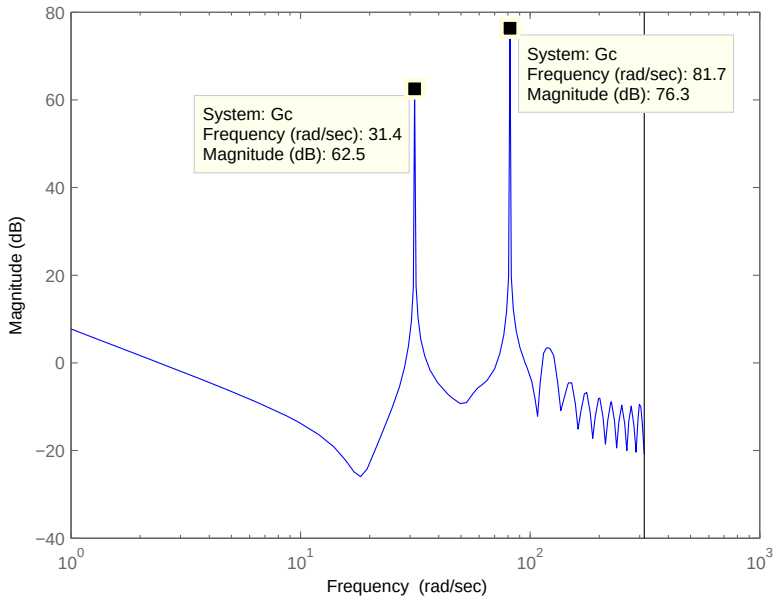

Figure 2.3 Bode magnitude plot of the adaptive controller at $t = 15$ sec. The adaptive controller places poles at the disturbance frequencies $\omega_1 = 5$ Hz and $\omega_2 = 13$ Hz. The controller magnitude $|G_c(e^{j\omega T_s})|$ is plotted for ω up to the Nyquist frequency $\omega_{\text{Nyq}} = \frac{\pi}{T_s} = 314$ rad/sec.

viewed as a consequence of how well the bound $\bar{H}_{1,k}$ models the first nonzero Markov parameter H_1.

For this mass-spring-dashpot example, slower adaptation can reduce peaks in the transient performance, but faster adaptation causes faster convergence. In fact, these observations hold for many open-loop stable systems; however, if the system is open-loop unstable, then the effects of adaptation speed differ. For the open-loop stable mass-spring-dashpot system, one might consider using slower adaptation when the controller is initially turned on, then increasing the adaptation speed. In particular, let $\zeta(k) = \exp(-3/k)$. Figure 2.5 shows a time history of the performance variable y. The system is allowed to run open loop for 5 seconds. Then the adaptive controller (2.98) and (2.113) with $n_c = 20$, $d = 1$, $\bar{H}_1 = 0.45$, and $\eta(k) = \exp(-3/k)\eta_{\text{opt}}(k)$ is implemented in feedback with the initial condition $\theta(0) = 0$. The performance variable y converges to zero with improved transient performance and good conver-

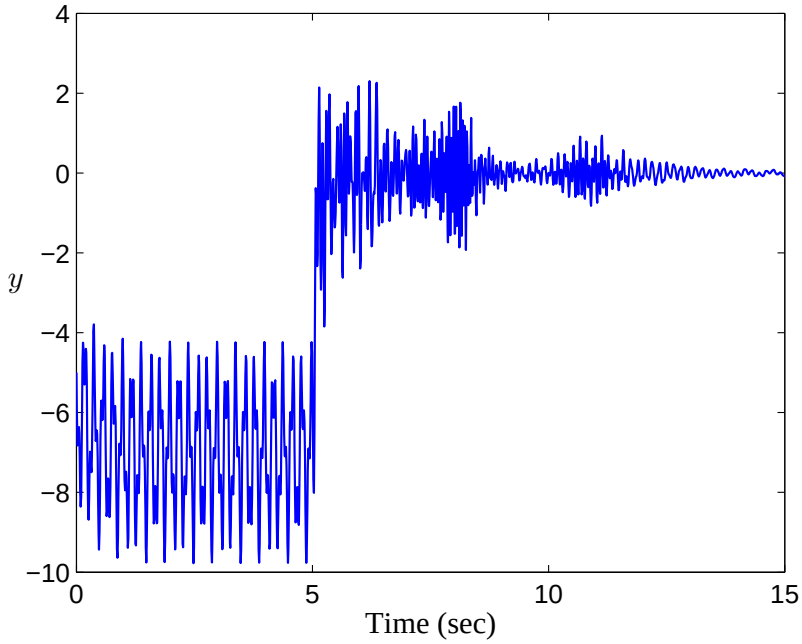

Figure 2.4 The adaptive controller with $\eta(k) = \frac{1}{5}\eta_{\text{opt}}(k)$ (that is, $\zeta(k) \equiv \frac{1}{5}$) is implemented in the feedback loop after 5 seconds. The performance variable y converges to zero with improved transient performance but much slower convergence compared to Figure 2.2.

gence time. Equivalently, setting $\zeta(k) \equiv 1$, $\psi(k) = \exp(3/k)$, and replacing $\bar{H}_1$ with $\bar{H}_{1,k} = 0.45\sqrt{\exp(3/k)}$ yields the same result.

2.8 Conclusion

We considered adaptive stabilization, command following, and disturbance rejection for multi-input, multi-output, linear, time-invariant, minimum-phase, discrete-time systems where the command and disturbance signals are generated by a linear system with unknown dynamics. The adaptive controller requires limited model information, specifically, knowledge of the open-loop system's relative degree and a bound on the first nonzero Markov parameter. We considered command and disturbance signals generated by Lyapunov-stable linear systems. Thus, the command and disturbance signals are combinations of discrete-time sinusoids and steps. We proved

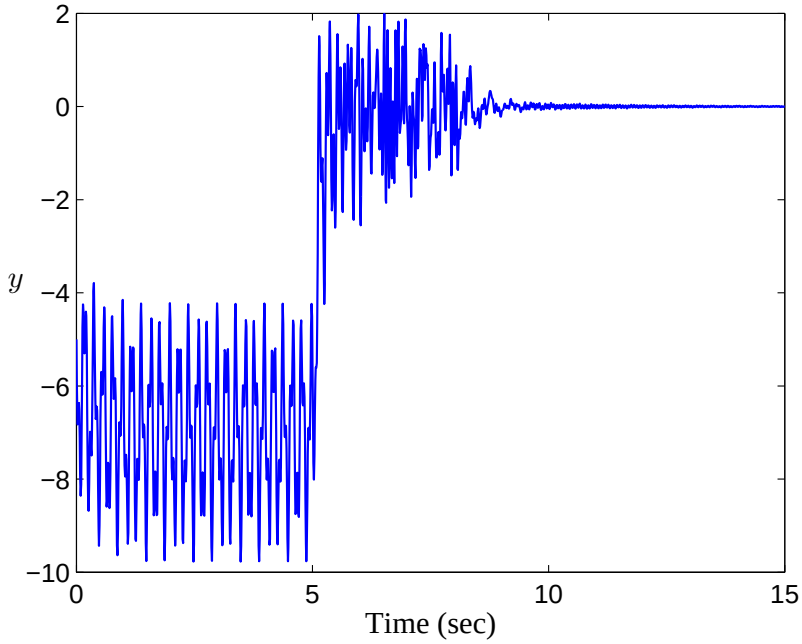

Figure 2.5 The adaptive controller with $\eta(k) = \exp(-3/k)\eta_{\text{opt}}(k)$ (that is, $\zeta(k) = \exp(-3/k)$) is implemented in the feedback loop after 5 seconds. The performance variable y converges to zero with improved transient performance compared to figures 2.2 and 2.4. Furthermore, the performance converges almost as quickly as in Figure 2.2 and more quickly than in Figure 2.4.

global asymptotic convergence for command following and disturbance rejection.

2.9 Appendix: Deadbeat Internal Model Control

Theorem 2.9.1. *Consider the discrete-time system*

$$\hat{x}(k+1) = \hat{A}\hat{x}(k) + \hat{B}u(k) + \hat{D}_1 w(k), \tag{2.161}$$

$$y(k) = \hat{C}\hat{x}(k) + \hat{D}_2 w(k), \tag{2.162}$$

where $\hat{x}(k) \in \mathbb{R}^{\hat{n}}$, $y(k) \in \mathbb{R}^{\hat{l}_y}$, $u(k) \in \mathbb{R}^{\hat{l}_u}$, $w(k) \in \mathbb{R}^{l_w}$, *and assume that the following conditions hold.*

(i) $(\hat{A}, \hat{B}, \hat{C})$ *is controllable and observable.*

(ii) $\hat{l}_u \geq \hat{l}_y$.

(iii) The exogenous signal $w(k)$ is generated from the output of the linear system

$$\hat{x}_w(k+1) = \hat{A}_w \hat{x}_w(k), \quad w(k) = \hat{C}_w \hat{x}_w(k), \tag{2.163}$$

where $\hat{x}_w(k) \in \mathbb{R}^{\hat{n}_w}$, $(\hat{A}_w, \hat{C}_w)$ is observable, for all $\lambda \in spec\left(\hat{A}_w\right)$, λ is not a transmission zero of $G(z) = \hat{C}(\mathbf{z}I - \hat{A})^{-1}\hat{B}$, and normal rank $G = min(\hat{l}_u, \hat{l}_y)$.

Furthermore, consider the linear time-invariant controller

$$\hat{x}_{\mathrm{c}}(k+1) = \hat{A}_{\mathrm{c}} \hat{x}_{\mathrm{c}}(k) + \hat{B}_{\mathrm{c}} y(k), \quad u(k) = \hat{C}_{\mathrm{c}} \hat{x}_{\mathrm{c}}(k), \tag{2.164}$$

where $\hat{x}_{\mathrm{c}}(k) \in \mathbb{R}^{n_{\mathrm{db}}}$ so that the closed-loop system is given by

$$x_{\mathrm{cl}}(k+1) = A_{\mathrm{cl}} x_{\mathrm{cl}}(k) + D_{\mathrm{cl}} w(k), \tag{2.165}$$

$$y(k) = C_{\mathrm{cl}} x_{\mathrm{cl}}(k) + D_2 w(k), \tag{2.166}$$

where

$$A_{\mathrm{cl}} \triangleq \begin{bmatrix} \hat{A} & \hat{B}\hat{C}_{\mathrm{c}} \\ \hat{B}_{\mathrm{c}}\hat{C} & \hat{A}_{\mathrm{c}} \end{bmatrix}, \quad D_{\mathrm{cl}} \triangleq \begin{bmatrix} \hat{D}_1 \\ \hat{B}_{\mathrm{c}}\hat{D}_2 \end{bmatrix}, \quad C_{\mathrm{cl}} \triangleq \begin{bmatrix} \hat{C} & 0 \end{bmatrix}, \quad x_{\mathrm{cl}} \triangleq \begin{bmatrix} \hat{x} \\ \hat{x}_{\mathrm{c}} \end{bmatrix}. \tag{2.167}$$

Then, for all $n_{\mathrm{db}} \geq \hat{n} + 2\hat{n}_w \hat{l}_y$, there exists $(\hat{A}_{\mathrm{c}}, \hat{B}_{\mathrm{c}}, \hat{C}_{\mathrm{c}})$ such that A_{cl} is nilpotent. Consequently, for all initial conditions $x_{\mathrm{cl}}(0)$ and $\hat{x}_w(0)$, and, for all $k \geq 2\left(\hat{n} + \hat{n}_w \hat{l}_y\right)$, $y(k) = 0$.

Proof. A straightforward extension of the arguments used in Section 2.2 to show that A_w can be chosen to have distinct eigenvalues shows that, without loss of generality, $\hat{A}_w$ can be assumed to be cyclic. We consider the open-loop system (2.161)-(2.162) connected in cascade with an internal model of the exogenous dynamics

$$\hat{x}_1(k+1) = A_W \hat{x}_1(k) + B_W y(k), \tag{2.168}$$

where $A_W \triangleq I_{\hat{l}_y} \otimes \hat{A}_w$, $B_W \triangleq I_{\hat{l}_y} \otimes \hat{B}_w$, and $\hat{B}_w \in \mathbb{R}^{\hat{n}_w}$ is chosen such that $(\hat{A}_w, \hat{B}_w)$ is controllable [14, Fact 5.12.6] or [15, Fact 5.14.7]. Note that the dynamics (2.168) contains $\hat{l}_y$ copies of the exogenous dynamics $\hat{A}_w$. The cascade (2.161), (2.162), and (2.168) is

$$\begin{bmatrix} \hat{x}(k+1) \\ \hat{x}_1(k+1) \end{bmatrix} = \begin{bmatrix} \hat{A} & 0 \\ B_W\hat{C} & A_W \end{bmatrix} \begin{bmatrix} \hat{x}(k) \\ \hat{x}_1(k) \end{bmatrix} + \begin{bmatrix} \hat{B} \\ 0 \end{bmatrix} u(k) + \begin{bmatrix} \hat{D}_1 \\ B_W\hat{D}_2 \end{bmatrix} w(k), \tag{2.169}$$

$$\begin{bmatrix} y(k) \\ \hat{x}_1(k) \end{bmatrix} = \begin{bmatrix} \hat{C} & 0 \\ 0 & I \end{bmatrix} \begin{bmatrix} \hat{x}(k) \\ \hat{x}_1(k) \end{bmatrix} + \begin{bmatrix} \hat{D}_2 \\ 0 \end{bmatrix} w(k). \tag{2.170}$$

Now, we show that the augmented system (2.169), (2.170) is controllable and observable. First, define the stable region

$$\mathcal{S} \triangleq \{\lambda \in \mathbb{C} : |\lambda| < 1\}, \tag{2.171}$$

and the unstable region $\mathcal{U} \triangleq \mathbb{C} \backslash \mathcal{S}$. Let $\mathbf{z} \in \mathcal{U}$ and $\lambda \in \operatorname{spec}\left(\hat{A}_w\right) \subset \mathcal{U}$. Since $(\hat{A}, \hat{B})$ is controllable, it follows that

$$\begin{aligned} \operatorname{rank} \begin{bmatrix} \hat{A} - \mathbf{z}I & \hat{B} & 0 \\ B_W\hat{C} & 0 & A_W - \mathbf{z}I \end{bmatrix} &\geq \operatorname{rank} \begin{bmatrix} \hat{A} - \lambda I & \hat{B} & 0 \\ B_W\hat{C} & 0 & A_W - \lambda I \end{bmatrix} \\ &\geq \operatorname{rank} \left(\begin{bmatrix} I_{\hat{n}} & 0 & 0 \\ 0 & B_W & A_W - \lambda I \end{bmatrix} \begin{bmatrix} \hat{A} - \lambda I & \hat{B} & 0 \\ \hat{C} & 0 & 0 \\ 0 & 0 & I_{\hat{l}_y\hat{n}_w} \end{bmatrix} \right). \end{aligned} \tag{2.172}$$

Conditions *(ii)* and *(iii)* imply that rank $\begin{bmatrix} \hat{A}-\lambda I & \hat{B} & 0 \\ \hat{C} & 0 & 0 \\ 0 & 0 & I_{\hat{l}_y\hat{n}_w} \end{bmatrix} = \hat{n}+\hat{l}_y+\hat{l}_y\hat{n}_w$, which is full row rank. Therefore,

$$\hat{n}+\hat{l}_y\hat{n}_w \geq \text{rank} \begin{bmatrix} \hat{A}-\mathbf{z}I & \hat{B} & 0 \\ B_W\hat{C} & 0 & A_W-\mathbf{z}I \end{bmatrix} \geq \text{rank} \begin{bmatrix} I_{\hat{n}} & 0 & 0 \\ 0 & B_W & A_W-\lambda I \end{bmatrix}. \tag{2.173}$$

Since (A_W, B_W) is controllable, rank $\begin{bmatrix} I_{\hat{n}} & 0 & 0 \\ 0 & B_W & A_W-\lambda I \end{bmatrix} = \hat{n}+\hat{l}_y\hat{n}_w$, and thus

$$\text{rank} \begin{bmatrix} \hat{A}-\mathbf{z}I & \hat{B} & 0 \\ B_W\hat{C} & 0 & A_W-\mathbf{z}I \end{bmatrix} = \hat{n}+\hat{l}_y\hat{n}_w. \tag{2.174}$$

Hence $\left(\begin{bmatrix} \hat{A} & 0 \\ B_W\hat{C} & A_W \end{bmatrix}, \begin{bmatrix} \hat{B} \\ 0 \end{bmatrix} \right)$ is controllable. Since, in addition, $(\hat{A}, \hat{C})$ is observable, it follows that $\left(\begin{bmatrix} \hat{A} & 0 \\ B_W\hat{C} & A_W \end{bmatrix}, \begin{bmatrix} \hat{C} & 0 \\ 0 & I \end{bmatrix} \right)$ is observable. Thus, there exists an observer-based controller that stabilizes the augmented system (2.169)-(2.170) and yields a closed-loop system with nilpotent dynamics. It follows that, for all $n_{\text{db}} \geq \hat{n}+2\hat{n}_w\hat{l}_y$, there exists a linear time-invariant controller (2.164) of order n_{db}, such that the equilibrium of the closed-loop system (2.165)-(2.167) is asymptotically stable, where A_{cl} is nilpotent and, for all initial conditions $x_{\text{cl}}(0)$ and $\hat{x}_w(0)$, $\lim_{k\to\infty} y(k) = 0$.

The closed-loop system (2.165)-(2.167) with exogenous input $w(k)$, can be written

as

$$x_s(k+1) = A_s x_s(k), \quad y(k) = C_s x_s(k), \tag{2.175}$$

where

$$A_s \triangleq \begin{bmatrix} A_{\rm cl} & D_{\rm cl}\hat{C}_w \\ 0 & \hat{A}_w \end{bmatrix}, \quad C_s \triangleq \begin{bmatrix} C_{\rm cl} & \hat{D}_2\hat{C}_w \end{bmatrix}, \tag{2.176}$$

and $x_s \triangleq \begin{bmatrix} x_{\rm cl} \\ \hat{x}_w \end{bmatrix}$. Since $\lim_{k\to\infty} y(k) = 0$ and $A_{\rm cl}$ is asymptotically stable, it follows from [40, 44, Lemma 2.1] there exists $S \in \mathbb{R}^{2\left(\hat{n}+\hat{n}_w\hat{l}_y\right)\times\hat{n}_w}$ such that

$$A_{\rm cl}S - S\hat{A}_w = D_{\rm cl}\hat{C}_w, \tag{2.177}$$

$$C_{\rm cl}S = \hat{D}_2\hat{C}_w. \tag{2.178}$$

Now define $Q \triangleq \begin{bmatrix} I & -S \\ 0 & I \end{bmatrix}$, and consider the change of basis

$$\bar{A}_s \triangleq Q^{-1}A_sQ = \begin{bmatrix} A_{\rm cl} & 0 \\ 0 & \hat{A}_w \end{bmatrix}, \bar{C}_s \triangleq C_sQ = \begin{bmatrix} C_{\rm cl} & 0 \end{bmatrix}. \tag{2.179}$$

Then, we have $y(k) = \bar{C}_s\bar{A}_s^kQ^{-1}x_s(0) = C_{\rm cl}A_{\rm cl}^k\left[x_{\rm cl}(0) + S\hat{x}_w(0)\right]$. Since $A_{\rm cl} \in \mathbb{R}^{2\left(\hat{n}+\hat{n}_w\hat{l}_y\right)\times 2\left(\hat{n}+\hat{n}_w\hat{l}_y\right)}$ is nilpotent, it follows that, for all initial conditions $x_{\rm cl}(0)$ and $\hat{x}_w(0)$ and for all $k \geq 2\left(\hat{n}+\hat{n}_w\hat{l}_y\right)$, $y(k) = 0$. □

2.10 Appendix: Inverse System Bounds

Consider the discrete-time system (2.1), (2.2), where $y(k) \in \mathbb{R}^l$, $u(k) \in \mathbb{R}^l$. To derive the inverse system, we increment (2.2) by d steps, yielding

$$\begin{aligned} y(k+d) &= Cx(k+d) + D_2 w(k+d) && (2.180) \\ &= CA^d x(k) + H_d u(k) \\ &\quad + \begin{bmatrix} D_2 & CD_1 & \cdots & CA^{d-1}D_1 \end{bmatrix} \begin{bmatrix} w(k+d) \\ \vdots \\ w(k) \end{bmatrix}, && (2.181) \end{aligned}$$

where $H_d \triangleq CA^{d-1}B$ is the first nonzero Markov parameter from u to y. It follows from (2.181) and assumption (A4) that

$$\begin{aligned} u(k) &= -H_d^{-1}CA^d x(k) + H_d^{-1} y(k+d) \\ &\quad - H_d^{-1} \begin{bmatrix} D_2 & CD_1 & \cdots & CA^{d-1}D_1 \end{bmatrix} \begin{bmatrix} w(k+d) \\ \vdots \\ w(k) \end{bmatrix}. \end{aligned}$$

The inverse system is thus given by

$$x(k+1) = A_{\mathrm{R}} x(k) + B_{\mathrm{R}} y_d(k) + D_{1\mathrm{R}} W_d(k), \tag{2.182}$$

$$u(k) = C_{\mathrm{R}} x(k) + D_{\mathrm{R}} y_d(k) + D_{2\mathrm{R}} W_d(k), \tag{2.183}$$

where

$$A_{\mathrm{R}} \triangleq A - BH_d^{-1}CA^d, \qquad B_{\mathrm{R}} \triangleq BH_d^{-1},$$

$$C_{\mathrm{R}} \triangleq -H_d^{-1}CA^d, \qquad D_{\mathrm{R}} \triangleq H_d^{-1},$$

$$D_{1\mathrm{R}} \triangleq \left[\begin{array}{cccc} -BH_d^{-1}D_2 & -BH_d^{-1}CD_1 & \cdots & -BH_d^{-1}CA^{d-2}D_1 \quad D_1 - BH_d^{-1}CA^{d-1}D_1 \end{array} \right],$$

$$D_{2\mathrm{R}} \triangleq \left[\begin{array}{ccc} -H_d^{-1}D_2 & -H_d^{-1}CD_1 & \cdots - H_d^{-1}CA^{d-1}D_1 \end{array} \right],$$

$$y_d(k) \triangleq y(k+d), \qquad W_d(k) \triangleq \left[\begin{array}{c} w(k+d) \\ \vdots \\ w(k) \end{array} \right]. \tag{2.184}$$

Since, by assumption (A1), (A, B, C) is minimal, it follows from [125, Proposition 4.2] that the eigenvalues of A_{R} consist of the invariant zeros of (A, B, C) as well as $n - d$ eigenvalues equal to 0. Therefore, by assumption (A2), A_{R} is asymptotically stable.

Theorem 2.10.1. *Consider the system (2.1), (2.2) and its inverse (2.182), (2.183). Let p be a positive integer. Then, subject to assumptions (A1), (A2), (A4), and (A8), there exist $c_1 > 0$ and $c_2 > 0$ such that*

$$\|\tilde{U}(k-d)\|_2^2 \leq c_1 + c_2\|\tilde{Y}(k)\|_2^2, \tag{2.185}$$

where

$$\tilde{U}(k) \triangleq \left[\begin{array}{c} u(k-1) \\ \vdots \\ u(k-p) \end{array} \right], \tilde{Y}(k) \triangleq \left[\begin{array}{c} y(k-1) \\ \vdots \\ y(k-p-1) \end{array} \right]. \tag{2.186}$$

Proof. By successive substitution,

$$u(k) = C_{\mathrm{R}} A_{\mathrm{R}}^{k} x(0) + D_{\mathrm{R}} y_d(k) + D_{2\mathrm{R}} W_d(k) + \sum_{i=1}^{k} C_{\mathrm{R}} A_{\mathrm{R}}^{i-1} B_{\mathrm{R}} y_d(k-i) + \sum_{i=1}^{k} C_{\mathrm{R}} A_{\mathrm{R}}^{i-1} D_{1\mathrm{R}} W_d(k-i).$$

Taking the norm of both sides yields

$$\|u(k)\|^2 \leq 5 \left\{ \|C_{\mathrm{R}}\|^2 \|A_{\mathrm{R}}^{k}\|^2 \|x(0)\|^2 + \|D_{\mathrm{R}}\|^2 \|y_d(k)\|^2 + \|D_{2\mathrm{R}}\|^2 \|W_d(k)\|^2 + \left[\sum_{i=1}^{k} \|C_{\mathrm{R}}\| \|A_{\mathrm{R}}^{i-1}\| \|B_{\mathrm{R}}\| \|y_d(k-i)\| \right]^2 + \left[\sum_{i=1}^{k} \|C_{\mathrm{R}}\| \|A_{\mathrm{R}}^{i-1}\| \|D_{1\mathrm{R}}\| \|W_d(k-i)\| \right]^2 \right\},$$

where $\|\cdot\|$ is the Euclidean norm. Since A_{R} is asymptotically stable, it follows that there exist $\lambda \in [0, 1)$ and $c > 0$ such that, for every positive integer k, $\|A_{\mathrm{R}}^{k}\| \leq c\lambda^{k}$. Therefore, there exists $c_3 > 0$ such that

$$\|u(k)\|^2 \leq c_3 \left[\lambda^{2k} + \|y_d(k)\|^2 + \left(\sum_{i=1}^{k} \lambda^{i-1} \|y_d(k-i)\| \right)^2 + \|W_d(k)\|^2 + \left(\sum_{i=1}^{k} \lambda^{i-1} \|W_d(k-i)\| \right)^2 \right].$$

Since, by assumption (A8), $w(k)$ is bounded for all k, it follows that $\|W_d(k)\|^2$ is also bounded, that is, there exists $\rho > 0$ such that $\|W_d(k)\|^2 \leq \rho$ for all k. Thus, there exists $c_4 > 0$ such that

$$\|u(k)\|^2 \leq c_4 \left[\rho + \lambda^{2k} + \|y_d(k)\|^2 + \left(\sum_{i=1}^{\infty} \lambda^{i-1} \right) \times \left(\sum_{i=1}^{k} \lambda^{i-1} \|y_d(k-i)\|^2 \right) + \left(\rho \sum_{i=1}^{\infty} \lambda^{i-1} \right)^2 \right].$$

Since $|\lambda| < 1$, it follows that $\sum_{i=1}^{\infty} \lambda^{i-1} = \frac{1}{1-\lambda}$, where $0^0 \triangleq 1$. Thus, it follows that there exist $c_5 > 0$ and $c_6 > 0$ such that

$$\|u(k)\|^2 \leq c_5 \left[c_6 + \|y_d(k)\|^2 + \sum_{i=1}^{k} \lambda^{i-1} \|y_d(k-i)\|^2 \right]. \tag{2.187}$$

Summing both sides of (2.187) from $k-p$ to $k-1$ yields

$$\sum_{j=k-p}^{k-1} \|u(j)\|^2 \leq c_5 \left[c_7 + \sum_{j=k-p}^{k-1} \|y_d(j)\|^2 + \sum_{j=k-p}^{k-1} \sum_{i=1}^{j} \lambda^{i-1} \|y_d(j-i)\|^2 \right], \tag{2.188}$$

where $c_7 > 0$. Introducing $\tau \triangleq j - i$ yields

$$\begin{aligned} \sum_{j=k-p}^{k-1} \|u(j)\|^2 &\leq c_5 \left[c_7 + \sum_{j=k-p}^{k-1} \|y_d(j)\|^2 + \sum_{\tau=k-p}^{k-2} \sum_{j=\tau+1}^{k-1} \lambda^{j-\tau-1} \|y_d(\tau)\|^2 \right] \\ &\leq c_8 \left[c_7 + \sum_{j=k-p}^{k-1} \|y_d(j)\|^2 + \sum_{\tau=k-p-1}^{k-2} \|y_d(\tau)\|^2 \right] \\ &\leq c_1 + c_2 \sum_{j=k-p-1}^{k-1} \|y_d(j)\|^2, \end{aligned} \tag{2.189}$$

where $c_8 > 0$. Decrementing (2.189) by d steps and using the definitions of $y_d(k)$, $\tilde{U}(k)$, and $\tilde{Y}(k)$ from (2.184) and (2.186), (yields 2.185). □

Chapter 3

Adaptive Retrospective-Cost-Based Full-State Feedback

In the previous chapter, we developed a gradient-based adaptive control algorithm for stabilization, command following, and disturbance rejection of multi-input, multi-output, linear, time-invariant, minimum-phase, discrete-time systems. A seemingly obvious extension would be to use the theory and methods developed in Chapter 2 to generalize the adaptive control algorithm for handling nonminimum-phase systems. Unfortunately, the same method of proof used in the previous chapter will not work for nonminimum-phase systems. Specifically, the development of the ideal fixed-gain controller in Section 2.4 requires a precompensator to exactly cancel the zeros of the open-loop plant. If nonminimum-phase zeros were present, this would cause unstable pole-zero cancellation in the loop. Even though the ideal fixed-gain controller is never implemented in practice, it must be shown to exist for the development of the adaptive control algorithm. In addition, the stability and convergence analysis of the adaptive controller in Section 2.6 requires that the control inputs u be bounded by the performance measurements y. For minimum-phase systems, this follows from Theorem 2.10.1, but the same is not true in general for systems with nonminimum-phase zeros.

To overcome nonminimum-phase zero restrictions, lifting techniques [4, 10–12, 71], which transform a high-rate nonminimum-phase system into a low-rate minimum-phase system, were explored. Lifting is able to transform a nonminimum-phase system into a minimum-phase system by forcing the system to run open loop, that is $u = 0$, over a periodic window of time. However, when operating the system open loop, the performance measurement y will not converge to zero if there are additional commands and/or disturbances driving the plant. The same is true for systems that are open-loop unstable.

This chapter marks a shift in the focus of this dissertation from gradient-based adaptive control to retrospective-cost-based adaptive control. In particular, this chapter investigates full-state-feedback stabilization in multi-input, linear, time-invariant, discrete-time systems. The results of this chapter support and motivate the retrospective-cost-based adaptive controllers developed in Chapters 4 and 5 by providing a basis for retrospective cost optimization. Retrospective cost optimization [127] is a measure of performance at the current time based on a past window of data and without assumptions about the command or disturbance signals. In particular, retrospective cost optimization acts as an inner loop to the adaptive control algorithm by modifying the performance variables based on the difference between the actual past control inputs and the recomputed past control inputs based on the current control law.

The novel features of this chapter include a Lyapunov-based stability and convergence proof for a special case. We also present numerical examples to illustrate the robustness of the algorithm under conditions of Markov parameter uncertainty. Theoretical and numerical results suggest that the converged adaptive controller has a downward adaptive gain margin of 6 dB and an infinite upward adaptive gain margin, which is reminiscent of continuous-time fixed-gain LQR control.

3.1 Introduction

Modern control engineering primarily focuses on state-space methods. Of these approaches, the full-state-feedback stabilization problem is perhaps the most well known. Given a linear, time-invariant system, the full-state-feedback problem is to find a stabilizing static feedback gain such that the closed-loop system with state feedback is asymptotically stable. Under certain conditions, namely controllability of the pair (A, B), it is possible to arbitrarily assign the closed-loop system's eigenvalues by appropriate feedback of the system state x. Further details are discussed in [6, 97].

The most well-developed approaches to the full-state-feedback problem are to use pole-placement or eigenvalue-assignment schemes. For a scalar-input plant, a stabilizing feedback gain can be found graphically through root locus or Nyquist techniques. Alternatively, a stabilizing feedback gain K can be obtained directly by constructing a desired closed-loop characteristic equation $\det(sI - A + BK)$ [6]. Another well-known approach is to use a linear quadratic regulator (LQR) for full-state-feedback. Instead of directly assigning closed-loop eigenvalues, LQR places the closed-loop poles based on the optimization of a cost function. One drawback of these approaches is that they all depend on an accurate model of the system. Since adaptive controllers can accommodate (to an extent) inaccurate models of the system and adapt online to the true system, this motivates the use of adaptive control for full-state-feedback stabilization.

The goal of this chapter is to present a discrete-time, adaptive, full-state-feedback control law that is effective for systems that are multi-input and/or unstable. The algorithm is developed in discrete time based on a discrete-time plant model obtained by either plant discretization or discrete-time system identification so that the controller can be implemented directly as embedded code without an intermediate controller discretization step.

The results of this chapter support and motivate the retrospective-cost-based

adaptive controllers developed in Chapters 4 and 5 by providing a basis for retrospective cost optimization. This method is used to adapt dynamic compensators for disturbance rejection, adaptive stabilization, adaptive command following, and model reference adaptive control in [113, 127]. Retrospective cost optimization is a measure of performance at the current time based on a past window of data and without assumptions about the command or disturbance signals. In particular, retrospective cost optimization acts as an inner loop to the adaptive control algorithm by modifying the performance variables based on the difference between the actual past control inputs and the recomputed past control inputs based on the current control law. We prove Lyapunov stability of the closed-loop error system for a special scalar case.

We present numerical examples to illustrate the algorithm's effectiveness in handling systems that are unstable to provide insight into the modeling information required for controller implementation. This information includes a limited number of Markov parameters, and in many cases, only a bound on the input matrix B need be known. For full-state feedback, these numerical results suggest that the retrospective-cost adaptive controller has downward and upward gain margins of 6 dB and ∞ dB, respectively, which is reminiscent of continuous-time fixed-gain LQR control.

3.2 Problem Formulation

Consider the discrete-time system

$$x(k+1) = Ax(k) + Bu(k), \tag{3.1}$$

where $x(k) \in \mathbb{R}^n$, $u(k) \in \mathbb{R}^m$, $A \in \mathbb{R}^{n\times n}$, $B \in \mathbb{R}^{n\times m}$, and $k \geq 0$. We assume that (A, B) is controllable and that measurements of x are available for feedback. Our goal is to develop an adaptive full-state-feedback controller such that x converges to

zero.

For a nonnegative integer r, we define the *extended state vector* $X(k) \in \mathbb{R}^{nr}$ and the *extended input vector* $U(k) \in \mathbb{R}^{mr}$ by

$$X(k) \triangleq \begin{bmatrix} x(k-r+1) \\ \vdots \\ x(k) \end{bmatrix}, \quad U(k) \triangleq \begin{bmatrix} u(k-r+1) \\ \vdots \\ u(k) \end{bmatrix}. \tag{3.2}$$

Note that (3.1) can be rewritten as

$$X(k+1) = \mathcal{A}X(k) + \mathcal{B}U(k), \tag{3.3}$$

where $\mathcal{A} \in \mathbb{R}^{nr \times nr}$ and $\mathcal{B} \in \mathbb{R}^{nr \times mr}$ are given by

$$\mathcal{A} \triangleq \begin{bmatrix} A & 0 & \cdots & 0 \\ A^2 & \vdots & & \vdots \\ \vdots & & \ddots & \\ A^r & 0 & \cdots & 0 \end{bmatrix}, \quad \mathcal{B} \triangleq \begin{bmatrix} H_1 & 0 & \cdots & 0 \\ H_2 & H_1 & \ddots & \vdots \\ \vdots & & \ddots & 0 \\ H_r & H_{r-1} & \cdots & H_1 \end{bmatrix}, \tag{3.4}$$

where, for all $i > 0$, the Markov parameters $H_i \in \mathbb{R}^{n \times m}$ of the system (3.1) are

$$H_i \triangleq A^{i-1}B. \tag{3.5}$$

In particular, $H_1 = B$.

3.3 Retrospective Cost Optimization

Let

$$u(k) = K(k)x(k), \tag{3.6}$$

where $K(k) \in \mathbb{R}^{m\times n}$ is the *gain matrix*. From (3.6), it follows that the extended input vector $U(k)$ can be rewritten as

$$U(k) = \sum_{i=1}^{r} L_i K(k-i+1)x(k-i+1), \tag{3.7}$$

where

$$L_i \triangleq \begin{bmatrix} 0_{(r-i)m\times m} \\ I_m \\ 0_{(i-1)m\times m} \end{bmatrix} \in \mathbb{R}^{mr\times m}. \tag{3.8}$$

Next, for $\mathcal{K} \in \mathbb{R}^{m\times n}$, define the *retrospective state vector* $\hat{X}(\mathcal{K}, k) \in \mathbb{R}^{nr}$ by

$$\hat{X}(\mathcal{K}, k+1) \triangleq \mathcal{A}X(k) + \mathcal{B}\hat{U}(\mathcal{K}, k), \tag{3.9}$$

where $\hat{U}(\mathcal{K}, k) \in \mathbb{R}^{mr}$ is the *recomputed input vector*, given by

$$\hat{U}(\mathcal{K}, k) \triangleq \sum_{i=1}^{r} L_i \mathcal{K} x(k-i+1). \tag{3.10}$$

Subtracting (3.3) from (3.9) yields

$$\hat{X}(\mathcal{K}, k+1) = X(k+1) - \mathcal{B}\left[U(k) - \hat{U}(\mathcal{K}, k)\right]. \tag{3.11}$$

Note that

$$\hat{U}(\mathcal{K}, k) = E(k)\text{vec } \mathcal{K}, \tag{3.12}$$

where

$$E(k) \triangleq \sum_{i=1}^{r} x^{\mathrm{T}}(k-i+1) \otimes L_i \in \mathbb{R}^{mr \times mn}, \tag{3.13}$$

vec is the column-stacking operator, and $\otimes$ represents the Kronecker product. Furthermore,

$$\hat{X}(\mathcal{K}, k+1) = f(k) + D(k)\text{vec } \mathcal{K}, \tag{3.14}$$

where

$$f(k) \triangleq X(k+1) - \mathcal{B}U(k) \in \mathbb{R}^{nr}, \tag{3.15}$$

$$D(k) \triangleq \mathcal{B}E(k) \in \mathbb{R}^{nr \times mn}. \tag{3.16}$$

Now consider the *retrospective cost function*

$$J(\mathcal{K}, k) \triangleq \hat{X}^{\mathrm{T}}(\mathcal{K}, k+1) R_1(k) \hat{X}(\mathcal{K}, k+1) + \alpha(k) \text{tr} \left[(\mathcal{K} - K(k))^{\mathrm{T}} (\mathcal{K} - K(k)) \right], \tag{3.17}$$

where, for all $k \geq 0$, $R_1(k) \in \mathbb{R}^{nr \times nr}$ is positive semidefinite and the *learning rate* $\alpha(k) \in \mathbb{R}$ satisfies

$$0 < \alpha(k) \leq \alpha_{\mathrm{u}} \triangleq \sup_{j \geq 0} \alpha(j) < \infty. \tag{3.18}$$

Substituting (3.14) into (3.17) yields

$$J(\mathcal{K}, k) = c(k) + b^{\mathrm{T}}(k)\mathrm{vec}\ \mathcal{K} + (\mathrm{vec}\ \mathcal{K})^{\mathrm{T}} M(k)\mathrm{vec}\ \mathcal{K}, \tag{3.19}$$

where

$$M(k) \triangleq D^{\mathrm{T}}(k)R_1(k)D(k) + \alpha(k)I_{mn}, \tag{3.20}$$

$$b(k) \triangleq 2D^{\mathrm{T}}(k)R_1(k)f(k) - 2\alpha(k)\mathrm{vec}\ K(k), \tag{3.21}$$

$$c(k) \triangleq f^{\mathrm{T}}(k)R_1(k)f(k) + \alpha(k)\mathrm{tr}\left[K^{\mathrm{T}}(k)K(k)\right]. \tag{3.22}$$

Since $M(k)$ is positive definite, $J(\mathcal{K}, k)$ has the strict global minimizer $K(k+1)$ given by

$$K(k+1) = -\frac{1}{2}\mathrm{vec}^{-1}\left[M^{-1}(k)b(k)\right]. \tag{3.23}$$

Since $K(k+1)$ depends on $x(k+1)$ through the dependence of $b(k)$ on $X(k+1)$, it follows that $u(k+1) = K(k+1)x(k+1)$ can be implemented at step $k+1$.

Note that $M(k)$ and $b(k)$ depend on $D(k)$ and $f(k)$, which in turn depend on the Markov parameter matrix $\mathcal{B}$. Since $\mathcal{B}$ may not be known in practice, we replace $\mathcal{B}$ by an estimate $\hat{\mathcal{B}}$ in $D(k)$, $f(k)$, and $K(k+1)$. Therefore, for all $k \geq 1$, the implemented control gain $\hat{K}(k)$ depends on $\hat{\mathcal{B}}$, that is,

$$u(k) = \hat{K}(k)x(k), \tag{3.24}$$

$$\hat{K}(k+1) \triangleq -\frac{1}{2}\mathrm{vec}^{-1}\left[\hat{M}^{-1}(k)\hat{b}(k)\right], \tag{3.25}$$

where

$$\hat{M}(k) \triangleq \hat{D}^{\mathrm{T}}(k)R_1(k)\hat{D}(k) + \alpha(k)I_{mn}, \tag{3.26}$$

$$\hat{b}(k) \triangleq 2\hat{D}^{\mathrm{T}}(k)R_1(k)\hat{f}(k) - 2\alpha(k)\mathrm{vec}\ \hat{K}(k), \tag{3.27}$$

and

$$\hat{f}(k) \triangleq X(k+1) - \hat{\mathcal{B}}U(k), \tag{3.28}$$

$$\hat{D}(k) \triangleq \hat{\mathcal{B}}E(k), \tag{3.29}$$

$$\hat{\mathcal{B}} \triangleq \begin{bmatrix} \hat{H}_1 & 0 & \cdots & 0 \\ \hat{H}_2 & \hat{H}_1 & \ddots & \vdots \\ \vdots & & \ddots & 0 \\ \hat{H}_r & \hat{H}_{r-1} & \cdots & \hat{H}_1 \end{bmatrix}, \tag{3.30}$$

where, for all $i = 1, \ldots, r$, $\hat{H}_i$ is an estimate of H_i. For convenience, we specialize (3.20)–(3.22) and (3.26), (3.27) with $R_1(k) \triangleq I_{nr}$.

The learning rate $\alpha(k)$ affects the convergence speed of the adaptive control algorithm. As $\alpha(k)$ is increased, convergence speed is lowered. Likewise, as $\alpha(k)$ is decreased, convergence speed is raised. By varying $\alpha(k)$, we study tradeoffs between transient performance and convergence speed.

3.4 Closed-loop System

For all $k \geq 0$, the closed-loop system is given by

$$X(k+1) = \begin{bmatrix} 0 & I_n & 0 & \cdots & 0 \\ \vdots & \ddots & \ddots & \ddots & \vdots \\ \vdots & & \ddots & \ddots & 0 \\ \vdots & & & 0 & I_n \\ 0 & \cdots & \cdots & 0 & A + B\hat{K}(k) \end{bmatrix} X(k), \tag{3.31}$$

$$\text{vec } \hat{K}(k+1) = -\frac{1}{2}\hat{M}^{-1}(k)\hat{b}(k), \tag{3.32}$$

$$\begin{bmatrix} \text{vec } \hat{K}(k) \\ \text{vec } \hat{K}(k-1) \\ \vdots \\ \text{vec } \hat{K}(k-r+2) \end{bmatrix} = \begin{bmatrix} I_{mn} & 0 & \cdots & \cdots & 0 \\ 0 & \ddots & \ddots & & \vdots \\ \vdots & \ddots & \ddots & 0 & 0 \\ 0 & \cdots & 0 & I_{mn} & 0 \end{bmatrix} \begin{bmatrix} \text{vec } \hat{K}(k) \\ \text{vec } \hat{K}(k-1) \\ \vdots \\ \text{vec } \hat{K}(k-r+1) \end{bmatrix}. \tag{3.33}$$

Note that the order of the closed-loop system is $(m+1)nr$.

Let $m = 1$ so that $E(k) = \sum_{i=1}^{r} L_i x^{\mathrm{T}}(k-i+1)$. Then, for all $k \geq 0$, (3.32) can be written as

$$\begin{aligned} &\text{vec } \hat{K}(k+1) = \\ &\text{vec } \left(\left[\alpha(k)\hat{K}(k) - X^{\mathrm{T}}(k+1)\hat{\mathcal{B}}E(k) + \sum_{i=1}^{r} x^{\mathrm{T}}(k-i+1)\hat{K}^{\mathrm{T}}(k-i+1)L_i^{\mathrm{T}}\hat{\mathcal{B}}^{\mathrm{T}}\hat{\mathcal{B}}E(k) \right] \right. \\ &\quad \left. \cdot \left[\alpha(k)I_n + E^{\mathrm{T}}(k)\hat{\mathcal{B}}^{\mathrm{T}}\hat{\mathcal{B}}E(k) \right]^{-1} \right). \end{aligned} \tag{3.34}$$

3.5 Closed-Loop Error System ($m = r = 1$)

Let $m = r = 1$. Then, for all $k \geq 0$, the closed-loop system with gain matrix $\hat{K}(k)$ is given by

$$x(k+1) = \left[A + B\hat{K}(k)\right] x(k), \tag{3.35}$$

$$\hat{K}(k+1) = \hat{K}(k) - \frac{x^{\mathrm{T}}(k+1)\hat{B}}{\alpha(k) + \hat{B}^{\mathrm{T}}\hat{B}x^{\mathrm{T}}(k)x(k)}x^{\mathrm{T}}(k). \tag{3.36}$$

Let $K^* \in \mathbb{R}^{m\times n}$ be a gain matrix that renders the ideal closed-loop system nilpotent, that is,

$$x^*(k+1) = \mathcal{N}x^*(k), \tag{3.37}$$

where $x^*(k) \in \mathbb{R}^n$, and the matrix $\mathcal{N} \triangleq A + BK^* \in \mathbb{R}^{n\times n}$ is nilpotent. Consequently, for all $k \geq n$, $x^*(k) = 0$. Define the error states $\tilde{x}(k) \in \mathbb{R}^n$ and $\tilde{K}(k) \in \mathbb{R}^{m\times n}$ by

$$\tilde{x}(k) \triangleq x(k) - x^*(k), \tag{3.38}$$

$$\tilde{K}(k) \triangleq \hat{K}(k) - K^*. \tag{3.39}$$

Thus, for all $k \geq n$, $\tilde{x}(k) = x(k)$. Therefore, for all $k \geq n$, substituting $\hat{K}(k) = \tilde{K}(k) + K^*$ into (3.35) and (3.36) yields the closed-loop error system

$$x(k+1) = \left[\mathcal{N} + B\tilde{K}(k)\right] x(k), \tag{3.40}$$

$$\tilde{K}(k+1) = \tilde{K}(k) - \frac{x^{\mathrm{T}}(k+1)\hat{B}}{\alpha(k) + \hat{B}^{\mathrm{T}}\hat{B}x^{\mathrm{T}}(k)x(k)}x^{\mathrm{T}}(k). \tag{3.41}$$

By substituting (3.40) into (3.41), the closed-loop error system can be rewritten

for all $k \geq n$ as

$$x(k+1) = \left[\mathcal{N} + B\tilde{K}(k)\right] x(k), \tag{3.42}$$

$$\tilde{K}^{\mathrm{T}}(k+1) = \mathcal{A}(k)\tilde{K}^{\mathrm{T}}(k) - \frac{\hat{B}^{\mathrm{T}}\mathcal{N}x(k)}{\alpha(k) + \hat{B}^{\mathrm{T}}\hat{B}x^{\mathrm{T}}(k)x(k)}x(k), \tag{3.43}$$

where

$$\mathcal{A}(k) \stackrel{\triangle}{=} I_n - \frac{\hat{B}^{\mathrm{T}}B}{\alpha(k) + \hat{B}^{\mathrm{T}}\hat{B}x^{\mathrm{T}}(k)x(k)}x(k)x^{\mathrm{T}}(k). \tag{3.44}$$

The multispectrum of $\mathcal{A}(k)$ is given by

$$\mathrm{mspec}\left[\mathcal{A}(k)\right] = \left\{1, \ldots, 1, 1 - \frac{\hat{B}^{\mathrm{T}}Bx^{\mathrm{T}}(k)x(k)}{\alpha(k) + \hat{B}^{\mathrm{T}}\hat{B}x^{\mathrm{T}}(k)x(k)}\right\}. \tag{3.45}$$

Proposition 3.5.1. *Assume that $B^{\mathrm{T}}B < 2\hat{B}^{\mathrm{T}}B$ and consider (3.45). Then, for all $k \geq n$,*

$$1 - \frac{B^{\mathrm{T}}B}{\hat{B}^{\mathrm{T}}B} < 1 - \frac{\hat{B}^{\mathrm{T}}Bx^{\mathrm{T}}(k)x(k)}{\alpha(k) + \hat{B}^{\mathrm{T}}\hat{B}x^{\mathrm{T}}(k)x(k)} \leq 1. \tag{3.46}$$

Furthermore,

$$\left|1 - \frac{B^{\mathrm{T}}B}{\hat{B}^{\mathrm{T}}B}\right| < 1. \tag{3.47}$$

Proof. Let $k \geq n$. Since $B^{\mathrm{T}}B < 2\hat{B}^{\mathrm{T}}B$, we have

$$0 < \frac{B^{\mathrm{T}}B}{\hat{B}^{\mathrm{T}}B} < 2,$$

and thus,

$$\left|1 - \frac{B^{\mathrm{T}}B}{\hat{B}^{\mathrm{T}}B}\right| < 1.$$

Now, since $0 < \alpha(k)B^{\mathrm{T}}B$, we have

$$0 \leq \hat{B}^{\mathrm{T}}B\hat{B}^{\mathrm{T}}Bx^{\mathrm{T}}(k)x(k) < \alpha(k)B^{\mathrm{T}}B + \hat{B}^{\mathrm{T}}B\hat{B}^{\mathrm{T}}Bx^{\mathrm{T}}(k)x(k).$$

Therefore,

$$0 \leq \hat{B}^{\mathrm{T}}B\hat{B}^{\mathrm{T}}Bx^{\mathrm{T}}(k)x(k) < B^{\mathrm{T}}B\left[\alpha(k) + \hat{B}^{\mathrm{T}}\hat{B}x^{\mathrm{T}}(k)x(k)\right],$$

and thus,

$$0 \leq \frac{\hat{B}^{\mathrm{T}}Bx^{\mathrm{T}}(k)x(k)}{\alpha(k) + \hat{B}^{\mathrm{T}}\hat{B}x^{\mathrm{T}}(k)x(k)} < \frac{B^{\mathrm{T}}B}{\hat{B}^{\mathrm{T}}B},$$

which implies

$$1 - \frac{B^{\mathrm{T}}B}{\hat{B}^{\mathrm{T}}B} < 1 - \frac{\hat{B}^{\mathrm{T}}Bx^{\mathrm{T}}(k)x(k)}{\alpha(k) + \hat{B}^{\mathrm{T}}\hat{B}x^{\mathrm{T}}(k)x(k)} \leq 1. \qquad \square$$

It follows from Proposition 3.5.1 that the singular values of $\mathcal{A}(k)$ are given by

$$\sigma\left[\mathcal{A}(k)\right] = \left\{1, \ldots, 1, \left|1 - \frac{\hat{B}^{\mathrm{T}}Bx^{\mathrm{T}}(k)x(k)}{\alpha(k) + \hat{B}^{\mathrm{T}}\hat{B}x^{\mathrm{T}}(k)x(k)}\right|\right\}. \tag{3.48}$$

3.6 Special Case ($n = m = r = 1$)

Let $n = m = r = 1$ and define $K^* \triangleq -A/B$, which yields $x^*(k) \equiv 0$ for all $k \geq 1$. Consequently, for all $k \geq 1$, $\tilde{x}(k) = x(k)$. Therefore, for all $k \geq 1$, it follows from (3.42), (3.43) that the closed-loop error system is

$$x(k+1) = B\tilde{K}(k)x(k), \tag{3.49}$$

$$\tilde{K}(k+1) = \Gamma(\gamma(k)x^2(k))\tilde{K}(k), \tag{3.50}$$

where, for $\lambda \geq 0$,

$$\Gamma(\lambda) \triangleq \frac{1+\eta\lambda}{1+\lambda}, \tag{3.51}$$

$\eta \triangleq 1 - 1/\delta$, $\delta \triangleq \hat{B}/B$, and $\gamma(k) \triangleq \hat{B}^2/\alpha(k)$. Note that $\Gamma(0) = 1$, $\Gamma(\lambda) \to \eta$ as $\lambda \to \infty$, and $\Gamma(\lambda)$ is a decreasing function of λ on $[0, \infty)$. Also, note that $\eta \in (-1, 1)$ if and only if $\delta > \frac{1}{2}$.

Further simplification is possible when B is known. In particular $\eta = 0$ if and only if $\hat{B} = B$. In this case, (3.49), (3.50) simplify to

$$x(k+1) = B\tilde{K}(k)x(k), \tag{3.52}$$

$$\tilde{K}(k+1) = \frac{1}{1+\gamma(k)x^2(k)}\tilde{K}(k). \tag{3.53}$$

Lemma 3.6.1. *Assume that $\delta > \frac{1}{2}$ and consider (3.49), (3.50). Then, for all $k \geq 1$, $\eta < \Gamma(\gamma(k)x^2(k)) \leq 1$. Furthermore, for all $k \geq 1$ such that $x(k) \neq 0$, $\eta < \Gamma(\gamma(k)x^2(k)) < 1$, and thus $|\Gamma(\gamma(k)x^2(k))| < 1$.*

Proof. Let $k \geq 1$. Since $\eta \in (-1, 1)$, it follows that

$$\eta < 1 \leq 1 + (1-\eta)\,\gamma(k)x^2(k).$$

Therefore,

$$\eta\left[1 + \gamma(k)x^2(k)\right] < 1 + \eta\gamma(k)x^2(k) \leq 1 + \gamma(k)x^2(k),$$

and thus,

$$\eta < \Gamma(\gamma(k)x^2(k)) \leq 1.$$

Furthermore, for all $k \geq 1$ such that $x(k) \neq 0$, it follows that $-1 < \eta < \Gamma(\gamma(k)x^2(k)) < 1$. □

Theorem 3.6.2. *Assume that $n = m = r = 1$, assume that $\delta > \frac{1}{2}$, and consider the open-loop system (3.1) and the adaptive feedback controller (3.24), (3.25). Then, for all initial conditions $x(0)$ and $\hat{K}(0)$, the following statements hold:*

(i) $\hat{K}(k)$ *is bounded.*

(ii) $\lim_{k\to\infty} x(k) = 0$.

(iii) $\{|\tilde{K}(k)|\}_{k=1}^{\infty}$ *is nonincreasing.*

(iv) $\lim_{k\to\infty} |\tilde{K}(k)| < 1/|B|$.

(v) There exists $k_0 \geq 1$ such that $\{|x(k)|\}_{k=k_0}^{\infty}$ is decreasing.

(vi) The zero solution of the closed-loop error system (3.49), (3.50) is Lyapunov stable.

Proof. Let $k \geq 1$ so that $\tilde{x}(k) = x(k)$. Consider the positive-definite, radially unbounded Lyapunov candidate

$$V(x, \hat{K}) \stackrel{\triangle}{=} \ln\left(1 + \gamma_0 x^2\right) + a\tilde{K}^2, \tag{3.54}$$

where $\gamma_0 \stackrel{\triangle}{=} \hat{B}^2/\alpha_{\mathrm{u}} > 0$ and $a > 0$ is specified below. The Lyapunov difference is thus given by

$$\Delta V(k) \stackrel{\triangle}{=} V(x(k+1), \hat{K}(k+1)) - V(x(k), \hat{K}(k)). \tag{3.55}$$

Evaluating $\Delta V(k)$ along the trajectories of the closed-loop error system (3.49), (3.50) yields

$$\begin{aligned}
\Delta V(k) &= \ln\left(1+\gamma_0 x^2(k+1)\right) - \ln\left(1+\gamma_0 x^2(k)\right) + a\left(\tilde{K}^2(k+1) - \tilde{K}^2(k)\right) \\
&= \ln\left(1+\gamma_0 B^2 \tilde{K}^2(k) x^2(k)\right) - \ln\left(1+\gamma_0 x^2(k)\right) \\
&\quad + a\left[\frac{\left(1+\eta\gamma(k)x^2(k)\right)^2}{\left(1+\gamma(k)x^2(k)\right)^2}\tilde{K}^2(k) - \tilde{K}^2(k)\right] \\
&= \ln\left[\frac{1+\gamma_0 B^2 \tilde{K}^2(k) x^2(k)}{1+\gamma_0 x^2(k)}\right] \\
&\quad + a\left[\frac{1+2\eta\gamma(k)x^2(k)+\eta^2\gamma^2(k)x^4(k)}{\left(1+\gamma(k)x^2(k)\right)^2} - 1\right]\tilde{K}^2(k) \\
&= \ln\left[1+\frac{\gamma_0 B^2 \tilde{K}^2(k) x^2(k) - \gamma_0 x^2(k)}{1+\gamma_0 x^2(k)}\right] \\
&\quad + a\left[\frac{2(\eta-1)\gamma(k)x^2(k)+(\eta^2-1)\gamma^2(k)x^4(k)}{\left(1+\gamma(k)x^2(k)\right)^2}\right]\tilde{K}^2(k) \\
&= \ln\left[1+\frac{\left(B^2\tilde{K}^2(k)-1\right)\gamma_0 x^2(k)}{1+\gamma_0 x^2(k)}\right] \\
&\quad + a\left[\frac{2(\eta-1)\gamma(k)x^2(k)+(\eta^2-1)\gamma^2(k)x^4(k)}{\left(1+\gamma(k)x^2(k)\right)^2}\right]\tilde{K}^2(k). \qquad (3.56)
\end{aligned}$$

Defining $b_1(k) \triangleq 1+\gamma_0 x^2(k)$ and $b_2(k) \triangleq 1+\gamma(k)x^2(k)$, it follows that

$$\begin{aligned}
\Delta V(k) &= \ln\left[1+\frac{\left(B^2\tilde{K}^2(k)-1\right)\gamma_0 x^2(k)}{b_1(k)}\right] \\
&\quad + a\left[\frac{2(\eta-1)\gamma(k)x^2(k)+(\eta^2-1)\gamma^2(k)x^4(k)}{b_2^2(k)}\right]\tilde{K}^2(k). \qquad (3.57)
\end{aligned}$$

Since, for all $z > 0$, $\ln z \leq z - 1$, we have

$$\begin{aligned}
\Delta V(k) \leq & \frac{\left(B^2\tilde{K}^2(k) - 1\right)\gamma_0 x^2(k)}{b_1(k)} \\
& + a\left[\frac{2(\eta-1)\gamma(k)x^2(k) + (\eta^2-1)\gamma^2(k)x^4(k)}{b_2^2(k)}\right]\tilde{K}^2(k) \\
= & \frac{(B^2\tilde{K}^2(k) - 1)\gamma_0 b_2^2(k)x^2(k)}{b_1(k)b_2^2(k)} \\
& + \frac{2a(\eta-1)\gamma(k)b_1(k)x^2(k)\tilde{K}^2(k) + a(\eta^2-1)\gamma^2(k)b_1(k)x^4(k)\tilde{K}^2(k)}{b_1(k)b_2^2(k)} \\
= & \frac{\left[B^2\gamma_0 b_2^2(k) + 2a(\eta-1)\gamma(k)b_1(k) + a(\eta^2-1)\gamma^2(k)x^2(k)b_1(k)\right]x^2(k)\tilde{K}^2(k)}{b_1(k)b_2^2(k)} \\
& - \frac{\gamma_0 b_2^2(k)x^2(k)}{b_1(k)b_2^2(k)} \\
= & \frac{\left[2a(\eta-1)\gamma(k) + B^2\gamma_0 + \left(a(\eta^2-1) + B^2\right)\gamma_0\gamma^2(k)x^4(k)\right]x^2(k)\tilde{K}^2(k)}{b_1(k)b_2^2(k)} \\
& + \frac{\left[(2B^2\gamma_0 + 2a(\eta-1)\gamma_0 + a(\eta^2-1)\gamma(k))\,\gamma(k)x^2(k)\right]x^2(k)\tilde{K}^2(k)}{b_1(k)b_2^2(k)} \\
& - \frac{\gamma_0 b_2^2(k)x^2(k)}{b_1(k)b_2^2(k)}. \qquad (3.58)
\end{aligned}$$

Letting $a \triangleq \frac{\hat{B}^2}{2\delta-1} > 0$ and noting that, for all $k \geq 0$, $\gamma_0 \leq \gamma(k)$, it follows that

$$\Delta V(k) \leq \frac{-b_3\gamma_0\left[1 + \gamma(k)x^2(k)\right]x^2(k)\tilde{K}^2(k) - \gamma_0 b_2^2(k)x^2(k)}{b_1(k)b_2^2(k)}, \qquad (3.59)$$

where $b_3 \triangleq \frac{B^2}{2\delta-1}$. Thus,

$$\Delta V(k) \leq -W(x(k), \tilde{K}(k)), \qquad (3.60)$$

where

$$W(x(k),\tilde{K}(k)) \triangleq \frac{b_3\gamma_0\left[1+\gamma(k)x^2(k)\right]\tilde{K}^2(k)+\gamma_0 b_2^2(k)}{b_1(k)b_2^2(k)}x^2(k)$$
$$= \frac{\left[1+b_3\tilde{K}^2(k)\right]\gamma_0 x^2(k)+\left[2+b_3\tilde{K}^2(k)\right]\gamma_0\gamma(k)x^4(k)+\gamma_0\gamma^2(k)x^6(k)}{1+\left[2\gamma(k)+\gamma_0\right]x^2(k)+\left[2\gamma_0+\gamma(k)\right]\gamma(k)x^4(k)+\gamma_0\gamma^2(k)x^6(k)}. \tag{3.61}$$

To show *(i)*, summing (3.60) from 1 to $k-1$ and noting that, for all $k \geq 0$, $W(x(k),\tilde{K}(k)) \geq 0$, yields

$$\begin{aligned} V(x(k),\tilde{K}(k)) &= V(x(1)+\sum_{j=1}^{k-1}\Delta V(j),\tilde{K}(1)) \\ &\leq V(x(1)-\sum_{j=1}^{k-1}W(x(j),\tilde{K}(j)),\tilde{K}(1)) \\ &\leq V(x(1),\tilde{K}(1)). \end{aligned} \tag{3.62}$$

Thus, $V(x(k),\tilde{K}(k))$ is bounded. Since $V(x(k),\tilde{K}(k))$ is positive definite and radially unbounded, it follows that $x(k)$ and $\tilde{K}(k)$ are bounded. Thus, $\hat{K}(k)=\tilde{K}(k)+K^*$ is bounded.

Now, we show *(ii)*. Since V is positive definite, it follows from (3.60) that

$$\begin{aligned} 0 &\leq \lim_{k\to\infty}\sum_{j=1}^{k}W(x(j),\tilde{K}(j)) \\ &\leq -\lim_{k\to\infty}\sum_{j=1}^{k}\Delta V(j) \\ &= V(x(1),\tilde{K}(1))-\lim_{k\to\infty}V(x(k),\tilde{K}(k)) \\ &\leq V(x(1),\tilde{K}(1)), \end{aligned} \tag{3.63}$$

where all three limits exist. Thus $\lim_{k\to\infty}W(x(k),\tilde{K}(k))=0$. It now follows from

(3.61) that $\lim_{k\to\infty} x(k) = 0$.

We now show *(iii)*. Since, by Lemma 3.6.1, $-1 < \Gamma(\gamma(k)x^2(k)) \leq 1$ for all $k \geq 1$, it follows from (3.50) that $\{|\tilde{K}(k)|\}_{k=1}^{\infty}$ is nonincreasing. Let $\kappa \triangleq \lim_{k\to\infty} |\tilde{K}(k)|$, and note that $\kappa \geq 0$ and, for all $k \geq 1$, $|\tilde{K}(k)| \geq \kappa$.

To show *(iv)*, suppose that $\kappa \geq 1/|B|$. Then, for all $k \geq 1$, it follows that $|x(k+1)| \geq \kappa|B||x(k)| \geq |x(k)|$. Consequently, $\{|x(k)|\}_{k=1}^{\infty}$ is nondecreasing. Therefore, if $x(1) \neq 0$, then $\{|x(k)|\}_{k=1}^{\infty}$ does not converge to zero. Hence $\kappa < 1/|B|$.

We now show *(v)*. Since $\{|\tilde{K}(k)|\}_{k=1}^{\infty}$ is nonincreasing and $\kappa < 1/|B|$, it follows that there exists $k_0 \geq 1$ such that, for all $k \geq k_0$, $|\tilde{K}(k)| < 1/|B|$, and thus $|B\tilde{K}(k)| < 1$. Consequently, it follows from (3.49) that $\{|x(k)|\}_{k=k_0}^{\infty}$ is decreasing.

Finally, to show *(vi)*, let

$$\mathcal{X}(k) \triangleq \begin{bmatrix} x(k) \\ \tilde{K}(k) \end{bmatrix} \tag{3.64}$$

be the state of the closed-loop error system (3.49), (3.50). Since V is positive definite and, by (3.60), ΔV is negative semidefinite, it follows from [77, Lemma A.3.12] that the zero solution of the closed-loop error system is Lyapunov stable. □

A discussion about generalizations of this scalar proof is presented in Section 3.8.

3.7 Full-State-Feedback Examples

In each example below, the adaptive controller gain matrix $\hat{K}(k)$ is initialized to zero.

Example 3.7.1 (Scalar input and plant, unstable plant)**.** *Consider the unstable scalar*

plant

$$x(k+1) = 2x(k) - 0.1u(k), \tag{3.65}$$

with pole located at $\{2\}$*. Taking* $\alpha(k) \equiv 1$*, the closed-loop response is shown in Figure 3.1 for* $x_0 = -4.3$*. The state approaches zero within 6 time steps.* ■

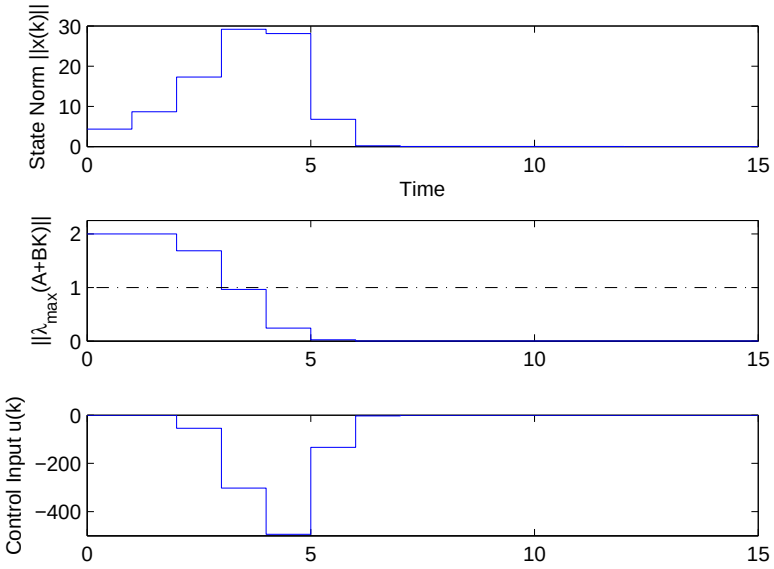

Figure 3.1 Closed-loop response for an unstable, scalar-input plant with $\alpha(k) \equiv 1$. The state approaches zero within 6 time steps.

Example 3.7.2 (Scalar input, asymptotically stable plant)**.** *Consider the stable plant*

$$x(k+1) = \begin{bmatrix} -0.1 & 0.4 & 0.45 \\ 1 & 0 & 0 \\ 0 & 1 & 0 \end{bmatrix} x(k) + \begin{bmatrix} 0 \\ 0 \\ 1 \end{bmatrix} u(k), \tag{3.66}$$

with poles located at $\{-0.5 \pm 0.5\jmath, 0.9\}$*. To demonstrate the effect of the learning rate, we take either* $\alpha(k) \equiv 1$ *or* $\alpha(k) \equiv 1000$*. The open and closed-loop responses are shown in Figure 3.2 for* $x_0 = [-4.3, -16.7, 1.3]^{\mathrm{T}}$*. With* $\alpha(k) \equiv 1$*,* x *approaches zero within 10 time steps, while, with* $\alpha(k) \equiv 1000$*,* x *approaches zero within 20 time steps.*

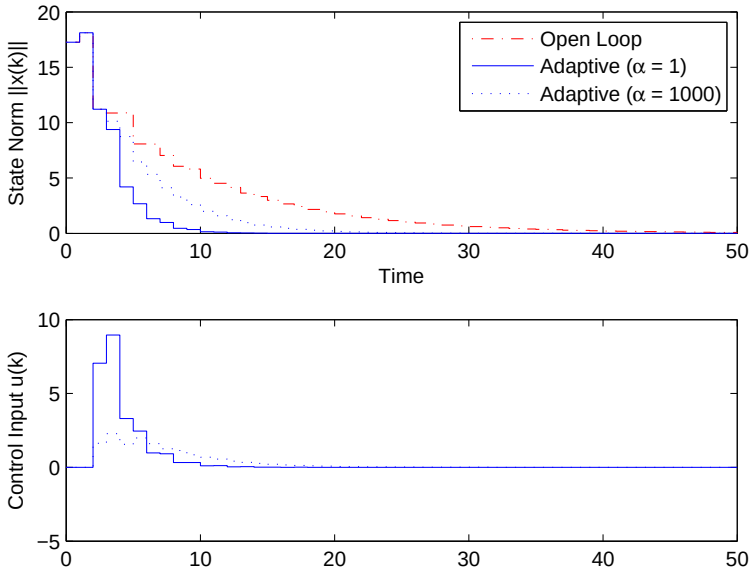

Figure 3.2 Closed-loop responses for a stable, scalar-input plant. To demonstrate the effect of the learning rate, we take either $\alpha(k) \equiv 1$ or $\alpha(k) \equiv 1000$. With $\alpha(k) \equiv 1$, x approaches zero within 10 time steps, while, with $\alpha(k) \equiv 1000$, x approaches zero within 20 time steps.

To develop a gain-margin metric, and thus demonstrate robustness of the adaptive control algorithm to knowledge of the input matrix $\hat{B}$, we take $\alpha(k) \equiv 1$ and $\hat{B} = \lambda B$, where $\lambda \in (0.5, 5]$ is a scale factor and $\hat{B}$ is the scaled input matrix to be used with the adaptive control algorithm. We define the performance metric

$$\min_k \frac{1}{5} \sum_{i=1}^{5} \|x(k-i+1)\| < 0.1, \tag{3.67}$$

which represents the minimum number of time steps for the average of the norm of the previous five state values to be below 0.1. A plot of the performance metric is shown in Figure 3.3. These results suggest that the converged adaptive control algorithm has a downward adaptive gain margin of 6 dB and an upward adaptive gain margin of at least 14 dB. This is consistent with the results of Theorem 3.6.2 for the case $n > 1$.

■

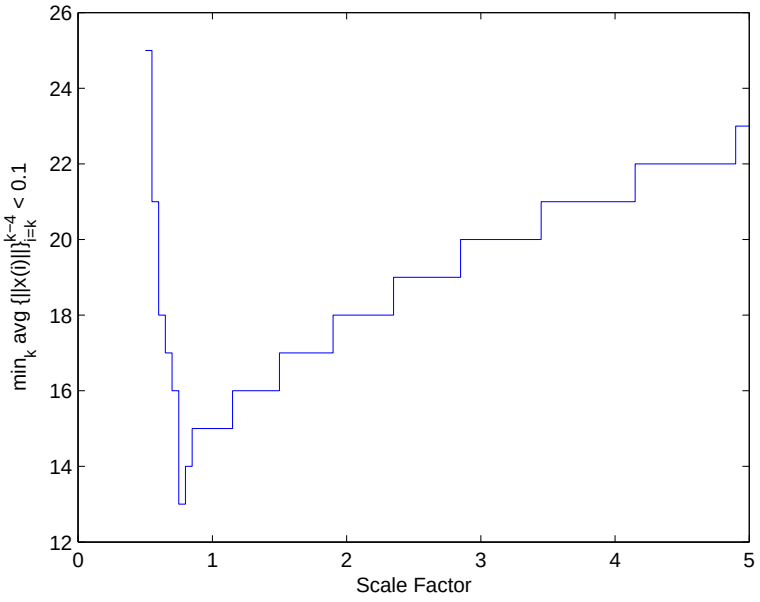

Figure 3.3 Performance metric to demonstrate robustness of the adaptive control algorithm to knowledge of the input matrix $\hat{B}$ for a stable, scalar-input plant. We take $\alpha(k) \equiv 1$ and $\hat{B} = \lambda B$, where $\lambda \in (0.5, 5]$ is a scale factor and $\hat{B}$ is the scaled input matrix to be used with the adaptive control algorithm. These results suggest that the converged adaptive control algorithm has a downward adaptive gain margin of 6 dB and an upward adaptive gain margin of at least 14 dB.

Example 3.7.3 (Scalar input, unstable plant)**.** *Consider the unstable plant*

$$x(k+1) = \begin{bmatrix} -0.38 & 0.46 & 1.03 \\ 1 & 0 & 0 \\ 0 & 1 & 0 \end{bmatrix} x(k) + \begin{bmatrix} 0 \\ 0 \\ 1 \end{bmatrix} u(k), \tag{3.68}$$

with poles located at $\{-\sqrt{2}/2 \pm \sqrt{2}/2, 1.03\}$*. To demonstrate the effect of the learning rate, we take either* $\alpha(k) \equiv 1$ *or* $\alpha(k) \equiv 1000$*. The open and closed-loop responses are shown in Figure 3.4 for* $x_0 = [-4.3, -16.7, 1.3]^{\mathrm{T}}$*. With* $\alpha(k) \equiv 1$*,* x *approaches zero within 10 time steps, while, with* $\alpha(k) \equiv 1000$*,* x *approaches zero within 20 time steps.*

To further develop a gain-margin metric, and thus demonstrate robustness of the adaptive control algorithm to knowledge of the input matrix $\hat{B}$*, we take* $\alpha(k) \equiv 1$ *and*

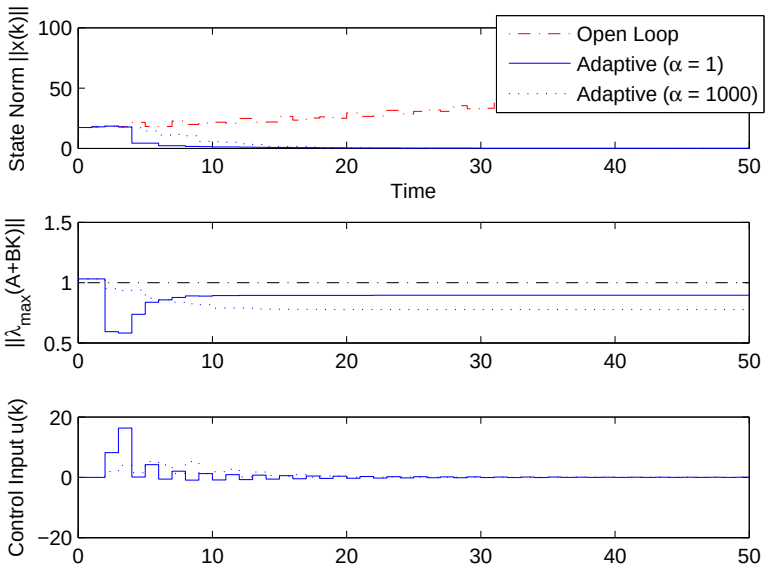

Figure 3.4 Closed-loop responses for an unstable, scalar-input plant with either $\alpha(k) \equiv 1$ or $\alpha(k) \equiv 1000$. With $\alpha(k) \equiv 1$, x approaches zero within 10 time steps, while, with $\alpha(k) \equiv 1000$, x approaches zero within 20 time steps.

$\hat{B} = \lambda B$, where $\lambda \in (0.5, 5]$ is a scale factor and $\hat{B}$ is the scaled input matrix to be used with the adaptive control algorithm. A plot of the performance metric (3.67) is shown in Figure 3.5. These results suggest that the converged adaptive control algorithm has a downward adaptive gain margin of 6 dB and an upward adaptive gain margin of at least 14 dB. This is consistent with the results of Theorem 3.6.2 for the case $n > 1$. ■

3.8 Algorithm Limitations

Although the retrospective-cost-based full-state-feedback adaptive control algorithm has been shown to work well with $r = 1$ in certain cases, there are situations that may require $r > 1$. We explore these cases through example.

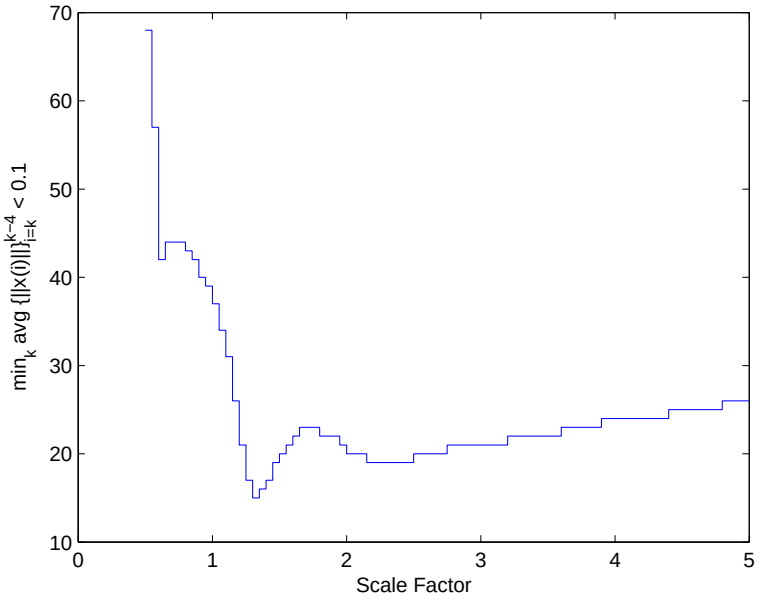

Figure 3.5 Performance metric to demonstrate robustness of the adaptive control algorithm to knowledge of the input matrix $\hat{B}$ for an unstable, scalar-input plant. We take $\alpha(k) \equiv 1$ and $\hat{B} = \lambda B$, where $\lambda \in (0.5, 5]$ is a scale factor and $\hat{B}$ is the scaled input matrix to be used with the adaptive control algorithm. These results suggest that the converged adaptive control algorithm has a downward adaptive gain margin of 6 dB and an upward adaptive gain margin of at least 14 dB.

Example 3.8.1 (Scalar input, unstable plant)**.** *Consider the unstable plant*

$$x(k+1) = \begin{bmatrix} 0 & 1 \\ 0 & -1.05 \end{bmatrix} x(k) + \begin{bmatrix} 1.05 \\ 1 \end{bmatrix} u(k), \tag{3.69}$$

with poles located at $\{0, -1.05\}$*. The closed-loop response is shown in Figure 3.6 for* $\alpha(k) \equiv 1$*,* $r = 1$*,* $\hat{K}(0) = 0$*, and* $\hat{B} = B$*. The state* x *does not go to zero, in fact, the closed-loop system is unstable. To understand what is happening, consider the closed-loop equations (3.35), (3.36) for* $m = r = 1$*. Letting* $\hat{K}(0) = 0$*, the equations*

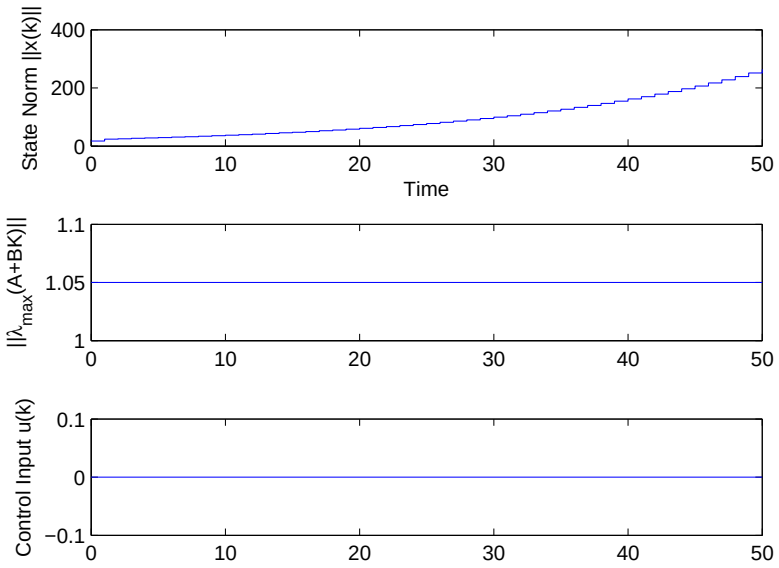

Figure 3.6 Closed-loop response for an unstable, scalar-input plant with $\alpha(k) \equiv 1$, $r = 1$, $\hat{K}(0) = 0$ and $\hat{B} = B$. The closed-loop system is unstable.

can be written as

$$x(1) = Ax(0), \tag{3.70}$$

$$\hat{K}(1) = -\frac{x^{\mathrm{T}}(1)\hat{B}}{\alpha(0) + \hat{B}^{\mathrm{T}}\hat{B}x^{\mathrm{T}}(0)x(0)}x^{\mathrm{T}}(0), \tag{3.71}$$

which further simplify to

$$x(1) = Ax(0), \tag{3.72}$$

$$\hat{K}(1) = -\frac{x^{\mathrm{T}}(0)A^{\mathrm{T}}\hat{B}}{\alpha(0) + \hat{B}^{\mathrm{T}}\hat{B}x^{\mathrm{T}}(0)x(0)}x^{\mathrm{T}}(0). \tag{3.73}$$

Since B lies in the null space of A^{T} and $\hat{B}$ is a scalar multiple of B, it follows that $A^{\mathrm{T}}\hat{B} = 0$, and hence, $\hat{K}(1) = 0$. In this case, the adaptive control algorithm doesn't compute a stabilizing feedback gain $\hat{K}(k)$ before $\hat{B}^{\mathrm{T}}x(k+1) = 0$. Therefore, since the open-loop system is unstable, the adaptive control algorithm does not stabilize the plant.

Now, we let $r = 2$ while keeping $\alpha(k) \equiv 1$, $\hat{K}(0) = 0$, and $\hat{B} = B$. The closed-loop response is shown in Figure 3.7, where, now the state x does go to zero. In this case $\hat{B}^{\mathrm{T}} x(k+1) \to 0$ as $k \to \infty$, but a stabilizing feedback gain $\hat{K}(k)$ is reached before the adaptive control gains converge. ■

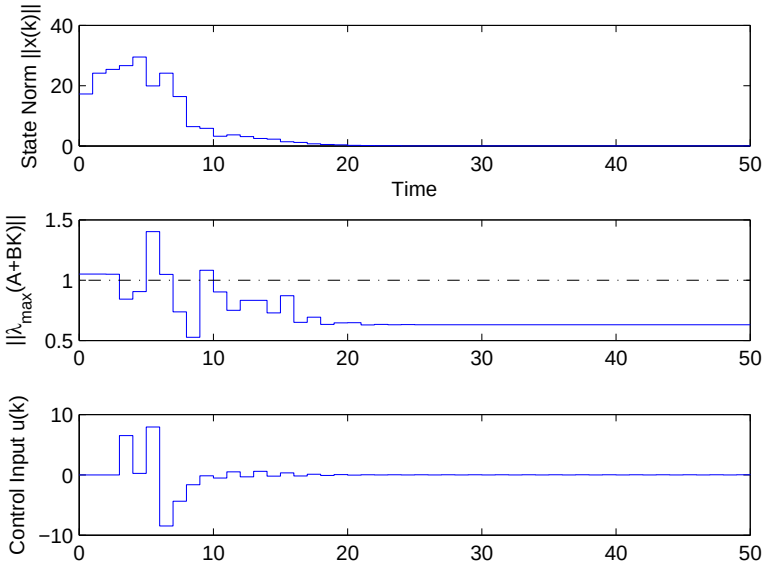

Figure 3.7 Closed-loop response for an unstable, scalar-input plant with $\alpha(k) \equiv 1$, $r = 2$, $\hat{K}(0) = 0$, and $\hat{B} = B$. The closed-loop system is stabilized.

Other cases can be constructed with similar properties to those of Example 3.8.1. It is found that $\hat{B}^{\mathrm{T}} x(k+1) \to 0$ as $k \to \infty$ whether or not $\hat{K}(k)$ is stabilizing. Therefore, in the cases where adaptation stops before a stabilizing feedback gain $\hat{K}(k)$ is computed, we must increase r. Based on numerical testing, Table 3.1 gives lower bounds on r, based on certain properties of the dynamics matrix A, that were found to stabilize all systems. In all cases, $r = n + 1$ was found to stabilize the open-loop system, though in many cases, $r = 1$ was sufficient. Although $r = n+1$ requires more knowledge of the Markov parameters than with $r = 1$, it is still less information than required to reconstruct a system model through techniques such as the eigenstructure realization algorithm (ERA), which generally requires $2n$ Markov parameters.

A	**Stable**	**Unstable**
Singular	$r \geq n+1$	$r \geq n+1$
Nonsingular	$r = 1$	$r \geq n+1$

Table 3.1 Guidelines for choosing r based on the properties of the dynamics matrix A to reach a stabilizing closed-loop feedback gain. In all cases, $r = n+1$ stabilizes the open-loop system, though in many cases, $r = 1$ is sufficient.

3.9 Conclusion

We presented a discrete-time, adaptive, full-state-feedback control algorithm based on retrospective cost optimization. We demonstrated the algorithm's effectiveness through numerical examples. We thus developed rules of thumb for choosing the parameters necessary for controller implementation.

A Lyapunov-based stability and convergence proof was presented for a special scalar case. Theoretical and numerical results suggest that the converged adaptive controller has a downward adaptive gain margin of 6 dB and an infinite upward adaptive gain margin. Future work includes extending the Lyapunov-based stability and convergence proof to the more general case to include multi-input, multi-dimensional plants with $r > 1$.

Chapter 4

Adaptive Retrospective-Cost-Based Static Output Feedback

The previous chapter considered retrospective-cost-based adaptive stabilization for systems with full-state feedback. In this chapter, we generalize those results to static-output-feedback stabilization. Specifically, this chapter considers retrospective-cost-based adaptive control for multi-input, multi-output, linear, time-invariant, discrete-time systems with knowledge of the sign of the high-frequency gain and a sufficient number of Markov parameters to approximate the nonminimum-phase zeros (if any). No additional information about the poles or zeros need be known. We also present numerical examples to illustrate the robustness of the algorithm under conditions of Markov parameter uncertainty. The results and methods of this chapter are published in [111].

4.1 Introduction

Given a linear, time-invariant system, the static-output-feedback problem is to find a stabilizing static feedback gain such that the closed-loop system with output feedback is asymptotically stable. While seemingly simple, this subject remains an

open problem in systems and control theory [13]. For full-state-feedback, as detailed in the previous chapter, a stabilizing feedback gain exists if the system is stabilizable. In the general output-feedback case, however, the conditions are much more subtle and further complicated by MIMO plants and the presence of transmission zeros. These issues are discussed in [121]

For a SISO plant, a stabilizing feedback gain can be found graphically through root locus or Nyquist techniques. Papers addressing MIMO static output feedback often require a minimum-phase assumption and/or a restriction on the plant's relative degree [121]. The minimum-phase assumption, while already not applicable to several real systems, added to a restriction on the plant's relative degree often leads to a strictly-positive-real (SPR) assumption, which is unrealistic and often impossible to prove in practice.

The most well-developed approach to the static-output-feedback problem is to use a pole-placement scheme, such as the algorithm in [105]. Other well-known approaches include eigenstructure assignment and the use of LQR for static-output-feedback [121]. Inverse linear quadratic approaches, such as [126], solve a modified LQR problem, but finding a solution to these problems can be difficult. Applying structural constraints [100] or coupled linear matrix inequalities (LMI) with quadratic Lyapunov functions [52] both lead to non-convex optimization problems, where iterative algorithms do not guarantee solution convergence.

The use of adaptive control for the static-output-feedback problem is motivated from the notion that this subject is still an open problem in systems and control theory [13]. The goal of this chapter is to present a discrete-time, adaptive, MIMO, static-output-feedback controller that is effective for systems that are unstable, nonsquare, and/or nonminimum-phase. The algorithm is developed in discrete time based on a discrete-time plant model obtained by either plant discretization or discrete-time system identification so that the controller can be implemented directly as embedded

code without an intermediate controller discretization step.

The adaptive controller presented in this chapter is based on retrospective cost optimization. This method is used to adapt dynamic compensators for disturbance rejection, adaptive stabilization, adaptive command following, and model reference adaptive control in [113, 127]. Retrospective cost optimization is a measure of performance at the current time based on a past window of data and without assumptions about the command or disturbance signals. In particular, retrospective cost optimization acts as an inner loop to the adaptive control algorithm by modifying the performance variables based on the difference between the actual past control inputs and the recomputed past control inputs based on the current control law.

We present numerical examples to illustrate the algorithm's effectiveness in handling systems that are unstable and/or nonminimum phase and to provide insight into the modeling information required for controller implementation. This information includes a sufficient number of Markov parameters to capture the sign of the high-frequency gain as well as to approximate the nonminimum-phase zeros (if any). These examples are intended to provide motivation for future proofs of stability and convergence.

4.2 Problem Formulation

Consider the MIMO discrete-time system

$$x(k+1) = Ax(k) + Bu(k), \tag{4.1}$$

$$y(k) = Cx(k), \tag{4.2}$$

$$z(k) = E_1 x(k), \tag{4.3}$$

where $x(k) \in \mathbb{R}^n$, $y(k) \in \mathbb{R}^{l_y}$, $z(k) \in \mathbb{R}^{l_z}$, $u(k) \in \mathbb{R}^{l_u}$, and $k \geq 0$. We assume that the open-loop system (4.1)-(4.3) is controllable and observable and that measurements of y and z are available for feedback. Our goal is to develop an adaptive static-output-feedback controller for performance stabilization, that is, convergence of the *performance variable* z to zero.

For a positive integer r, we define the *extended performance vector* $Z(k) \in \mathbb{R}^{l_z r}$ and the *extended input vector* $U(k) \in \mathbb{R}^{l_u r}$ by

$$Z(k) \triangleq \begin{bmatrix} z(k-r+1) \\ z(k-r+2) \\ \vdots \\ z(k) \end{bmatrix}, \quad U(k) \triangleq \begin{bmatrix} u(k-r) \\ u(k-r+1) \\ \vdots \\ u(k-1) \end{bmatrix}.$$

Note that $Z(k)$, $U(k)$, and $x(k)$ are related by

$$Z(k) = \Gamma x(k-r) + \mathcal{H} U(k), \tag{4.4}$$

where $\Gamma \in \mathbb{R}^{l_z r}$ and $\mathcal{H} \in \mathbb{R}^{l_z r \times l_u r}$ are given by

$$\Gamma \triangleq \begin{bmatrix} E_1 A \\ E_1 A^2 \\ \vdots \\ E_1 A^r \end{bmatrix}, \quad \mathcal{H} \triangleq \begin{bmatrix} H_1 & 0 & \cdots & 0 \\ H_2 & H_1 & \ddots & \vdots \\ \vdots & & \ddots & 0 \\ H_r & H_{r-1} & \cdots & H_1 \end{bmatrix},$$

and, for $i = 1, 2, \ldots$, the Markov parameters H_i of the system (4.1)–(4.3) from u to z are

$$H_i \triangleq E_1 A^{i-1} B. \tag{4.5}$$

Let d denote the *relative degree* of (A, B, E_1), that is, the smallest positive integer i such that the ith Markov parameter H_i is nonzero. Note that, if $r < d$, then $\mathcal{H} = 0$. Therefore, we assume that $r \geq d$.

4.3 Retrospective Cost Optimization

Let

$$u(k) = K(k)y(k), \tag{4.6}$$

where $K(k) \in \mathbb{R}^{l_u \times l_y}$ is the *gain matrix*. From (4.6), it follows that $U(k)$ can be rewritten as

$$U(k) = \sum_{i=1}^{r} L_i K(k-i)y(k-i), \tag{4.7}$$

where

$$L_i \triangleq \begin{bmatrix} 0_{(r-i)l_u \times l_u} \\ I_{l_u} \\ 0_{(i-1)l_u \times l_u} \end{bmatrix} \in \mathbb{R}^{l_u r \times l_u}. \tag{4.8}$$

Next, for $\mathcal{K} \in \mathbb{R}^{m \times n}$, define the *retrospective performance vector* $\hat{Z}(\mathcal{K}, k) \in \mathbb{R}^{l_z r}$ by

$$\hat{Z}(\mathcal{K}, k) \triangleq \Gamma x(k-r) + \mathcal{H}\hat{U}(\mathcal{K}, k), \tag{4.9}$$

where $\hat{U}(\mathcal{K}, k) \in \mathbb{R}^{l_u r}$ is the *recomputed input vector*, given by

$$\hat{U}(\mathcal{K}, k) \triangleq \sum_{i=1}^{r} L_i \mathcal{K} y(k-i). \tag{4.10}$$

Subtracting (4.4) from (4.9) yields

$$\hat{Z}(\mathcal{K},k) = Z(k) - \mathcal{H}\left[U(k) - \hat{U}(\mathcal{K},k)\right], \tag{4.11}$$

and hence,

$$\hat{Z}(\mathcal{K},k) = f(k) + D(k)\text{vec }\mathcal{K}, \tag{4.12}$$

where

$$f(k) \triangleq Z(k) - \mathcal{H}U(k) \in \mathbb{R}^{l_z r}, \tag{4.13}$$

$$D(k) \triangleq \sum_{i=1}^{r} y^{\mathrm{T}}(k-i) \otimes (\mathcal{H}L_i) \in \mathbb{R}^{l_z r \times l_u l_y}, \tag{4.14}$$

vec is the column-stacking operator, and $\otimes$ represents the Kronecker product.

Now consider the *retrospective cost function*

$$J(\mathcal{K},k) \triangleq \hat{Z}^{\mathrm{T}}(\mathcal{K},k)R_1(k)\hat{Z}(\mathcal{K},k) + \alpha(k)\text{tr}\left[(\mathcal{K}-K(k))^{\mathrm{T}}(\mathcal{K}-K(k))\right], \tag{4.15}$$

where, for all $k \geq 0$, $R_1(k) \in \mathbb{R}^{l_z r \times l_z r}$ is positive semidefinite and $\alpha(k) > 0$ is the *learning rate*. Substituting (4.12) into (4.15) yields

$$J(\mathcal{K},k) = c(k) + b^{\mathrm{T}}(k)\text{vec }\mathcal{K} + (\text{vec }\mathcal{K})^{\mathrm{T}} M(k)\text{vec}\mathcal{K}, \tag{4.16}$$

where

$$M(k) \triangleq D^{\mathrm{T}}(k)R_1(k)D(k) + \alpha(k)I_{l_u l_y}, \tag{4.17}$$

$$b(k) \triangleq 2D^{\mathrm{T}}(k)R_1(k)f(k) - 2\alpha(k)\text{vec }K(k), \tag{4.18}$$

$$c(k) \triangleq f^{\mathrm{T}}(k)R_1(k)f(k) + \alpha(k)\text{tr}\left[K^{\mathrm{T}}(k)K(k)\right]. \tag{4.19}$$

Since $M(k)$ is positive definite, $J(\mathcal{K}, k)$ has the strict global minimizer $K(k+1)$ given by

$$K(k+1) = -\frac{1}{2}\text{vec}^{-1}\left[M^{-1}(k)b(k)\right]. \tag{4.20}$$

Note that $M(k)$ and $b(k)$ depend on $D(k)$ and $f(k)$, which in turn depend on the Markov-parameter matrix $\mathcal{H}$. Since $\mathcal{H}$ may not be known in practice, we replace $\mathcal{H}$ by an estimate $\hat{\mathcal{H}}$ in $D(k)$, $f(k)$, and $K(k+1)$. Therefore, for all $k \geq 1$, the implemented control gain $\hat{K}(k)$ depends on $\hat{\mathcal{H}}$, that is

$$u(k) = \hat{K}(k)y(k), \tag{4.21}$$

$$\hat{K}(k+1) \triangleq -\frac{1}{2}\text{vec}^{-1}\left[\hat{M}^{-1}(k)\hat{b}(k)\right], \tag{4.22}$$

where

$$\hat{M}(k) \triangleq \hat{D}^{\mathrm{T}}(k)R_1(k)\hat{D}(k) + \alpha(k)I_{l_u l_y}, \tag{4.23}$$

$$\hat{b}(k) \triangleq 2\hat{D}^{\mathrm{T}}(k)R_1(k)\hat{f}(k) - 2\alpha(k)\text{vec}\ \hat{K}(k), \tag{4.24}$$

and

$$\hat{f}(k) \triangleq Z(k) - \hat{\mathcal{H}}U(k), \tag{4.25}$$

$$\hat{D}(k) \triangleq \sum_{i=1}^{r} y^{\mathrm{T}}(k-i) \otimes (\hat{\mathcal{H}}L_i), \tag{4.26}$$

$$\hat{\mathcal{H}} \triangleq \begin{bmatrix} \hat{H}_1 & 0 & \cdots & 0 \\ \hat{H}_2 & \hat{H}_1 & \ddots & \vdots \\ \vdots & & \ddots & 0 \\ \hat{H}_r & \hat{H}_{r-1} & \cdots & \hat{H}_1 \end{bmatrix}, \tag{4.27}$$

where, for all $i = 1, \ldots, r$, $\hat{H}_i$ is an estimate of H_i. For convenience, we specialize

(4.17)–(4.19) and (4.23), (4.24) with $R_1(k) \triangleq I_{l_z r}$.

The learning rate $\alpha(k)$ affects convergence speed of the adaptive control algorithm. As $\alpha(k)$ is increased, convergence speed is lowered. Likewise, as $\alpha(k)$ is decreased, convergence speed is raised. By varying $\alpha(k)$, we study tradeoffs between transient performance and convergence speed.

4.4 Static-Output-Feedback Examples

We now present numerical examples to investigate the effect of r and $\alpha(k)$ as well as the accuracy of $\hat{\mathcal{H}}$ on the adaptive control algorithm. The adaptive controller gains are initialized to zero, that is $\hat{K}(0) = 0$. Unless otherwise noted, we take $z(k) = y(k)$.

Example 4.4.1 (SISO, minimum-phase, asymptotically stable plant)**.** *Consider the asymptotically stable, minimum-phase plant*

$$x(k+1) = \begin{bmatrix} -0.4 & 0.33 & 0.76 \\ 1 & 0 & 0 \\ 0 & 1 & 0 \end{bmatrix} x(k) + \begin{bmatrix} 1 \\ 0 \\ 0 \end{bmatrix} u(k), \tag{4.28}$$

$$y(k) = \begin{bmatrix} 0 & 1 & -0.25 \end{bmatrix} x(k), \tag{4.29}$$

with poles $\{-0.65 \pm 0.65\jmath, 0.9\}$ *and zero* $\{0.25\}$*. The first 25 Markov parameters are shown in Figure 4.1.*

We investigate the effect of r *on the closed-loop response. Table 4.1 lists the roots of the Markov parameter polynomial* $p_r(\boldsymbol{q})$ *(as defined in* (A.10)*) as a function of* r*. Note that, since* $d = 2$*, we must choose* $r \geq 2$*, and, as* r *increases,* $p_r(\boldsymbol{q})$ *contains spurious roots, none of which approximates the zero. We consider* $r = 2$*,* $r = 3$*, or* $r = 4$ *with* $\alpha(k) \equiv 50$*. The open and closed-loop responses are shown in Figure 4.2 for* $x(0) = [-4.3, -16.7, 1.3]^{\mathrm{T}}$*. In each case, the adaptive controller reduces* z *faster than*

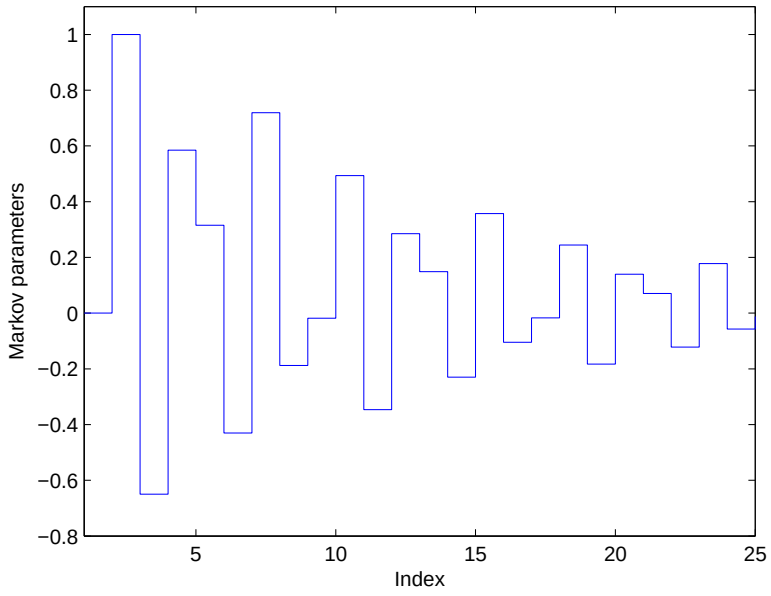

Figure 4.1 First 25 Markov parameters for the asymptotically stable, minimum-phase plant in Example 4.4.1.

r	$\mathbf{roots}(p_r(\mathbf{q}))$
2	$\{\cdot\}$
3	$\{0.65\}$
4	$\{0.33 \pm 0.69\jmath\}$
5	$\{-0.34, 0.50 \pm 0.82\jmath\}$

Table 4.1 Roots of $p_r(\mathbf{q})$ as a function of r for the asymptotically stable, minimum-phase plant in Example 4.4.1.

the open-loop response. As r increases from 2 to 3, the adaptive controller reduces z faster, but no additional performance is gained by increasing r from 3 to 4. ■

Example 4.4.2 (SISO, nonminimum-phase, asymptotically stable plant)**.** *Consider the asymptotically stable, nonminimum-phase plant*

$$x(k+1) = \begin{bmatrix} -0.4 & 0.33 & 0.76 \\ 1 & 0 & 0 \\ 0 & 1 & 0 \end{bmatrix} x(k) + \begin{bmatrix} 1 \\ 0 \\ 0 \end{bmatrix} u(k), \tag{4.30}$$

$$y(k) = \begin{bmatrix} 0 & 1 & -2 \end{bmatrix} x(k), \tag{4.31}$$

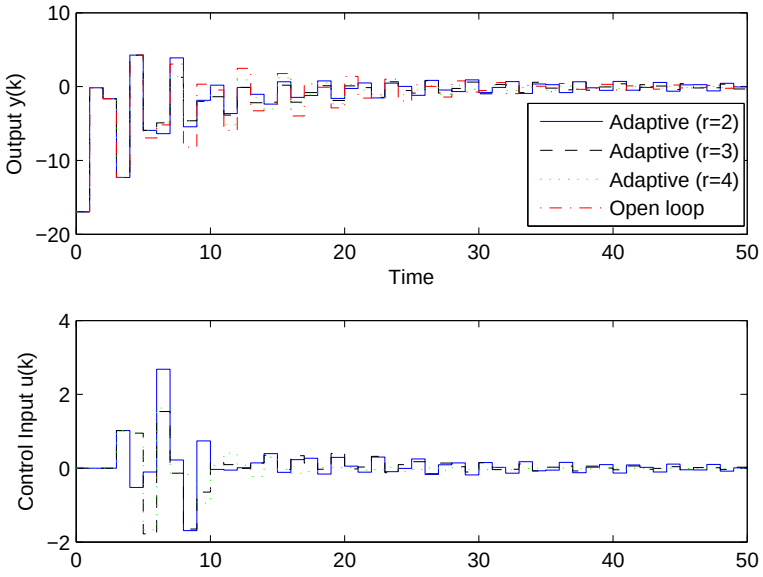

Figure 4.2 Closed-loop response for the asymptotically stable, minimum-phase, SISO plant in Example 4.4.1 with $\alpha(k) \equiv 50$ and either $r = 2$, $r = 3$, or $r = 4$. In each case, the adaptive controller reduces z faster than the open-loop response. As r increases from 2 to 3, the adaptive controller reduces z faster, but no additional performance is gained by increasing r from 3 to 4.

with poles $\{-0.65 \pm 0.65\jmath, 0.9\}$ *and zero* $\{2\}$. *The first 25 Markov parameters are shown in Figure 4.3.*

We demonstrate the effect of r *for this nonminimum-phase plant. Table 4.2 lists the roots of the Markov-parameter polynomial* $p_r(\boldsymbol{q})$ *as a function of* r. *It is seen that the roots of the Markov parameter polynomial include an estimate of the nonminimum-phase zero of the transfer function from* u *to* z. *As* r *increases, this approximation improves. For each value of* r, *the remaining roots play no role in the stability and convergence of the adaptive control algorithm, but what is important is the need to choose* r *sufficiently large to adequately approximate the nonminimum-phase zeros. Note that, as* r *increases, the nonminimum-phase zero at* $\boldsymbol{z} = 2$ *is more accurately modeled, but* $p_r(\boldsymbol{q})$ *also contains spurious roots, although these roots have no effect on the adaptive controller. For* $r \leq 3$, *the closed-loop simulation fails. We thus take* $r = 4$, $r = 5$, *or* $r = 6$ *with* $\alpha(k) \equiv 50$. *The open and closed-loop responses are shown*

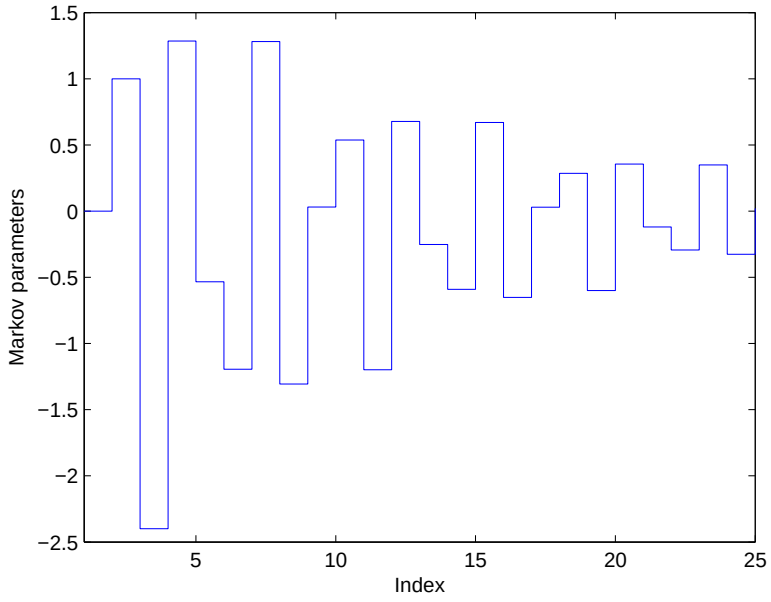

Figure 4.3 First 25 Markov parameters for the asymptotically stable, nonminimum-phase plant in Example 4.4.2.

r	$\mathbf{roots}(p_r(\mathbf{q}))$
3	$\{\mathbf{2.4}\}$
4	$\{0.81,\mathbf{1.59}\}$
5	$\{0.27\pm0.46\jmath,\mathbf{1.86}\}$
6	$\{-0.55,0.46\pm0.92\jmath,\mathbf{2.04}\}$

Table 4.2 Roots of $p_r(\mathbf{q})$ as a function of r for the asymptotically stable, nonminimum-phase plant in Example 4.4.2. As r increases, the nonminimum-phase zero at $\mathbf{z} = 2$ is more accurately modeled.

in Figure 4.4 for $x(0) = [-4.3, -16.7, 1.3]^{\mathrm{T}}$. *In each case, the adaptive controller reduces* z *faster than the open-loop response. In addition, as* r *increases, and thus the nonminimum-phase zero is more accurately modeled, the adaptive controller reduces* z *even faster.* ■

Example 4.4.3 (SISO, nonminimum-phase, unstable plant)**.** *Consider the unstable,*

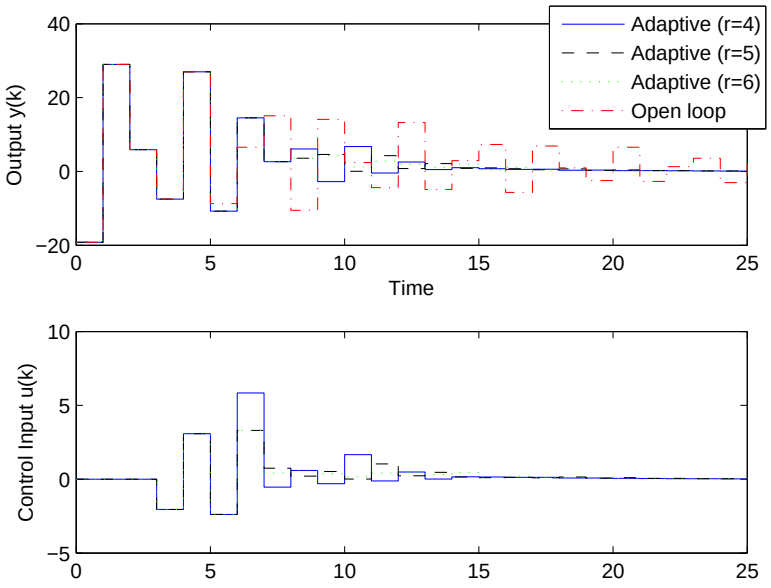

Figure 4.4 Closed-loop response for the asymptotically stable, nonminimum-phase, SISO plant in Example 4.4.2 with $\alpha(k) \equiv 50$ and either $r = 4$, $r = 5$, or $r = 6$. In each case, the adaptive controller reduces z faster than the open-loop response. In addition, as r increases, and thus the nonminimum-phase zero is more accurately modeled, the adaptive controller reduces z even faster.

nonminimum-phase plant

$$x(k+1) = \begin{bmatrix} -0.36 & 0.48 & 1.05 \\ 1 & 0 & 0 \\ 0 & 1 & 0 \end{bmatrix} x(k) + \begin{bmatrix} 1 \\ 0 \\ 0 \end{bmatrix} u(k), \tag{4.32}$$

$$y(k) = \begin{bmatrix} 0 & 1 & -4 \end{bmatrix} x(k), \tag{4.33}$$

$$z(k) = \begin{bmatrix} 1 & 1 & -6 \end{bmatrix} x(k), \tag{4.34}$$

with poles $\{-\sqrt{2}/2 \pm \sqrt{2}/2, 1.05\}$, *zeros* $\{2, -3\}$ *from* u *to* z, *and zero* $\{4\}$ *from* u *to* y. *Table 4.3 lists the roots of the Markov-parameter polynomial* $p_r(\boldsymbol{q})$ *as a function of* r. *Note that, as* r *increases, the nonminimum-phase zeros are more accurately modeled, but* $p_r(\boldsymbol{q})$ *also contains additional spurious roots. For* $r \leq 3$, *the closed-loop simulation fails. We thus take* $r = 4$ *and set* $\alpha(k) \equiv 100$. *The open and closed-loop*

r	$\mathbf{roots}(p_r(\mathbf{q}))$
3	{**2.1**,**-2.74**}
4	{0.73,**1.6**,**-2.97**}
5	{0.274±0.72$\jmath$,**1.91**,**-3.03**}
6	{-0.49,0.43±0.94$\jmath$,**2.0**,**-3.01**}

Table 4.3 Roots of $p_r(\mathbf{q})$ as a function of r for the unstable, nonminimum-phase plant in Example 4.4.3. As r increases, the nonminimum-phase zeros are more accurately modeled.

responses are shown in Figure 4.5 for $x(0) = [-4.3, -16.7, 1.3]^{\mathrm{T}}$. *The adaptive controller stabilizes the plant.* ■

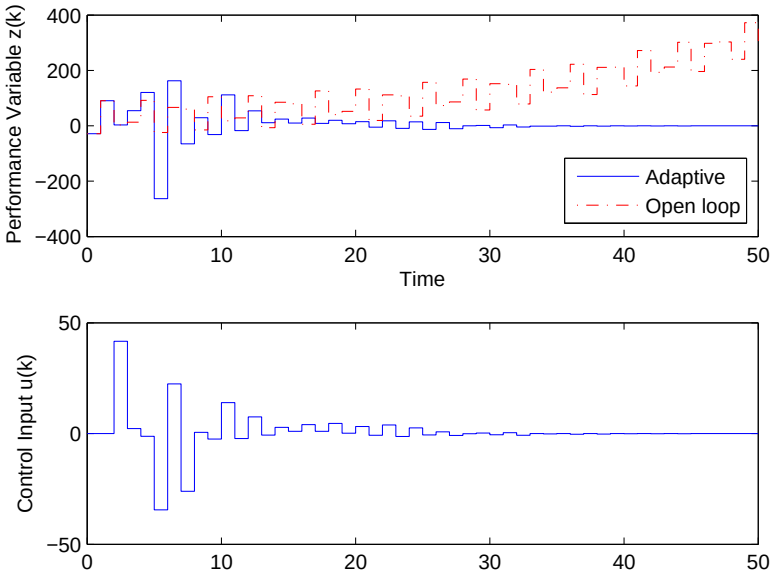

Figure 4.5 Closed-loop response for the unstable, nonminimum-phase, SISO plant in Example 4.4.3 with $\alpha(k) \equiv 100$ and $r = 4$. The adaptive controller stabilizes the plant.

These results, along with those of Example 4.4.2, suggest that, for nonminimum-phase plants, the adaptive controller requires a sufficient number of Markov parameters to capture the approximate locations of any nonminimum-phase zeros. In particular, Examples 4.4.2 and 4.4.3 require $r \geq n+1$. This bound is consistent with the numerical results of Chapter 3, and, in particular, Table 3.1. Furthermore, as seen from Tables 4.2 and 4.3, as the order of the Markov-parameter polynomial increases,

and hence r increases, the accuracy of all nonminimum-phase zeros improves.

Example 4.4.4 (SISO, non/minimum-phase, unstable plant)**.** *Consider the unstable plant with both minimum-phase and nonminimum-phase zeros, given by*

$$x(k+1) = \begin{bmatrix} -0.36 & 0.48 & 1.05 \\ 1 & 0 & 0 \\ 0 & 1 & 0 \end{bmatrix} x(k) + \begin{bmatrix} 1 \\ 0 \\ 0 \end{bmatrix} u(k), \tag{4.35}$$

$$y(k) = \begin{bmatrix} 0 & 1 & -2 \end{bmatrix} x(k), \tag{4.36}$$

$$z(k) = \begin{bmatrix} 0 & 1 & -0.1 \end{bmatrix} x(k), \tag{4.37}$$

with poles $\{-\sqrt{2}/2 \pm \sqrt{2}/2, 1.05\}$*, zero* $\{0.1\}$ *from* u *to* z*, and zero* $\{2\}$ *from* u *to* y*. Note that the transfer function from* u *to* y *contains a nonminimum-phase zero while the transfer function from* u *to* z *is minimum phase. We take* $\alpha(k) \equiv 500$ *and* $r = 2$*. The open and closed-loop responses are shown in Figure 4.6 for* $x(0) = [-4.3, -16.7, 1.3]^{\mathrm{T}}$*. The adaptive controller stabilizes the plant.* ■

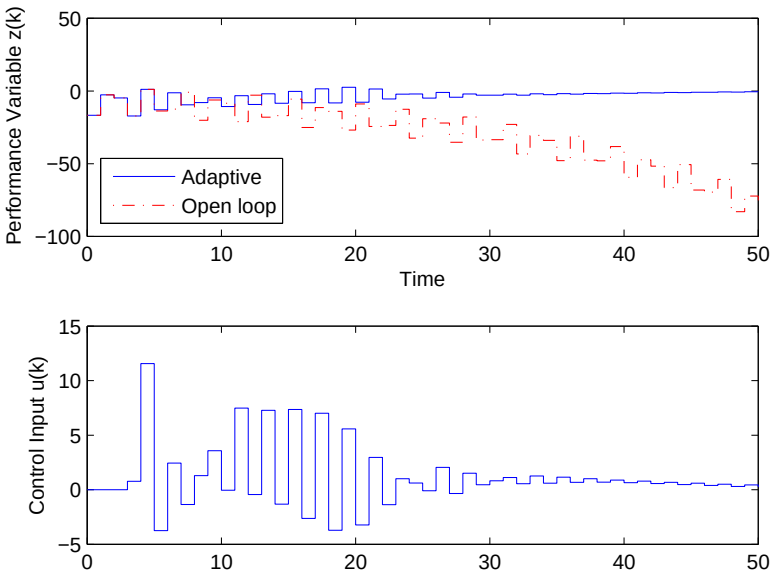

Figure 4.6 Closed-loop response for the unstable, non/minimum-phase, SISO plant in Example 4.4.4 with $\alpha(k) \equiv 500$ and $r = 2$. The adaptive controller stabilizes the plant.

Example 4.4.5 (SISO, minimum-phase, Lyapunov-stable plant)**.** *Consider a discrete-time model of a laboratory process obtained using identification techniques [70]. A state-space model for this system sampled at* $T_{\mathrm{s}} = 0.08\,\mathrm{sec}$ *is given by*

$$x(k+1) = \begin{bmatrix} 1.2885 & 1 & 6.555 & 0 \\ -0.4065 & 0 & 4.383 & 0 \\ 0 & 0 & 1 & 1 \\ 0 & 0 & 0 & 0 \end{bmatrix} x(k) + \begin{bmatrix} 0 \\ 0 \\ 0 \\ 1 \end{bmatrix} u(k), \tag{4.38}$$

$$y(k) = \begin{bmatrix} 1 & 0 & 0 & 0 \end{bmatrix} x(k). \tag{4.39}$$

This system is minimum phase and Lyapunov stable. A root locus plot is shown in Figure 4.7, where the range of stabilizing output-feedback gain is $-3.7\times10^{-3} < K < 0$*. We take* $\alpha(k) \equiv 10^8$ *and* $r = 3$*. The open and closed-loop responses are shown in Figure 4.8 for* $x(0) = [-0.43, -1.67, 0.13, 0.29]^{\mathrm{T}}$*. The adaptive controller stabilizes the plant, and the output-feedback gain converges to the steady-state value* -1.5×10^{-3}*.*

■

4.5 Conclusion

We presented a discrete-time, adaptive, static-output-feedback control algorithm based on retrospective cost optimization. We demonstrated the algorithm's effectiveness in handling nonminimum-phase zeros through numerical examples illustrating the response of the algorithm under conditions of uncertainty. We thus developed rules of thumb for choosing the parameters necessary for controller implementation. These numerical studies serve as motivation for future development of Lyapunov-based stability, robustness, and convergence proofs of the adaptive control algorithm.

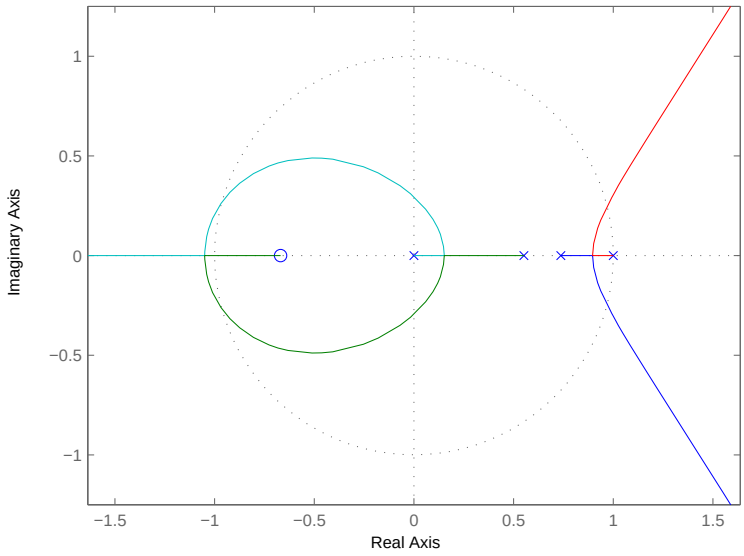

Figure 4.7 Root locus plot for the Lyapunov-stable, minimum-phase, SISO plant in Example 4.4.5. The range of stabilizing output-feedback gain is $-3.7 \times 10^{-3} < K < 0$.

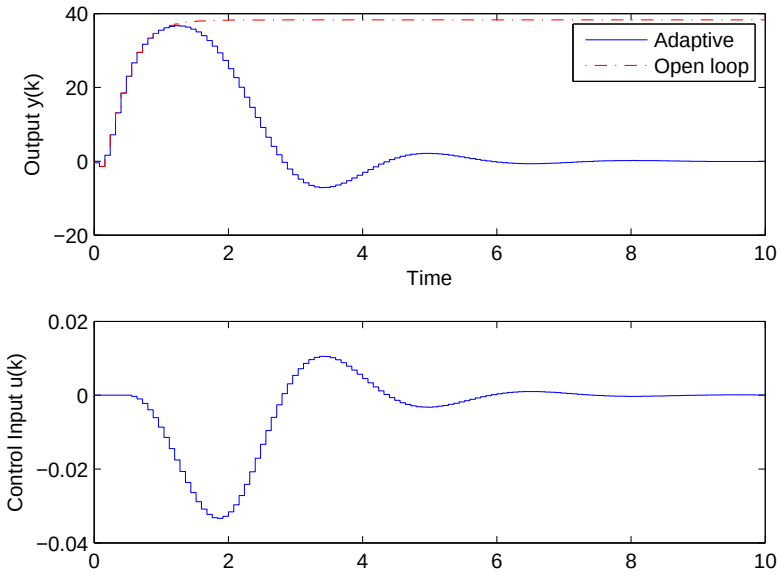

Figure 4.8 Closed-loop response for the Lyapunov-stable, minimum-phase, SISO plant in Example 4.4.5 with $\alpha(k) \equiv 10^8$ and $r = 3$. The adaptive controller stabilizes the plant, and the output-feedback gain converges to the steady-state value -1.5×10^{-3}.

Chapter 5

Adaptive Retrospective-Cost-Based Dynamic Compensation

The previous two chapters considered retrospective-cost-based adaptive stabilization for systems with static feedback. In this chapter, we generalize the results to dynamic compensation for stabilization, command following, disturbance rejection, and model reference adaptive control (MRAC). Specifically, this chapter considers retrospective-cost-based adaptive control for multi-input, multi-output, linear, time-invariant, discrete-time systems with knowledge of the sign of the high-frequency gain and a sufficient number of Markov parameters to approximate the nonminimum-phase zeros (if any). No additional information about the poles or the zeros need be known.

The adaptive control algorithm presented in this chapter is based on the adaptive control algorithm developed in [127]. The algorithm developed in [127] uses a gradient-based update with a fixed step-size. In contrast, the algorithms presented in Chapters 3-5 of this dissertation utilize an adjustable learning-rate parameter α which allows us to develop Newton-step-based adaptive update laws. In addition, this chapter further develops the theoretical link between Markov parameters and nonminimum-phase zeros. The development and analysis of this link is detailed in Appendix A. We also develop preliminary metrics for analyzing the gain and phase

margins for discrete-time adaptive systems. Finally, we present numerical examples to illustrate the robustness of the algorithm under conditions of uncertainty. The adaptive control algorithm is shown to be effective for systems that are unstable, MIMO, and/or nonminimum phase. The results and methods of this chapter are published in [113, 114]. In [117], the adaptive control algorithm developed in this chapter is used to identify multi-input, multi-output, linear, time-invariant, discrete-time systems.

5.1 Introduction

Unlike robust control, which fixes the control gains based on a prior, fixed level of modeling uncertainty, adaptive control algorithms tune the feedback gains in response to the true plant and exogenous signals, that is, commands and disturbances. Generally speaking, adaptive controllers require less prior modeling information than robust controllers, and thus can be viewed as highly parameter-robust control laws. The price paid for the ability of adaptive control laws to operate with limited prior modeling information is the complexity of analyzing and quantifying the stability and performance of the closed-loop system, especially in light of the fact that adaptive control laws, even for linear plants, are nonlinear.

Stability and performance analysis of adaptive control laws often entails assumptions on the dynamics of the plant. For example, a widely invoked assumption in adaptive control is passivity [90], which is restrictive and difficult to verify in practice. A related assumption is that the plant is minimum phase [33, 45], which may entail the same difficulties. In fact, sampled-data control may give rise to nonminimum-phase zeros whether or not the continuous-time system is minimum phase [8]. Beyond these assumptions, adaptive control laws are known to be sensitive to unmodeled dynamics and sensor noise [9, 104], which motivates robust adaptive control laws [50].

In addition to these basic issues, adaptive control laws may entail unaccept-

able transients during adaptation, which may be exacerbated by actuator limitations [60, 98, 135]. In fact, adaptive control under extremely limited modeling information such as uncertainty in the high-frequency gain [64, 69] may yield a transient response that exceeds the practical limits of the plant. Therefore, the type and quality of the available modeling information as well as the speed of adaptation must be considered in the analysis and implementation of adaptive control laws. These issues are discussed in [5].

Adaptive control laws have been developed in both continuous time and discrete time. In the present chapter we consider discrete-time adaptive control laws since these control laws can be implemented directly in embedded code without requiring an intermediate discretization step with potential loss of phase margin. Although discrete-time adaptive control laws are less developed than their continuous-time counterparts, the literature is substantial and growing [3, 32, 33, 35, 55, 77].

The goal of this chapter is to present a discrete-time adaptive control law that is effective for nonminimum-phase systems. In [33], a discrete-time adaptive control law with stability guarantees was developed under a minimum-phase assumption. Extensions given in Chapter 2 based on internal model control [44] and Lyapunov analysis also invoke this assumption. To circumvent the minimum-phase assumption, the zero annihilation periodic control law [10] uses lifting to move all of the plant's zeros to the origin.

The present chapter is motivated by the adaptive control laws given in Chapter 2, [45], and [127]. The control law given in [127] lacks a proof of stability, but is known numerically to be effective on nonminimum-phase plants without recourse to lifting. Accordingly, we present an adaptive control law based on [45] and [127] for systems that are unstable, MIMO, and/or nonminimum phase. The adaptive control algorithm provides guidelines concerning the modeling information needed for implementation. This information includes a sufficient number of Markov parameters to

capture the sign of the high-frequency gain as well as the nonminimum-phase zeros (if any). No additional information about the plant need be known.

The novel feature of this adaptive control law is the use of a retrospective correction filter (RCF). The RCF provides an inner loop to the adaptive control law by modifying the sensor measurements based on the difference between the actual past control inputs and the recomputed past control inputs based on the current control law. This technique is inherent in [127] in the use of the estimated performance variable, but is more fully developed in the present chapter.

The goal of the present chapter is to develop the RCF adaptive control algorithm and demonstrate its effectiveness in handling nonminimum-phase zeros. We thus present several numerical examples to illustrate the response of the algorithm under conditions of uncertainty in the relative degree and Markov parameters, measurement noise, and actuator and sensor saturations. To this end we systematically consider a sequence of examples of increasing complexity, ranging from SISO, minimum-phase plants to MIMO, nonminimum-phase plants, including stable and unstable cases. We then revisit these plants under off-nominal conditions, that is, with uncertainty in the required plant modeling information. In each case, we illuminate the role of the weighting parameter α, which governs the rate of convergence. Our goal is thus to develop rules of thumb for choosing α based on the level of model fidelity.

5.2 Problem Formulation

Consider the MIMO discrete-time system

$$x(k+1) = Ax(k) + Bu(k) + D_1 w(k), \tag{5.1}$$

$$y(k) = Cx(k) + D_2 w(k), \tag{5.2}$$

$$z(k) = E_1 x(k) + E_0 w(k), \tag{5.3}$$

where $x(k) \in \mathbb{R}^n$, $y(k) \in \mathbb{R}^{l_y}$, $z(k) \in \mathbb{R}^{l_z}$, $u(k) \in \mathbb{R}^{l_u}$, $w(k) \in \mathbb{R}^{l_w}$, and $k \geq 0$. Our goal is to develop an adaptive output feedback controller under which the performance variable z is minimized in the presence of the exogenous signal w. Note that w can represent either a command signal to be followed, an external disturbance to be rejected, or both. For example, if $D_1 = 0$ and $E_0 \neq 0$, then the objective is to have the output $E_1 x$ follow the command signal $-E_0 w$. On the other hand, if $D_1 \neq 0$ and $E_0 = 0$, then the objective is to reject the disturbance w from the performance measurement $E_1 x$. The combined command following and disturbance rejection problem is addressed when D_1 and E_0 are block matrices. More precisely, if $D_1 = \left[\begin{array}{cc} \hat{D}_1 & 0 \end{array} \right]$, $E_0 = \left[\begin{array}{cc} 0 & \hat{E}_0 \end{array} \right]$, and $w(k) = \left[\begin{array}{c} w_1(k) \\ w_2(k) \end{array} \right]$, then the objective is to have $E_1 x$ follow the command $-\hat{E}_0 w_2$ while rejecting the disturbance w_1. Lastly, if D_1 and E_0 are empty matrices, then the objective is output stabilization, that is, convergence of z to zero. We assume that the open-loop system (5.1)-(5.3) is controllable and observable and that measurements of y and z are available for feedback.

Model reference adaptive control (MRAC) is a special case of (5.1)–(5.3) where $z \triangleq y_1 - y_{\mathrm{m}}$ is the difference between the measured output of the plant G and reference model G_{m}. For MRAC, the exogenous command w is available to the controller as an additional measurement variable y_2, as shown in Figure 5.1.

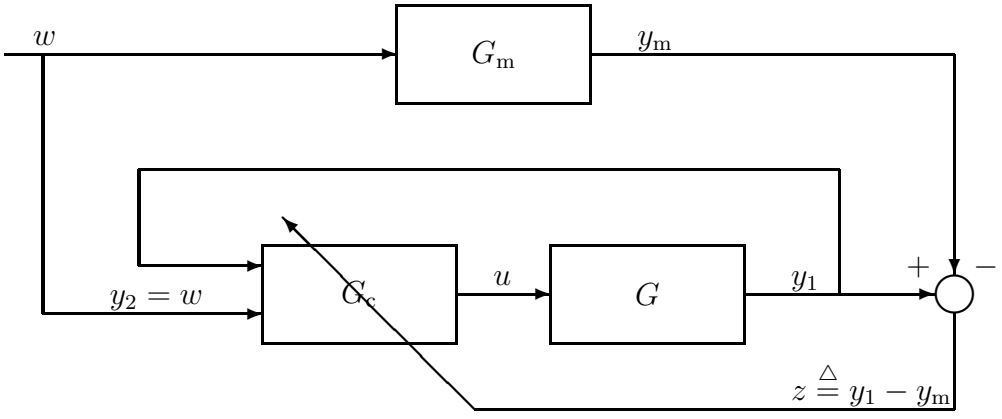

Figure 5.1 Model reference adaptive control problem.

5.3 Time-Series Modeling

Consider the time-series representation of (5.1)–(5.3) from u to z, given by

$$z(k) = \sum_{i=1}^{n} -\alpha_i z(k-i) + \sum_{i=d}^{n} \beta_i u(k-i) + \sum_{i=0}^{n} \gamma_i w(k-i), \tag{5.4}$$

where $\alpha_1, \ldots, \alpha_n \in \mathbb{R}$, $\beta_d, \ldots, \beta_n \in \mathbb{R}^{l_z \times l_u}$, $\gamma_0, \ldots, \gamma_n \in \mathbb{R}^{l_z \times l_w}$, and the *relative degree* d is the smallest positive integer i such that the ith Markov parameter $H_i \triangleq E_1 A^{i-1} B$ is nonzero.

Replacing k with $k-1$ in (5.4) and substituting the resulting relation back into (5.4) yields a *2-MARKOV* model. Repeating this procedure $r-1$ times yields the r-MARKOV model of (5.1)–(5.3)

$$\begin{aligned} z(k) = {} & \sum_{i=1}^{n} \alpha_{r,i} z(k-r-i+1) + \sum_{i=d}^{r} H_i u(k-i) + \sum_{i=2}^{n} \beta_{r,i} u(k-r-i+1) \\ & + \sum_{i=0}^{r} H_{zw,i} w(k-i) + \sum_{i=2}^{n} \gamma_{r,i} w(k-r-i+1), \end{aligned} \tag{5.5}$$

where $H_{zw,0} \triangleq E_0$, for all $i > 0$, $H_{zw,i} \triangleq E_1 A^{i-1} D_1$, and, for $i = 1, \ldots, n$, the coefficients $\alpha_{r,i} \in \mathbb{R}$, $\beta_{r,i} \in \mathbb{R}^{l_z \times l_u}$, and $\gamma_{r,i} \in \mathbb{R}^{l_z \times l_w}$ are given by

$$\begin{array}{lll} \alpha_{1,i} \triangleq -\alpha_i, & \beta_{1,i} \triangleq \beta_i, & \gamma_{1,i} \triangleq \gamma_i, \\ \vdots & \vdots & \vdots \\ \alpha_{r,i} \triangleq \alpha_{r-1,1}\alpha_{1,i} + \alpha_{r-1,i+1}, & \beta_{r,i} \triangleq \alpha_{r-1,1}\beta_{1,i} + \beta_{r-1,i+1}, & \gamma_{r,i} \triangleq \alpha_{r-1,1}\gamma_{1,i} + \gamma_{r-1,i+1}, \\ \vdots & \vdots & \vdots \\ \alpha_{r,n} \triangleq \alpha_{r-1,1}\alpha_{1,n}, & \beta_{r,n} \triangleq \alpha_{r-1,1}\beta_{1,n}, & \gamma_{r,n} \triangleq \alpha_{r-1,1}\gamma_{1,n}. \end{array} \tag{5.6}$$

Note that $H_r = \beta_{r,1}$ and $H_{zw,r} = \gamma_{r,1}$.

For a positive integer p, we define the *extended performance vector* $Z(k) \in \mathbb{R}^{pl_z}$

and the *extended control vector* $U(k) \in \mathbb{R}^{p_c l_u}$ by

$$Z(k) \triangleq \begin{bmatrix} z(k) \\ \vdots \\ z(k-p+1) \end{bmatrix}, \quad U(k) \triangleq \begin{bmatrix} u(k) \\ \vdots \\ u(k-p_c+1) \end{bmatrix}. \tag{5.7}$$

where $p_c \triangleq n + r + p - 1$. Then, (5.4) can be written in the form

$$Z(k) = W_{zw}\phi_{zw}(k) + B_{zu}U(k), \tag{5.8}$$

where

$$W_{zw} \triangleq \begin{bmatrix} -\alpha_{r,1}I_{l_z} & \cdots & -\alpha_{r,n}I_{l_z} & 0_{l_z} & \cdots & 0_{l_z} & H_{zw,0} & \cdots \\ 0_{l_z} & \ddots & & \ddots & \ddots & \vdots & 0_{l_z \times l_w} & \ddots \\ \vdots & \ddots & \ddots & & \ddots & 0_{l_z} & \vdots & \ddots \\ 0_{l_z} & \cdots & 0_{l_z} & -\alpha_{r,1}I_{l_z} & \cdots & -\alpha_{r,n}I_{l_z} & 0_{l_z \times l_w} & \cdots \end{bmatrix}$$

$$\begin{bmatrix} \cdots & H_{zw,r} & \gamma_{r,2} & \cdots & \gamma_{r,n} & 0_{l_z \times l_w} & \cdots & 0_{l_z \times l_w} \\ \ddots & & \ddots & \ddots & & \ddots & \ddots & \vdots \\ \ddots & \ddots & & \ddots & \ddots & & \ddots & 0_{l_z \times l_w} \\ \cdots & 0_{l_z \times l_w} & H_{zw,0} & \cdots & H_{zw,r} & \gamma_{r,2} & \cdots & \gamma_{r,n} \end{bmatrix},$$

$$B_{zu} \triangleq \begin{bmatrix} 0_{l_z \times l_u} & \cdots & 0_{l_z \times l_u} & H_d & \cdots & H_r & \beta_{r,2} & \cdots & \beta_{r,n} & 0_{l_z \times l_u} & \cdots & 0_{l_z \times l_u} \\ 0_{l_z \times l_u} & \ddots & & \ddots & \ddots & & \ddots & \ddots & & \ddots & \ddots & \vdots \\ \vdots & \ddots & \ddots & & \ddots & \ddots & & \ddots & \ddots & & \ddots & 0_{l_z \times l_u} \\ 0_{l_z \times l_u} & \cdots & 0_{l_z \times l_u} & 0_{l_z \times l_u} & \cdots & 0_{l_z \times l_u} & H_d & \cdots & H_r & \beta_{r,2} & \cdots & \beta_{r,n} \end{bmatrix},$$

and

$$\phi_{zw}(k) \triangleq \begin{bmatrix} z(k-r) \\ \vdots \\ z(k-r-p-n+2) \\ w(k) \\ \vdots \\ w(k-r-p-n+2) \end{bmatrix}. \tag{5.9}$$

5.4 Controller Construction

In this section we formulate an adaptive control algorithm for the general control problem represented by (5.1)–(5.3). We use a strictly proper time-series controller of order n_c, such that the control $u(k)$ is given by

$$u(k) = \sum_{i=1}^{n_c} P_i(k)u(k-i) + \sum_{i=1}^{n_c} Q_i(k)y(k-i), \tag{5.10}$$

where, for all $i = 1, \ldots, n_c$, $P_i(k) \in \mathbb{R}^{l_u \times l_u}$ and $Q_i(k) \in \mathbb{R}^{l_u \times l_y}$. The control (5.10) can be expressed as

$$u(k) = \theta(k)\phi(k), \tag{5.11}$$

where

$$\theta(k) \triangleq \begin{bmatrix} Q_1(k) & \cdots & Q_{n_c}(k) & P_1(k) & \cdots & P_{n_c}(k) \end{bmatrix} \in \mathbb{R}^{l_u \times n_c(l_u+l_y)} \tag{5.12}$$

is the *controller gain matrix*, and the *regressor vector* $\phi(k)$ is given by

$$\phi(k) \triangleq \begin{bmatrix} y(k-1) \\ \vdots \\ y(k-n_{\mathrm{c}}) \\ u(k-1) \\ \vdots \\ u(k-n_{\mathrm{c}}) \end{bmatrix} \in \mathbb{R}^{n_{\mathrm{c}}(l_u+l_y)}. \tag{5.13}$$

From (5.11), it follows that the extended control vector $U(k)$ can be written as

$$U(k) = \sum_{i=1}^{p_{\mathrm{c}}} L_i \theta(k-i+1)\phi(k-i+1), \tag{5.14}$$

where

$$L_i \triangleq \begin{bmatrix} 0_{(i-1)l_u \times l_u} \\ I_{l_u} \\ 0_{(p_{\mathrm{c}}-i)l_u \times l_u} \end{bmatrix} \in \mathbb{R}^{p_{\mathrm{c}} l_u \times l_u}. \tag{5.15}$$

Next, we define the *retrospective performance vector* $\hat{Z}(\hat{\theta}, k) \in \mathbb{R}^{pl_z}$ by

$$\hat{Z}(\hat{\theta}, k) \triangleq W_{zw}\phi_{zw}(k) + B_{zu}U(k) - \bar{B}_{zu}\left[U(k) - \hat{U}(\hat{\theta}, k)\right], \tag{5.16}$$

where $\hat{\theta} \in \mathbb{R}^{l_u \times n_{\mathrm{c}}(l_u+l_y)}$, $\bar{B}_{zu} \in \mathbb{R}^{pl_z \times p_{\mathrm{c}} l_u}$ is the *surrogate input matrix*, and

$$\hat{U}(\hat{\theta}, k) \triangleq \sum_{i=1}^{p_{\mathrm{c}}} L_i \hat{\theta}\phi(k-i+1) \tag{5.17}$$

is the *recomputed extended control vector*. In the special case $\bar{B}_{zu} = B_{zu}$, we have

$$\hat{Z}(k) = W_{zw}\phi_{zw}(k) + B_{zu}\hat{U}(k). \tag{5.18}$$

Substituting (5.8) into (5.16), yields

$$\hat{Z}(\hat{\theta}, k) = Z(k) - \bar{B}_{zu}\left[U(k) - \hat{U}(\hat{\theta}, k)\right]. \tag{5.19}$$

Taking the vec of $\bar{B}_{zu}\hat{U}(\hat{\theta}, k)$ yields

$$\hat{Z}(\hat{\theta}, k) = f(k) + D(k)\text{vec }\hat{\theta}, \tag{5.20}$$

where

$$f(k) \triangleq Z(k) - \bar{B}_{zu}U(k), \tag{5.21}$$

$$D(k) \triangleq \sum_{i=1}^{p_c} \phi^{\mathrm{T}}(k-i+1) \otimes \left(\bar{B}_{zu}L_i\right), \tag{5.22}$$

and $\otimes$ represents the Kronecker product.

Now, consider the *retrospective cost function*

$$\begin{aligned} J(\hat{\theta}, k) \triangleq{}& \hat{Z}^{\mathrm{T}}(\hat{\theta}, k)R_1(k)\hat{Z}(\hat{\theta}, k) + \hat{u}^{\mathrm{T}}(\hat{\theta}, k+1)R_2(k)\hat{u}(\hat{\theta}, k+1) \\ &+ \mathrm{tr}\left[R_3(k)\left(\hat{\theta} - \theta(k)\right)^{\mathrm{T}} R_4(k)\left(\hat{\theta} - \theta(k)\right)\right], \end{aligned} \tag{5.23}$$

where $R_1(k) = R_1^{\mathrm{T}}(k) \geq 0, R_2(k) \geq 0, R_3(k) = R_3^{\mathrm{T}}(k) > 0$, $R_4(k) = R_4^{\mathrm{T}}(k) > 0$, and

$$\hat{u}(\hat{\theta}, k) \triangleq \hat{\theta}\phi(k). \tag{5.24}$$

Substituting (5.20) into (5.23) yields

$$J(\hat{\theta},k) = c(k) + b^{\mathrm{T}}(k)\mathrm{vec}\ \hat{\theta} + \left(\mathrm{vec}\ \hat{\theta}\right)^{\mathrm{T}} M(k)\mathrm{vec}\ \hat{\theta}, \tag{5.25}$$

where

$$M(k) \triangleq D^{\mathrm{T}}(k)R_1(k)D(k) + \left[\phi^{\mathrm{T}}(k)\phi(k)\right] \otimes R_2(k) + R_3(k) \otimes R_4(k), \tag{5.26}$$

$$b(k) \triangleq 2D^{\mathrm{T}}(k)R_1(k)f(k) - 2\left[R_3(k) \otimes R_4(k)\right]\mathrm{vec}\ \theta(k), \tag{5.27}$$

$$c(k) \triangleq f^{\mathrm{T}}(k)R_1(k)f(k) + \mathrm{tr}\left[R_3(k)\theta^{\mathrm{T}}(k)R_4(k)\theta(k)\right]. \tag{5.28}$$

Since $M(k)$ is positive definite, $J(\hat{\theta},k)$ has the strict global minimizer $\theta(k+1)$ given by

$$\theta(k+1) = -\frac{1}{2}\mathrm{vec}^{-1}\left[M^{-1}(k)b(k)\right]. \tag{5.29}$$

For all future discussion, we specialize (5.26)–(5.28) with

$$R_1(k) \triangleq I_{pl_z}, \quad R_2(k) \triangleq 0_{l_u}, \quad R_3(k) \triangleq \alpha(k)I_{n_c(l_u+l_y)}, \quad R_4(k) \triangleq I_{l_u}, \tag{5.30}$$

where $\alpha(k) > 0$ is a scalar, yielding

$$M(k) = D^{\mathrm{T}}(k)D(k) + \alpha(k)I, \tag{5.31}$$

$$b(k) = 2D^{\mathrm{T}}(k)f(k) - 2\alpha(k)\mathrm{vec}\ \theta(k), \tag{5.32}$$

$$c(k) = f^{\mathrm{T}}(k)f(k) + \alpha(k)\mathrm{tr}\left[\theta^{\mathrm{T}}(k)\theta(k)\right]. \tag{5.33}$$

The weighting parameter $\alpha(k)$ introduced in (5.30) is called the *learning rate* since it affects convergence speed of the adaptive control algorithm. As $\alpha(k)$ is increased, a higher weight is placed on the difference between the previous control coefficients

and the current control coefficients, and, as a result, convergence speed is lowered. Likewise, as $\alpha(k)$ is decreased, converge speed is raised. By varying $\alpha(k)$, we study tradeoffs between transient performance and convergence speed.

In the particular case $z = y$, using the *retrospective performance variable* $\hat{z}$ in place of y in the regressor vector (5.13) results in faster convergence. Therefore, for $z = y$, we redefine (5.13) as

$$\phi(k) \triangleq \begin{bmatrix} \hat{z}(k-1) \\ \vdots \\ \hat{z}(k-n_{\mathrm{c}}) \\ u(k-1) \\ \vdots \\ u(k-n_{\mathrm{c}}) \end{bmatrix}. \tag{5.34}$$

The novel feature of the adaptive control algorithm (5.11), (5.29) is the use of the retrospective correction filter (RCF) (5.19), as shown in Figure 5.2 for $p = 1$. The RCF provides an inner loop to the adaptive control law by modifying the extended performance vector $Z(k)$ based on the difference between the actual past control inputs $U(k)$ and the recomputed past control inputs based on the current control law $\hat{U}(\hat{\theta}, k)$.

5.5 Smith-McMillan-Based Update

If information about the plant's nonminimum-phase zeros is available, we can use that information to construct $\bar{B}_{zu}$ for the adaptive control algorithm. We first represent G_{zu} (as given by (A.12) in Appendix A) in Smith-McMillan form. We then define the surrogate transfer function matrix $\hat{G}_{zu}$ to be identical to G_{zu} in Smith-McMillan form except that the minimum-phase transmission zeros of G_{zu} are replaced

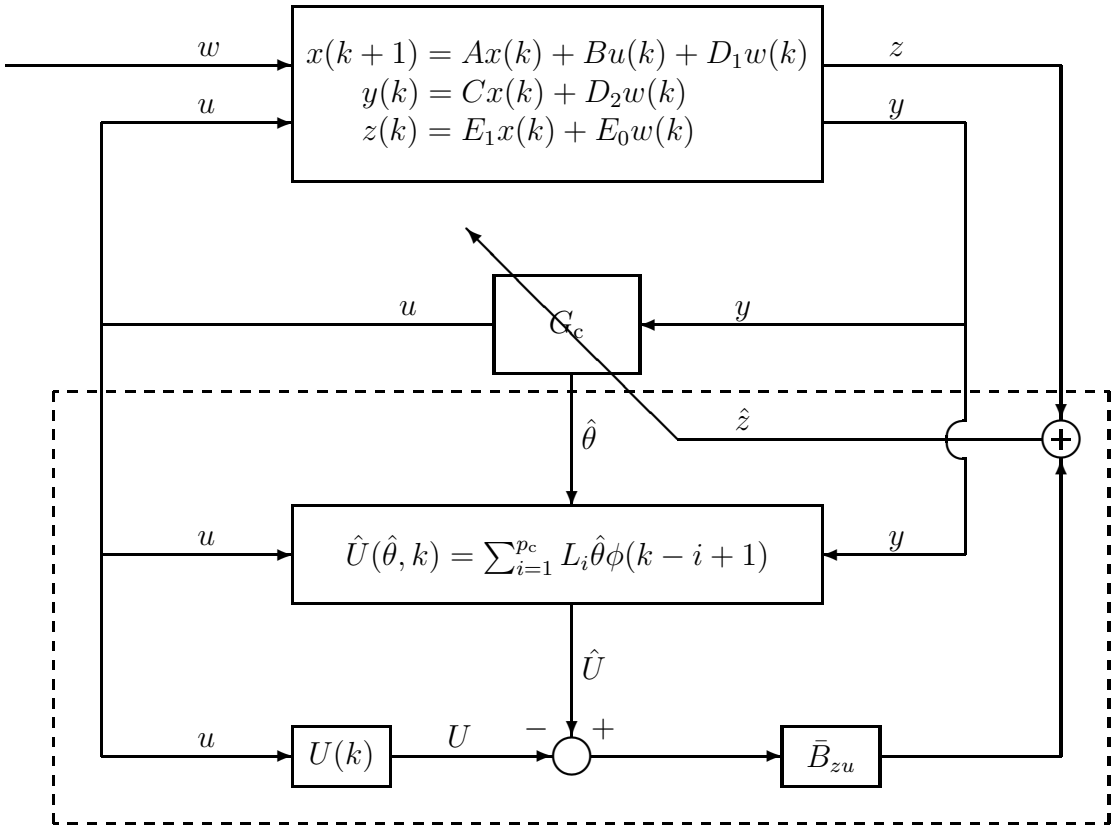

Figure 5.2 Closed-loop system including adaptive control algorithm with the retrospective correction filter (dashed box) for $p = 1$.

by transmission zeros at the origin. Thus $\hat{G}_{zu}$ has the form

$$\hat{G}_{zu}(\mathbf{z}) \triangleq \frac{1}{\mathbf{z}^n + \alpha_1\mathbf{z}^{n-1} + \cdots + \alpha_n}\left(\hat{\beta}_d\mathbf{z}^{n-d} + \hat{\beta}_{d+1}\mathbf{z}^{n-d-1} + \cdots + \hat{\beta}_n\right), \tag{5.35}$$

where $\hat{\beta}_d, \ldots, \hat{\beta}_n \in \mathbb{R}^{l_z \times l_u}$ are the *surrogate numerator coefficients* and $\hat{\beta}_d \triangleq H_d$. Then, using the numerator coefficients of $\hat{G}_{zu}(\mathbf{z})$, the Smith-McMillan-based con-

struction of $\bar{B}_{zu}$ is given by

$$\bar{B}_{zu} \triangleq \begin{bmatrix} 0_{l_z \times l_u} & \cdots & 0_{l_z \times l_u} & \hat{\beta}_d & \cdots & \hat{\beta}_n & 0_{l_z \times l_u} & \cdots & 0_{l_z \times l_u} & 0_{l_z \times l_u} & \cdots & 0_{l_z \times l_u} \\ 0_{l_z \times l_u} & \ddots & & \ddots & \ddots & & \ddots & \ddots & & \ddots & \ddots & \vdots \\ \vdots & \ddots & \ddots & & \ddots & \ddots & & \ddots & \ddots & & \ddots & \vdots \\ 0_{l_z \times l_u} & \cdots & 0_{l_z \times l_u} & 0_{l_z \times l_u} & \cdots & 0_{l_z \times l_u} & \hat{\beta}_d & \cdots & \hat{\beta}_n & 0_{l_z \times l_u} & \cdots & 0_{l_z \times l_u} \end{bmatrix}. \tag{5.36}$$

In the SISO case, this construction of $\bar{B}_{zu}$ requires knowledge of the relative degree d, the first nonzero Markov parameter H_d, and the location of nonminimum-phase zeros, if any. The MIMO case is more subtle, but still requires knowledge of the relative degree, first nonzero Markov parameter, and the location of any nonminimum-phase transmission zeros. The advantage in using the surrogate numerator coefficients $\hat{\beta}_d, \ldots, \hat{\beta}_n$ of $\hat{G}_{zu}$ as opposed to the actual numerator coefficients $\beta_d, \ldots, \beta_n$ of G_{zu} is faster convergence.

5.6 Markov Parameter-Based Update

In many cases, the number and location of any nonminimum-phase zeros may be difficult or even impossible to obtain. Therefore, an alternate construction of $\bar{B}_{zu}$ is available that makes use of Markov parameters. It is shown in Appendix A that there exists a theoretical connection between Markov parameters and nonminimum-phase zeros. Details of this connection are available in Section A.3.

Using the methods developed in Appendix A and the numerator coefficients of

(A.20), it follows that the Markov parameter-based construction of $\bar{B}_{zu}$ is given by

$$\bar{B}_{zu} \triangleq \begin{bmatrix} 0_{l_z \times l_u} & \cdots & 0_{l_z \times l_u} & H_d & \cdots & H_r & 0_{l_z \times l_u} & \cdots & 0_{l_z \times l_u} & 0_{l_z \times l_u} & \cdots & 0_{l_z \times l_u} \\ 0_{l_z \times l_u} & \ddots & & \ddots & \ddots & & \ddots & \ddots & & \ddots & \ddots & \vdots \\ \vdots & \ddots & \ddots & & \ddots & \ddots & & \ddots & \ddots & & \ddots & \vdots \\ 0_{l_z \times l_u} & \cdots & 0_{l_z \times l_u} & 0_{l_z \times l_u} & \cdots & 0_{l_z \times l_u} & H_d & \cdots & H_r & 0_{l_z \times l_u} & \cdots & 0_{l_z \times l_u} \end{bmatrix}. \tag{5.37}$$

The leading zeros in the first row of $\bar{B}_{zu}$ account for the nonzero relative degree d. The advantage in constructing $\bar{B}_{zu}$ using the Markov parameters H_i, $i = d, \ldots, r$, as opposed to using all of the numerator coefficients of (A.15) is faster convergence and ease of identification. The algorithm places no constraints on either the value of d or the rank of H_d or $\bar{B}_{zu}$. Unless otherwise noted, we will use the Markov-parameter-based construction of $\bar{B}_{zu}$ given by (5.37) in the following examples.

5.7 Numerical Examples - Nominal Case

We now present numerical examples to illustrate the response of the RCF adaptive control algorithm under nominal conditions. We consider a sequence of examples of increasing complexity, ranging from SISO, minimum-phase plants to MIMO, nonminimum-phase plants, including stable and unstable cases. Each plant can be viewed as a sampled-data discretization of a continuous-time plant sampled at $T_{\mathrm{s}} = 0.01\,\mathrm{sec}$. All examples assume $z = y$ and the adaptive controller gain matrix $\theta(k)$ is initialized to zero.

Unless otherwise noted, each example is taken to be a disturbance rejection simulation, that is, $E_0 = 0$, with unknown sinusoidal disturbance given by

$$w(k) = \begin{bmatrix} \sin 2\pi\nu_1 kT_{\mathrm{s}} \\ \sin 2\pi\nu_2 kT_{\mathrm{s}} \end{bmatrix}, \tag{5.38}$$

where $\nu_1 = 5$ Hz and $\nu_2 = 13$ Hz. The RCF adaptive control algorithm requires no information about w. With each plant realized in controllable canonical form, we take $D_1 = \begin{bmatrix} I_2 \\ 0 \end{bmatrix}$, and, therefore, the disturbance is not matched.

Example 5.7.1 (SISO, Nonminimum Phase, FIR Plant)**.** *Consider an FIR plant of order* $n = 8$ *and zeros* $\{0.3 \pm 0.7\jmath, -0.7 \pm 0.3\jmath, 2 \pm 0.5\jmath\}$. *We take* $n_c = 15$, $p = 2$, $r = 8$, *and* $\alpha(k) \equiv 25$. *The closed-loop response is shown in Figure 5.3. The control is turned on at* $t = 2\,\text{sec}$, *and the performance variable reduces to zero within* $3\,\text{sec}$.■

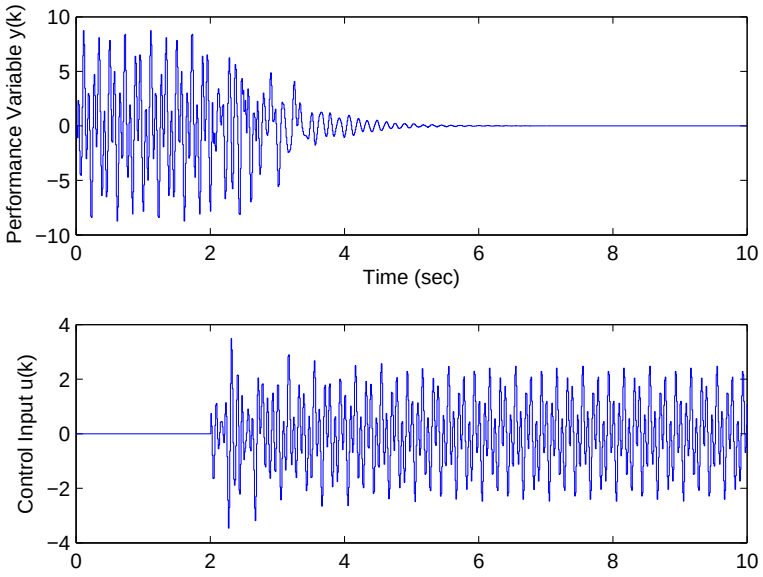

Figure 5.3 Closed-loop disturbance rejection response for an FIR, nonminimum phase, SISO plant. The control is turned on at $t = 2\,\text{sec}$. The controller order is $n_c = 15$ with parameters $p = 2, r = 8, \alpha(k) \equiv 25$.

Example 5.7.2 (SISO, Minimum Phase, Stable Plant)**.** *Consider a plant with poles* $\{0.5 \pm 0.5\jmath, -0.5 \pm 0.5\jmath, \pm 0.9, \pm 0.7\jmath\}$ *and zeros* $\{0.3 \pm 0.7\jmath, -0.7 \pm 0.3\jmath, 0.5\}$. *We take* $n_c = 15$, $p = 1$, $r = 3$, *and* $\alpha(k) \equiv 25$. *The closed-loop response is shown in Figure 5.4. The control is turned on at* $t = 2\,\text{sec}$, *and the performance variable reduces to zero within* $1\,\text{sec}$. *The control algorithm converges to an internal model controller with high gain at the disturbance frequencies, as seen in Figure 5.5.* ■

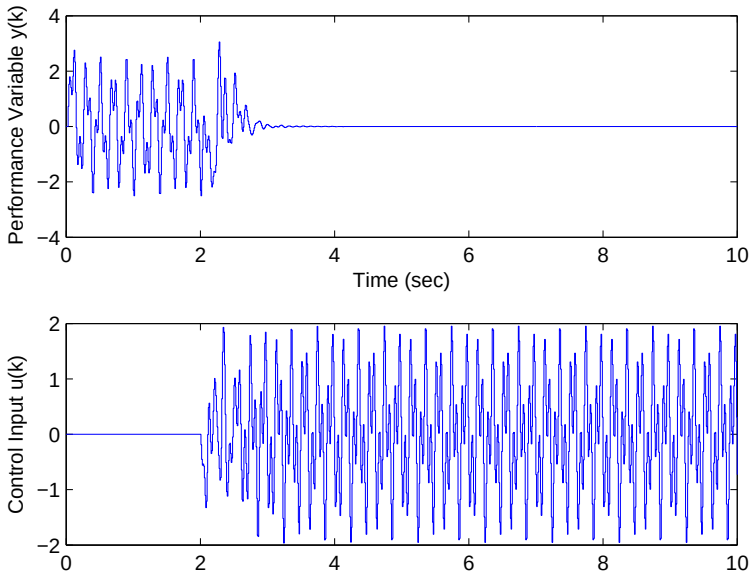

Figure 5.4 Closed-loop disturbance rejection response for a stable, minimum phase, SISO plant. The control is turned on at $t = 2\,\text{sec}$. The controller order is $n_c = 15$ with parameters $p = 1, r = 3, \alpha(k) \equiv 25$.

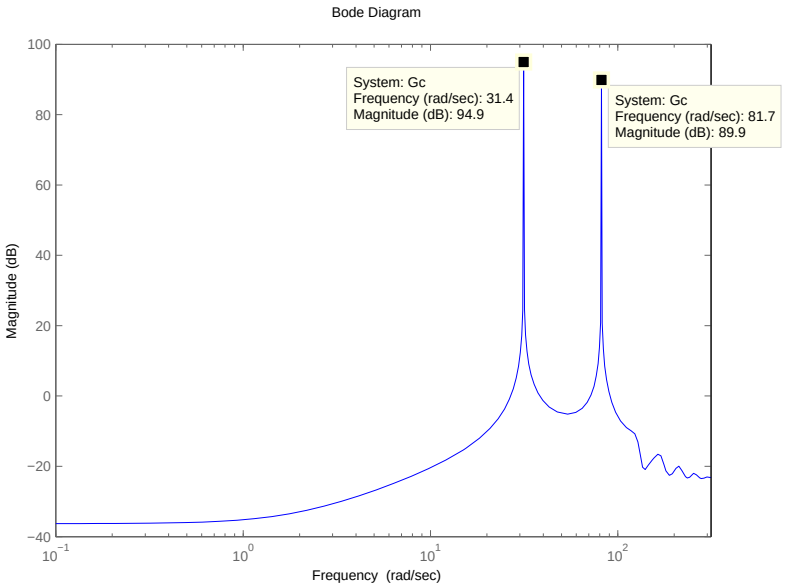

Figure 5.5 Bode magnitude plot of the adaptive controller at $t = 10$ sec. The adaptive controller places poles at the disturbance frequencies $\nu_1 = 5$ Hz and $\nu_2 = 13$ Hz. The controller magnitude $|G_c(e^{j\omega T_s})|$ is plotted for ω up to the Nyquist frequency $\omega_{\text{Nyq}} = \frac{\pi}{T_s} = 314$ rad/sec.

Example 5.7.3 (SISO, Nonminimum Phase, Stable Plant)**.** *Consider a plant with poles* $\{0.5 \pm 0.5\jmath, -0.5 \pm 0.5\jmath, \pm 0.9, \pm 0.7\jmath\}$ *and zeros* $\{0.3 \pm 0.7\jmath, -0.7 \pm 0.3\jmath, 2\}$*. We take* $n_{\mathrm{c}} = 15$*,* $p = 1$*,* $r = 7$*, and* $\alpha(k) \equiv 25$*. Note that the Markov parameter polynomial used to construct* $\bar{B}_{zu}$ *is given by*

$$p_7(\boldsymbol{q}) = \boldsymbol{q}^4 - 1.2\boldsymbol{q}^3 - 0.96\boldsymbol{q}^2 - 0.56\boldsymbol{q} - 0.75,$$

with corresponding roots $\{0.01 \pm 0.71\jmath, -0.77, 1.94\}$*. The closed-loop response is shown in Figure 5.6. The control is turned on at* $t = 2\,\mathrm{sec}$*, and, after a slight transient, the performance variable reduces to zero.*

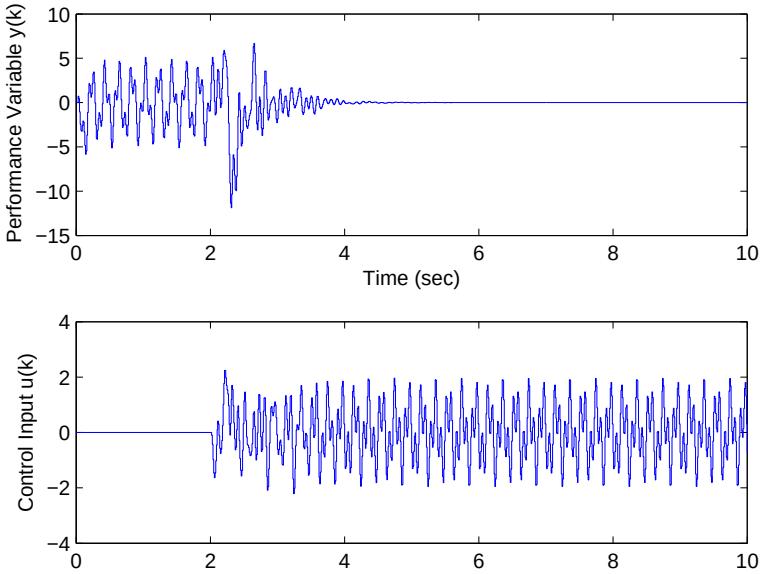

Figure 5.6 Closed-loop disturbance rejection response for a stable, nonminimum phase, SISO plant. The control is turned on at $t = 2\,\mathrm{sec}$. The controller order is $n_{\mathrm{c}} = 15$ with parameters $p = 1, r = 7, \alpha(k) \equiv 25$.

Alternatively, consider the Smith-McMillan-based construction of $\bar{B}_{zu}$ *given by (5.36), which is constructed using the first nonzero Markov parameter* $H_3 = 1$ *and the location of the nonminimum-phase zero at* $\boldsymbol{z} = 2$*. We take* $n_{\mathrm{c}} = 15$*,* $p = 1$*,* $r = 1$*, and* $\alpha(k) \equiv 25$*. The closed-loop response is shown in Figure 5.7. The control is turned on at* $t = 2\,\mathrm{sec}$*, and, after a transient, the performance variable reduces to*

zero. Note that the simulation using the Markov-parameter-based construction of $\bar{B}_{zu}$ (Figure 5.6) yields a better transient response than the simulation using the Smith-McMillan-based construction of $\bar{B}_{zu}$ (Figure 5.7). ■

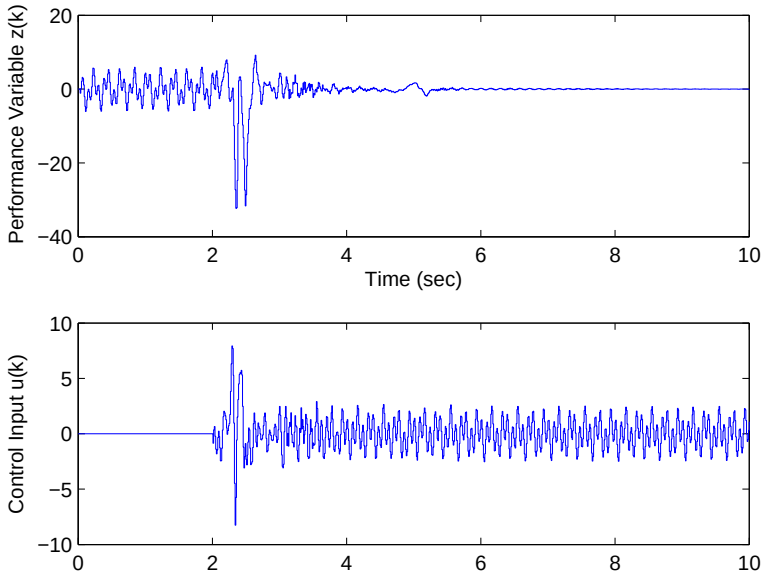

Figure 5.7 Closed-loop disturbance rejection response for a stable, nonminimum phase, SISO plant using the Smith-McMillan-based construction of $\bar{B}_{zu}$. The control is turned on at $t = 2\,\text{sec}$. The controller order is $n_c = 15$ with parameters $p = 1, r = 1, \alpha(k) \equiv 25$.

Example 5.7.4 (SISO, Minimum Phase, Unstable Plant)**.** *Consider a plant with poles* $\{0.5 \pm 0.5\jmath, -0.5 \pm 0.5\jmath, \pm 1.04, 0.1 \pm 1.025\jmath\}$ *and zeros* $\{0.3 \pm 0.7\jmath, -0.7 \pm 0.3\jmath, 0.5\}$. *We take* $n_c = 15$, $p = 1$, $r = 10$, *and* $\alpha(k) \equiv 25$. *The closed-loop response is shown in Figure 5.8. The control is turned on at* $t = 2\,\text{sec}$, *and, after a transient, the performance variable reduces to zero.* ■

Example 5.7.5 (MIMO, Minimum Phase, Stable Plant)**.** *Consider a two-input, two-output plant with poles* $\{-0.5 \pm 0.5\jmath, 0.9, \pm 0.7\jmath, -0.5 \pm 0.5\jmath, 0.9, \pm 0.7\jmath\}$ *and transmission zeros* $\{0.3 \pm 0.7\jmath, 0.5, 0.5\}$. *We take* $n_c = 15$, $p = 1$, $r = 10$, *and* $\alpha(k) \equiv 1$. *The closed-loop response is shown in Figure 5.9. The control is turned on at* $t = 2\,\text{sec}$,

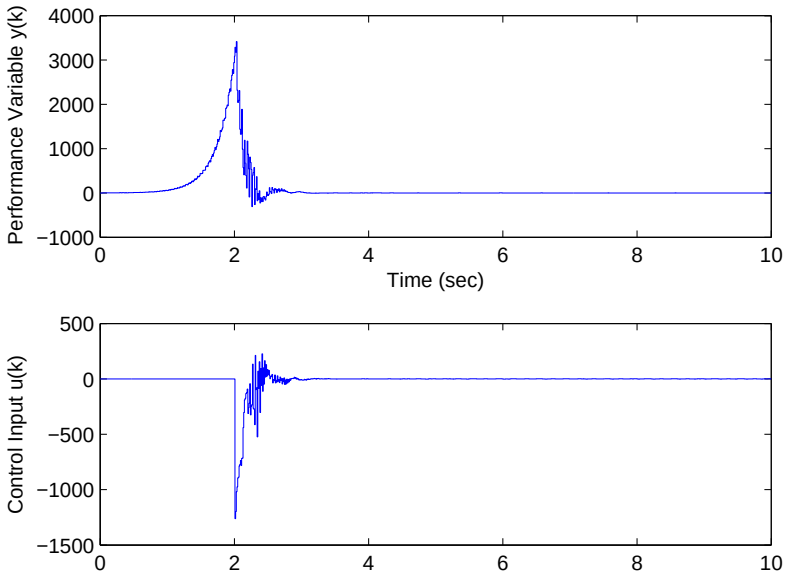

Figure 5.8 Closed-loop disturbance rejection response for an unstable, minimum phase, SISO plant. The control is turned on at $t = 2\,\text{sec}$. The controller order is $n_c = 15$ with parameters $p = 1, r = 10, \alpha(k) \equiv 25$.

and the performance variable reduces to zero. ■

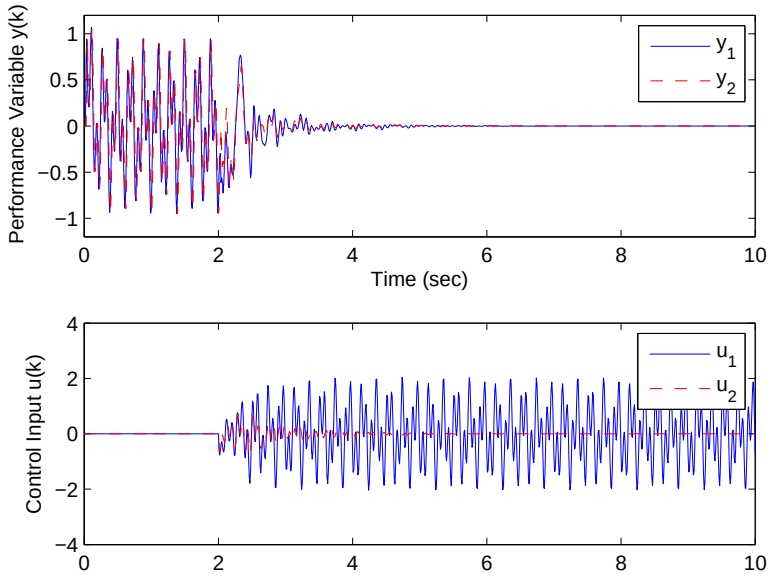

Figure 5.9 Closed-loop disturbance rejection response for a stable, minimum phase, two-input two-output plant. The control is turned on at $t = 2\,\text{sec}$. The controller order is $n_c = 15$ with parameters $p = 1, r = 10, \alpha(k) \equiv 1$.

Example 5.7.6 (MIMO, Nonminimum Phase, Stable Plant)**.** *Consider a two-input, two-output plant with poles* $\{-0.5 \pm 0.5\jmath, 0.9, -0.5 \pm 0.5\jmath, 0.9\}$ *and transmission zero* $\{2\}$*. We take* $n_c = 20$*,* $p = 1$*,* $r = 6$*, and* $\alpha(k) \equiv 1$*. The closed-loop response is shown in Figure 5.10. The control is turned on at* $t = 2\,\text{sec}$*, and, after a slight transient, the performance variable reduces to zero.* ■

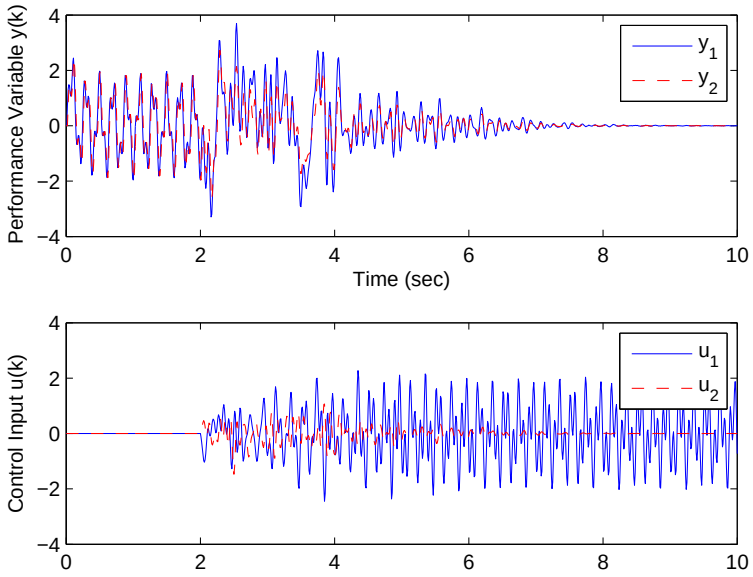

Figure 5.10 Closed-loop disturbance rejection response for a stable, nonminimum phase, two-input two-output plant. The control is turned on at $t = 2\,\text{sec}$. The controller order is $n_c = 20$ with parameters $p = 1, r = 6, \alpha(k) \equiv 1$.

Example 5.7.7 (MIMO, Nonminimum Phase, Unstable Plant)**.** *Consider a two-input, two-output plant with poles* $\{-0.5 \pm 0.5\jmath, \pm 0.7\jmath, 0.1 \pm 1.025\jmath, -0.4, 0.9\}$ *and transmission zeros* $\{0.5, 2\}$*. We take* $n_c = 10$*,* $p = 1$*,* $r = 10$*, and* $\alpha(k) \equiv 1$*. The closed-loop response is shown in Figure 5.11. The control is turned on at* $t = 2\,\text{sec}$*, and, after a slight transient, the performance variable reduces to zero.* ■

Example 5.7.8 (Ex. 5.7.2 with Command Following and Disturbance Rejection)**.** *We consider a combined step-command following and disturbance rejection problem*

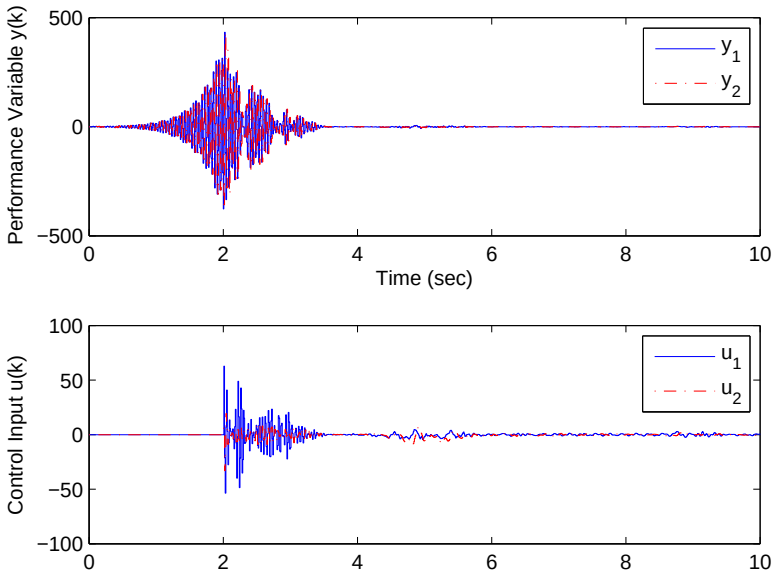

Figure 5.11 Closed-loop disturbance rejection response for an unstable, nonminimum phase, two-input two-output plant. The control is turned on at $t = 2\,\text{sec}$. The controller order is $n_c = 10$ with parameters $p = 1, r = 10, \alpha(k) \equiv 1$.

with command and disturbance given by

$$w(k) = \begin{bmatrix} w_1(k) \\ w_2(k) \end{bmatrix} = \begin{bmatrix} \sin 2\pi\nu_1 k T_s \\ 5 \end{bmatrix}. \tag{5.39}$$

With the plant realized in controllable canonical form, we take $D_1 = \begin{bmatrix} 1 & 0 \\ 0 & 0 \end{bmatrix}$ *and* $E_0 = \begin{bmatrix} 0 & -1 \end{bmatrix}$. *Therefore,* w_1 *is the disturbance to be rejected, while* w_2 *is the command to be followed.*

We take $n_c = 20$, $p = 1$, $r = 3$, *and* $\alpha(k) \equiv 50$. *The closed-loop response is shown in Figure 5.12. The control is turned on at* $t = 2\,\text{sec}$, *and the performance variable reduces to zero, that is, the disturbance* w_1 *is rejected while the command* w_2 *is followed.* ■

Example 5.7.9 (Command Following with Unstable Plant)**.** *We consider a dou-*

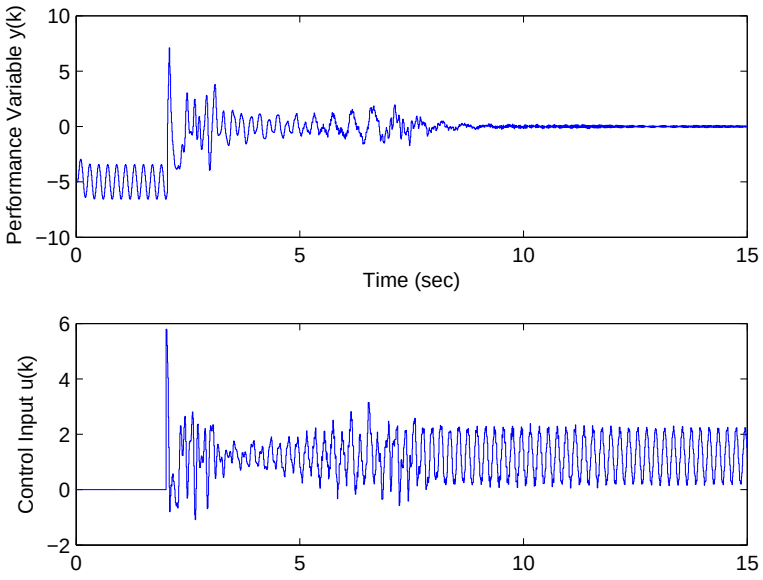

Figure 5.12 Closed-loop response for a stable, minimum phase, SISO plant with a step command and sinusoidal disturbance. The control is turned on at $t = 2\,\text{sec}$. The controller order is $n_c = 20$ with parameters $p = 1, r = 3, \alpha(k) \equiv 50$.

ble integrator plant with command given by $w(k) = 1$. *With the plant realized in controllable canonical form, we take* $D_1 = 0$ *and* $E_0 = -1$.

The SISO plant is unstable and minimum phase with poles $\{0.5 \pm 0.5\jmath, -0.5 \pm 0.5\jmath, 1, 1\}$ *and zeros* $\{0.3 \pm 0.7\jmath, 0.5\}$. *We take* $n_c = 10$, $p = 5$, $r = 10$, *and* $\alpha(k) \equiv 5$. *The closed-loop response is shown in Figure 5.13. The control is turned on at* $t = 2\,\text{sec}$, *and, after a transient, the performance variable reduces to zero, that is, the step-command* w *is followed.* ■

5.8 Numerical Examples - Off-nominal Cases

We now present numerical examples to illustrate the response of the RCF adaptive control algorithm under conditions of uncertainty in the relative degree and Markov parameters, measurement noise, and actuator and sensor saturations. Therefore, we

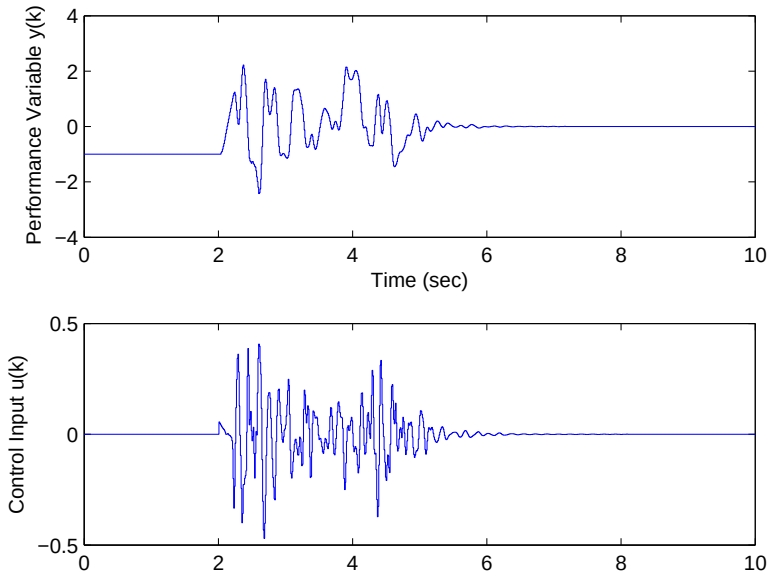

Figure 5.13 Closed-loop response for an unstable, minimum phase, SISO plant with a step command. The control is turned on at $t = 2\,\text{sec}$. The controller order is $n_c = 10$ with parameters $p = 5, r = 10, \alpha(k) \equiv 5$.

revisit examples from the previous section under off-nominal conditions, that is, with uncertainty in the required plant modeling information. In each case, we illuminate the role of the learning rate α, which governs the rate of convergence. Our goal is thus to develop rules of thumb for choosing α based on the level of model fidelity. Each example is taken to be a disturbance rejection simulation with $z = y$, as presented in Section 5.7. In each example below, the adaptive controller gain matrix $\theta(k)$ is initialized to zero.

Example 5.8.1 (Ex. 5.7.3 with Relative Degree Error and Unknown Latency - Phase Margin)**.** *Consider model error in the relative degree. The system has relative degree* $d = 3$.

First, for controller implementation, we use the erroneous $\hat{d} = 2$. *We take* $n_c = 15$, $p = 1$, $r = 10$, *and* $\alpha(k) \equiv 1000$. *The closed-loop response is shown in Figure 5.14. The control is turned on at* $t = 2\,\text{sec}$, *and the performance variable reduces to zero.*

Now let $\hat{d} = 4$. *We take* $n_c = 15$, $p = 1$, $r = 10$, *and* $\alpha(k) \equiv 1000$. *The closed-*

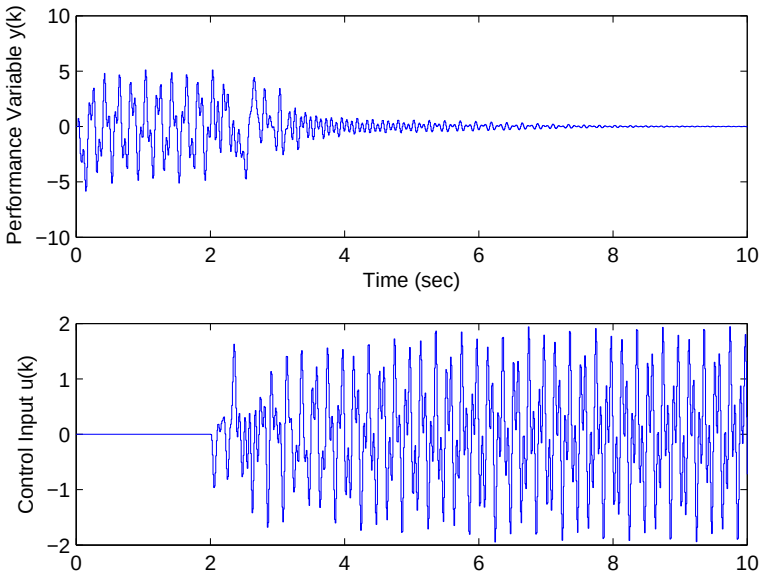

Figure 5.14 Closed-loop disturbance rejection response for a stable, nonminimum phase, relative degree $d = 3$ SISO plant where the controller is created assuming the plant has relative degree $\hat{d} = 2$. The control is turned on at $t = 2\,\text{sec}$. The controller order is $n_c = 15$ with parameters $p = 1, r = 10, \alpha(k) \equiv 1000$. To compensate for uncertainty in the relative degree d, α is increased to slow down the adaptation.

loop response is shown in Figure 5.15. The control is turned on at $t = 2\,\text{sec}$*, and the performance variable converges to zero.*

These simulations show that the adaptive controller is sensitive to errors in relative degree, which is equivalent to an unknown latency, that is, implementation delay. However, the effect of a known *latency of* l *steps can be addressed by simply replacing* d *by* $d + l$ *in the construction of* $\bar{B}_{zu}$*. These simulations suggest that it is a natural extension to use relative degree error and latency as potential metrics for analyzing phase margins of discrete-time adaptive systems.* ■

Example 5.8.2 (Ex. 5.7.2 with Uncertain H_d - Gain Margin)**.** *We now assess the algorithm's robustness to knowledge of the first nonzero Markov parameter* H_d*. The first nonzero Markov parameter is* $H_3 = 1$*.*

We first assume that the first nonzero Markov parameter is $\hat{H}_3 = 0.05H_3$*. We take* $n_c = 15$*,* $p = 1$*,* $r = 3$*, and* $\alpha(k) \equiv 25$*. The closed-loop response is shown in Figure*

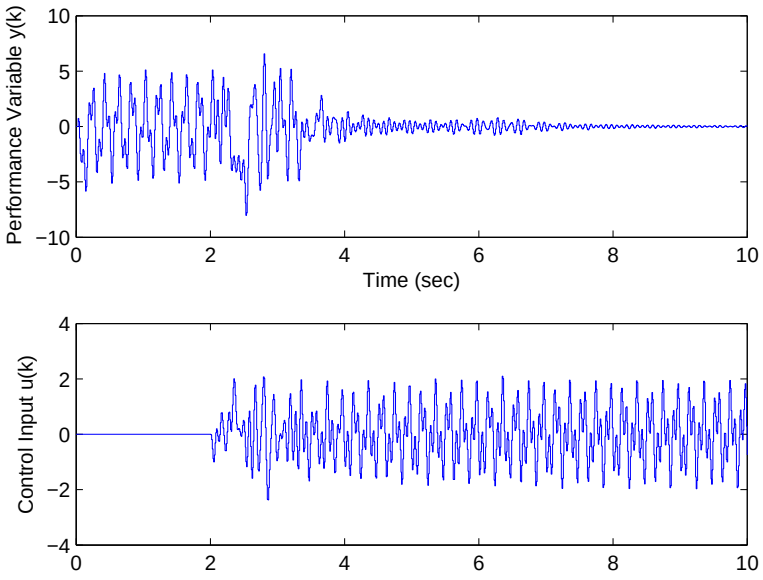

Figure 5.15 Closed-loop disturbance rejection response for a stable, nonminimum phase, relative degree $d = 3$ SISO plant where the controller is created assuming the plant has relative degree $\hat{d} = 4$. The control is turned on at $t = 2\,\text{sec}$. The controller order is $n_c = 15$ with parameters $p = 1, r = 10, \alpha(k) \equiv 1000$.

5.16. The control is turned on at $t = 2\,\text{sec}$*, and the performance variable converges within* $6\,\text{sec}$*. In this case, the Markov parameter scaling is equivalent to at least a 26 dB downward adaptive gain margin.*

Now, we assume that the first nonzero Markov parameter is $\hat{H}_3 = 20H_3$*. We take* $n_c = 15$*,* $p = 1$*,* $r = 3$*, and* $\alpha(k) \equiv 25$*. The closed-loop response is shown in Figure 5.17. The control is turned on at* $t = 2\,\text{sec}$*, and the performance variable converges to zero. In this case, the Markov parameter scaling is equivalent to at least a 26 dB upward adaptive gain margin.*

In the case where the sign of the first nonzero Markov parameter is wrong, that is, $\hat{H}_3 = -H_3$*, the simulation fails. As the fidelity of* H_d *decreases, convergence is slowed. From these results it is seen that increasing error in* H_d *is equivalent to increasing* α*, and thus slowing down the convergence. These simulations suggest that it is a natural extension to use linear Markov parameter scaling as a potential metric*

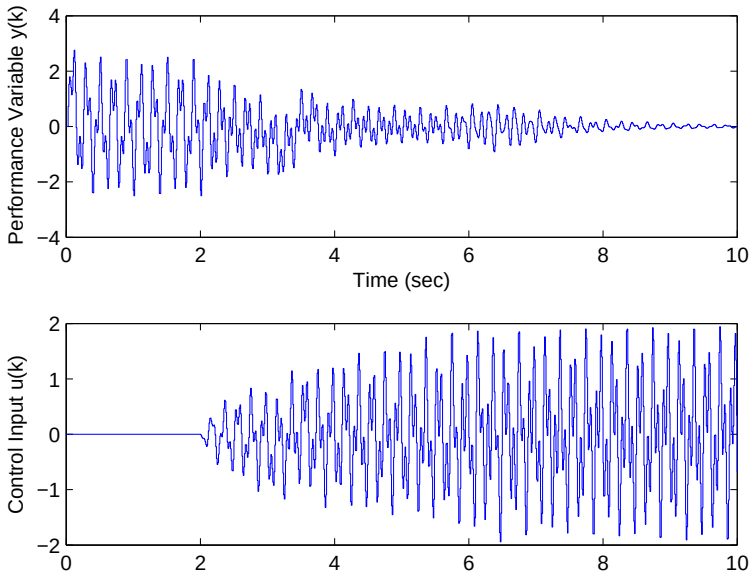

Figure 5.16 Closed-loop disturbance rejection response for a stable, minimum phase, SISO plant with $H_d = 1$ where the controller is created with $\hat{H}_d = 0.05$. The control is turned on at $t = 2\,\text{sec}$. The controller order is $n_c = 15$ with parameters $p = 1, r = 3, \alpha(k) \equiv 25$. With H_d underestimated, the closed-loop converges more slowly than in the nominal case.

for analyzing gain margins of discrete-time adaptive systems. ■

Example 5.8.3 (Noisy Markov Parameters)**.** *We investigate model error in the Markov parameters.*

First, consider Example 5.7.2. The system has relative degree $d = 3$ with $H_3 = 1$. For controller implementation, we perturb each Markov parameter H_i, $i = 1 \ldots r$, by adding zero-mean Gaussian white noise with standard deviation $\sigma = 0.25$. We take $n_c = 15$, $p = 1$, $r = 3$, and $\alpha(k) \equiv 25$. The closed-loop response is shown in Figure 5.18. The control is turned on at $t = 2\,\text{sec}$, and the performance variable reduces to zero.

Next, consider Example 5.7.3 with model error in the Markov parameters. The system has relative degree $d = 3$ with $H_3 = 1$. For controller implementation, we perturb each Markov parameter H_i, $i = 1 \ldots r$, by adding zero-mean Gaussian white noise with standard deviation $\sigma = 0.25$. We take $n_c = 15$, $p = 1$, $r = 10$, and

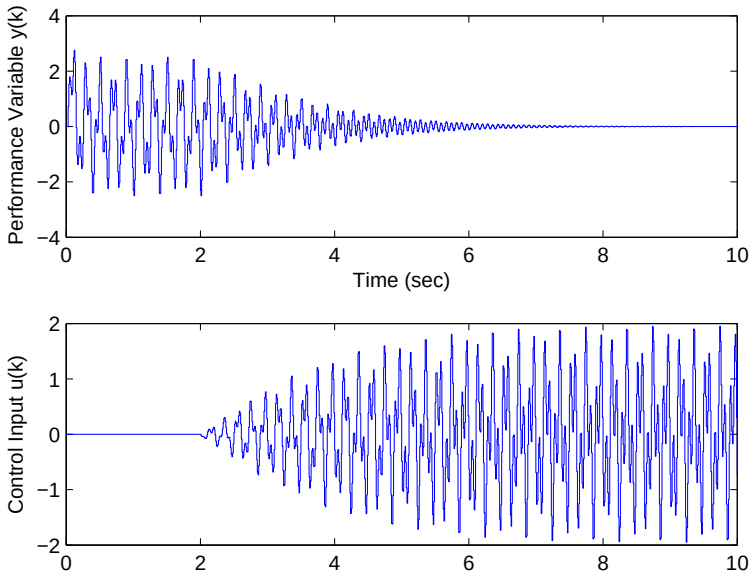

Figure 5.17 Closed-loop disturbance rejection response for a stable, minimum phase, SISO plant with $H_d = 1$ where the controller is created with $\hat{H}_d = 20$. The control is turned on at $t = 2\,\text{sec}$. The controller order is $n_c = 15$ with parameters $p = 1, r = 3, \alpha(k) \equiv 25$. With H_d overestimated, the closed-loop converges more slowly than in the nominal case.

$\alpha(k) \equiv 25$. *The closed-loop response is shown in Figure 5.19. The control is turned on at* $t = 2\,\text{sec}$, *and the performance variable reduces to zero.*

These simulations show that the adaptive control algorithm is robust to errors in the Markov parameters. ■

Example 5.8.4 (Ex. 5.7.2 with Noisy Measurements)**.** *To assess the performance of the adaptive algorithm with added sensor noise, we modify the sensor equation (5.2) by*

$$y(k) = Cx(k) + D_2 w(k) + v(k), \tag{5.40}$$

where $v(k) \in \mathbb{R}^{l_y}$ *is zero-mean Gaussian white noise with standard deviation* $\sigma = 0.1$.

We take $n_c = 15$, $p = 1$, $r = 3$, *and* $\alpha(k) \equiv 25$. *The closed-loop response is shown in Figure 5.20. The control is turned on at* $t = 2\,\text{sec}$, *and the performance variable is reduced to the level of the additive sensor noise* $v(k)$. *Analogous results*

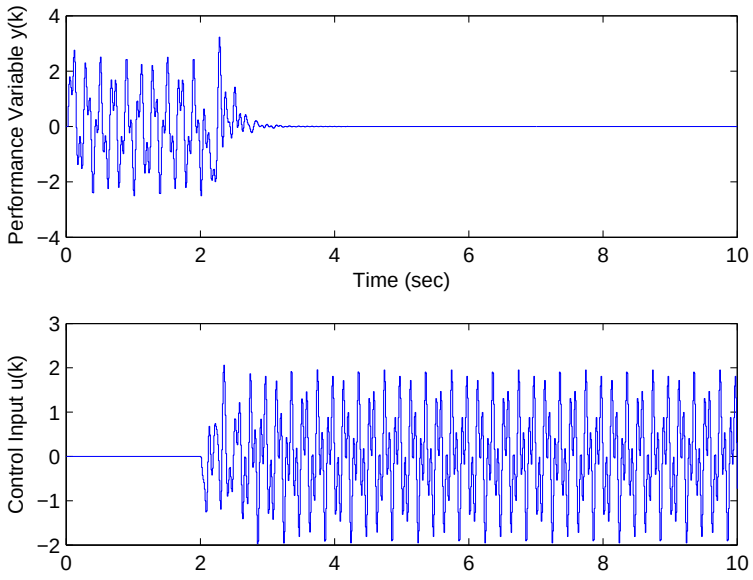

Figure 5.18 Closed-loop disturbance rejection response for a stable, minimum phase, relative degree $d = 3$, SISO plant where the controller is created with Markov parameters perturbed by zero-mean Gaussian white noise with standard deviation $\sigma = 0.25$. The control is turned on at $t = 2\,\text{sec}$. The controller order is $n_c = 15$ with parameters $p = 1, r = 3$, and $\alpha(k) \equiv 25$.

are obtained for sinusoidal sensor noise and measurement bias, that is, constant measurement noise. Bursting was not observed in any of the simulations. ■

Example 5.8.5 (Ex. 5.7.2 with Actuator and Sensor Saturation)**.** *In addition to the issues discussed above, physical systems are constrained by actuator and sensor limitations. In particular, we consider the performance of the adaptive algorithm under actuator and sensor saturation.*

The control input $u(k)$ is subject to saturation at ± 1.5, while the sensor measurement $y(k)$ is subject to saturation at ± 2. We take $n_c = 15$, $p = 1$, $r = 3$, and $\alpha(k) \equiv 25$. The closed-loop response is shown in Figure 5.21. The control is turned on at $t = 2\,\text{sec}$, and the performance variable is reduced to a level consistent with what the saturated control can provide. ■

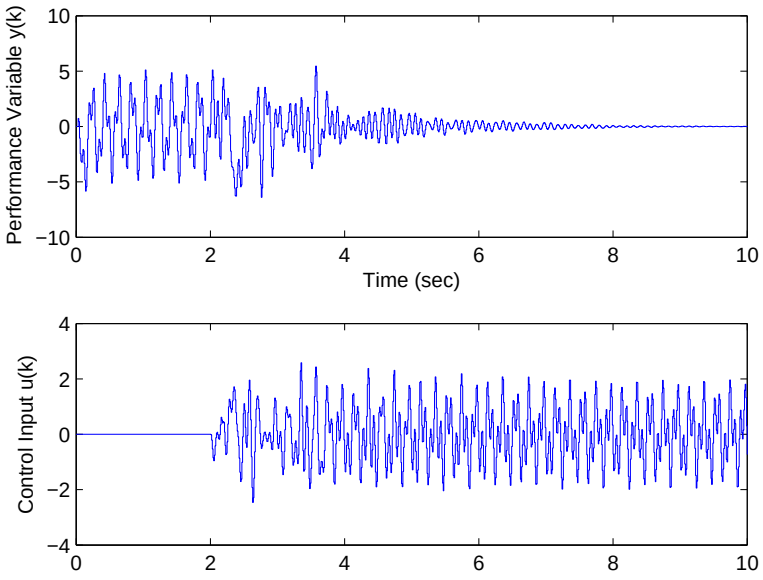

Figure 5.19 Closed-loop disturbance rejection response for a stable, nonminimum phase, relative degree $d = 3$, SISO plant where the controller is created with Markov parameters perturbed by zero-mean Gaussian white noise with standard deviation $\sigma = 0.25$. The control is turned on at $t = 2\,\text{sec}$. The controller order is $n_c = 15$ with parameters $p = 1, r = 10$, and $\alpha(k) \equiv 25$.

Example 5.8.6 (Ex. 5.7.2 Command Following with Actuator Saturation)**.** *We consider a command given by* $w(k) = 1$. *With the plant realized in controllable canonical form, we take* $D_1 = 0$ *and* $E_0 = -1$.

First, consider the case with no actuator saturation. We take $n_c = 15$, $p = 1$, $r = 3$, *and* $\alpha(k) \equiv 25$. *The closed-loop response is shown in Figure 5.22. The control is turned on at* $t = 2\,\text{sec}$, *and, after a transient, the performance variable reduces to zero, that is, the step-command* w *is followed.*

Now, consider the case with actuator saturation at ± 0.1. *We take* $n_c = 15$, $p = 1$, $r = 3$, *and* $\alpha(k) \equiv 25$. *The closed-loop response is shown in Figure 5.23. The control is turned on at* $t = 2\,\text{sec}$, *and the performance variable reduces to a level consistent with what the saturated control can provide.* ■

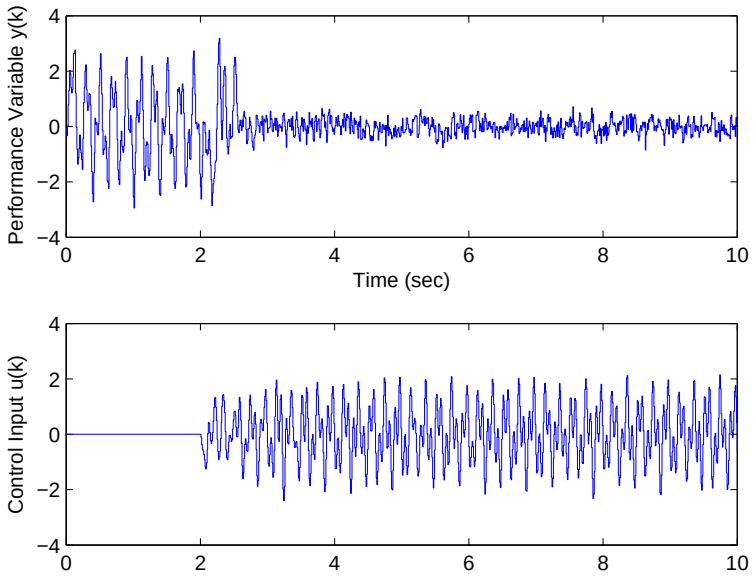

Figure 5.20 Closed-loop disturbance rejection response for a stable, minimum phase, SISO plant with random white noise added to the measurement. The control is turned on at $t = 2\,\text{sec}$. The controller order is $n_c = 15$ with parameters $p = 1, r = 3, \alpha(k) \equiv 25$. The performance variable $y(k)$ is reduced to the level of the additive sensor noise $v(k)$.

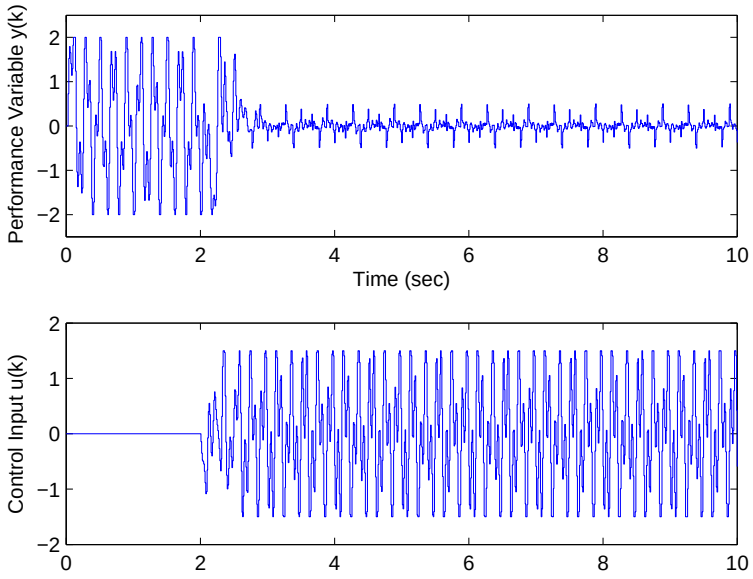

Figure 5.21 Closed-loop disturbance rejection response for a stable minimum phase SISO plant where the actuator is saturated at ± 1.5 and the sensor is saturated at ± 2. The control is turned on at $t = 2\,\text{sec}$. The controller order is $n_c = 15$ with parameters $p = 1, r = 3, \alpha(k) \equiv 25$. The saturations reduce overall steady-state performance.

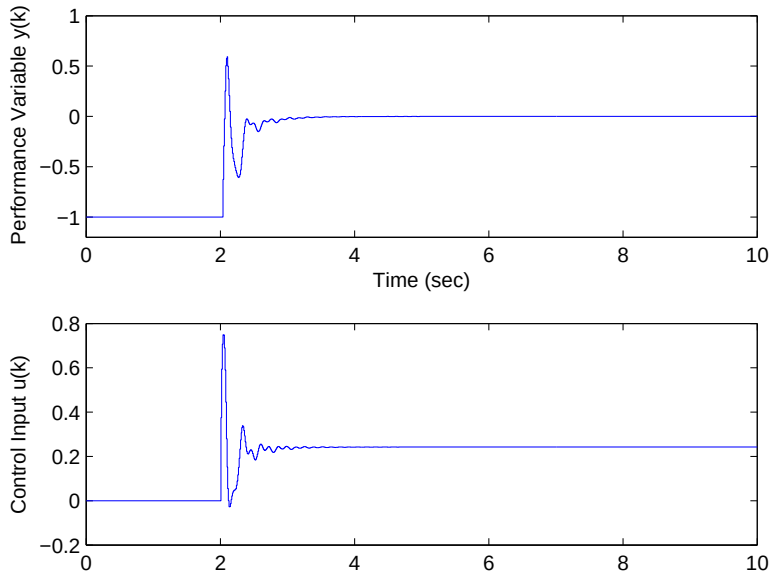

Figure 5.22 Closed-loop response for a stable, minimum phase, SISO plant with a step command. The control is turned on at $t = 2\,\text{sec}$. The controller order is $n_c = 15$ with parameters $p = 1, r = 3, \alpha(k) \equiv 25$.

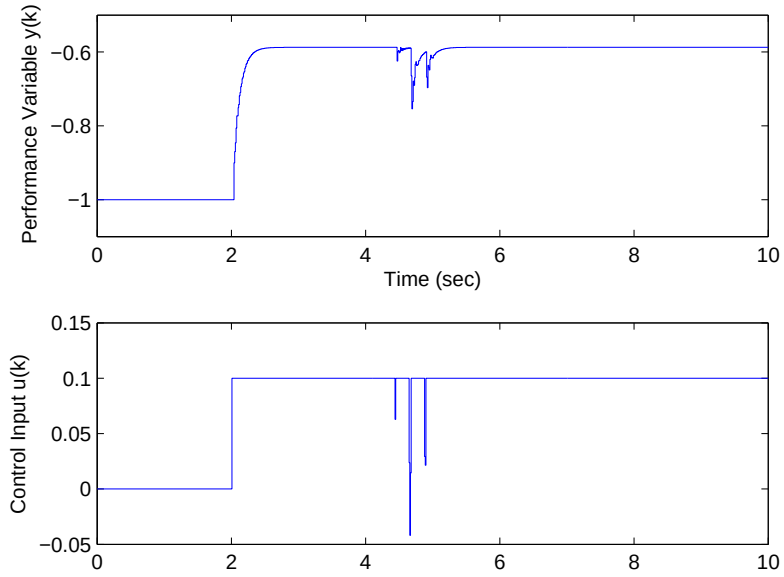

Figure 5.23 Closed-loop response for a stable, minimum phase, SISO plant with a step command subject to actuator saturation at ± 0.1. The control is turned on at $t = 2\,\text{sec}$. The controller order is $n_c = 15$ with parameters $p = 1, r = 3, \alpha(k) \equiv 25$.

5.9 Numerical Examples - Model Reference Adaptive Control

We now present numericals example to illustrate the response of the RCF adaptive control algorithm for model reference adaptive control (see Figure 5.1). Unless otherwise noted, the adaptive controller gain matrix $\theta(k)$ is initialized to zero.

5.9.1 Boeing 747 longitudinal dynamics

Consider the longitudinal dynamics of a Boeing 747 aircraft, linearized about steady flight at 40,000 ft and 774 ft/sec. The inputs to the dynamical system are taken to be elevator deflection and thrust. The output of the dynamical system is taken to be pitch angle. The continuous-time equations of motion are thus given by

$$\begin{bmatrix} \dot{u} \\ \dot{w} \\ \dot{q} \\ \dot{\theta} \end{bmatrix} = \begin{bmatrix} -0.003 & 0.039 & 0 & -0.322 \\ -0.065 & -0.319 & 7.74 & 0 \\ 0.020 & -0.101 & -0.429 & 0 \\ 0 & 0 & 1 & 0 \end{bmatrix} \begin{bmatrix} u \\ w \\ q \\ \theta \end{bmatrix} + \begin{bmatrix} 0.010 & 1 \\ -0.180 & -0.040 \\ -1.160 & 0.598 \\ 0 & 0 \end{bmatrix} \begin{bmatrix} \delta_{\mathrm{e}} \\ \delta_{\mathrm{T}} \end{bmatrix}, \tag{5.41}$$

$$y = \begin{bmatrix} y_1 \\ y_2 \end{bmatrix} = \begin{bmatrix} 0 & 0 & 0 & 1 \\ 0 & 0 & 0 & 0 \end{bmatrix} \begin{bmatrix} u \\ w \\ q \\ \theta \end{bmatrix} + \begin{bmatrix} 0 \\ 1 \end{bmatrix} w, \tag{5.42}$$

$$z = y_1 - y_{\mathrm{m}}, \tag{5.43}$$

where w is the exogenous command and y_m is the output of the reference model

$$G_{\mathrm{m}}(s) = \frac{Y_{\mathrm{m}}(s)}{W(s)} = \frac{0.0131}{s^2 + 0.16s + 0.0131}. \tag{5.44}$$

We discretize (5.41)–(5.44) using a zero-order hold and sampling time $T_s = 0.01$ sec. The reference command is taken to be a 1 deg step command in pitch angle. The controller order is $n_c = 10$ with parameters $p = 1, r = 10, \alpha(k) \equiv 40$. The closed-loop response is shown in Figure 5.24. The controller is turned on immediately and the performance variable reduces to zero within about 20 sec.

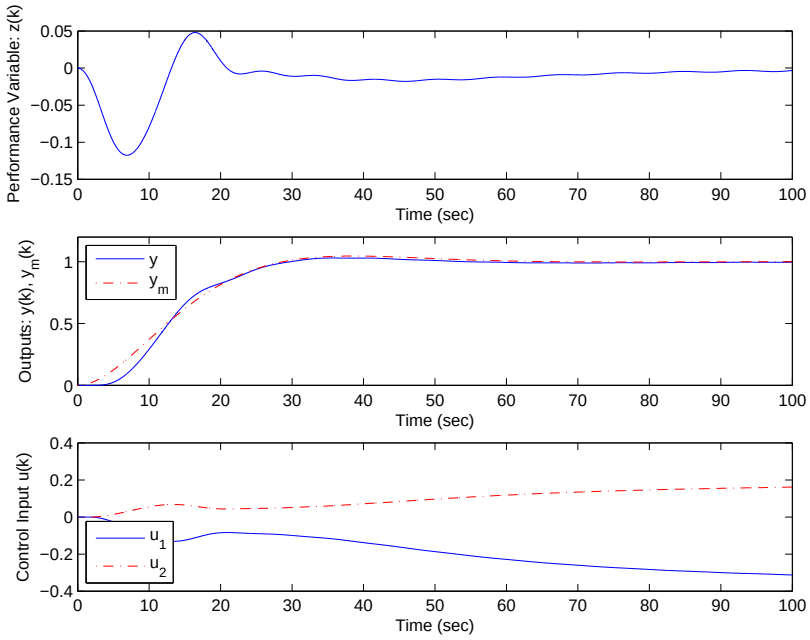

Figure 5.24 Closed-loop model reference adaptive control of Boeing 747 longitudinal dynamics. The controller order is $n_c = 10$ with parameters $p = 1, r = 10, \alpha(k) \equiv 40$. The performance variable converges within about 20 sec.

5.9.2 Missile Longitudinal Dynamics

We now present numerical examples for MRAC of missile longitudinal dynamics under off-nominal or damage situations. The basic missile longitudinal plant [89] is derived from the short period approximation of the longitudinal equations of motion,

given by

$$\dot{x} = \begin{bmatrix} -1.064 & 1 \\ 290.26 & 0 \end{bmatrix} x + \lambda \begin{bmatrix} -0.25 \\ -331.4 \end{bmatrix} u, \tag{5.45}$$

$$y = \begin{bmatrix} -123.34 & 0 \\ 0 & 1 \end{bmatrix} x + \lambda \begin{bmatrix} -13.51 \\ 0 \end{bmatrix} u, \tag{5.46}$$

where

$$x \triangleq \begin{bmatrix} \alpha \\ q \end{bmatrix}, \quad y \triangleq \begin{bmatrix} A_z \\ q \end{bmatrix},$$

and $\lambda \in (0, 1]$ represents the control effectiveness. Nominally $\lambda = 1$.

The open-loop system (5.45), (5.46) is statically unstable. To overcome this instability, a classical three-loop autopilot [89] is wrapped around the basic missile longitudinal plant. The adaptive controller then augments the closed-loop system to provide control in off-nominal cases, that is, when $\lambda < 1$. The autopilot and adaptive controller inputs are denoted u_{ap} and u_{ac}, respectively. Thus, the total control input $u = u_{\mathrm{ap}} + u_{\mathrm{ac}}$. The reference model G_{m} consists of the basic missile longitudinal plant with $\lambda = 1$ and the classical three-loop autopilot. An actuator saturation of ± 30 deg is included in the model, but no actuator or sensor dynamics are included.

Our goal is for the missile to follow a pitch acceleration command w consisting of a 1-g amplitude 1-Hz square wave. The performance variable z is the difference between the measured pitch acceleration A_z and the reference model pitch acceleration A_z^*, that is, $z \triangleq A_z - A_z^*$. The closed-loop response is shown in Figure 5.25 for $\lambda = 1$. Since the plant and reference model are identical in the nominal case, the adaptive control input $u_{\mathrm{ac}} = 0$.

All of the following examples use the same adaptive controller parameters. The adaptive controller is implemented at a sampling rate of 300 Hz. We take $n_{\mathrm{c}} = 3$, $p = 1$, and $r = 20$. A time-varying learning rate α is used such that, initially, con-

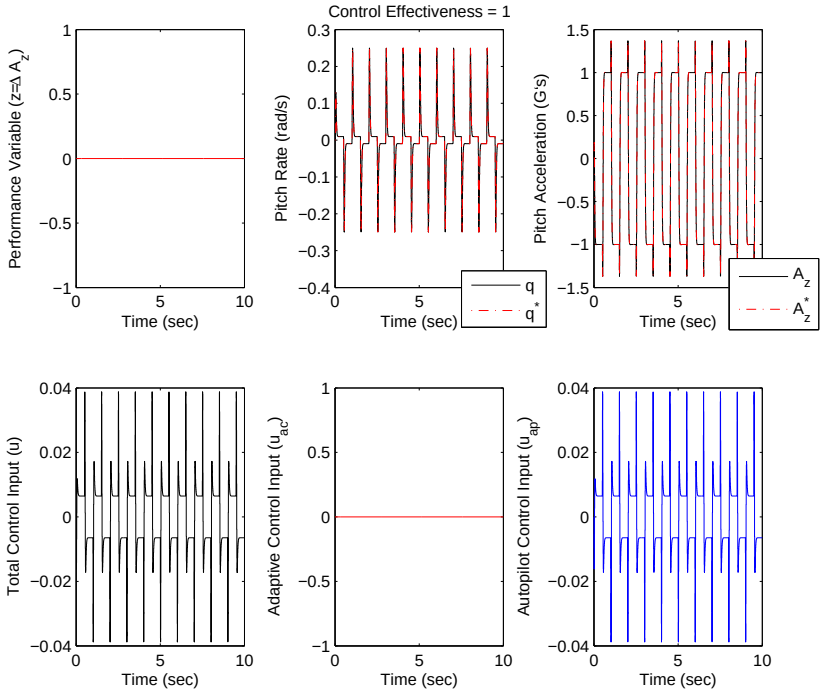

Figure 5.25 Closed-loop model reference adaptive control of missile longitudinal dynamics. The control effectiveness $\lambda = 1$, thus the plant and reference model are identical. Therefore, the adaptive control input $u_{\text{ac}} = 0$.

troller adaptation is fast, and, as performance improves, the adaptation slows. The learning rate is identical for each simulation. System identification using the Observer/Kalman filter identification (OKID) algorithm [57] is used to obtain the 20 Markov parameters required for controller implementation. The offline identification procedure is performed with a nominal simulation ($\lambda = 1$) by injecting band-limited white noise at the adaptive controller input u_{ac} and recording the performance variable z while the autopilot is in-the-loop. No external disturbances are assumed to be present during the identification procedure.

Example 5.9.1 (75% Control Effectiveness)**.** *Consider* $\lambda = 0.75$. *First, Figure 5.26 shows simulation results with the adaptive controller turned off, that is, autopilot-only control.*

Now, with the adaptive controller turned on, that is, augmented autopilot plus

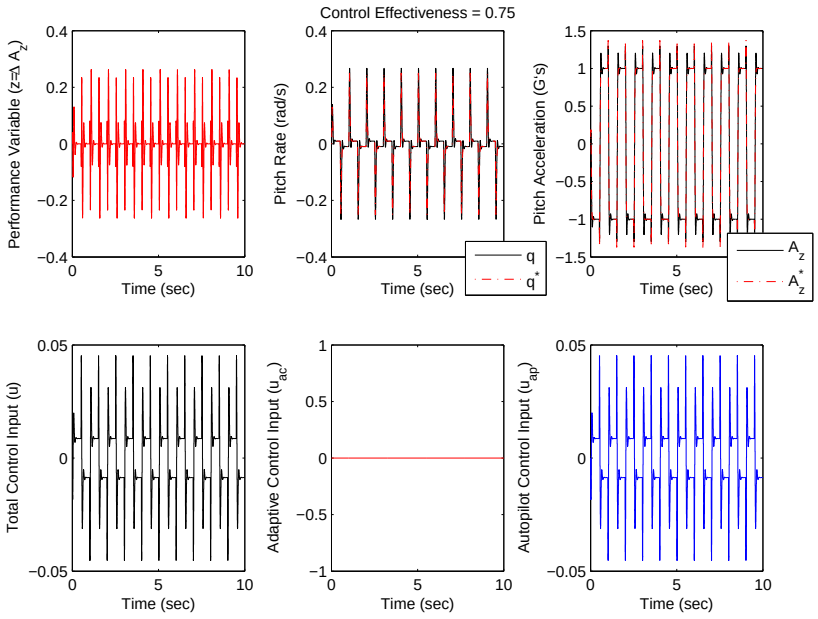

Figure 5.26 Missile longitudinal dynamics with control effectiveness $\lambda = 0.75$ and adaptive controller turned off, that is, autopilot-only control.

adaptive controller, simulation results are shown in Figure 5.27. After a small transient, the augmented controllers result in better performance than the autopilot-only simulation. ■

Example 5.9.2 (50% Control Effectiveness)**.** *Consider* $\lambda = 0.50$. *First, Figure 5.28 shows simulation results with the adaptive controller turned off, that is, autopilot-only control.*

Now, with the adaptive controller turned on, that is, augmented autopilot plus adaptive controller, simulation results are shown in Figure 5.29. After a transient, the augmented controllers result in better performance than the autopilot-only simulation. ■

Example 5.9.3 (25% Control Effectiveness)**.** *Consider* $\lambda = 0.25$. *With the adaptive controller turned off, that is, autopilot-only control, the simulation fails. With the adaptive controller turned on, that is, augmented autopilot plus adaptive con-*

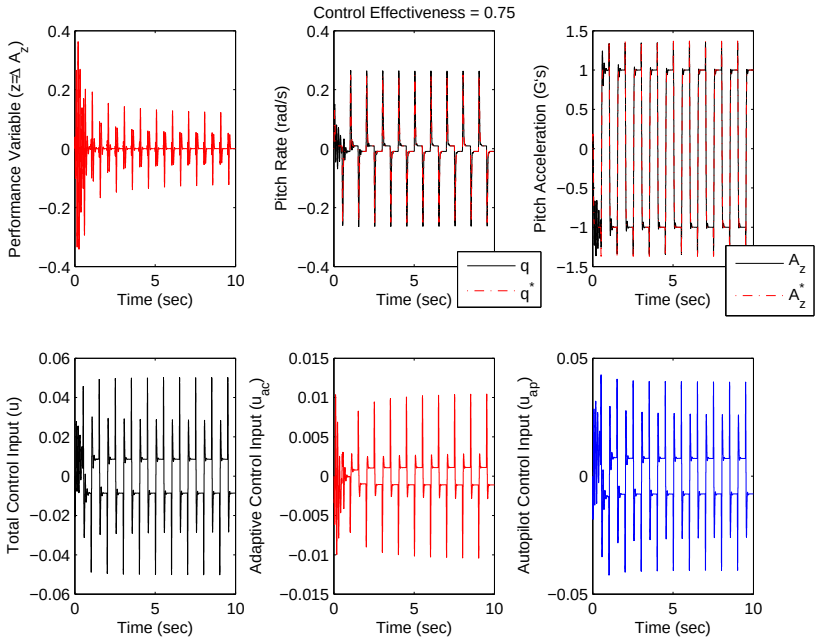

Figure 5.27 Closed-loop model reference adaptive control of missile longitudinal dynamics with control effectiveness $\lambda = 0.75$. The augmented controllers result in better performance than the autopilot-only simulation.

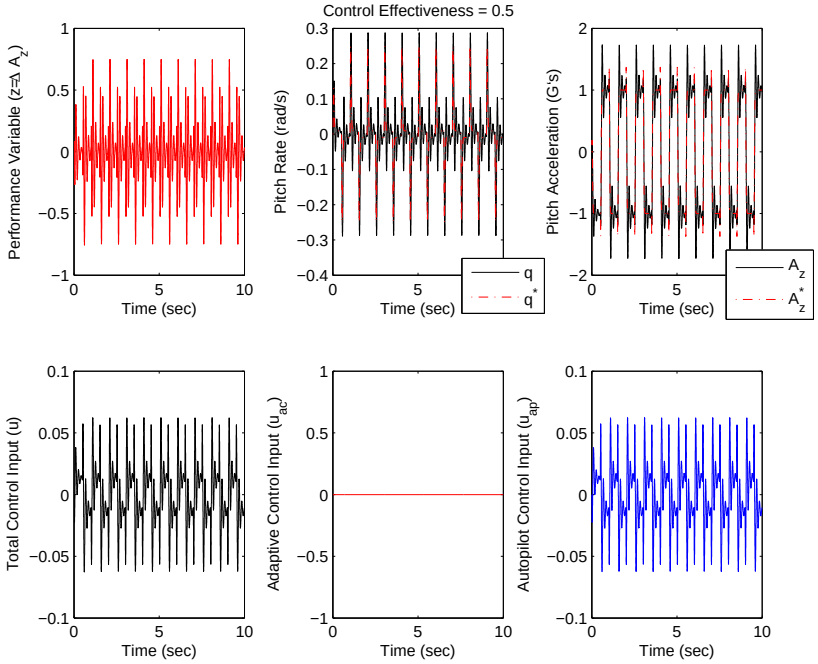

Figure 5.28 Missile longitudinal dynamics with control effectiveness $\lambda = 0.50$ and adaptive controller turned off, that is, autopilot-only control.

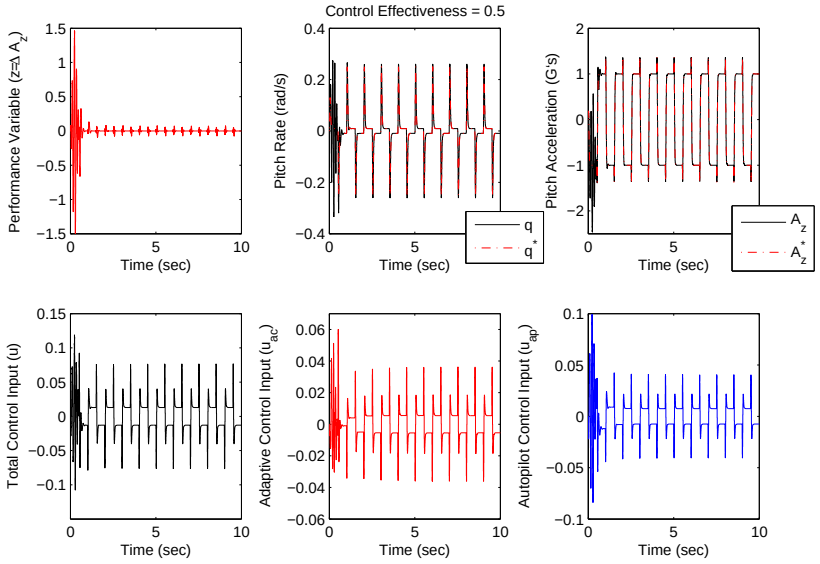

Figure 5.29 Closed-loop model reference adaptive control of missile longitudinal dynamics with control effectiveness $\lambda = 0.50$. The augmented controllers result in better performance than the autopilot-only simulation.

troller, simulation results are shown in Figure 5.30. After a transient, the augmented controllers stabilize the system whereas the autopilot-only simulation fails.

Figure 5.30 shows that the total control input u reaches the actuator saturation level of $\pm 30\,\text{deg}$. *To reduce the initial transient, a more finely tuned learning rate can be implemented or the adaptive controller can be initialized with nonzero gains. Therefore, we now initialize the adaptive controller with the converged control gains* θ *from the 50% control effectiveness case. We use the gains of the 50% case since it is a median starting point. Simulation results are shown in Figure 5.31. The initial transient is reduced as compared with initializing the control gains to zero. In this case, the actuator saturation level is never reached.* ■

5.10 Algorithm Limitations

For practical reasons such as sensor or actuator failure, control engineers can be reluctant to use unstable controllers for the purpose of stabilization. It thus follows

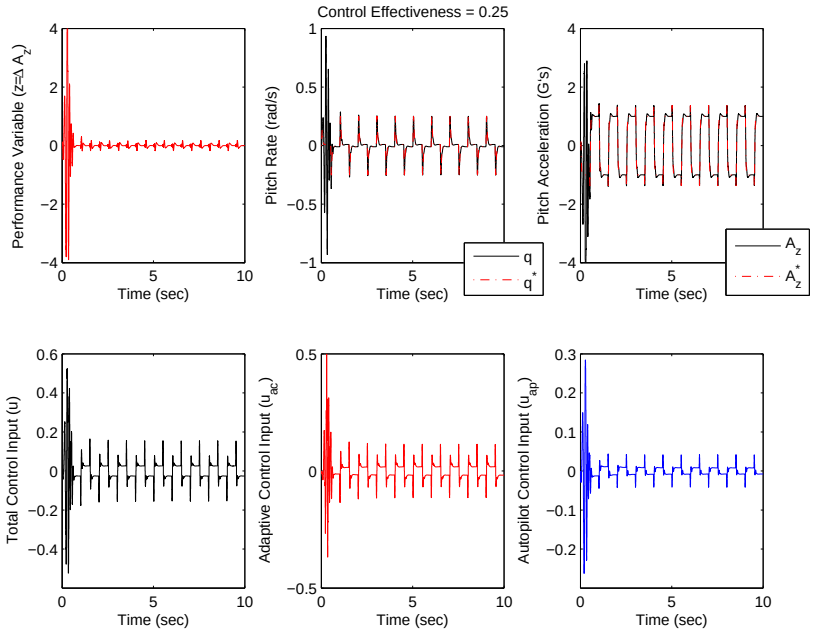

Figure 5.30 Closed-loop model reference adaptive control of missile longitudinal dynamics with control effectiveness $\lambda = 0.25$. After a transient, the augmented controllers stabilize the system whereas the autopilot-only simulation fails. Note that the system is stabilized despite the total control input u reaching the actuator saturation level of ± 30 deg.

that we are interested in plants that are strongly stabilizable [129]. A dynamical system G is said to be *strongly stabilizable* if there exists a stable controller G_c that stabilizes the open-loop system G. It is well known that a stable controller which stabilizes the system exists if and only if the plant satisfies the parity interlacing property [133]. In SISO continuous-time systems, a plant satisfies the parity interlacing property if it has an even number of poles between each pair of zeros on the positive real axis. Similar results apply for both discrete-time and MIMO systems.

After gain convergence, every simulation presented in this chapter resulted in a stable adaptive controller. No simulations performed with the RCF adaptive control algorithm have resulted in an unstable controller after gain convergence. Without converging to an unstable controller, it follows that the simulation fails if the RCF adaptive control algorithm is used to stabilize a plant that is not strongly stabilizable. No other cases have been identified which cause the RCF adaptive control algorithm

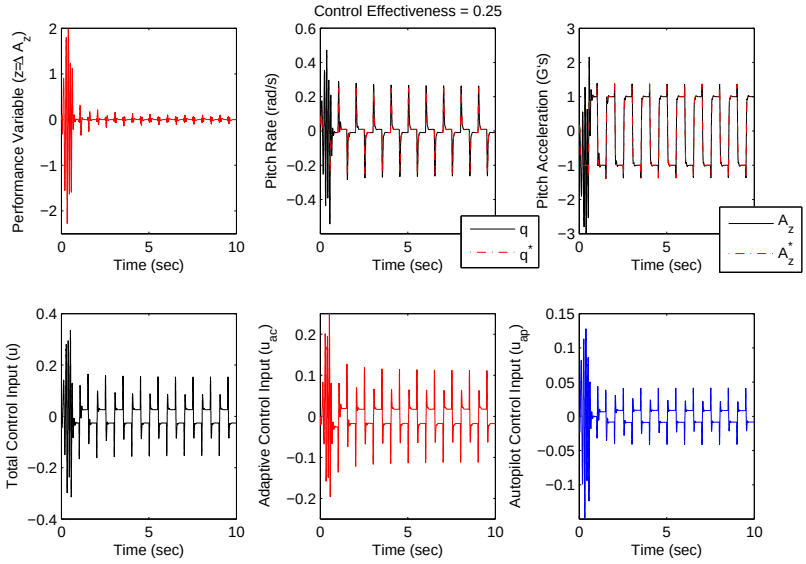

Figure 5.31 Closed-loop model reference adaptive control of missile longitudinal dynamics with control effectiveness $\lambda = 0.25$. The adaptive controller is initialized with the converged gains from the 50% control effectiveness case. The initial transient is reduced as compared with initializing the control gains to zero. In this case, the actuator saturation level is never reached.

to fail. Obtaining a linear bound of the control inputs u by the measurement variables y (as required in Theorem 2.6.1) is not possible in general for nonminimum-phase systems. However, this linear bounding condition does hold for systems that are stabilized with a stable controller. Future work includes incorporating this strongly stabilizing property into a Lyapunov-based stability analysis of the RCF adaptive control algorithm.

Linear Quadratic Gaussian (LQG) techniques have been shown to work well with broadband disturbances, but LQG controllers require complete knowledge of the system parameters. In practice, reliable knowledge of the system parameters may be impossible to obtain. Therefore, it is desirable to use adaptive controllers with minimal modeling requirements for broadband disturbance rejection. While the RCF adaptive control algorithm was shown to work well with commands and disturbances generated from Lyapunov-stable linear systems, that is, sums of discrete sinusoids and steps, it has been found to provide only marginal performance improvements for

broadband disturbance rejection applications. Future work includes the development of a theoretical foundation for analyzing broadband disturbance rejection properties of the controller.

5.11 Conclusion

We presented the RCF adaptive control algorithm and demonstrated its effectiveness in handling nonminimum-phase zeros through numerical examples illustrating the response of the algorithm under conditions of uncertainty in the relative degree and Markov parameters, measurement noise, and actuator and sensor saturations. We thus developed rules of thumb for choosing the learning rate α for stable response and acceptable transient behavior. Bursting was not observed in any of the simulations. We also developed preliminary metrics for analyzing the gain and phase margins for discrete-time adaptive systems. Future work includes the development of Lyapunov-based stability and robustness analysis of the RCF adaptive control algorithm as well as development of a theoretical foundation for analyzing broadband disturbance rejection properties of the controller.

Chapter 6

Indirect Retrospective-Cost-Based Adaptive Control with RLS-Based Estimation

In the previous chapter, we presented a direct adaptive control algorithm which required a priori information about the sign of the high-frequency gain as well as information about the locations of the nonminimum-phase zeros. In this chapter, we augment the adaptive controller developed in Chapter 5 with recursive least-squares estimation to form a discrete-time indirect adaptive control law that is effective for systems that are multi-input, multi-output, and/or nonminimum phase. Recursive least-squares estimation is used for concurrent Markov parameter updating. We present numerical examples to illustrate the algorithm's effectiveness in handling nonminimum-phase zeros as plant changes occur. The results and methods of this chapter are published in [112].

6.1 Introduction

Adaptive control algorithms can be classified as either direct or indirect, depending on whether they employ an explicit parameter estimation algorithm within the overall adaptive scheme; see [32, 50, 77, 90]. Most direct adaptive control algorithms,

with the exception of universal adaptive control algorithms [46, 47, 64, 79, 81, 86, 87, 96, 106, 130, 132], require some prior modeling information, such as the sign of the high-frequency gain. By updating the required modeling information, perhaps through closed-loop identification, a direct adaptive control algorithm can be converted to an indirect adaptive control algorithm, which may have greater versatility in practice.

The goal of the present chapter is to present an indirect discrete-time adaptive control algorithm as an extension of the direct adaptive control algorithm developed in Chapter 5. This algorithm, based on a retrospective correction filter (RCF), requires prior estimates of the Markov parameters of the transfer function from the control inputs to the performance (error) variables. These Markov parameter estimates capture the sign of the high-frequency gain as well as the locations of the nonminimum-phase zeros (if any) in the relevant transfer function. Since no parameter estimation is performed online, the algorithm developed in Chapter 5 is a direct adaptive control algorithm. In some applications, however, prior modeling or identification is not possible, whereas, in other applications, the dynamics of the plant may change unexpectedly during operation. In both cases, the required Markov parameters must be estimated online.

With this motivation in mind, the present chapter investigates the performance of the RCF-based adaptive control algorithm with concurrent Markov-parameter estimation. The resulting adaptive control algorithm is thus indirect. For parameter estimation we use a standard recursive least-squares (RLS) algorithm. The scenario we consider begins with discrete-time RCF-based direct adaptive control with prior estimates of the Markov parameters. The RLS identification algorithm operates concurrently with the control adaptation to update the Markov parameters when a plant change occurs.

We demonstrate the indirect RCF algorithm on several numerical examples. Of

particular interest is the case in which a plant change occurs, in which a minimum phase zero becomes nonminimum phase. These results are noteworthy since nonminimum-phase zeros are known to be challenging for adaptive control algorithms [5]. Numerical results show that the algorithm is able to update the Markov parameters and maintain stabilization of the system. These numerical examples are intended to provide motivation for future proofs of stability and convergence.

6.2 Recursive Least-Squares Markov Parameter Update

To obtain the required Markov parameters for constructing $\bar{B}_{zu}$, we implement the standard recursive least-squares algorithm as in [70] for the r-MARKOV plant structure (5.5). A forgetting factor is not used since no benefit was observed by including it. We initialize the parameter matrix to zero and the covariance matrix of the parameter estimation error to the identity matrix. At each time step, we take the computed Markov parameters H_i, $i = 0, \ldots, r$, and construct $\bar{B}_{zu}$ as in (5.37). The identification input for RLS is taken to be the output of the adaptive controller, that is, the control input u to the plant, while the identification output for RLS is taken to be the performance variable z. The closed-loop system including the RCF adaptive control algorithm with concurrent RLS identification for Markov parameter, and thus $\bar{B}_{zu}$, updates is shown in Figure 6.1. No probing input is used to identify the Markov parameters, and disturbances are assumed to be present while the online identification takes place.

6.3 Numerical Examples

We now present numerical examples to illustrate the response of the RCF adaptive control algorithm with concurrent RLS identification. We consider a sequence of ex-

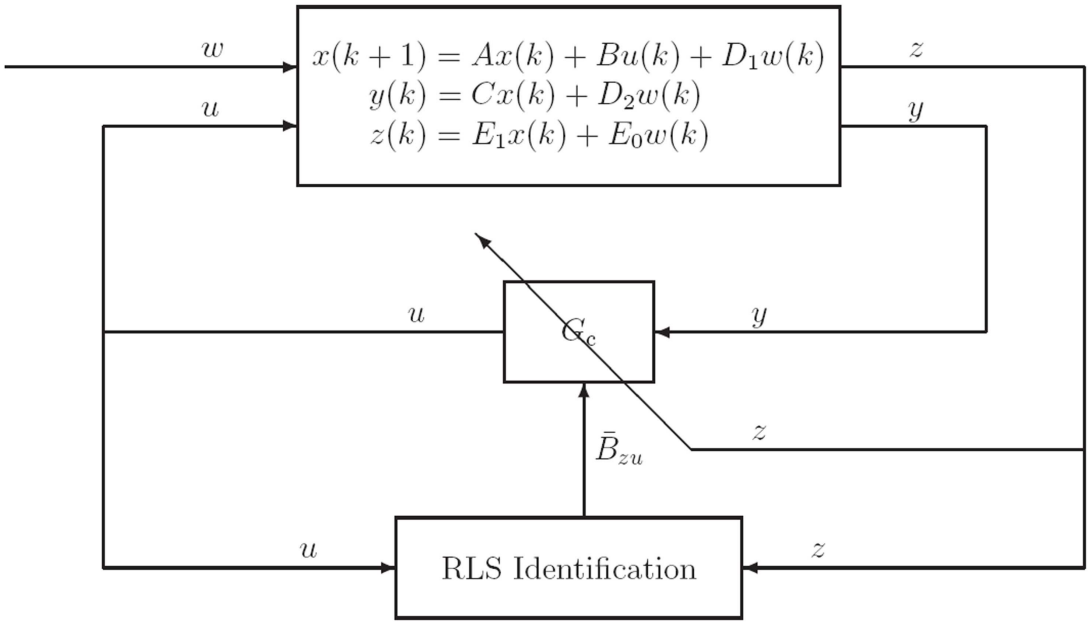

Figure 6.1 Closed-loop system including the RCF adaptive control algorithm with concurrent RLS identification for Markov parameter updates.

amples of increasing complexity. In each case, we start with a nominal plant in closed loop with the RCF adaptive control algorithm and concurrent RLS identification. At some time during the simulation, a plant change occurs, which requires updating the Markov parameters for the adaptive controller. As RLS identification runs concurrently with the adaptive controller, the Markov parameters are updated in real time. Each plant can be viewed as a sampled-data discretization of a continuous-time plant sampled at $T_{\mathrm{s}} = 0.01\,\mathrm{sec}$. All examples assume $z = y$ and the adaptive controller gain matrix $\theta(k)$ is initialized to zero.

For simplicity, each example, unless otherwise noted, is taken to be a disturbance rejection simulation, that is, $E_0 = 0$, with unknown sinusoidal disturbance given by

$$w(k) = \begin{bmatrix} \sin 2\pi\nu_1 kT_{\mathrm{s}} \\ \sin 2\pi\nu_2 kT_{\mathrm{s}} \end{bmatrix}, \tag{6.1}$$

where $\nu_1 = 5$ Hz and $\nu_2 = 13$ Hz. The RCF adaptive control algorithm requires no information about w. With each plant realized in controllable canonical form, we take $D_1 = \begin{bmatrix} I_2 \\ 0 \end{bmatrix}$, and, therefore, the disturbance is not matched.

Example 6.3.1 (Change in control effectiveness)**.** *Consider a stable, minimum-phase, SISO plant with poles* $\{0.5 \pm 0.5\jmath, -0.5 \pm 0.5\jmath, \pm 0.9, \pm 0.7\jmath\}$ *and zeros* $\{0.3 \pm 0.7\jmath, -0.7 \pm 0.3\jmath, \pm 0.5\}$. *We take* $n_c = 15$, $p = 1$, $r = 3$, *and* $\alpha(k) \equiv 25$. *The closed-loop response is shown in Figure 6.2. The control is turned on at* $t = 5\,\text{sec}$, *and the performance variable reduces to zero within* $2\,\text{sec}$. *At* $t = 15\,\text{sec}$, *the system suffers a 75% loss of control effectiveness, that is, the control input* u *entering the plant is multiplied by a scaling factor* $\lambda = 0.25$. *The Markov parameters are updated online, and the adaptive control algorithm reduces the performance variable to zero within* $2\,\text{sec}$. *Figure 6.3 shows a time-history plot of the first 3 Markov parameters obtained from online RLS identification.* ■

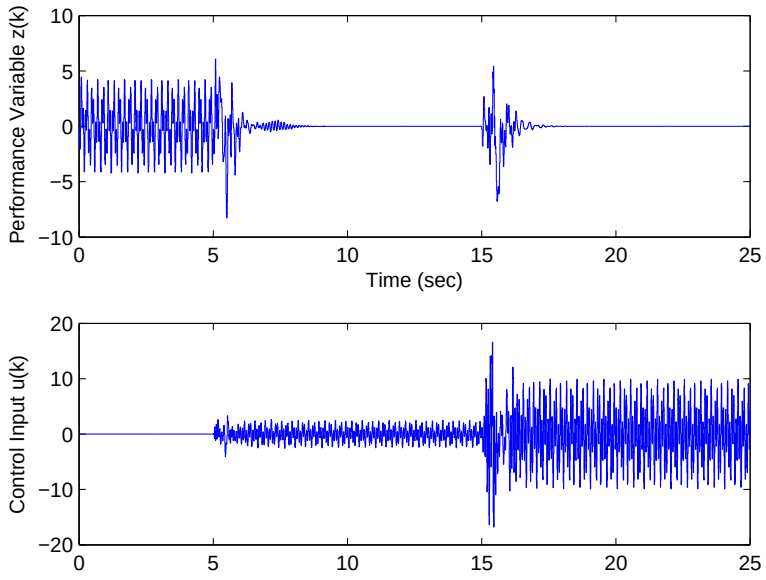

Figure 6.2 Closed-loop disturbance rejection response for a stable, minimum-phase, SISO plant. The control is turned on at $t = 5\,\text{sec}$, and, at $t = 15\,\text{sec}$, the system suffers a 75% loss of control effectiveness. The controller order is $n_c = 15$ with parameters $p = 1, r = 3, \alpha(k) \equiv 25$.

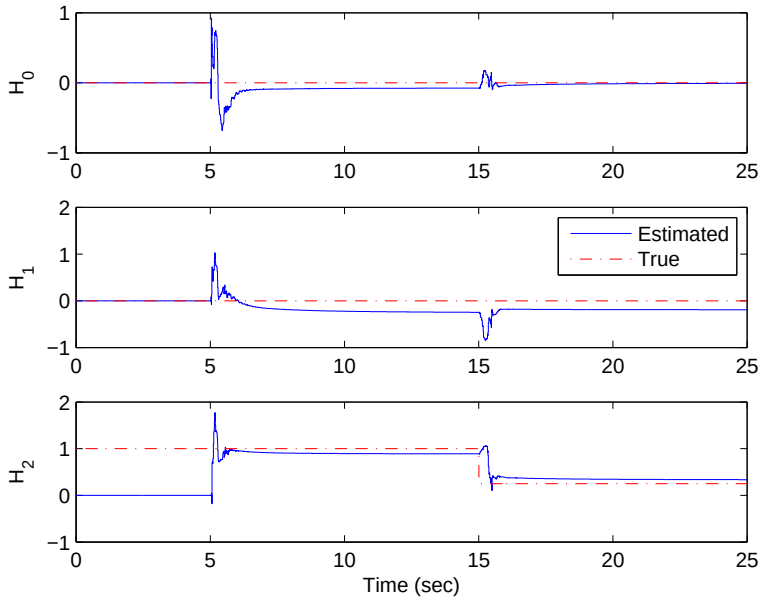

Figure 6.3 Time history of the first 3 Markov parameters obtained from online RLS identification. The control is turned on at $t = 5\,\text{sec}$, and, at $t = 15\,\text{sec}$, the system suffers a 75% loss of control effectiveness. The estimated Markov parameters are used in the adaptive controller update law.

Example 6.3.2 (Change in zero characteristics)**.** *Consider a stable, minimum-phase, SISO plant with poles* $\{0.5\pm0.5\jmath, -0.5\pm0.5\jmath, \pm0.9, \pm0.7\jmath\}$ *and zeros* $\{0.3\pm0.7\jmath, -0.7\pm 0.3\jmath, \pm0.5\}$*. We take* $n_c = 20$*,* $p = 1$*,* $r = 20$*, and* $\alpha(k) \equiv 1000$*. The closed-loop response is shown in Figure 6.4. The control is turned on at* $t = 5\,\text{sec}$*, and the performance variable reduces to zero. At* $t = 15\,\text{sec}$*, the minimum-phase zero at* $\boldsymbol{z} = 0.5$ *is changed to a nonminimum-phase zero at* $\boldsymbol{z} = 2$*. After a transient, the adaptive control algorithm reduces the performance variable to zero.* ■

Example 6.3.3 (Change in poles and zeros)**.** *Consider an order* $n = 8$ *FIR, nonminimum-phase, SISO plant with zeros* $\{0.3 \pm 0.7\jmath, -0.7 \pm 0.3\jmath, 0.5, 2\}$*. We take* $n_c = 15$*,* $p = 1$*,* $r = 10$*, and* $\alpha(k) \equiv 25$*. The closed-loop response is shown in Figure 6.5. The control is turned on at* $t = 5\,\text{sec}$*, and the performance variable reduces to zero. At* $t = 15\,\text{sec}$*, the nonminimum-phase zero at* $\boldsymbol{z} = 2$ *is changed to a minimum-phase zero at* $\boldsymbol{z} = 0.5$ *and the plant's poles are changed to*

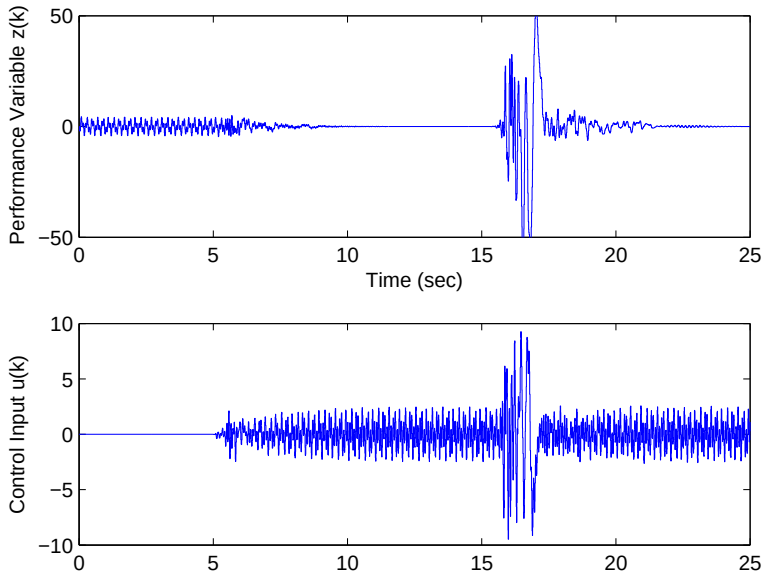

Figure 6.4 Closed-loop disturbance rejection response for a stable, minimum-phase, SISO plant. The control is turned on at $t = 5\,\text{sec}$, and, at $t = 15\,\text{sec}$, one of the plant's minimum-phase zeros is replaced with a nonminimum-phase zero. The controller order is $n_c = 20$ with parameters $p = 1, r = 20, \alpha(k) \equiv 1000$.

$\{0.5 \pm 0.5\jmath, -0.5 \pm 0.5\jmath, \pm 0.7\jmath\}$. *After a slight transient, the adaptive control algorithm reduces the performance variable to zero.* ■

Example 6.3.4 (Change in relative degree)**.** *Consider a stable, nonminimum-phase, SISO plant with poles* $\{0.5 \pm 0.5\jmath, -0.5 \pm 0.5\jmath, \pm 0.9, \pm 0.7\jmath\}$ *and zeros* $\{0.3 \pm 0.7\jmath, -0.7 \pm 0.3\jmath, 0.5, 2\}$. *We take* $n_c = 15$, $p = 2$, $r = 10$, *and* $\alpha(k) \equiv 50$. *The closed-loop response is shown in Figure 6.6. The control is turned on at* $t = 5\,\text{sec}$, *and the performance variable reduces to zero. At* $t = 15\,\text{sec}$, *the plant's relative degree is changed from* $d = 2$ *to* $d = 4$ *by adding two poles at the origin. The RLS algorithm identifies the shifted Markov parameters due to latency and recovers performance. Without RLS, the RCF algorithm is shown in [114] to be sensitive to unknown delays.* ■

Example 6.3.5 (Command following with change in zeros)**.** *We now consider a step-command following problem with command given by a square wave of frequency* $2\pi\nu_1 T_s$

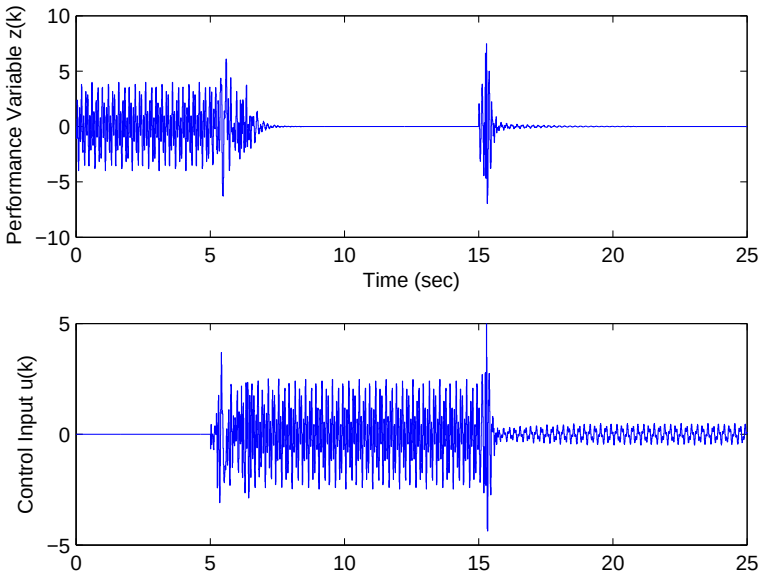

Figure 6.5 Closed-loop disturbance rejection response for an FIR, nonminimum-phase, SISO plant. The control is turned on at $t = 5\,\text{sec}$, and, at $t = 15\,\text{sec}$, the plant's nonminimum-phase zero is replaced with a minimum-phase zero and the plant's poles are relocated to stable poles away from the origin. The controller order is $n_c = 15$ with parameters $p = 1, r = 10, \alpha(k) \equiv 25$.

cycles/sample, where $\nu_3 = 0.1$ *Hz. With the plant realized in controllable canonical form, we take* $D_1 = 0$ *and* $E_0 = -1$.

Consider a stable, nonminimum-phase, SISO plant with poles $\{0.5 \pm 0.5\jmath, -0.5 \pm 0.5\jmath, \pm 0.9, \pm 0.7\jmath\}$ *and zeros* $\{0.3 \pm 0.7\jmath, -0.7 \pm 0.3\jmath, 0.5, 2\}$. *We take* $n_c = 15$, $p = 2$, $r = 25$, *and* $\alpha(k) \equiv 250$. *The closed-loop response is shown in Figure 6.7. The control is turned on at* $t = 5\,\text{sec}$, *and the performance variable reduces to zero. At* $t = 15\,\text{sec}$, *the minimum-phase zero at* $\boldsymbol{z} = 0.5$ *disappears from the plant, while the nonminimum-phase zero at* $\boldsymbol{z} = 2$ *is changed to a nonminimum-phase zero at* $\boldsymbol{z} = 2.5$. *After a transient, the adaptive control algorithm reduces the performance variable to zero and follows the step command.* ■

Example 6.3.6 (MRAC for Missile Longitudinal Dynamics)**.** *We now present a numerical example for MRAC of missile longitudinal dynamics under an off-nominal or damage situation. The MRAC control architecture is shown in Figure 5.1. The basic*

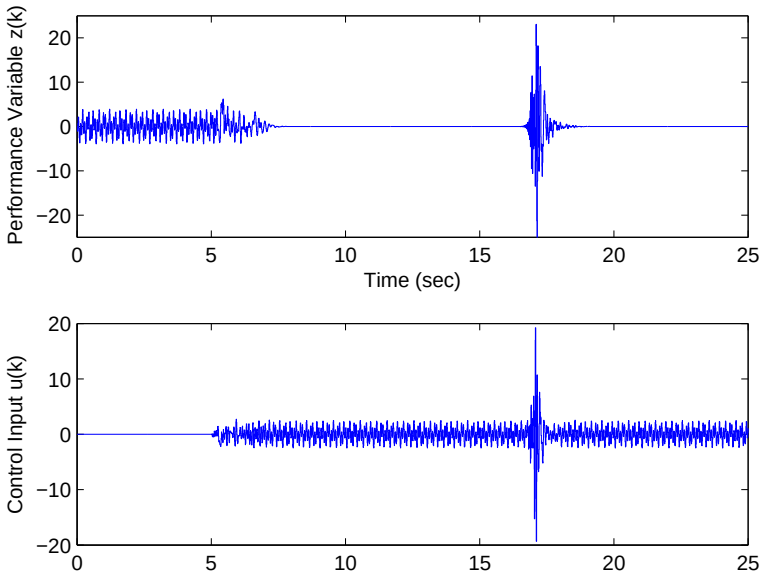

Figure 6.6 Closed-loop disturbance rejection response for a stable, nonminimum-phase, SISO plant. The control is turned on at $t = 5\,\text{sec}$, and, at $t = 15\,\text{sec}$, the plant's relative degree changes from $d = 2$ to $d = 4$. The controller order is $n_c = 15$ with parameters $p = 2, r = 10$, and $\alpha(k) \equiv 50$.

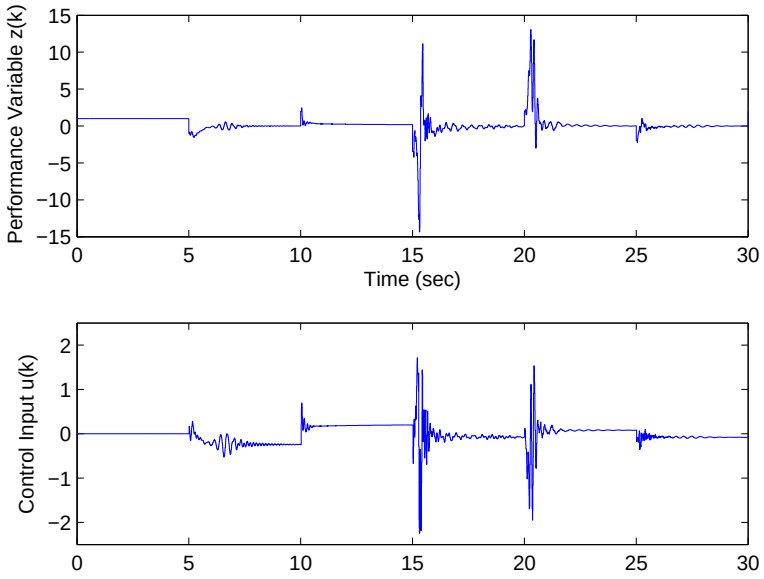

Figure 6.7 Closed-loop command following response for a stable, nonminimum-phase, SISO plant. The control is turned on at $t = 5\,\text{sec}$, and, at $t = 15\,\text{sec}$, one of the plant's minimum-phase zeros is removed while the location of the plant's nonminimum-phase zero is changed. The controller order is $n_c = 15$ with parameters $p = 2, r = 25, \alpha(k) \equiv 250$.

missile longitudinal plant of [89] is derived from the short period approximation of the longitudinal equations of motion, given by

$$\dot{x} = \begin{bmatrix} -1.064 & 1 \\ 290.26 & 0 \end{bmatrix} x + \lambda \begin{bmatrix} -0.25 \\ -331.4 \end{bmatrix} u, \tag{6.2}$$

$$y = \begin{bmatrix} -123.34 & 0 \\ 0 & 1 \end{bmatrix} x + \lambda \begin{bmatrix} -13.51 \\ 0 \end{bmatrix} u, \tag{6.3}$$

where

$$x \triangleq \begin{bmatrix} \alpha \\ q \end{bmatrix}, \quad y \triangleq \begin{bmatrix} A_z \\ q \end{bmatrix},$$

and $\lambda \in (0, 1]$ *represents the control effectiveness. Nominally* $\lambda = 1$.

The open-loop system (6.2), (6.3) is statically unstable. To overcome this instability, a classical three-loop autopilot from [89] is wrapped around the basic missile longitudinal plant. The adaptive controller then augments the closed-loop system to provide control in off-nominal cases, that is, when $\lambda < 1$. *The autopilot and adaptive controller inputs are denoted* u_{ap} *and* u_{ac}, *respectively. Thus, the total control input* $u = u_{\mathrm{ap}} + u_{\mathrm{ac}}$. *The reference model* G_{m} *consists of the basic missile longitudinal plant with* $\lambda = 1$ *and the classical three-loop autopilot. An actuator saturation of* $\pm 30\,\mathrm{deg}$ *is included in the model, but no actuator or sensor dynamics are included.*

Our goal is to have the missile follow a pitch acceleration command w *consisting of a 1-g amplitude, 1-Hz square wave. The performance variable* z *is the difference between the measured pitch acceleration* A_z *and the reference model pitch acceleration* A_z^*, *that is,* $z \triangleq A_z - A_z^*$. *The adaptive controller is implemented at a sampling rate of* 300 *Hz. We take* $n_{\mathrm{c}} = 3$, $p = 1$, *and* $r = 20$. *A time-varying learning rate* α *is used such that, initially, controller adaptation is fast, and, as performance improves, the adaptation slows.*

Figure 6.8 shows closed-loop MRAC simulation results. Initially, $\lambda = 1$, *and thus,*

the adaptive controller is not used. At $t = 5\,\text{sec}$, we change $\lambda = 0.5$, but, to demonstrate autopilot-only control, we do not turn on the adaptive controller. At $t = 10\,\text{sec}$, the adaptive controller is turned on. After a transient, the augmented controllers result in better performance than the autopilot-only control. ■

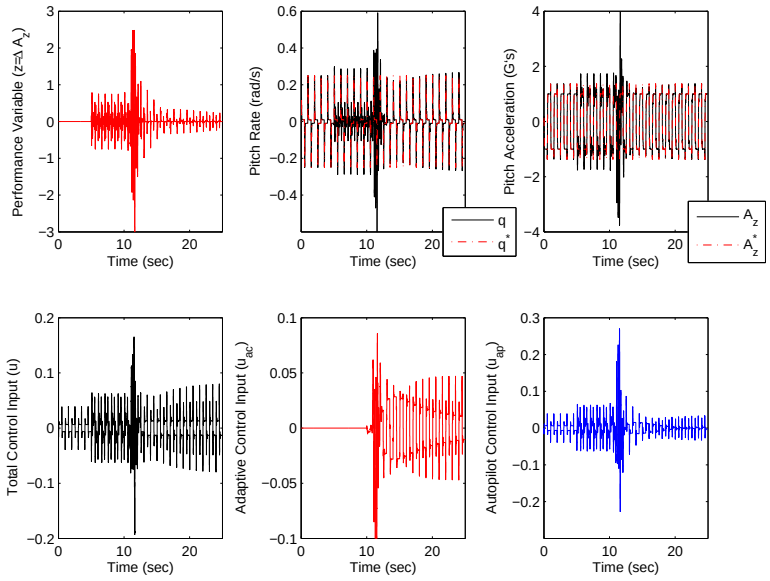

Figure 6.8 Closed-loop model reference adaptive control of missile longitudinal dynamics. Initially, $\lambda = 1$. At $t = 5\,\text{sec}$, we change $\lambda = 0.5$ but the adaptive controller remains off. At $t = 10\,\text{sec}$, the adaptive controller is turned on. After a transient, the augmented controllers result in better performance than the autopilot-only control.

6.4 Conclusion

We presented the indirect RCF adaptive control algorithm and demonstrated its effectiveness, through numerical examples, in handling nonminimum-phase zeros while plant changes occur. The adaptive control algorithm requires a sufficient number of Markov parameters to capture the sign of the high-frequency gain as well as the nonminimum-phase zeros. Recursive least-squares estimation was used for concurrent Markov parameter updating. Future work includes the development of Lyapunov-based stability and robustness analysis for the RCF adaptive control algorithm.

Chapter 7

Conclusion

This dissertation presented advances in adaptive control of multi-input, multi-output, linear, time-invariant, discrete-time systems. Chapter 2 focused on gradient-based adaptive control, while Chapters 3-6 related to retrospective-cost-based adaptive control.

Chapter 2 provided an extension of the work presented in [36, Chapter VII], where an adaptive controller was developed that requires limited model information for stabilization, command following, and disturbance rejection for multi-input, multi-output, linear, time-invariant, minimum-phase, discrete-time systems. Specifically, the controller requires knowledge of the open-loop system's relative degree and a bound on the first nonzero Markov parameter. Notably, the controller does not require knowledge of the command or disturbance spectrum as long as the command and disturbance signals are generated by Lyapunov-stable linear systems. Thus the command and disturbance signals are combinations of discrete-time sinusoids and steps. We proved global asymptotic convergence for command following and disturbance rejection.

Chapter 2 incorporated a logarithmic Lyapunov function to prove Lyapunov stability for systems whose exogenous dynamics are unknown and unmeasured. In addition, the adaptive update law was constructed as a gradient-based adaptive control algo-

rithm. Since an ideal deadbeat internal model controller was proven to exist, the gradient-based construction allowed us to compute and implement an optimal gradient step size. Furthermore, the gradient-based construction provided a framework for directly analyzing tradeoffs between transient performance and modeling accuracy. Finally, an inverse system representation was derived for multi-input, multi-output, minimum-phase systems which was necessary for the proof of Theorem 2.6.1.

Since the adaptive control method presented in Chapter 2 has been shown to perform well in simulation on broadband disturbances that are not generated by Lyapunov-stable linear systems, future work includes developing a theoretical foundation for analyzing and proving the broadband disturbance rejection properties of the controller.

Chapter 3 began the main topic of this dissertation. Since the method of proof for the gradient-based adaptive control algorithm presented in Chapter 2 could not be extended to nonminimum-phase systems, we focused on retrospective-cost-based adaptive control. To review, retrospective cost optimization is a measure of performance at the current time based on a past window of data and without assumptions about the command or disturbance signals. In particular, retrospective cost optimization acts as an inner loop to the adaptive control algorithm by modifying the performance variables based on the difference between the actual past control inputs and the recomputed past control inputs based on the current control law.

In particular, Chapter 3 investigated full-state-feedback stabilization in multi-input, linear, time-invariant, discrete-time systems. The results of Chapter 3 supported and motivated the retrospective-cost-based adaptive controllers developed in Chapters 4 and 5 by providing a basis for retrospective cost optimization. Specifically, a retrospective-cost-based adaptive controller was developed for full-state-feedback stabilization. Furthermore, Lyapunov stability of the closed-loop error system was proven for a special case. Numerical examples illustrated the robustness of the algo-

rithm under conditions of Markov-parameter uncertainty. Theoretical and numerical results suggested that the converged adaptive controller has a downward adaptive gain margin of 6 dB and an infinite upward adaptive gain margin, which is reminiscent of continuous-time fixed-gain LQR control.

Although the retrospective-cost-based full-state-feedback adaptive control algorithm developed in Chapter 3 was shown to work well in many cases with $r = 1$, there were situations that required $r > 1$. However, in all cases, $r = n + 1$ was found to stabilize the open-loop system. Although $r = n + 1$ requires more knowledge of the Markov parameters than with $r = 1$, it is still less information than required to reconstruct a system model through techniques such as the eigenstructure realization algorithm, which generally requires $2n$ Markov parameters. Future work includes extending the specialized Lyapunov-based stability and convergence proof to the more general case to include multi-input, multi-dimensional plants with $r > 1$.

As an extension to the results of Chapter 3, Chapter 4 investigated static-output-feedback stabilization in multi-input, multi-output, linear, time-invariant, discrete-time systems with knowledge of the sign of the high-frequency gain and a sufficient number of Markov parameters to approximate the nonminimum-phase zeros (if any). No additional information about the poles or zeros need be known. In addition, a theoretical link between nonminimum-phase zero information and Markov parameters was developed and explored through simulation. Numerical examples illustrated the robustness of the algorithm under conditions of Markov parameter uncertainty.

The results of Chapter 4 suggest that $r = n + 1$ was sufficient to stabilize the open-loop system. However, future work includes the development of a Lyapunov-based stability and convergence proof for the adaptive control algorithm presented in Chapter 4. In addition, the theoretical link between nonminimum-phase zero information and Markov parameters needs to be explored further, especially for multi-input, multi-output systems, where the presence of transmission zeros complicates the anal-

ysis.

Chapter 5 provided an extension to the work presented in [127] as well as Chapter 3 and Chapter 4 of this dissertation. Specifically, Chapter 5 generalized the results of Chapter 3 and Chapter 4 to dynamic compensation for stabilization, command following, disturbance rejection, and model reference adaptive control. A retrospective-cost-based adaptive controller was developed for multi-input, multi-output, linear, time-invariant, discrete-time systems with knowledge of the sign of the high-frequency gain and a sufficient number of Markov parameters to approximate the nonminimum-phase zeros (if any). No additional information about the poles or the zeros need be known.

The adaptive control algorithms developed in Chapters 3-5 of this dissertation incorporated an adjustable learning-rate parameter α which allowed us to develop Newton-step-based adaptive update laws. In addition, Chapter 5 further developed the theoretical link between Markov parameters and nonminimum-phase zeros. We also developed preliminary metrics for analyzing the gain and phase margins for discrete-time adaptive systems. Numerical robustness analysis with uncertainty in the required modeling information was presented for plants that are multi-input, multi-output, nonminimum phase, and possibly unstable. These numerical studies showed that the adaptive control algorithm is effective for handling nonminimum-phase zeros under minimal modeling assumptions. These numerical studies serve as guidance with regard to the future development of system identification algorithms that can estimate the required plant parameters with suitable accuracy.

Future work includes development of the learning-rate parameter α as a function of the performance objective z as well as the development of Lyapunov-based stability and robustness analysis for the retrospective-cost-based adaptive control algorithm presented in Chapter 5. While the RCF adaptive control algorithm was shown to work well with commands and disturbances generated from Lyapunov-stable linear systems,

that is, sums of discrete sinusoids and steps, it was found to provide only marginal performance improvements for broadband disturbance rejection applications. Future work includes the development of a theoretical foundation for analyzing and proving the broadband disturbance rejection properties of the adaptive controller presented in Chapter 5.

Finally, Chapter 6 extended the results of Chapter 5. Specifically, the direct adaptive controller developed in Chapter 5 was augmented with recursive least-squares estimation to form a discrete-time indirect adaptive control law that is effective for systems that are multi-input, multi-output, and/or nonminimum phase. Recursive least-squares estimation was used for concurrent Markov parameter updating. Numerical examples illustrated the algorithm's effectiveness in handling nonminimum-phase zeros as plant changes occured. Numerical results showed that the algorithm was able to update the Markov parameters and maintain stabilization of the system.

Appendix A

Properties of the Markov Parameter Polynomial

A.1 Problem Formulation

Consider the MIMO discrete-time system

$$x(k+1) = Ax(k) + Bu(k), \tag{A.1}$$

$$y(k) = Cx(k), \tag{A.2}$$

$$z(k) = E_1 x(k), \tag{A.3}$$

where $x(k) \in \mathbb{R}^n$, $y(k) \in \mathbb{R}^{l_y}$, $z(k) \in \mathbb{R}^{l_z}$, $u(k) \in \mathbb{R}^{l_u}$, and $k \geq 0$. For a positive integer r, we define the *extended performance vector* $Z(k) \in \mathbb{R}^{l_z r}$ and the *extended input vector* $U(k) \in \mathbb{R}^{l_u r}$ by

$$Z(k) \triangleq \begin{bmatrix} z(k-r+1) \\ z(k-r+2) \\ \vdots \\ z(k) \end{bmatrix}, \quad U(k) \triangleq \begin{bmatrix} u(k-r) \\ u(k-r+1) \\ \vdots \\ u(k-1) \end{bmatrix}.$$

Note that $Z(k)$, $U(k)$, and $x(k)$ are related by

$$Z(k) = \Gamma x(k-r) + \mathcal{H}U(k), \tag{A.4}$$

where $\Gamma \in \mathbb{R}^{l_z r}$ and $\mathcal{H} \in \mathbb{R}^{l_z r \times l_u r}$ are given by

$$\Gamma \triangleq \begin{bmatrix} E_1 A \\ E_1 A^2 \\ \vdots \\ E_1 A^r \end{bmatrix}, \quad \mathcal{H} \triangleq \begin{bmatrix} H_1 & 0 & \cdots & 0 \\ H_2 & H_1 & \ddots & \vdots \\ \vdots & & \ddots & 0 \\ H_r & H_{r-1} & \cdots & H_1 \end{bmatrix},$$

and, for $i = 1, 2, \ldots$, the Markov parameters H_i of the system (A.1)–(A.3) from u to z are

$$H_i \triangleq E_1 A^{i-1} B. \tag{A.5}$$

Let d denote the *relative degree* of (A, B, E_1), that is, the smallest positive integer i such that the ith Markov parameter H_i is nonzero. Note that, if $r < d$, then $\mathcal{H} = 0$. Therefore, we assume that $r \geq d$.

A.2 Markov Parameter Polynomial

From (A.4), the expression for $z(k)$ is

$$z(k) = E_1 A^r x(k-r) + H_1 u(k-1) + H_2 u(k-2) + \cdots + H_r u(k-r). \tag{A.6}$$

In terms of the forward-shift operator $\mathbf{q}$, (A.6) can be rewritten as

$$z(k) = E_1 A^r \mathbf{q}^{-r} x(k) + \left[H_1 \mathbf{q}^{-1} + H_2 \mathbf{q}^{-2} + \cdots + H_r \mathbf{q}^{-r}\right] u(k). \tag{A.7}$$

Shifting (A.7) forward by r steps gives

$$z(k+r) = E_1 A^r x(k) + p_r(\mathbf{q})u(k), \tag{A.8}$$

where

$$p_r(\mathbf{q}) \stackrel{\triangle}{=} H_1\mathbf{q}^{r-1} + H_2\mathbf{q}^{r-2} + \cdots + H_r \tag{A.9}$$

is the *Markov parameter polynomial*. For $r < d$, note that $p_r(\mathbf{q}) = 0$, whereas, if $r \geq d$, then

$$p_r(\mathbf{q}) = H_d\mathbf{q}^{r-d} + H_{d+1}\mathbf{q}^{r-d-1} + \cdots + H_r. \tag{A.10}$$

The Markov parameter polynomial contains information about the system's relative degree and sign of the high-frequency gain in the case $l_u = l_z = 1$.

The following fact states that, for SISO transfer functions, the roots of the Markov parameter polynomial include an estimate of each nonminimum-phase zero of the transfer function from u to z. As r increases, this approximation improves.

Fact A.2.1. *Consider $l_u = l_z = 1$ and let $\boldsymbol{p}$ be a zero of the transfer function from u to z. For each r, let $\mathcal{R}_r \stackrel{\triangle}{=} \{\boldsymbol{p}_{r,1}, \ldots, \boldsymbol{p}_{r,r-d}\}$ be the set of roots of $p_r(\boldsymbol{q})$. Then, there exists a sequence $\{\boldsymbol{p}_{r,i_r}\}_{r=1}^{\infty}$ that converges to $\boldsymbol{p}$ as $r \to \infty$.*

A.3 Time-Series Modeling

Consider the time-series representation of (A.1) - (A.3) from u to z, given by

$$z(k) = \sum_{i=1}^{n} -\alpha_i z(k-i) + \sum_{i=d}^{n} \beta_i u(k-i), \tag{A.11}$$

where $\alpha_1, \ldots, \alpha_n \in \mathbb{R}$ and $\beta_d, \ldots, \beta_n \in \mathbb{R}^{l_z \times l_u}$. The transfer function matrix $G_{zu}(\mathbf{z}) \stackrel{\triangle}{=} E_1(\mathbf{z}I - A)^{-1}B$ from u to z can be equivalently represented by

$$G_{zu}(\mathbf{z}) = \frac{1}{\mathbf{z}^n + \alpha_1 \mathbf{z}^{n-1} + \cdots + \alpha_n} \cdot \left(\beta_d \mathbf{z}^{n-d} + \beta_{d+1}\mathbf{z}^{n-d-1} + \cdots + \beta_n\right). \tag{A.12}$$

It follows that $\beta_d = H_d$.

Replacing k with $k-1$ in (A.11) and substituting the resulting relation back into (A.11) yields a *2-MARKOV* model. Repeating this procedure $r-1$ times yields the r-MARKOV model from u to z of (A.1) - (A.3)

$$z(k) = \sum_{i=1}^{n} \alpha_{r,i} z(k-r-i+1) + \sum_{i=d}^{r} H_i u(k-i) + \sum_{i=2}^{n} \beta_{r,i} u(k-r-i+1), \tag{A.13}$$

where, for $i = 1 \ldots n$, the coefficients $\alpha_{r,i} \in \mathbb{R}$ and $\beta_{r,i} \in \mathbb{R}^{l_z \times l_u}$ are given by

$$\begin{aligned}
&\alpha_{1,i} \stackrel{\triangle}{=} -\alpha_i, && \beta_{1,i} \stackrel{\triangle}{=} \beta_i, \\
&\quad\vdots && \quad\vdots \\
&\alpha_{r,i} \stackrel{\triangle}{=} \alpha_{r-1,1}\alpha_{1,i} + \alpha_{r-1,i+1}, && \beta_{r,i} \stackrel{\triangle}{=} \alpha_{r-1,1}\beta_{1,i} + \beta_{r-1,i+1}, \\
&\quad\vdots && \quad\vdots \\
&\alpha_{r,n} \stackrel{\triangle}{=} \alpha_{r-1,1}\alpha_{1,n}, && \beta_{r,n} \stackrel{\triangle}{=} \alpha_{r-1,1}\beta_{1,n}.
\end{aligned} \tag{A.14}$$

Note that $H_r = \beta_{r,1}$.

Equation (A.13) can be equivalently represented as the *r-MARKOV transfer function*

$$G_{r,zu}(\mathbf{z}) = \frac{1}{\mathbf{z}^{r+n-1} + \alpha_{r,1}\mathbf{z}^{n-1} + \cdots + \alpha_{r,n}} \cdot \left(H_d \mathbf{z}^{r+n-d-1} + \cdots + H_{r-1}\mathbf{z}^n + \beta_{r,1}\mathbf{z}^{n-1} + \cdots + \beta_{r,n}\right). \tag{A.15}$$

This system representation is nonminimal, overparameterized, order $n+r-1$, and the coefficients of the terms $\mathbf{z}^{n+r-2}$ through $\mathbf{z}^n$ in the denominator are zero. It follows that (A.15) can be rewritten as

$$\begin{aligned} G_{r,zu}(\mathbf{z}) &= \frac{(\mathbf{z}^{r-1} + \alpha_{1,1}\mathbf{z}^{r-2} + \cdots + \alpha_{r-1,1}) \cdot \left(\beta_d \mathbf{z}^{n-d} + \beta_{d+1}\mathbf{z}^{n-d-1} + \cdots + \beta_n\right)}{(\mathbf{z}^{r-1} + \alpha_{1,1}\mathbf{z}^{r-2} + \cdots + \alpha_{r-1,1}) \cdot (\mathbf{z}^n + \alpha_1 \mathbf{z}^{n-1} + \cdots + \alpha_n)} \\ &= \frac{R_r(\mathbf{z})}{R_r(\mathbf{z})} \cdot G_{zu}(\mathbf{z}), \end{aligned} \tag{A.16}$$

where

$$R_r(\mathbf{z}) \stackrel{\triangle}{=} \mathbf{z}^{r-1} + \alpha_{1,1}\mathbf{z}^{r-2} + \cdots + \alpha_{r-1,1} \tag{A.17}$$

is the *ring polynomial*.

Fact A.3.1 (SISO, zeros and ring)**.** *Consider $l_u = l_z = 1$ and let $P(\boldsymbol{z})$ and $Q(\boldsymbol{z})$ denote the polynomials whose roots are the minimum-phase and nonminimum-phase zeros from u to z, respectively, of* (A.1)-(A.3)*. Then*

$$\begin{aligned} &roots\left[H_d \boldsymbol{z}^{r+n-d-1} + \cdots + H_{r-1}\boldsymbol{z}^n + \beta_{r,1}\boldsymbol{z}^{n-1} + \cdots + \beta_{r,n}\right] \\ &\quad = roots\left[P(\boldsymbol{z})\right] \cup roots\left[Q(\boldsymbol{z})\right] \cup roots\left[R_r(\boldsymbol{z})\right]. \end{aligned} \tag{A.18}$$

The Laurent series expansion of $G_{zu}(\mathbf{z})$ about $\mathbf{z} = \infty$ is given by

$$\begin{aligned} G_{zu}(\mathbf{z}) &= E_1(\mathbf{z}I - A)^{-1}B \\ &= \frac{1}{\mathbf{z}}E_1(I - \frac{1}{\mathbf{z}}A)^{-1}B \\ &= \sum_{i=1}^{\infty} \frac{1}{\mathbf{z}^i}E_1A^{i-1}B \\ &= \frac{1}{\mathbf{z}}E_1B + \frac{1}{\mathbf{z}^2}E_1AB + \cdots \\ &= \frac{1}{\mathbf{z}}H_1 + \frac{1}{\mathbf{z}^2}H_2 + \cdots \\ &= \frac{1}{\mathbf{z}^d}H_d + \frac{1}{\mathbf{z}^{d+1}}H_{d+1} + \cdots \\ &= \sum_{i=d}^{\infty} \mathbf{z}^{-i}H_i. \end{aligned} \tag{A.19}$$

Truncating the numerator and denominator of (A.15) is equivalent to the r-th order Laurent series expansion about $\mathbf{z} = \infty$, given by

$$\begin{aligned} \bar{G}_{r,zu}(\mathbf{z}) &= \frac{1}{\mathbf{z}^{r+n-1}} \cdot \left(H_d\mathbf{z}^{r+n-d-1} + \cdots + H_{r-1}\mathbf{z}^n + \beta_{r,1}\mathbf{z}^{n-1}\right) \\ &= \frac{1}{\mathbf{z}^{r+n-1}} \left(H_d\mathbf{z}^{r+n-d-1} + \cdots + H_{r-1}\mathbf{z}^n + H_r\mathbf{z}^{n-1}\right) \\ &= \frac{1}{\mathbf{z}^r} \left(H_d\mathbf{z}^{r-d} + \cdots + H_{r-1}\mathbf{z} + H_r\right) \\ &= \sum_{i=d}^{r} \mathbf{z}^{-i}H_i. \end{aligned} \tag{A.20}$$

Note that the numerator coefficients of the truncated transfer function (A.20) are identical to the coefficients of the Markov parameter polynomial (A.10). The following example and conjectures remark that, as r is increased, some roots of the Markov parameter polynomial $p_r(\mathbf{q})$, and hence, the numerator of the truncated transfer function $\bar{G}_{r,zu}(\mathbf{z})$, approximate the locations of any nonminimum-phase zeros from u to z of (A.1)-(A.3). The remaining roots are either located at the origin or form an approximate ring close to a circle with radius equal to the spectral radius of the

r	$\mathbf{roots}_{\mathrm{nmp}}(p_r(\mathbf{q}))$
6	$\{\mathbf{0.94}, \mathbf{-1.54}\}$
8	$\{\mathbf{1.17}, \mathbf{-1.50}\}$
10	$\{\mathbf{1.21}, \mathbf{-1.50}\}$
15	$\{\mathbf{1.24}, \mathbf{-1.50}\}$
20	$\{\mathbf{1.25}, \mathbf{-1.50}\}$

Table A.1 Approximate nonminimum-phase zero locations obtained as roots of $p_r(\mathbf{q})$ as a function of r for the stable, nonminimum-phase plant in Example A.3.1. As r increases, the nonminimum-phase zeros are more accurately modeled.

dynamics matrix A.

Example A.3.1 (SISO, Nonminimum Phase, Stable Plant)**.** *Consider a plant with poles* $\{0.5 \pm 0.5\jmath, -0.5 \pm 0.5\jmath, \pm 0.95, \pm 0.7\jmath\}$ *and zeros* $\{0.3 \pm 0.7\jmath, -0.7 \pm 0.3\jmath, 1.25, -1.5\}$. *Table A.1 lists the approximated nonminimum-phase zero locations obtained as roots of* $p_r(\boldsymbol{q})$ *as a function of* r. *Note that as* r *increases, the approximation of the nonminimum-phase zero locations improves.*

Figure A.1 shows the roots of $p_{20}(\boldsymbol{q})$. *The dotted line denotes* $sprad(A) = 0.95$. *Note that the approximated nonminimum-phase zero locations are close to the true locations. The remaining roots are either located at the origin or form an approximate ring close to a circle with radius equal to the spectral radius of the dynamics matrix* A. ■

It follows from Example A.3.1 that, for each finite value of r, the roots of the Markov parameter polynomial $p_r(\mathbf{q})$ contain an approximation to the nonminimum-phase zeros of $G_{zu}(\mathbf{z})$. For increasing r, this approximation improves. In addition, Markov parameters may not be known exactly and therefore must be estimated. Hence, the estimated Markov parameters will introduce further error into the approximation of the nonminimum-phase zeros of $G_{zu}(\mathbf{z})$. Future work includes a study of sensitivity of the nonminimum-phase zero information to the number of Markov parameters in $p_r(\mathbf{q})$ as well as the Markov parameter estimation error.

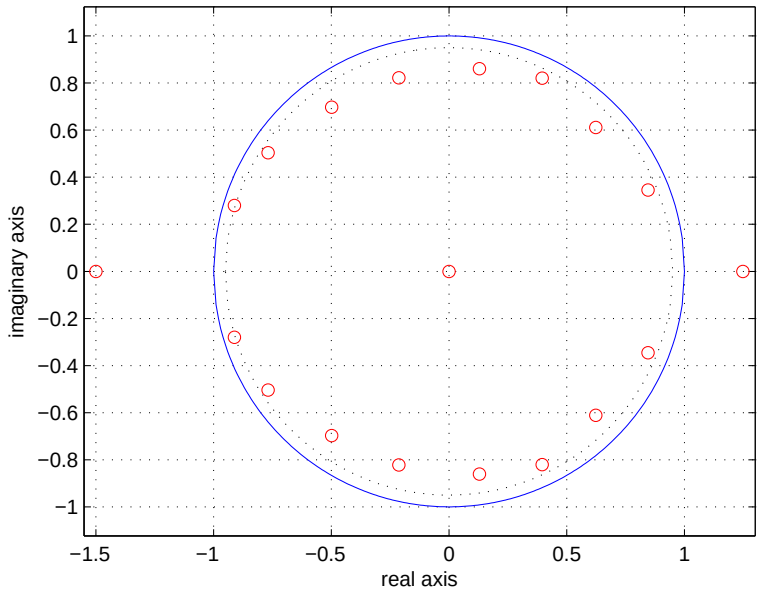

Figure A.1 Roots of $p_{20}(\mathbf{q})$ for the stable, nonminimum-phase plant in Example A.3.1. The dotted line denotes $\text{sprad}(A) = 0.95$. Note that the approximated nonminimum-phase zero locations are close to the true locations. The remaining roots are either located at the origin or form an approximate ring close to a circle with radius equal to the spectral radius of the dynamics matrix A.

Conjecture A.3.1 (SISO, stable, truncated polynomial)**.** *Consider* $l_u = l_z = 1$, $\|\lambda_{\max}(A)\| < 1$, *and let* $P(\boldsymbol{z})$ *and* $Q(\boldsymbol{z})$ *denote the polynomials whose roots are the minimum-phase and nonminimum-phase zeros from* u *to* z, *respectively, of* (A.1)-(A.3).

If $max(abs(roots\,[P(\boldsymbol{z})])) < \|\lambda_{\max}(A)\|$, *then*

$$\lim_{r\to\infty} roots\left[H_d\boldsymbol{z}^{r+n-d-1} + \cdots + H_{r-1}\boldsymbol{z}^{n} + \beta_{r,1}\boldsymbol{z}^{n-1}\right] = roots\,[Q(\boldsymbol{z})] \cup roots\left[\bar{R}_r(\boldsymbol{z})\right] \cup 0_{n-1}, \tag{A.21}$$

where $\bar{R}_r(\boldsymbol{z})$ *is a* perturbed ring polynomial. *The nonminimum phase zeros are retained while the remaining roots are either located at the origin or form an approximate ring close to a circle with radius equal to the spectral radius of* A. *A total of* $n-1$ *roots are located at the origin.*

Otherwise, if max(abs(roots$[P(\boldsymbol{z})]$*)) >* $\|\lambda_{\max}(A)\|$*, then*

$$\lim_{r\to\infty} roots\left[H_d\boldsymbol{z}^{r+n-d-1}+\cdots+H_{r-1}\boldsymbol{z}^{n}+\beta_{r,1}\boldsymbol{z}^{n-1}\right] = roots\left[Q(\boldsymbol{z})\right]\cup roots\left[\bar{P}(\boldsymbol{z})\right]\cup roots\left[\bar{\bar{R}}_r(\boldsymbol{z})\right]\cup 0_{n-1}, \tag{A.22}$$

where $\bar{P}(\boldsymbol{z})$ *is a subset of* $P(\boldsymbol{z})$ *containing all roots* p_i *of* $P(\boldsymbol{z})$ *such that, for* $i=1\ldots n_{\bar{p}}$, $\|p_i\| > \|\lambda_{\max}(A)\|$, *and* $\bar{\bar{R}}_r(\boldsymbol{z})$ *is another perturbed ring polynomial. The nonminimum-phase zeros, as well as any minimum-phase zeros whose magnitude is greater than* $\|\lambda_{\max}(A)\|$, *are retained, while the remaining roots are either located at the origin or form an approximate ring close to a circle with radius equal to the spectral radius of A. A total of* $n-1$ *roots are located at the origin.*

Conjecture A.3.2 (SISO, unstable, truncated polynomial)**.** *Consider* $l_u = l_z = 1$, $\|\lambda_{\max}(A)\| > 1$, *and let* $P(\boldsymbol{z})$ *and* $Q(\boldsymbol{z})$ *denote the polynomials whose roots are the minimum-phase and nonminimum-phase zeros from u to z, respectively, of* (A.1)-(A.3).

If max(abs(roots$[Q(\boldsymbol{z})]$*)) <* $\|\lambda_{\max}(A)\|$*, then*

$$\lim_{r\to\infty} roots\left[H_d\boldsymbol{z}^{r+n-d-1}+\cdots+H_{r-1}\boldsymbol{z}^{n}+\beta_{r,1}\boldsymbol{z}^{n-1}\right] = roots\left[\bar{R}_r(\boldsymbol{z})\right]\cup 0_{n-1}, \tag{A.23}$$

where $\bar{R}_r(\boldsymbol{z})$ *is a perturbed ring polynomial. The nonminimum-phase zeros are not retained. The roots are either located at the origin or form an approximate ring close to a circle with radius equal to the spectral radius of A. A total of* $n-1$ *roots are located at the origin.*

Otherwise, if max(abs(roots$[Q(\boldsymbol{z})]))$ > $\|\lambda_{\max}(A)\|$*, then*

$$\lim_{r\to\infty} \mathit{roots}\left[H_d\boldsymbol{z}^{r+n-d-1} + \cdots + H_{r-1}\boldsymbol{z}^{n} + \beta_{r,1}\boldsymbol{z}^{n-1}\right] = \mathit{roots}\left[\bar{Q}(\boldsymbol{z})\right] \cup \mathit{roots}\left[\bar{\bar{R}}_r(\boldsymbol{z})\right] \cup 0_{n-1}, \tag{A.24}$$

where $\bar{Q}(\boldsymbol{z})$ *is a subset of* $Q(\boldsymbol{z})$ *containing all roots* q_i *of* $Q(\boldsymbol{z})$ *such that, for* $i = 1 \ldots n_{\bar{q}}$, $\|q_i\| > \|\lambda_{\max}(A)\|$, *and* $\bar{\bar{R}}_r(\boldsymbol{z})$ *is another perturbed ring polynomial. The nonminimum-phase zeros whose magnitude is greater than* $\|\lambda_{\max}(A)\|$ *are retained, while the remaining roots are either located at the origin or form an approximate ring close to a circle with radius equal to the spectral radius of* A*. A total of* $n-1$ *roots are located at the origin.*

Conjecture A.3.3 (SISO, truncated ring polynomial)**.** *Consider* $l_u = l_z = 1$ *and let* $\bar{R}_r(\boldsymbol{z})$ *denote a* perturbed ring polynomial*, obtained as above. For each* r*, let* $\bar{\mathcal{R}}_r \stackrel{\triangle}{=} \{\boldsymbol{z}_{r,1}, \ldots, \boldsymbol{z}_{r,r-1}\}$ *be the set of roots of* $\bar{R}_r(\boldsymbol{z})$*. Then, for each* $i = 1, \ldots, r-1$*, the sequence* $\{\boldsymbol{z}_{r,i}\}_{r=1}^{\infty}$ *converges to* $\|\lambda_{\max}(A)\|$ *as* $r \to \infty$*, that is, as* $r \to \infty$*, the radius of each root* $\boldsymbol{z}_{r,i}$ *of the perturbed ring polynomial* $\bar{R}_r(\boldsymbol{z})$ *approaches the spectral radius of the dynamics matrix* A*.*

Bibliography

[1] S. Akhtar and D. S. Bernstein. Optimal adaptive feedback disturbance rejection. In *Proc. ACTIVE 04*, Williamsburg, VA, September 2004.

[2] S. Akhtar and D. S. Bernstein. Logarithmic Lyapunov functions for direct adaptive stabilization with normalized adaptive laws. *Int. J. Contr.*, 77:630–638, 2004.

[3] S. Akhtar and D. S. Bernstein. Lyapunov-stable discrete-time model reference adaptive control. *Int. J. Adaptive Contr. Signal Proc.*, 19:745–767, 2005.

[4] P. Albertos. Block multirate input-output model for sampled-data control systems. *IEEE Trans. Autom. Contr.*, 35:1085–1088, 1990.

[5] B. D. O. Anderson. Topical problems of adaptive control. In *Proc. European Contr. Conf.*, pages 4997–4998, Kos, Greece, July 2007.

[6] K. J. Åström and R. M. Murray. *Feedback Systems: An Introduction for Scientists and Engineers*. Princeton University Press, 2008.

[7] K. J. Åström and B. Wittenmark. *Adaptive Control*. Addison-Wesley, Reading, MA, second edition, 1995.

[8] K. J. Åström, P. Hagander, and J. Sternby. Zeros of sampled systems. *Automatica*, 20:31–38, 1984.

[9] E. W. Bai and S. S. Sastry. Persistency of excitation, sufficient richness and parameter convergence in discrete-time adaptive control. *Sys. Contr. Lett.*, 6: 153–163, 1985.

[10] D. S. Bayard. Extended horizon liftings for stable inversion of nonminimum-phase systems. *IEEE Trans. Autom. Contr.*, 39:1333–1338, 1994.

[11] D. S. Bayard. Stable direct adaptive periodic control using only plant order knowledge. *Int. J. Adaptive Contr. Signal Processing*, 10:551–570, 1996.

[12] D. S. Bayard and D. Boussalis. Noncolocated structural vibration suppression using zero annihilation periodic control. In *Proc. Conf. Contr. Appl.*, pages 141–146, Vancouver, B.C., 1993.

[13] D. S. Bernstein. Some open problems in matrix theory arising in linear systems and control. *Linear Algebra and Its Applications*, 162-164:409–432, 1992.

[14] D. S. Bernstein. *Matrix Mathematics*. Princeton University Press, 2005.

[15] D. S. Bernstein. *Matrix Mathematics*. Princeton University Press, 2nd edition, 2009.

[16] R. R. Bitmead, M. Gevers, and V. Wertz. *Adaptive Optimal Control: The Thinking Man's GPC*. Prentice Hall, Victoria, Australia, 1990.

[17] E. Bullinger and F. Allgöwer. Adaptive λ-tracking for nonlinear higher relative degree systems. *Automatica*, 41:1191–1200, 2005.

[18] C. I. Byrnes and J. C. Willems. Adaptive stabilization of multivariable linear systems. In *Proc. Conf. Dec. Contr.*, pages 1574–1577, Las Vegas, NV, 1984.

[19] E. F. Camacho and C. Bordons. *Model Predictive Control*. Springer, London, England, 2004.

[20] K. C. Chan and J. L. Lin. On the minimum phase property of mass-dashpot-spring sampled systems. *J. Dynamical Systems, Measurement, and Contr.*, 127: 642–647, 2005.

[21] Y. C. Cho, M. Fledderjohn, M. Holzel, B. Jayaraman, M. Santillo, D. S. Bernstein, and W. Shyy. Adaptive flow control of low reynolds number aerodynamics using a dielectric barrier discharge actuator. In *AIAA Aerosp. Sciences Mtg.*, Orlando, FL, January 2009. AIAA-2009-0378.

[22] M. J. Corless and A. E. Frazho. *Linear Systems and Control*. Marcel Dekker, New York, 2003.

[23] J. Daams and J. W. Polderman. Almost optimal adaptive LQ control: SISO case. *Math. Contr., Signals, Sys.*, 15(15):71–100, 2002.

[24] A. Datta. *Adaptive Internal Model Control*. Springer-Verlag, London, England, 1998.

[25] J. C. Doyle, B. A. Francis, and A. R. Tannenbaum. *Feedback Control Theory*. Macmillan, New York, 1992.

[26] B. Egardt. *Stability of Adaptive Controllers*. Springer-Verlag, Berlin, Germany, 1979.

[27] B. Egardt. Stability analysis of continuous-time adaptive control. *SIAM J. Contr. Optim.*, 18:540–558, 1980.

[28] G. Feng. A robust discrete-time direct adaptive control algorithm. *Sys. Contr. Lett.*, 22:203–208, 1994.

[29] A. L. Fradkov. Synthesis of an adaptive system for linear plant stabilization. *Automation and Remote Control*, 35:1960–1966, 1974.

[30] P. J. Gawthrop, L. Wang, and P. C. Young. Continuous-time non-minimal state-space design. *Int. J. Contr.*, 80:1690–1697, 2007.

[31] S. G. Goodhart, K. J. Burnham, and D. J. G. James. A retrospective self-tuning controller. *Int. J. Adaptive Contr. Signal Proc.*, 5:283–292, 1991.

[32] G. C. Goodwin and K. S. Sin. *Adaptive Filtering, Prediction, and Control*. Prentice Hall, 1984.

[33] G. C. Goodwin, P. J. Ramadge, and P. E. Caines. Discrete-time multivariable adaptive control. *IEEE Trans. Autom. Contr.*, 25:449–456, 1980.

[34] W. M. Haddad, T. Hayakawa, and A. Leonessa. Direct adaptive control for discrete-time nonlinear uncertain dynamical systems. In *Proc. Amer. Contr. Conf.*, pages 1773–1778, Anchorage, AK, 2002.

[35] T. Hayakawa, W. M. Haddad, and A. Leonessa. A Lyapunov-based adaptive control framework for discrete-time non-linear systems with exogenous disturbances. *Int. J. Contr.*, 77:250–263, 2004.

[36] J. B. Hoagg. *Advances in adaptive stabilization, command following, and disturbance rejection*. PhD thesis, University of Michigan, 2006.

[37] J. B. Hoagg and D. S. Bernstein. Discrete-time adaptive feedback disturbance rejection using a retrospective performance measure. In *Proc. ACTIVE 04*, Williamsburg, VA, 2004.

[38] J. B. Hoagg and D. S. Bernstein. Robust stabilization of discrete-time systems. In *Proc. Conf. Dec. Contr.*, pages 2346–2351, Paradise Island, The Bahamas, 2004.

[39] J. B. Hoagg and D. S. Bernstein. Discrete-time adaptive command following and disturbance rejection with unknown exogenous dynamics. In *Proc. Conf. Dec. Contr.*, pages 471–476, San Diego, CA, December 2006.

[40] J. B. Hoagg and D. S. Bernstein. Deadbeat internal model control for command following and disturbance rejection in discrete-time systems. In *Proc. Amer. Contr. Conf.*, pages 194–199, Minneapolis, MN, 2006.

[41] J. B. Hoagg and D. S. Bernstein. Direct adaptive stabilization of minimum-phase systems with bounded relative degree. *IEEE Trans. Autom. Contr.*, 52: 610–621, 2007.

[42] J. B. Hoagg, D. S. Bernstein, S. L. Lacy, and R. Venugopal. Adaptive control of a flexible membrane using acoustic excitation and optical sensing. In *Proc. Guid. Nav. Contr. Conf.*, Austin, TX, 2003. AIAA-2003-5430.

[43] J. B. Hoagg, S. L. Lacy, and D. S. Bernstein. Broadband adaptive disturbance rejection for a deployable optical telescope testbed. In *Proc. Amer. Contr. Conf.*, pages 4953–4958, Portland, OR, 2005.

[44] J. B. Hoagg, M. A. Santillo, and D. S. Bernstein. Internal model control in the shift and delta domains. *IEEE Trans. Autom. Contr.*, 53:1066–1072, 2008.

[45] J. B. Hoagg, M. A. Santillo, and D. S. Bernstein. Discrete-time adaptive command following and disturbance rejection with unknown exogenous dynamics. *IEEE Trans. Autom. Contr.*, 53:912–928, 2008.

[46] A. Ilchmann. *Non-Identifier-Based High-Gain Adaptive Control*. Springer-Verlag, London, England, 1993.

[47] A. Ilchmann. Universal adaptive stabilization of nonlinear systems. *Dynamics and Contr.*, 7:199–213, 1997.

[48] A. Ilchmann and E. P. Ryan. On gain adaptation in adaptive control. *IEEE Trans. Autom. Contr.*, 48:895–899, 2003.

[49] P. Ioannou and B. Fidan. *Adaptive Control Tutorial*. SIAM, Philadelphia, 2006.

[50] P. Ioannou and J. Sun. *Robust Adaptive Control*. Prentice Hall, 1996.

[51] T. Ionescu and R. Monopoli. Discrete model reference adaptive control with an augmented error signal. *Automatica*, 13:507–517, 1977.

[52] T. Iwasaki and R. Skelton. Parameterization of all stabilizing controllers via quadratic Lyapunov functions. *J. Optim. Theory Appl.*, 85(2):291–307, 1995.

[53] R. Johansson. Lyapunov functions for adaptive systems. In *Proc. Conf. Dec. Contr.*, pages 449–454, San Antonio, TX, 1983.

[54] R. Johansson. Stability of direct adaptive control with RLS identification. In *Modeling, Identification, and Robust Control*, pages 29–43, North Holland, Amsterdam, 1986.

[55] R. Johansson. Global Lyapunov stability and exponential convergence of direct adaptive control. *Int. J. Contr.*, 50:859–869, 1989.

[56] R. Johansson. Supermartingale analysis of minimum variance adaptive control. *Contr. – Theory and Advanced Technology*, 10:993–1013, 1995.

[57] J. N. Juang. *Applied System Identification*. Prentice-Hall, Upper Saddle River, NJ, 1993.

[58] T. Kailath. *Linear Systems*. Prentice Hall, Englewood Cliffs, New Jersey, 1980.

[59] I. Kanellakopoulos. A discrete-time adaptive nonlinear system. *IEEE Trans. Autom. Contr.*, 39:2362–2365, 1994.

[60] S. P. Karason and A. M. Annaswamy. Adaptive control in the presence of input constraints. *IEEE Trans. Autom. Contr.*, 39:2325–2330, 1994.

[61] H. Kaufman, I. Barkana, and K. Sobel. *Direct Adaptive Control Algorithms: Theory and Applications*. Springer, New York, 2nd edition, 1998.

[62] S. M. Kuo and D. R. Morgan. *Active Noise Control Systems*. Wiley, New York, 1996.

[63] S. L. Lacy, R. Venugopal, and D. S. Bernstein. ARMARKOV adaptive control of self-excited oscillations of a ducted flame. In *Proc. Conf. Dec. Contr.*, pages 4527–4528, Tampa, FL, December 1998.

[64] W. C. Lai and P. A. Cook. A discrete-time universal regulator. *Int. J. Contr.*, 62:17–32, 1995.

[65] I. D. Landau. *Adaptive Control: The Model Reference Approach*. Marcel Dekker, New York, 1979.

[66] I. D. Landau and H. M. Silveira. A stability theorem with applications to adaptive control. *IEEE Trans. Autom. Contr.*, 24:305–312, 1979.

[67] I. D. Landau, R. Lozano, and M. M'Sadd. *Adaptive Control*. Springer, London, England, 1998.

[68] J. Li, X. Xie, and W. Chen. Direct model reference adaptive control using $K_p = LDU$ factorization for multivariable discrete-time plants. *J. Contr. Thy. Appl.*, 6:392–298, 2008.

[69] A. Lindquist and V. A. Yakubovich. Universal regulators for optimal tracking in discrete-time systems affected by harmonic disturbances. *IEEE Trans. Autom. Contr.*, 44:1688–1704, 1999.

[70] L. Ljung. *System Identification: Theory for the User*. Prentice-Hall Information and Systems Sciences, Upper Saddle River, NJ, 2nd edition, 1999.

[71] R. Lozano-Leal. Robust adaptive regulation without persistent excitation. *IEEE Trans. Autom. Contr.*, 34:1260–1267, 1989.

[72] J. Lu and T. Yahagi. Discrete-time model reference adaptive control for non-minimum phase systems with disturbances using approximate inverse systems. *IEE Proc.-Control Theory Appl.*, 144(5):447–454, 1997.

[73] J. M. Maciejowski. *Multivariable Feedback Design*. Addison-Wesley, Great Britain, 1989.

[74] J. M. Maciejowski. *Predictive Control with Constraints*. Prentice Hall, Harlow, Essex, 2002.

[75] M. Makoudi and L. Radouane. A robust model reference adaptive control for non-minimum phase systems with unknown or time-varying delay. *Automatica*, 36:1057–1065, 2000.

[76] I. Mareels. A simple selftuning controller for stably invertible systems. *Sys. Contr. Lett.*, 4:5–16, 1984.

[77] I. Mareels and J. W. Polderman. *Adaptive Systems: An Introduction*. Birkhäuser, Boston, MA, 1996.

[78] R. Marino and G. L. Santosuosso. Regulation of linear systems with unknown exosystems of uncertain order. *IEEE Trans. Autom. Contr.*, 52:352–359, 2007.

[79] B. Martensson. The order of any stabilizing regulator is sufficient a priori information for adaptive stabilization. *Sys. Contr. Lett.*, 6:87–91, 1985.

[80] W. Messner and M. Bodson. Design of adaptive feedforward algorithms using internal model equivalence. *Int. J. Adaptive Contr. Signal Processing*, 9: 199–212, 1995.

[81] D. E. Miller and E. J. Davison. An adaptive controller which provides Lyapunov stability. *IEEE Trans. Autom. Contr.*, 34:599–609, 1989.

[82] R. V. Monopoli. Model reference adaptive control with an augmented error signal. *IEEE Trans. Autom. Contr.*, 19:474–484, 1974.

[83] K. L. Moore. *Iterative Learning Control for Deterministic Systems*. Springer-Verlag, London, England, 1993.

[84] K. L. Moore. Iterative learning control - an expository overview. *Applied and Computational Controls, Signal Processing, and Circuits*, 1:151–214, 1998.

[85] A. S. Morse. Global stability of parameter adaptive control systems. *IEEE Trans. Autom. Contr.*, 25:433–440, 1980.

[86] A. S. Morse. A three-dimensional universal controller for the adaptive stabilization of any strictly proper minimum phase system with relative degree not exceeding two. *IEEE Trans. Autom. Contr.*, 30:1188–1191, 1985.

[87] A. S. Morse. A $4(n+1)$-dimensional model reference adaptive stabilizer for any relative degree one or two, minimum phase system of dimension n or less. *Automatica*, 23:123–125, 1987.

[88] E. Mosca. *Optimal Predictive and Adaptive Control*. Prentice Hall, Englewood Cliffs, New Jersey, 1995.

[89] C. Mracek and D. Ridgely. Missile longitudinal autopilots: Connections between optimal control and classical topologies. In *Proc. Guid. Nav. Contr. Conf.*, San Francisco, CA, August 2005. AIAA-2005-6381.

[90] K. S. Narendra and A. M. Annaswamy. *Stable Adaptive Systems*. Prentice Hall, Englewood Cliffs, New Jersey, 1989.

[91] K. S. Narendra and Y. H. Lin. Stable discrete adaptive control. *IEEE Trans. Autom. Contr.*, 25:456–461, 1980.

[92] K. S. Narendra and L. S. Valavani. Stable adaptive controller design – Direct control. *IEEE Trans. Autom. Contr.*, 23:570–583, 1978.

[93] K. S. Narendra and C. Xiang. Adaptive control of discrete-time systems using multiple models. *IEEE Trans. Autom. Contr.*, 45:1669–1686, 2000.

[94] K. S. Narendra, Y. H. Lin, and L. S. Valavani. Stable adaptive controller design, part II: Proof of stability. *IEEE Trans. Autom. Contr.*, 25:440–448, 1980.

[95] P. A. Nelson and S. J. Elliot. *Active Control of Sound*. Academic, New York, 1992.

[96] R. D. Nussbaum. Some remarks on a conjecture in parameter adaptive control. *Sys. Contr. Lett.*, 3:243–246, 1983.

[97] K. Ogata. *Modern Control Engineering*. Prentice Hall, New Jersey, 2001.

[98] F. Ohkawa and Y. Yonezawa. A discrete model reference adaptive control system for a plant with input amplitude constraints. *Int. J. Contr.*, 36:747–753, 1982.

[99] B. L. Pence, M. A. Santillo, and D. S. Bernstein. Markov-parameter-based adaptive control of 3-axis angular velocity in a six-degree-of-freedom Stewart platform. In *Proc. Amer. Contr. Conf.*, pages 4767–4772, Seattle, WA, June 2008.

[100] P. Peres, J. Geromel, and S. Souza. Optimal H_2 control by output feedback. In *Proc. Conf. Dec. Contr.*, pages 102–107, San Antonio, TX, December 1993.

[101] J. W. Polderman. A state space approach to the problem of adaptive pole assignment. *Math. Contr. Signal Processing*, 2:71–94, 1989.

[102] J. W. Polderman and I. Mareels. High gain adaptive control revisited: first and second order case. In *Proc. Conf. Dec. Contr.*, pages 3329–3333, Phoenix, AZ, December 1999.

[103] M. A. Rizzo, M. A. Santillo, A. K. Padthe, J. B. Hoagg, S. Akhtar, K. Powell, and D. S. Bernstein. CFD-based identification for adaptive flow control using ARMARKOV disturbance rejection. In *Proc. Amer. Contr. Conf.*, pages 3783–3788, Minneapolis, MN, June 2006.

[104] C. Rohrs, L. Valavani, M. Athans, and G. Stein. Robustness of continuous-time adaptive control algorithms in the presence of unmodeled dynamics. *IEEE Trans. Autom. Contr.*, 30:881–889, 1985.

[105] J. Rosenthal and X. Wang. Output feedback pole placement with dynamic compensators. Technical Report BS-R9516, CWI, P.O. Box 94079, 1090 GB Amsterdam, The Netherlands, 1995.

[106] E. P. Ryan. A universal adaptive stabilizer for a class of nonlinear systems. *Sys. Contr. Lett.*, 16:209–218, 1991.

[107] J. M. M. Sanchez and J. Rodellar. *Adaptive Predictive Control: From the concepts to plant optimization*. Prentice Hall, Cornwall, U.K., 1996.

[108] H. Sane and D. S. Bernstein. Active noise control using an acoustic servovalve. In *Proc. Amer. Contr. Conf.*, pages 2621–2625, Philadelphia, PA, June 1998.

[109] H. Sane, R. Venugopal, and D. S. Bernstein. Robustness of ARMARKOV adaptive control disturbance rejection algorithm. In *Proc. Amer. Contr. Conf.*, pages 2035–2039, San Diego, CA, June 1999.

[110] H. Sane, R. Venugopal, and D. S. Bernstein. Disturbance rejection using ARMARKOV adaptive control with simultaneous identification. *IEEE Trans. Contr. Sys. Tech.*, 9:101–106, 2001.

[111] M. A. Santillo and D. S. Bernstein. Adaptive static-output-feedback stabilization using retrospective cost optimization. In *Proc. Conf. Dec. Contr.*, Shanghai, China, December 2009. (submitted).

[112] M. A. Santillo and D. S. Bernstein. Indirect adaptive control using retrospective cost optimization with RLS-based estimation for concurrent markov-parameter updating. In *Proc. Conf. Dec. Contr.*, Shanghai, China, December 2009. (submitted).

[113] M. A. Santillo and D. S. Bernstein. A retrospective correction filter for discrete-time adaptive control of nonminimum phase systems. In *Proc. Conf. Dec. Contr.*, pages 690–695, Cancun, Mexico, December 2008.

[114] M. A. Santillo and D. S. Bernstein. Inherent robustness of minimal modeling discrete-time adaptive control to flight anomalies. In *Proc. Guid. Nav. Contr. Conf.*, Honolulu, HI, August 2008. AIAA-2008-7289.

[115] M. A. Santillo, J. B. Hoagg, D. S. Bernstein, and K. Powell. CFD-based adaptive flow control for steady flow field modification. In *Proc. Conf. Dec. Contr.*, pages 3105–3110, San Diego, CA, December 2006.

[116] M. A. Santillo, J. B. Hoagg, D. S. Bernstein, and K. Powell. Adaptive disturbance rejection for flow in a duct with time-varying upstream velocity. In *Proc. Amer. Contr. Conf.*, pages 2226–2231, New York, NY, July 2007.

[117] M. A. Santillo, A. M. D'Amato, and D. S. Bernstein. System identification using a retrospective correction filter for adaptive feedback model updating. In *Proc. Amer. Contr. Conf.*, pages 4392–4397, St. Louis, MO, June 2009.

[118] S. Sastry and M. Bodson. *Adaptive Control: Stability, Convergence, and Robustness*. Prentice Hall, Englewood Cliffs, New Jersey, 1989.

[119] U. Shaked. Guaranteed stability margins for the discrete-time linear quadratic optimal regulator. *IEEE Trans. Autom. Contr.*, 31:162–165, 1986.

[120] S. Skogestad and I. Postlethwaite. *Multivariable Feedback Control*. Wiley, New York, 2nd edition, 2005.

[121] V. L. Syrmos, C. T. Abdallah, P. Dorato, and K. Grigoriadis. Static output feedback - a survey. *Automatica*, 33:125–137, 1997.

[122] G. Tao. *Adaptive Control Design and Analysis*. Wiley, Hoboken, New Jersey, 2003.

[123] G. Tao and P. A. Ioannou. Model reference adaptive control for plants with unknown relative degree. In *Proc. Amer. Contr. Conf.*, pages 2297–2302, Pittsburgh, PA, June 1989.

[124] C. J. Taylor, A. Chotai, and P. C. Young. State space control system design based on non-minimal state-variable feedback: Further generalization and unification results. *Int. J. Contr.*, 73:1329–1345, 2000.

[125] J. Tokarzewski. *Finite Zeros in Discrete-Time Control Systems*. Springer, Berlin, 2006.

[126] A. Trofino-Neto and V. Kučera. Stabilization via static output feedback. *IEEE Trans. Autom. Contr.*, 38:764–765, 1993.

[127] R. Venugopal and D. S. Bernstein. Adaptive disturbance rejection using ARMARKOV/Toeplitz models. *IEEE Trans. Contr. Sys. Tech.*, 8:257–269, 2000.

[128] R. Venugopal, V. Rao, and D. S. Bernstein. Lyapunov-based backward-horizon adaptive stabilization. *Int. J. Adaptive Contr. Signal Proc.*, 17:67–84, 2003.

[129] M. Vidyasagar. *Control System Synthesis: A Factorization Approach*. M.I.T. Press, Boston, MA, 1985.

[130] J. C. Willems and C. I. Byrnes. Global adaptive stabilization in the absence of information on the sign of the high frequency gain. *Lecture Notes Contr. and Info. Sciences*, 62:49–57, 1984.

[131] X. Xie and J. Li. A robustness analysis of discrete-time direct model reference adaptive control. *Int. J. Contr.*, 79:1196–1204, 2006.

[132] Y. Xudong. Universal λ-tracking for nonlinearly-perturbed systems without restrictions on the relative degree. *Automatica*, 35:109–119, 1999.

[133] D. C. Youla, J. J. Bongiorno, and C. N. Lu. Single-loop feedback stabilization of linear multivariable dynamical plants. *Automatica*, 10:159–173, 1974.

[134] P. Young, M. A. Benzadi, C. L. Wang, and A. Chotai. Direct digital and adaptive control by input-output state variable feedback pole assignment. *Int. J. Contr.*, 46:1867–1881, 1987.

[135] C. Zhang and R. J. Evans. Amplitude constrained adaptive control. *Int. J. Contr.*, 46:53–64, 1987.

[136] K. Zhou. *Robust and Optimal Control*. Prentice Hall, Upper Saddle River, New Jersey, 1996.